THE UNIVERSITY OF OKLAHOMA

GRADUATE COLLEGE

POLYMER SOLUTION RHEOLOGY AND DISPLACEMENT PROCESSES

A DISSERTATION

SUBMITTED TO THE GRADUATE FACULTY

in partial fulfillment of the requirements for the

degree of

DOCTOR OF PHILOSOPHY

BY

HOSSEIN H. NOURI

Norman, Oklahoma

1971

POLYMER SOLUTION RHEOLOGY AND DISPLACEMENT PROCESSES

APPROVED BY

Paul J. Root

Kenneth E. Starling

Carl A. Moore

Jim T. Hays

D E Menzie

DISSERTATION COMMITTEE

ACKNOWLEDGEMENTS

In any undertaking of this magnitude there is always an individual who is instrumental in providing the counsel and encouragement at times when it is most necessary. Dr. Paul J. Root has been such an individual for me, and I am pleased to convey my gratitude for his confidence and support throughout the entire program of advanced study leading to this work.

I also wish to express my thanks and profound gratitude to Drs. C. M. Sliepcevich and J. Reed Welker for their guidance and assistance during the completion of this investigation.

I am indebted to Dr. Don E. Menzie for his assistance throughout the years of my study at the University of Oklahoma and to the other members of my doctoral committee, Drs. Kenneth E. Starling, Jimmy F. Harp and Carl A. Moore, who gave so freely of their time to serve on my committee.

I am thankful to Mr. N. S. Knight for his help in construction of the apparatus, to Mrs. Joyce Gerald, Mrs. Priscilla Tullis, Mrs. Danna S. Sowell, Mrs. Nedra Eaton, and Miss Jan Trantham for their assistance in preparing this manuscript.

I am grateful to the various industrial organizations who provided partial financial assistance over the course of this research and I wish to acknowledge their support. Among these are the Socony Mobil Oil Company and Gulf Research and Development Company, each of whom contributed a fellowship toward my support.

Finally, I am sincerely grateful to my family for their continued encouragement, patience and understanding during the course of this work.

Hossein H. Nouri

ABSTRACT

Flow and displacement theories for non-Newtonian polymer solutions in porous media have not been advanced to nearly the extent as those for the Newtonian fluids. At present, reliable field and experimental data concerning the mechanism of flow of polymer solutions through porous media are scarce and fragmentary. In particular, basic investigations which determine whether or not the efficiency of the polymer displacement process is a function only of the mobility ratio have not been reported. Both experimental and theoretical research in development of a more satisfactory theory to describe the flow behavior of polymer solutions in porous media are urgently needed.

In this work a method is designed to study the role of mobility ratio for a process in which oil is displaced from a porous medium by a polymer solution. A reduced friction factor-Reynolds number correlation is developed to predict the flow of various polymer solutions through consolidated porous media and a theory is advanced to explain more truly the flow behavior of a polymer solution as it passes through the cores.

The cone and plate viscometer data obtained for a total of 88 solutions of twelve different polymers more frequently used by the petroleum industry appeared to fit the power law equation quite well. The effects of temperature, sodium chloride concentration, polymer molecular weight and polymer concentration on solution viscosity are also discussed.

TABLE OF CONTENTS

TABLE OF CONTENTS (Continued)

TABLE OF CONTENTS (Continued)

LIST OF TABLES

LIST OF TABLES (Continued)

LIST OF TABLES (Continued)

LIST OF TABLES (Continued)

LIST OF TABLES (Continued)

LIST OF TABLES (Continued)

LIST OF TABLES (Continued)

LIST OF TABLES (Continued)

LIST OF TABLES (Continued)

LIST OF TABLES (Continued)

LIST OF ILLUSTRATIONS AND GRAPHS

LIST OF ILLUSTRATIONS AND GRAPHS (Continued)

LIST OF ILLUSTRATIONS AND GRAPHS (Continued)

LIST OF ILLUSTRATIONS AND GRAPHS (Continued)

LIST OF ILLUSTRATIONS AND GRAPHS (Continued)

LIST OF ILLUSTRATIONS AND GRAPHS (Continued)

POLYMER SOLUTION RHEOLOGY AND DISPLACEMENT PROCESSES

CHAPTER I

INTRODUCTION

For many years oil has been one of the most important sources of the world's fuel energy. Today with the high rate of population increase and the vast technological progress, an ever increasing demand for petroleum products is imminent. To combat this demand, the oil industry can either find new petroleum resources or develop a more efficient process to recover more oil from known oil reservoirs. Oil reservoirs which have reached the economic limit of their productivity by natural flow, gas lift, and various methods of pumping, still contain, as a rule, at least 30 percent of their original petroleum hydrocarbons. At present such secondary recovery methods as water flooding, gas repressuring, in-situ combustion, steam flooding, etc., are being used in order to produce a part of this remaining oil. Undoubtedly other methods will some day be developed to recover still higher percentages of this crude oil from the reservoir.

Among the methods of secondary recovery which have been used is one which involves the injection of high-viscosity water through the reservoir to improve the mobility ratio and thereby increase the displacement efficiency. The mobility ratio, when two immisicible fluids displace each other, is defined as the ratio of the mobility of the displacing fluid to that of the displaced fluid:

$$M = \frac{(K/\mu)\ \text{displacing}}{(K/\mu)\ \text{displaced}} \qquad (1\text{-}1)$$

The mobility ratio is a very important factor in secondary recovery predictions, governing the displacement efficiency of the oil by the displacing fluid. A mobility ratio of greater than one will result in an uneven displacement and a poor oil recovery (18). On the other hand a mobility ratio of one or less will result in a more piston-like displacement process and a higher oil production.

The use of additives to increase the viscosity of injection water is not new. Natural gums, fatty acid soaps, sucrose, glycerine, alginates, and lately water soluble polymers have been used as viscosity-increasing agents to improve the efficiency of a secondary recovery program. Of these, the water soluble polymers appear to be the most suitable additives. In general only a small concentration of polymer is required to increase the viscosity of water significantly. An increase in the viscosity of the displacing

fluid will provide a more favorable mobility ratio, and therefore an increase in oil recovery.

Problems relating to the use of high molecular weight polymer solutions for secondary recovery of oil have been given attention during the past few years. A number of attempts have been made (18,28,45) to modify the D'Arcy's linear fluid flow equation to fit a particular fluid flow-porous medium system by expressing the viscosity term as a function of pressure gradient, rheological properties of the polymer solution and characteristics of the porous media. Others (14,33,67) have tried to correlate the flow behavior of the polymer solution through porous media by a friction factor-Reynolds number relationship, expressed in terms of the various hydraulic radius principles, essentially applicable to the flow through unconsolidated porous media.

At present there are no published results that truly describe the flow behavior of the polymer solution through porous media nor is there a general expression relating the flow characteristics of the polymer solutions to the properties of the porous media. Basic investigations which determine whether or not the displacement efficiency of polymer flooding is a function only of the mobility ratio have not been reported, nor have techniques for predicting the displacement behavior from single laboratory experiments been developed. It was with the intent of contributing to the preceding areas of interest that this experimental study was conducted. In

particular, this dissertation is an investigation of the polymer solution rheology, the polymer solution behavior in porous media and the polymer solution displacement efficiency.

CHAPTER II

BACKGROUND AND REVIEW OF PREVIOUS INVESTIGATIONS

During the past decade, a great number of technical papers have been devoted to the studies of the behavior of polymer solutions in porous media. In particular, many experimental studies have been concerned with the determination of the variables that control the amount of oil which can be displaced from a porous matrix by an aqueous polymer solution. Only recently have the results of these studies been employed to any great extent in the prediction of actual reservoir performance. That such studies were of great practical value, can be demonstrated by the significant increase in the amount of oil produced by secondary recovery methods using polymer solutions during the last ten years. These studies can be divided into two groups: those which were concerned with the development of theories which would describe the flow of polymer solutions in porous media, and those which were more concerned with displacement behavior of polymer solutions in the particular system under study. A rather extensive review of the literature concerning the

behavior of polymer solutions in porous media has been completed with particular emphasis being placed on those features of the published literature having the most direct bearing on the subject matter covered by this investigation.

Polymer Background

Although the high molecular weight compounds, like rubber, protein resins, cellulose and gum had been known to chemists for years, they were believed to be made up of colloid aggregates of small molecules which were held together by some undefined force. Not until 1930 was the fundamental concept that high polymers are actually high molecular weight compounds containing "covalent bonds" as the force holding together atoms or smaller molecular fragments accepted.

Actually it was in 1871 that Haberman and Hlasiwetz (35) stated that these naturally occurring substances were polymeric in nature, as we define polymeric today. Their concept was not very widely received by organic chemists mainly because of their inability to isolate pure molecular compounds which could be defined by a simple molecular weight. A procedure developed by the organic chemists has proven to be very successful, but it depended on elementary analysis and molecular weight determination. Unfortunately, there were no accurate methods of determining the molecular weights of high molecular weight compounds at that time.

Another barrier to the progress of the polymeric theory was the inability of scientists to account for the end groups. Since ozanalysis of natural rubber produced levulinic acid, the chain structure was rejected in favor of a cyclic dimer:

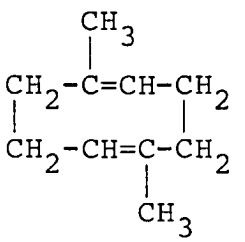

Later, the dimer structure was changed in favor of larger rings. The same ideas were carried over to synthetic polymers. Generally, colloidal aggregates of simple molecules were formulated, and, in order to account for end groups, cyclic monomers and dimers were depicted.

In 1920 the chain formulas for polyoxymethylene:

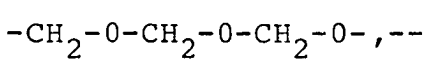

and polystyrene:

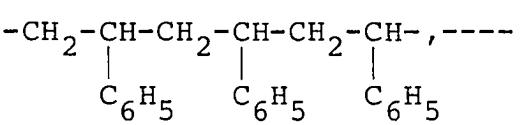

were proposed by Staudinger (24). Despite the extensive investigation and further proof of the nature of polymers, his views were not widely accepted until ten years later. During this ten-years period, Mayer and Mark (44) added

support to the high molecular weight theory with several x-ray investigations of polymer structure. In 1929 Carothers (12) reported a series of experiments in which polymeric molecules were prepared through known organic reactions and the properties of the products were then correlated with polymer structure. His work was particularly effective in breaking the last barrier to the new theories and opening up the field of polymer chemistry to synthetic polymers.

Polymer Definition and Classification

The term polymer means many members (24) and it was first used to specify compounds with same composition but different molecular weight. Carothers (12) defined polymerization as a reaction which is functionally capable of proceeding indefinitely. The structure of a polymeric substance is customarily described in terms of its structural units. These may be defined in the most general terms as groups having a valence of two or more and are connected to one another in the polymer molecule, or polymeric structure, by covalent bonds.

The structural units can be connected together in any conceivable pattern. In the simplest polymer, "the linear polymer," the structural units are connected to one another in linear sequence such as:

$$P'\text{-}P\text{-}P\text{-}P\text{-}P\cdots\cdots\text{-}P'' \text{ or } P'(\text{-}P\text{-})_{y-2} - P''$$

where P is a basic structural unit or a monomer and y is the degree of polymerization, or number of structural units in the molecule. The chain of structural units P is terminated on either end by P' and P". The structural units, other than the terminal units, P', and P", must necessarily be bivalent in this case. The group P' may be identical with P", but neither can be identical with P.

Alternatively, the structural units of the polymer may be connected together in such a way as to form "nonlinear or branched," structures. At least some of the units must then possess a valency greater than two:

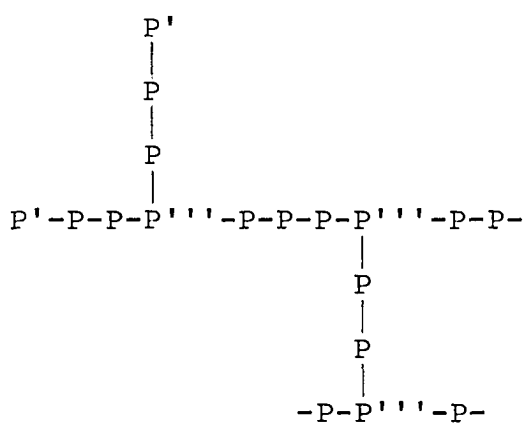

where P''' is a trivalent branching unit. The polymer molecules of this kind can be interconnected to form a "network structure" which may be a "planar network" or a three-dimensional "space network."

Often the end groups for a polymer are not known and the polymer structure is written only in terms of the structural unit, the end groups being left off. Even end groups on different polymer chains produced from the same

polymerization reaction can be different. According to the functionality concept introduced by Carothers (12), all monomers which when polymerized may join with two, and only two, other monomers are termed "bifunctional." Similarly, a bifunctional unit is one which is attached to two other units. It is clear then that linear polymers are composed exclusively of bifunctional units. Nonlinear polymers are on the other hand made from monomers at least some of which possess a functionality exceeding two. In other words, nonlinear polymers are made of "polyfunctional" monomers.

Polymers consisting of a single repeating unit are called "homopolymers." This kind of polymer is made from one monomer and is homogeneous in this respect. Polymeric substances containing two or more structural units combined more or less in random sequence are then referred to as "copolymers."

In 1929 the need for classification of high molecular weight polymers was first recognized by Carothers (12). He classified all polymers into two groups: "addition polymers," in which the molecular formula of the structural unit (or units) is identical with that of the monomer from which the polymer is derived, and "condensation polymers," in which the molecular formula of the structural unit (or units) lacks certain atoms present in the monomer from which it is formed, or to which it may be degraded by chemical means. Condensation polymers may be formed from monomers

having two or more reactive groups of such a character that they may condense intermolecularly with the elimination of a by-product, usually water. A prime example is polyester:

$$nHO\text{-}R\text{-}COOH \rightarrow HO[\text{-}R\text{-}COO\text{-}]_{n-1}\ R\text{-}COOH + (n-1)H_2O$$

An addition polymer is made from a bifunctional or polyfunctional monomer by the addition of one monomer to another without the loss of any portion of the monomer. The most important class of addition polymers consists of those derived from the unsaturated monomers, such as the vinyl monomers:

$$nCH_2 = \underset{\displaystyle Y}{\overset{\displaystyle |}{CH}}\rightarrow \left[\ CH_2\text{-}\underset{\displaystyle Y}{\overset{\displaystyle |}{CH}}\ \right]_n$$

where y may be halogen, acetoxy, phenyl, etc. The above terminology can be applied also to the processes by which the polymers are formed. Thus the first reaction is a condensation polymerization, and the second one is an addition polymerization.

Flory (24) has pointed out that the significant difference between addition and condensation polymerization is not a matter of similarity or difference in the composition of the monomer and structural unit, but is a matter of the reactions which form the polymers. Condensation polymerization proceed by a stepwise intermolecular condensation,

while addition polymerizations are associated with a chain mechanism involving active centers on the growing chain.

Polymer hydrolyzation is a process in which a base such as sodium hydroxide is reacted with the polymer to hydrolyze about 0.8 to 10 percent of the amide groups present in the polymer. The result is a long hydrocarbon chain with alternating carbon atoms bearing either carboxylic or amide groups with ratio of carboxylic to amide groups being somewhere between 1/9 and 1/124 (15).

Polymer Solution Displacement Processes

Sadowski (68) was one of the first to investigate the flow of non-Newtonian polymer solutions through porous media. He was concerned with the characterization of non-Newtonian fluids by a rheological equation of state more generally applicable than the commonly used power law model, and the measurement and correlation of friction factor data for non-Newtonian flow through packed beds.

For his viscometric data, as obtained from either a capillary tube or core and plate viscometer, the three-parameter Ellis model:

$$\gamma_{ij} = -\frac{1}{\mu_o}\left[1 + \left(\frac{\sqrt{1/2\ \pi_\tau}}{\tau_{1/2}}\right)^{\beta-1}\right]\tau_{ij} \qquad (2\text{-}1)$$

was found to give an excellent fit. Here γ_{ij} are the cartesian

components of the rate of deformation tensor, τ_{ij} are the cartesian components of shear stress tensor, μ_o is the lower limiting viscosity, constant in Ellis' model, $\pi_\tau = \Sigma_i \Sigma_j \tau_{ij} \tau_{ji}$, and $\tau_{1/2}$ and β are constants in Ellis' model and are determined experimentally. The average error in the shear rate calculated from this model varied from 1.3 to 3.4 percent for shear rates up to 14,000 sec^{-1}. His data represented fourteen different aqueous solutions of polyethylene glycol, hydorxyethyl cellulose, and polyvinyl alcohol. His work with flow of non-Newtonian polymer solutions through packed beds gave results which depended very much upon the experimental procedure. If the flow rate of the fluid passing through a packed bed was held constant, the observed results were both steady and reversible. If the pressure applied to a packed bed was held constant, for sufficiently small particles and sufficiently large polymer concentrations, the observed results were both unsteady and irreversible. Sadowski's application of the capillary model to porous media, using the hydraulic radius concept and the Kozeny equation, and application of the Ellis model to a non-Newtonian fluid led to a modified form of D'Arcy's law:

$$V = \frac{K}{\mu_e} \frac{\Delta p}{L} \qquad (2\text{-}2)$$

A modified Ergun's friction factor:

$$F = \left(\frac{\Delta p}{\rho V^2}\right) \left(\frac{\phi^3}{1 - \phi}\right) \frac{D}{L} \tag{2-3}$$

and a modified Reynolds number:

$$R_e = \left(\frac{DV\rho}{\mu_e}\right) \left(\frac{1}{1 - \phi}\right) \left[1 + \frac{4}{\beta + 3} \left(\frac{\tau_R}{\tau_{1/2}}\right)^{\beta-1}\right] \tag{2-4}$$

In each case the Newtonian viscosity was replaced by an effective viscosity:

$$\frac{1}{\mu_e} = \frac{1}{\mu_o} \left[f(\beta) \left(\frac{\tau_R}{\tau_{1/2}}\right)^{\beta-1} + 1\right] \tag{2-5}$$

where

$$\tau_R = \frac{1}{6} \left(\frac{\Delta p}{L}\right) \left(\frac{D\phi}{1 - \phi}\right) \tag{2-6}$$

ϕ is the bed porosity, D is the particle diameter and $\Delta P/L$ is the pressure gradient. In the range, $1.0 < \beta < 7$, the function $f(\beta)$ was approximated to within 2 percent by:

$$f(\beta) = 1.27 - 0.75 \text{ Log } \beta \tag{2-7}$$

In his constant flow rate experiments, the data for the polymer solutions of low and medium molecular weights were successfully correlated for values of the effective Reynolds number less than ten. The average error in the friction factor was found to be 6.6 percent for 93 experimental

points representing seven fluids. For the polymer solutions of high molecular weight an additional parameter $\frac{1}{\lambda} = \mu_o/\tau_{1/2}$ and a dimensionless group, $(DG/(1 - \phi)\mu_o)(V/D\lambda)$, were introduced in which G is mass velocity, and V is superficial velocity. He designated the parameter $1/\lambda$ as a relaxation time characteristic of fluids which were exhibiting viscoelastic behavior.

A tentative explanation given for the unsteady and irreversible flow behavior observed for the constant pressure runs was that polymer adsorption and gel formation occurred throughout the bed. It was also suggested that the permeability of the bed was a function both of the effective Reynolds number and of the volumetric flow rate.

Gogarty (29) was concerned with rheological properties of pseudoplastic fluids in porous media. As part of his investigation, the average shear rate in a core was related to the permeability, porosity and the frontal velocity of the core as follows:

$$\bar{\gamma} = \left[\frac{V_o}{f(K)\,(K/\phi)^{1/2}}\right]^x \qquad (2\text{-}8)$$

where $\bar{\gamma}$ is the average shear rate, V_o is the frontal velocity, x is a constant, and f(K) is a linear function of the logarithm of the permeability, and to some degree, accounts for the interaction between a flowing non-Newtonian fluid and the porous media.

The rheological and flow results were also correlated to develop an expression for calculating effective viscosities, for use in the D'Arcy's equation, given as:

$$\mu_e = \frac{\mu_o}{f(\bar{\gamma}) + \frac{\mu_o}{a(\bar{\gamma})^n} g(\bar{\gamma})} \qquad (2\text{-}9)$$

where μ_e and μ_o are the effective and Newtonian viscosity respectively, a and n are constants derived from the power law portion of his curve, $f(\bar{\gamma})$ and $g(\bar{\gamma})$ are functions of the average shear rate and are defined as:

$$f(\bar{\gamma}) = \frac{1}{1 + (b\bar{\gamma})^s} \qquad (2\text{-}10)$$

$$g(\bar{\gamma}) = \frac{1}{1 + (d/\bar{\gamma})^t} \qquad (2\text{-}11)$$

where, b, d, s, and t are constants. This model was specifically developed to account for the rapidity with which the fluids change with shear rate from Newtonian to non-Newtonian character.

The three fluid systems used in this investigation were surfactant-stabilized dispersions of water in hydrocarbon, which exhibit time-independent pseudoplastic rheological behavior. For porous media, Berea sandstone cores with different permeabilities were used. They were heat treated to minimize change in permeability. With the correlation

obtained for determining effective viscosity, experimental and theoretical values were compared for each fluid system by determining average and maximum errors.

Gogarty concluded that his average shear rate relationship is more general than predicted by previous researchers and the rheological model developed fits data for fluids whose character changes rapidly with shear rate from Newtonian to non-Newtonian. At high velocity in a core the average shear rate becomes proportional to the frontal velocity raised to a fractional power, and the experimental relationship developed represents the power law equation for the flow of non-Newtonian fluids through porous media.

Pasini (57) has also examined the flow of polymer solutions through low permeability porous sandstone cores, containing low viscosity crude oil, in an effort to study the feasibility of a full scale polymer flood of the Spindletop field of West Virginia.

Two linear floods were conducted through two cores, prepared from low permeability (2.10 and 3.75 md) Cow Run sandstone of Spindletop field. They were approximately 21 centimeters long and 5 centimeters in diameter. Three plugs were placed end to end and mounted in steel pipe by filling the annular space with epoxy resin. Isopropyl alcohol was used to clean the cores, a low viscosity crude oil to saturate them, and two solutions of zero and 30 percent hydrolyzed polyacrylamide polymer to flood them.

The results of this experiment were presented in the form of oil recovered versus water cut, and cumulative volume of polymer solution injected versus apparent viscosity of the solution after breakthrough. Pasini's results indicated that the partially hydrolyzed polyacrylamide solution produced more oil than the ordinary water flood or the flood with unhydrolyzed polyacrylamide solution. The effect of polymer deposition on the inlet surface of the sand, on permeability of the sand and on concentration of polymer behind the flood is also discussed. The most significant aspect of his results was the fact that the polymer flooding was proven to be as applicable to low permeability porous rocks as to high ones.

Pye (62) conducted laboratory tests to develop a more efficient water-soluble polymer viscosity builder. He experienced a rather unusual phenomenon in flowing aqueous solutions of polyacrylamide through porous media. He reported that the apparent viscosities of the solutions calculated from D'Arcy's fluid flow equation were much higher than the viscosities determined from the Ostwald viscometer. This anamalously high apparent viscosity may be attributed to the use of brine permeabilities in place of the polymer solution permeabilities of the cores. There is considerable evidence (11,62,67) to indicate that some of the polymers will be adsorbed to the rock surfaces and decrease the permeability. For that reason it is very difficult to distinguish a reduced

permeability from an unusually high apparent viscosity. Pye reported that there was no plugging of the cores and no permanent reduction of the permeabilities.

For the study of areal sweep efficiency he used compressed glass wool as the porous media with colored water solutions of glycol of different viscosities adjusted to represent mobility ratios. His model consisted of a sandwich-like structure made of a steel plate on the bottom, a thin rubber sheet membrane, then a layer of 1/2 inch fiberglass insulation mat which was sealed on the edge with latex. A 3/4 inch plexiglas sheet top was bolted through the steel which compressed the mat to about 1/16 inch thick. The model was flooded through simulated wells drilled in the transparent sheet, and flood program was recorded with a time-lapse movie camera and a still camera. The results of these tests presented in the form of percent areal coverage versus water-oil ratio indicated sweep efficiencies of 40 and 85 percent for mobility ratios of 50 and 1 respectively at water-oil ratio of one.

Adsorption, rheology, transport and oil recovery efficiency of polymer solutions were the subject of a research performed by Mungan, Smith, and Thompson (53). They used Berea sandstone for displacement tests, Alundum cores and Bartlesville sandstone for mobility measurements, Berea sandstone, powdered silica and sintered glass discs for adsorption tests. Two different types of non-Newtonian

fluids used in this experiment were polyethylene oxide and polyacrylamide solutions.

They devised two methods to determine adsorption; a static technique in which polymer solution and adsorbent were equilibrated in stoppered Pyrex bottles and the decrease in the polymer concentration determined; and a dynamic technique in which a material balance on the polymer was calculated from known injected and produced concentrations during core displacement tests. Polymer solution concentrations were determined by viscosity measurement. To describe mobility changes caused by flow of the polymer through the porous medium, an arbitrary procedure was used. They started with polymer injection and later switched to water injection. Throughout the flood the mobility of injection fluid was calculated at numerous cumulative injections. These mobilities were then divided into the mobilities observed from the same cumulative injection of only brine in the same core during the control flood. The resulting ratios were called relative mobility and were plotted versus cumulative injection to describe the mobility reduction taking place as a polymer flood progresses and to show how the mobility is recovered when brine follows the polymer. Their rheological data were presented in the form of shear rate versus apparent relative viscosity, defined as the ratio of polymer viscosity to that of solvent viscosity. These curves showed typical shear rate dependence and pseudoplastic characteristics of the kind of polymer used in their experiment.

They concluded that the mobility of water can be decreased considerably by addition of polymer. The nature and extent of the mobility reduction depends on the particular polymer used. The reduction of water mobility by polymers is due in part to increase in solution viscosity and in part to core permeability reduction. Furthermore, for any polymer the mobility reduction depends on the NaCl content of water, the pH, the capillary properties of the rock, the crude oil and the shear rate. Polymer flooding will increase oil recovery by improving volumetric sweep efficiency. The increase in oil recovery would have to be sufficient to pay for the additional polymer expenses and also make a profit. Connate water always decreased the benefits which would have otherwise resulted from a certain reduction of mobility ratio.

Burcik (8) has also found results similar to those of Mungan and et al. (53) by flowing a solution of partially hydrolyzed polyacrylamide through a Berea sandstone disc approximately one inch in diameter and 1/8 inch thick under a constant pressure head. He concluded that the decrease in mobility is due to the presence of polymer particles within the pore openings. He flowed brine, polymer solution, and again brine through a sintered glass disc and noted that the final brine flow rate was substantially less than the original rate. He then flowed distilled water through the disc and the result was a nearly plugged core. When he flushed the distilled water with ethyl alcohol, mobility of

ethyl alcohol, after correction for viscosity, was identical to the initial brine mobility. He argued that the alcohol collapsed the acrylic polymer particles and, consequently, flow of alcohol was undisturbed. He then flushed the alcohol with distilled water and the result was again a nearly plugged core. This indicated the existence of polymer molecules within the pore openings.

Results of a number of laboratory and pilot flood tests of polymer solutions were reported by Sandiford (69). The polymer flood tests were run in linear and radial systems with different water soluble polymers and under varying conditions of flow, including reservoir conditions of temperature, pressure and fluid composition. The non-Newtonian fluids used in this research were two high molecular weight, partially hydrolyzed polyacrylamide polymer solutions specified only as Polymer A, and Polymer B.

For a series of linear flow tests his laboratory models consisted of unconsolidated sand packs, the length of which varied from 4 inches to 5 feet with 1 to 6-inch diameters. Using conventional procedures similar water and polymer floods were run on sand packs containing either refined or crude oil at restored state. The results of two different groups of runs presented in the form of oil recovered, percent of original oil in place, versus water-oil ratio showed that recoveries at water-oil ratio of ten were about 10-15 percent higher for the polymer floods than for

ordinary water floods of cores saturated with 62-cp refined oil. A similar test of a uniform sand pack saturated with a 2-cp refined oil resulted in the same oil recovery for the polymer flood as for the water flood. This was attributed to the fact that the water flood of the low viscosity oil in the linear, homogeneous sand pack was a very efficient displacement process. In fact, sixty six percent of the initial oil of the core was recovered at a producing water-oil ratio of 10, both with the ordinary water and with the polymer flood.

In another group of runs the porous medium was a consolidated oil reservoir core 2.5 in. long and 3.5 in. in diameter. The sides and ends of which were covered with epoxy resin; the injection and production wells were holes drilled parallel to the core axis. Again using conventional procedures, water and polymer flood were run on consolidated cores containing 62-cp refined oil. Recoveries in these series of tests were reported to be about 20 percent higher at a given producing water-oil ratio than recoveries in an ordinary water flood. In a similar group of tests using 2-cp refined oil resulted in a significant increase in oil recovery, in contrast to the linear flood involving 2-cp refined oil which showed no increase.

For his pilot flood experiment he conducted four field tests in which he injected slugs of water containing partially hydrolyzed polyacrylamide during a regular water

flood. The slugs were very small, 0.1 to 0.5 percent of the original stock-tank oil volumes, and polymer concentration was 0.37 percent. The result of one of the four tests, run on the West Coast Canyon field of Santa Barbara, California was included in this report. It was sufficiently encouraging to warrant a continued program of field testing on a larger scale. The conclusions reached by Sandiford included the following: Water mobility can be reduced and oil recovery increased by addition of certain polymer solutions to flood water. A seven-fold reduction in the mobility ratio, due to the presence of polymer, in many cases, is greater than would be expected from conventional viscosity measurements. A polymer flood would increase the recovery of low viscosity oil from a multidimensional system or non-homogeneous medium and would increase the recovery of high viscosity oil from any system or medium. When the sweep efficiency is poor, the polymer solutions have a good chance of increasing oil recovery. Since in most actual oil reservoirs the sweep efficiency is low enough that an improvement is desirable, it would appear that many reservoirs are candidates for polymer flooding.

Christopher and Middleman (14) have reported the results of a study performed on laminar flow of non-Newtonian fluids through packed and porous media. They used a "capillary model" to develop a modified Blake-Kozeny equation for use in the laminar flow of non-Newtonian power law fluids through porous media.

The packed beds were constructed of brass pipes with an inside diameter of 1.0 inch and lengths of 3, 5.375, and 10 inches. The particles used were superbrite glass beads with average diameters of 710 to 840 microns. The non-Newtonian fluid used was aqueous solutions of carbonxymethyl-cellulose (CMC Type 70, high molecular weight, Hercules Powder Company), and a toluene solution of polyisobutylene (PIB L100, Enjay Company).

They started with Blake-Kozeny equation for a laminar flow of a Newtonian fluid through porous media:

$$V = \frac{\phi^3 \, \Delta P \, D_p^2}{150(1 - \phi)^2 \, \mu L} \tag{2-12}$$

which was originally derived from D'Arcy's equation:

$$V_o = \frac{KA}{\mu} \frac{\Delta P}{L} \tag{2-13}$$

and a permeability expression:

$$K = \frac{\phi^3 \, D_p^2}{150(1 - \phi)^2} \tag{2-14}$$

where D_p is the mean particle diameter of the bed. Next they used Hagen-Poiseuille equation for laminar flow of a power law fluid through a capillary:

$$\bar{V} = \left(\frac{\Delta P}{2aL}\right)^{1/n} \left(\frac{n}{3n + 1}\right) D^{\left(1 + \frac{1}{n}\right)} \tag{2-15}$$

where a and n are defined by the relationship between shear stress and shear rate for a power law fluid, D the diameter of capillary, L the length, ΔP pressure drop, and $\bar{V}$ the average flow velocity.

Introducing the expression for hydraulic radius, $R_h = \frac{D_p}{6} \frac{\phi}{1 - \phi}$; $D = 4\ R_h$, superficial velocity, $V = \frac{V_o}{\phi}$, and replacing L by a tortousity factor, 25/12 L in Equation 2-15, the final result is the modified Blake-Kozeny equation:

$$V = \left(\frac{6\Delta P}{25aL}\right)^{1/n} \left(\frac{D_p \phi}{3(1 - \phi)}\right)^{1 + \frac{1}{n}} \left(\frac{n\phi}{1 + 3n}\right) \qquad (2\text{-}16)$$

Assuming the permeability of the porous medium is the same for all identical bed configurations, independent of flow conditions in the bed, and introducing the permeability Equation 2-14 into Equation 2-16, Equation 2-17 is written as:

$$V = \left(\frac{K}{F} \frac{\Delta P}{L}\right)^{\frac{1}{n}} \qquad (2\text{-}17)$$

where F is a factor which accounts for the additional dependence of V on K and ϕ due to non-Newtonian behavior and it is given by:

$$F = \frac{a}{12} \left(\frac{3}{n} + 9\right)^n (150\ K\ \phi)^{(1-n)/2} \qquad (2\text{-}18)$$

They have presented their results in the form of a Reynolds number versus friction factor relationship. The Reynolds

number was given by:

$$Re = \frac{D_R \, G^{(2-n)} \, \rho^{(n-1)}}{150(1 - \phi)F} \qquad (2\text{-}19)$$

and the friction factor as:

$$f = \frac{\Delta P \, D_p \, \phi^3 \, \rho}{LG^2(1 - \phi)} \qquad (2\text{-}20)$$

where G is the mass flow rate and is defined by:

$$G = V\rho \qquad (2\text{-}21)$$

They concluded that the power law can be used to represent the rheological behavior of their non-Newtonian fluids. Equation 2-17 can easily be used by measuring permeability, K, with a Newtonian fluid, measuring the porosity, ϕ, and determining the fluid rheological parameters a and n. The data obtained, using the modified Blake-Kozeny equation can be correlated with an average error of 18%, over a range of three orders of magnitude of the modified Reynolds number.

Clay (15) studied the possible use of various ionic polymers as conventional waterflood additives. In all of his tests, first, a 50,000 ppm brine solution was used as the displacing medium and afterward a polymer solution was used as the displacing medium. A total of four cores and four ionic polymers were investigated. Unsteady state flow

tests of conventional waterflood and a polymer flood were conducted through each of the four cores used. The results of a conventional waterflood and a polymer flood were compared by plotting graphs of the relative permeability ratio, cumulative oil produced, and mobility ratio.

He concluded that an increase in oil recovery at breakthrough resulted when the cores were flooded with NP-20 or AP-30 polymer solutions. This increase in recovery ranged from 7.60 to 10.76 percent of the original oil in place. The cumulative oil produced was greater when NP-20 or AP-30 polymer was added to the flood-water. The absolute permeability to water was reduced when polymer solution was flowed through the cores. The absolute permeability to oil was also reduced. However, the reduction in absolute permeability to water was greater than the reduction in absolute permeability to oil.

Clay noted that the addition of polymer to flood-water reduced the oil to water viscosity ratio which in turn resulted in less fingering of the displacing medium and a more piston-like displacement of the flood front. He attributed the increase in oil recovery and the reduction in permeability to water in the polymer floods to the thickening effect of the polymer additives.

Dauben and Menzie (19) examined the physical parameters involved in the flow of polymer solutions through porous media. Their porous matrix consisted of a stainless

steel flow cell packed with glass beads. The beads were made from high grade optical crown glass, soda lime type, and had a silica content of not less than sixty-eight percent. They were believed to be true spheres, essentially free of surface scoring and foreign matter, and ranged from 53 to 300 microns in diameter. They used aqueous solution of polyethylene oxide, manufactured by Union Carbide Corporation under the trade name of "polyox," the molecular weights of which ranged from 200,000 for "polyox" WSR-35 to over 5,000,000 for polyox coagulant.

The characterization of the polymer solutions used in their research was done with the means of a capillary viscometer and a parallel plate instrument designed similar to that of Tamura (79). They have concluded that the famous power law model described their polymer solution data quite well.

Their results are in apparent contradiction to those obtained by Sadowski (67) and Christopher (14). They found that the apparent viscosity of polymer solutions flowing through the porous media increased as the rate of flow increased. This anomalously high flow resistance of the solutions was attributed to interaction between the macromolecules and the walls of the flow channels, and the behavior of viscoelastic fluids in the inlet and exit region of a pore. The apparent viscosities of the solutions were also found to increase with increase in polymer molecular weight and

concentration, and decrease with increase in pore size. In contrast to most of the research reported with aqueous solutions of polymer, there was little indication of permeability reduction with polyethylene oxide solutions.

Harvey (33) was also concerned with the mechanism of flow of high molecular weight polymer solutions through porous media. He continued the research, initiated earlier by Dauben (18), to develop a more satisfactory theory to describe the flow of non-Newtonian polymers through packed beds and to investigate rheological properties of certain polymer solutions.

He modified the Ergun's friction factor equation for non-Newtonian fluids empirically to predict the flow of polyethylene oxide, polyacrylamide, and polysaccharide through unconsolidated porous media. Using a parallel plate viscometer he noted that none of the solutions of polyacrylamide, and polysaccharide tested for viscoelasticity, were found to be sufficiently viscoelastic to indicate that polymer floods using these solutions would develop a Deborah number high enough to cause significant viscoelastic flow resistance.

Harvey concluded that the polysaccharide Kelzan M solutions behave approximately in the manner predicted by the modified Ergun's correlation. He suggested that if this behavior persisted under reservoir conditions there would be less loss of polymer with polysaccharide Kelzan M than with

other polymers. He also suggested that the use of polymer solution in secondary recovery of oil might reduce oil recovery under unfavorable reservoir conditions. He based his argument on the fact that many of his polymer solutions did not pass through a rather coarse filter. He then argued that it is not hard to imagine a situation in which a low permeability lens of oil sand would be by-passed because the polymer solution could not enter the small pore spaces.

CHAPTER III

THEORETICAL CONSIDERATION

Polymer Solution Rheological Behavior and Mathematical Modeling

Rheology is "the science of deformation and flow of matter." A body is said to be deformed when an appropriate force system alters the shape or size of the body. A body is said to flow if its degree of deformation changes continually with time. The aim of rheology is prediction of the force system necessary to cause a given deformation or flow in a body, or conversely, prediction of the deformation or flow resulting from the application of a given force system to a body.

Fluid Behavior Classification

Fluids are generally classified according to their laminar flow characteristics. One of the most general and widely used classifications is as follows:

Group I - Newtonian

Group II - Non-Newtonian

(a) Time-independent fluids

1. Bingham plastic
2. Pseudoplastic
3. Dilatant

(b) Time-dependent fluids

1. Thixotropic
2. Rheopectic

(c) Viscoelastic fluids

Group III - Magnetic Fluids

Fluids for which shear rate depends on shear stress and intensity of an imposed magnetic field.

Group IV -

Fluids which must be considered as being made of discrete particles rather than as continuous media.

The rate of shear that any fluid undergoes when it flows between fixed boundaries is a function of the shear stress applied. In other words, the change of velocity with distance from the boundary is a function of the shearing force:

$$-\frac{du}{dy} = -\gamma = f(\tau) \qquad (3\text{-}1)$$

where u is the velocity, y is the distance from boundary, τ is shear stress, and $\frac{du}{dy} = \gamma$ is the velocity gradient or rate of shear.

Newton formulated the basic concept of viscosity when he proposed that the shear rate is directly proportional

to shear stress. Thus Equation 3-1 becomes:

$$\tau_{yx} = - \mu \frac{du}{dy} = - \mu \gamma \qquad (3\text{-}2)$$

where τ_{yx} is a shear stress acting in the x-direction on a surface normal to the y-direction, and the constant of proportionality, μ, is called the Newtonian viscosity. The Newtonian viscosity depends only on temperature and pressure and is independent of the rate of shear. All fluids obeying the Newtonian concept are known as Newtonian fluids. A diagram relating shear stress and shear rate for Newtonian fluids, known as "flow curve," is a straight line of slope μ and the single constant, μ, completely characterizes the fluid. Newtonian behavior is demonstrated by fluids in which the dissipation of viscous energy is due to the collision of comparatively small molecular species.

All the other fluids for which the flow curve is not linear through the origin at a given temperature and pressure are called non-Newtonian fluids. Non-Newtonian fluids may be time-independent, time-dependent, or viscoelastic.

Time-independent fluids are those for which the rate of shear at any point is some function of shearing stress at that point and nothing else. They may conveniently be devided into three types:

1. Bingham plastic-fluids which are characterized by a flow curve, Figure III-1, that is a straight line having an intercept τ_y on the shear-stress axis. The rheological equation for a Bingham plastic fluid may be written as:

$$\tau - \tau_y = - \mu_p \gamma \; ; \; \tau > \tau_y \qquad (3\text{-}3)$$

2. Pseudoplastic fluids which show no yield value and the typical flow curve for these materials indicates that the ratio of shear stress to the shear rate, which may be termed apparent viscosity decreases progressively with shear rate.

3. Dilatant fluids which are similar to pseudoplastic fluids in one respect that they show no yield stress but the apparent viscosity for these materials increases with increasing rate of shear.

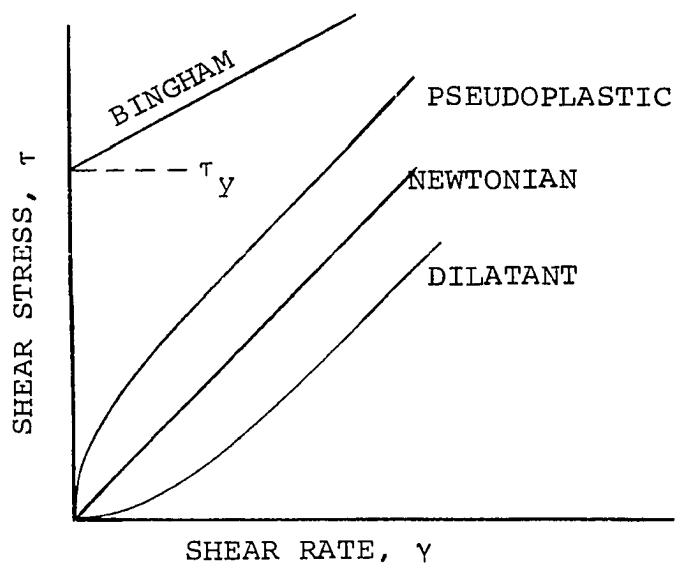

Figure III-1. A Typical Flow Curve for Various Types of Time-independent Non-Newtonian Fluids.

Typical flow curves for these three fluids are shown in Figure III-1 together with a linear relation typical of Newtonian fluids.

Time-dependent fluids: Fluids which undergo a reversible thickening or thinning with time when the imposed shear stress is held constant are called time-dependent. Fluids which thicken when at rest are called Thixotropic fluids. This thickening appears to be caused by the formation of weak bonds between suspended particles in the fluid. The rate of formation of these bonds is dependent on the number of unbonded linkages available at any time and is therefore comparable to a first order chemical reaction. When thixotropic fluids are sheared, the shearing breaks the bonds, thereby reducing the apparent viscosity of the fluid. For a constant rate of shear an equilibrium between bond breakage and bond formation will occur, in time, yielding a constant apparent viscosity. Some fluids become thicker when sheared at low rates but thin when at rest. These fluids are called rheopectic fluids.

Viscoelastic fluids: The term viscoelasticity is used to describe materials which are both viscous like liquids and elastic like solids. In steady laminar flow, the extent of elastic deformation of a viscoelastic fluid is constant because the shear stress does not vary with time. Viscoelasticity is therefore not observed in such cases. In unsteady flow, variations of shear stress with time cause

detectable change in the elastic deformation of these fluids. In turbulent flow, it is theorized that elastic energy is stored by molecular translations and later returned to the bulk fluid, thereby minimizing the ordinary conversion of turbulent energy to heat. Although the term viscoelasticity is becoming accepted in the industry, it is felt that such a term might be misleading, since the viscosity is primarily associated with the bulk fluid and the elasticity is more probably associated with specific molecular structures of dissolved molecules in the fluid.

A General Form of Newtonian Model

The basic laws governing the isothermal flow of fluids are the equations of change:

$$\frac{\partial \rho}{\partial t} = - (\nabla \cdot \rho u) \tag{3-4}$$

$$\rho \frac{Du}{Dt} = - \nabla P - (\nabla \cdot \bar{\bar{\tau}}) + \rho g \tag{3-5}$$

Equation 3-4 is the equation of continuity, which expresses the principle of conservation of matter and Equation 3-5 is the equation of motion, which expresses the principle of the conservation of momentum. These equations, ignoring electrical and magnetic effects, are valid for all fluids irrespective of their other properties. In order to take account of the nature of different fluids, one introduces a rheological equation of state, or constitutive equation,

which identifies the basic characteristics of the fluids. In particular, one must specify, in Equation 3-5, a relation between the viscous part of the momentum-flux tensor $\bar{\bar{\tau}}$ and the rate of deformation tensor $\bar{\bar{\gamma}}$. With the rheological equation of state and the equations of change a theory is constructed and found acceptable until such time as the phenomena predicted by the theory do not agree with the experimental results.

A very useful and practical constitution relation is that of the so-called generalized Newtonian fluid equation:

$$\tau_{ij} = - \mu \gamma_{ij} \tag{3-6}$$

where $\gamma_{ij} = \frac{\partial u_i}{\partial x_j} + \frac{\partial u_j}{\partial x_i}$, is the cartesian component of the rate of deformation tensor, $\bar{\bar{\gamma}}$, τ_{ij} is the cartesian component of the shearing stress tensor, $\bar{\bar{\tau}}$, and μ is the viscosity. The relation is analogous to Newton's law except that μ depends on all γ_{ij}. The relation is a simplified form of the Reiner-Rivlin-Pranger (61) relation:

$$\tau_{ij} = - \mu\gamma_{ij} - \mu_c \Sigma_k \gamma_{ik}\gamma_{kj} \tag{3-7}$$

where μ and the cross viscosity μ_c are, in general, functions of the scalar invariants of the $\bar{\bar{\gamma}}$ tensor:

$$I_1 = (\bar{\bar{\gamma}}:\bar{\delta}) = \Sigma_i \gamma_{ii} \tag{3-8}$$

$$I_2 = (\bar{\bar{\gamma}}:\bar{\bar{\gamma}}) = \Sigma_i \Sigma_j \gamma_{ij} \gamma_{ji} \tag{3-9}$$

$$I_3 = \det \bar{\bar{\gamma}} = \Sigma_i \Sigma_j \Sigma_k \epsilon_{ijk} \gamma_{1i} \gamma_{2j} \gamma_{3k} \qquad (3\text{-}10)$$

Equation 3-7 is the most general relation between $\bar{\bar{\tau}}$ and $\bar{\bar{\gamma}}$ which does not involve space or time derivation of either $\bar{\bar{\tau}}$ or $\bar{\bar{\gamma}}$. The exclusion of time effects restricts the relation to inelastic fluids. One other restriction on Equations 3-4, 3-5, and 3-7 is that the net entropy production rate must be negative.

The reduction of Equation 3-7 to 3-6 depends upon several assumptions. First, in all cases, the fluid will be considered to be incompressible. Here the first invariant I_1 is identically equal to zero. Second, the cross viscosity effects will be neglected, $\mu_c = 0$. There is little known about cross viscosity effects. Some investigators (61,63), assumed μ_c to be constant. Leigh (40), however, has shown that thermodynamic principles require that μ_c not be constant. Most investigators are content to ignore this function. Third, it will be assumed that there exists no functional dependence of the viscosity μ on the third invariant I_3. There is little known about the effect of I_3 on fluid flow. In simple flow geometries, such as flow through a tube or a slit, the third invarient is identically zero (3). In more complex geometries this is generally not true. For flow around spheres Slattery and Bird (75) show that, for an incompressible fluid, if the cross viscosity is zero, and if

$\bar{\bar{\tau}}$, as a function of $\bar{\bar{\gamma}}$, introduces a potential σ such that $\bar{\bar{\tau}} = \frac{\partial \sigma}{\partial \gamma}$ then $\mu = \mu(I_2)$ only. The fact that they are able to correlate data for flow of non-Newtonian fluids around sphere without the incorporation of I_3 leads them to suspect that its contribution is small. It is adequate, therefore, for many cases, to use the generalized Newtonian equation:

$$\tau_{ij} = - \mu(I_2)\gamma_{ij} \qquad (3\text{-}11)$$

which, in summary describes an inelastic incompressible fluid for which the effects of third invariant and a cross viscosity are ignored.

Rheological Models

A number of empirical equations of the form of Equation 3-11 have been presented in the literature. Any proposed rheological model should represent the actual behavior of fluid with convenience, accuracy, and simplicity. There is no known model to describe the behavior of all non-Newtonian fluids with a reasonable number of constants. Different models may be necessary to describe different fluids, or even the same fluid under different conditions. The best model for a given fluid is not necessarily known until an experiment is made on the fluid under the specific working condition to relate τ_{ij} and γ_{ij}. It is known however, that if the model is to be a reasonable approximation to reality, two conditions must be satisfied.

1. The viscosity should approach a constant value, μ_o, at very low shear stress.

2. The viscosity should approach a constant value, μ_∞, at very high shear stresses.

A fluid may be expected to exhibit a constant viscosity at the lowest flow rates which are generally encountered in the flow of very viscous fluids through porous media. The fulfillment of Condition 2 is not critical. The upper limiting viscosity, μ_∞, usually requires severe flow conditions which are not likely to be found in most flow systems.

One of the most familiar and widely used rheological model is the power law (Ostwald-de-Waele) model. This relation, which was originally proposed by Ostwald may be written as:

$$\tau_{yx} = - k\gamma^n \qquad (3\text{-}12)$$

where k and n are fluid parameters determinable from viscometric measurements: k is a measure of consistency of the fluid, the higher the value of k the more viscous the fluid; n is a measure of the degree of non-Newtonian behavior, and the greater the departure from unity the more pronounced are the non-Newtonian properties of the fluid. This model does not describe either the lower limiting viscosity, μ_o, or the upper limiting viscosity, μ_∞. It is important to note that although n is nearly constant in many cases over wide

ranges of shear stress-shear rate it is not a true constant for real fluid over all possible ranges of shear. This is not a serious problem in engineering applications because all that is needed is a rheological equation which describes the fluid over the particular range of shear rate encountered in the particular problem. Over such a range, n may often be regarded as constant. It should also be noted that the dimensions of k depends on the index n and this fact has led to many objections to the use of the power law model. Nevertheless, the model generally gives an adequate description of fluid behavior over an intermediate range of shear rates. More important, other empirical models are extensions of the power law model.

A very simple extension of the power law model is the three constant Sisko (71) model:

$$\tau_{yx} = - a\gamma - b\gamma^{n} \qquad (3\text{-}13)$$

where a, b and n are fluid parameters. The model has been primarily used to describe the flow of lubricating greases. Although this model describes the flow behavior of this system more adequately than does the power law model, it does not describe the lower limiting viscosity, μ_o, whereas $n < 1$, an upper limiting viscosity, a, is described.

Ellis (73) and more recently Gee and Lyon (27) proposed another extension of the power law model, similar in

form to the Sisko model:

$$\tau_{yx} = - \frac{1}{A_o + A_1 \tau_{yx}^{n-1}} \gamma \qquad (3\text{-}14)$$

$$\gamma = - \left(A_o + A_1 \tau_{yx}^{n-1} \right) \tau_{yx} \qquad (3\text{-}15)$$

where A_o, A_1, and n are the fluid parameters. The Ellis model does not describe an upper limiting viscosity, μ_∞, but it does describe the lower limiting viscosity $\mu_o = \frac{1}{A_o}$.

A modified form of the Ellis model has been proposed by Bird (4):

$$\gamma = - \frac{1}{\mu_o} \left[1 + \left(\frac{\tau_{yx}}{\tau_{1/2}} \right)^{n-1} \right] \tau_{yx} \qquad (3\text{-}16)$$

where n and μ_o and $\tau_{1/2}$ are the fluid parameters. The shear stress $\tau_{1/2}$ is that value of shear stress for which the corresponding non-Newtonian viscosity has dropped off to one-half of the value of the lower limiting viscosity, μ_o. Bird introduced the fluid parameter $\tau_{1/2}$ as a result of Meter's success in correlating turbulent tube flow data with this parameter. Also, the form of Equation 3-16 eliminates the dimensionality objection to Equation 3-15.

Another three-parameter model which does describe both the lower and upper limiting viscosity is the Powell-Eyring (60) model:

$$\tau_{yx} = - \left[a\,\gamma + \frac{1}{b}\,\mathrm{Sinh}^{-1}\left(\frac{1}{c}\gamma\right)\right] \qquad (3\text{-}17)$$

where a, b, and c are the fluid parameters. Whereas the other models are little more than curve fits, Eyring (22) from the theory of rate process, attempted to develop a rheological model which considers the molecular structure of matter. Ree and Eyring (64) discuss several successful applications of Equation 3-17 to polymeric and colloidal systems.

Meter (46) proposed a four-constant generalized form of the Ellis model in which there is both a lower limiting and upper limiting viscosity:

$$\tau_{yx} = - \left[\mu_\infty + \frac{\mu_o - \mu_\infty}{1 + \left(\frac{\tau_{yx}}{\tau_m}\right)^m} \right] \gamma \qquad (3\text{-}18)$$

where m, μ_o, μ_∞ and τ_m are the fluid parameters. The meter model reduces to the Reiner-Philippoff (66) model for m = 2:

$$\tau_{yx} = - \left[\mu_\infty + \frac{\mu_o - \mu_\infty}{1 + \left(\tau_{yx}/\tau_m\right)^2} \right] \gamma \qquad (3\text{-}19)$$

The constant τ_m is the value of the shear stress for which the corresponding non-Newtonian viscosity has dropped off to the arithmetic mean of the limiting viscosities. Meter

has successfully used this model to describe the turbulent flow through tubes of several hydroxyethylcellulose solutions.

Meter has also modified the Bird model to come up with:

$$\gamma = -\frac{1}{\mu_o}\left[\frac{1 + \left(\tau_{yx}/\tau_m\right)^{n-1}}{1 + \left(\tau_{yx}/\tau_m\right)^{n-1}\left(\frac{\mu_\infty}{\mu_o}\right)}\right] \qquad (3\text{-}20)$$

where, according to Meter's notation, $n = m + 1$. Sadowski (68) has shown that for many of his solutions, μ_∞ is at least an order of magnitude smaller than μ_o. So he proposed that the Equation 3-20 be rewritten as: (3-21)

$$\gamma = -\frac{1}{\mu_o}\left\{\left[1 + \left(\frac{\tau_{yx}}{\tau_m}\right)^{n-1}\right]\left[\sum_{i=0}^{\infty}\left(1 - \frac{\mu_\infty}{\mu_o}\left(\frac{\tau_{yx}}{\tau_m}\right)^{n-1}\right)^i\right]\right\}\tau_{yx}$$

He then suggested that the Meter model in this form may be considered to be the Ellis model with a small perturbation on it. It is important to note that for the limit in which $\tau_{1/2}$, or τ_m, approaches infinity, Equations 3-16, 3-18, 3-20 and 3-21 reduce to Newton's law.

For steady-state laminar behavior in simple flow systems, the power law model appears to be the simplest and most generally useful two-constant empirical model of the generalized Newtonian model. This model will be used, for

the most part, to examine the rheological characteristics of the polymer solutions studied in this project.

CHAPTER IV

EXPERIMENTAL APPARATUS AND MATERIALS

The accurate measurement of fluid properties is the essential prerequisite to progress in the development of engineering design procedure. It has been seen that at least two experimental measurements must be made on any non-Newtonian fluid in order to define its rheological properties whereas a Newtonian fluid requires only one measurement, namely the viscosity.

Although many types of viscometers are avialable, most of them are quite unsuitable for collecting scientific or engineering data. This is because various features of their construction make it impossible to determine both shear stress and rate of shear at the same known point in the equipment. The flow curve therefore can not be constructed from data obtained with such devices. Most of these instruments give readings which are complex functions of several fluid properties. They are consequently of some use for production quality control purposes, inasmuch as a change in reading denotes variation of some property of

the product from a standardized level. However, for the study of the flow mechanism undertaken in this work, they would not be adequate. In the next section the principles determining the performances of a cone and plate viscometer used to obtain rheological data of this investigation will be discussed.

Cone and Plate Viscometer

The cone and plate viscometer, which is shown in Figure IV-1, consists of a flat plate and a rotating cone with a very obtuse angle. The apex of the cone just touches the plate surface and the fluid fills the narrow gap formed by the cone and plate. Temperature control is usually applied to the lower plate. If the axis of the nearly flat conical surface is perpendicular to a flat plate with the cone's apex lying in the plane of the plate, and if either the cone or the plate is rotated with respect to the other about the axis, fluid in the space between the two will be subjected to a uniform shear rate. This, except for small edge effects, follows from the fact that the rate of movement of any point on either surface is proportional to its distance from the axis and the separation of the surfaces at that point is equivalently proportional to the same radius. The ratio of the rate of movement of the surface (at any point) to the distance of separation is fixed for any speed of rotation, and constant over the entire surface. Since rate of shear is by definition this ratio, it is therefore constant.

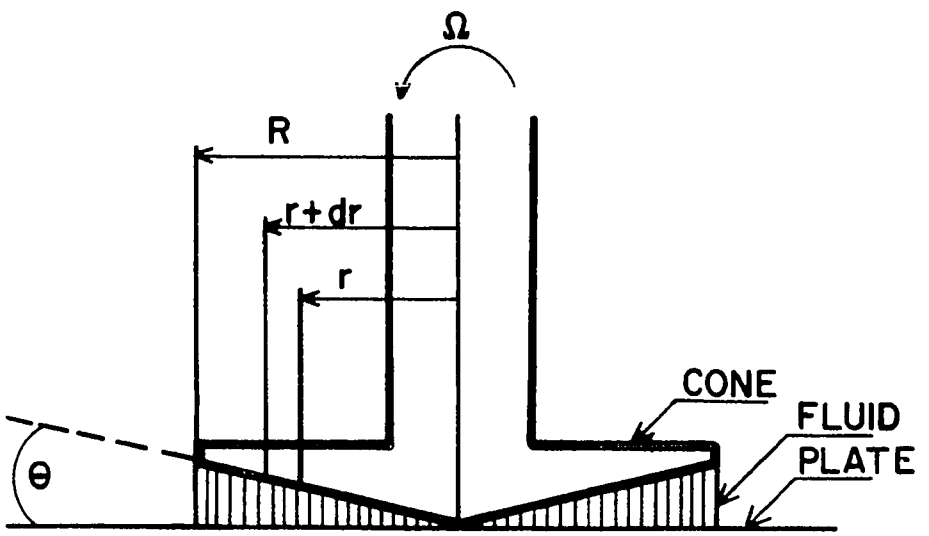

Figure IV-1. Schematic Diagram of the Cone and Plate Viscometer.

When the angle θ is very small, and the average gap width is correspondingly small, the whole sample will be subjected to a constant rate of shear and the end effects will be negligible. This simplifies the analysis of the non-Newtonian fluids data, because it gives the apparent viscosity as a function of shear rate directly. By using small angles between cone and plate, substantial rates of shear and hence shearing stress, can also be achieved with comparatively low rotational speed, low viscosity and small samples.

When the cone rotates at a constant speed Ω rpm, the linear velocity at radius r is $2\pi r\Omega$ and the gap width at radius r is r (tan θ). Hence the rate of shear at radius r is given by:

$$\frac{du}{dr} = \frac{2\pi r\Omega}{r \tan\theta} = \frac{2\pi\Omega}{\tan\theta} \qquad (4\text{-}1)$$

If θ is very small, $\tan\theta = \theta$, the magnitude of the shear rate can be estimated by $\frac{2\pi\Omega}{\theta}$. Equation 4-1 indicates that the rate of shear is constant over the range $0 \leq r \leq R$ so that shear stress must also be constant over this range.

Skelland (73) suggests that a relationship between the measured torque T and shear stress can be written as follows:

$$dT = (2\pi r dr)\tau r = 2\pi\tau r^2 dr \qquad (4\text{-}2)$$

Integrating Equation 4-2 from 0 to R

$$T = 2\pi \tau \int_0^R r^2 dr \qquad (4\text{-}3,$$

$$T = \frac{2}{3} \pi R^3 \tau \qquad (4\text{-}4)$$

then

$$\tau = \frac{3T}{2\pi R^3} \qquad (4\text{-}5)$$

The cone and plate viscometer, shown in Figure IV-2, is an eight speed, 0.3, 0.6, 1.5, 3.0, 6.0, 12.0, 30, 60 rpm, Wells-Brookfield Micro viscometer model LVT, with a model A laboratory stand, a type N constant temperature bath, and an immersion syrings assembly. The viscometer has a cone 2.4 cm in radius, with an angle of 1.57 degrees and a full scale torque of 673.7 dyne-cm.

A well insulated jacket (see Figure IV-3) built around the plate accommodates circulation of the bath liquid around the plate, keeping the sample temperature the same as that of the bath at all times and preventing increase in the temperature of the sample resulting from shearing.

The magnitude of the shear rate is precalculated by the manufacturer and is given in a range versus speed chart, the shear stress is calculated from Equation 4-5. The apparent viscosities of non-Newtonian fluids are calculated by simply dividing the shear stress by the corresponding rate of shear.

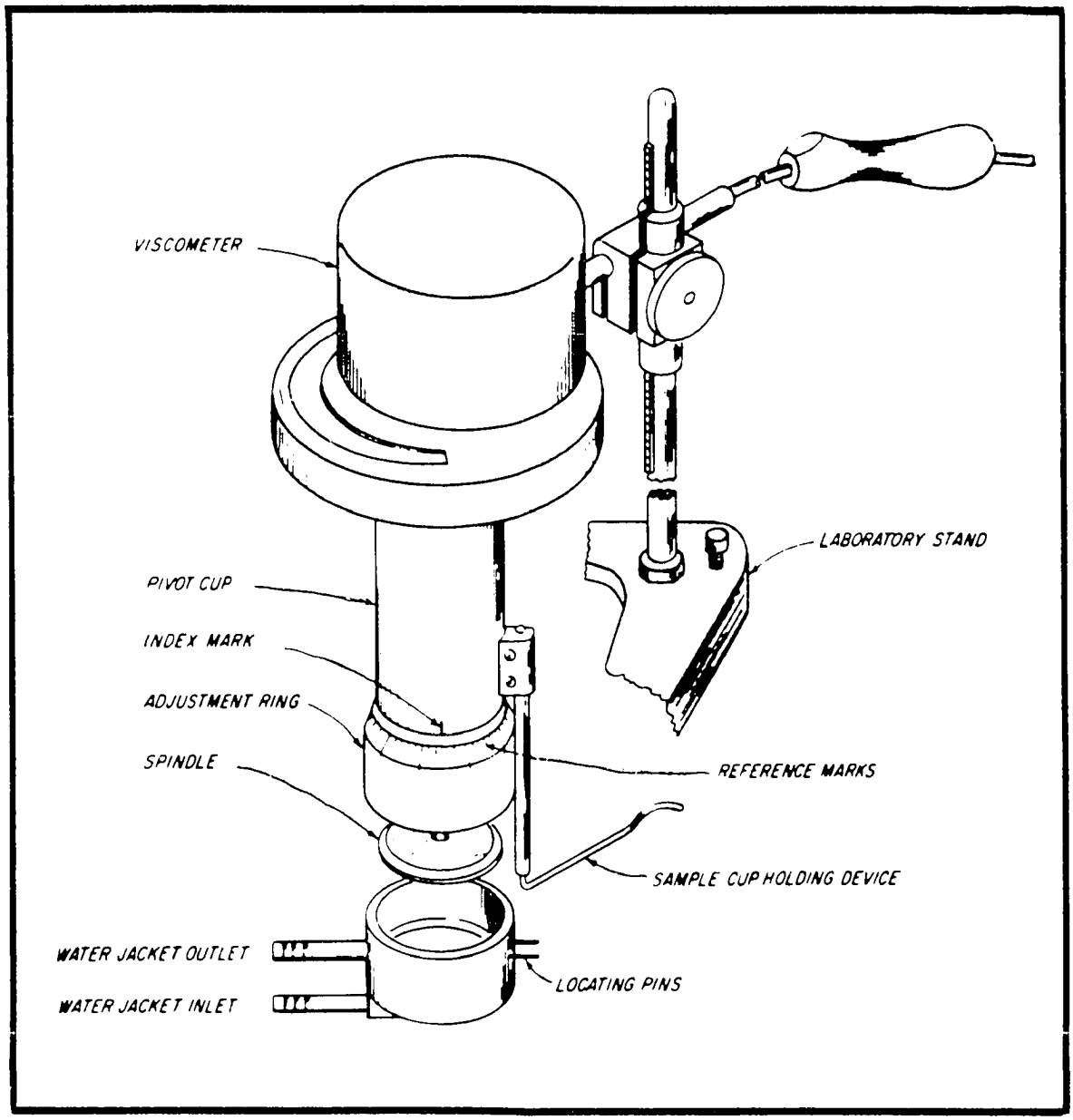

Figure IV-2. Wells-Brookfield Micro Viscometer (courtesy of Brookfield Laboratories Inc.).

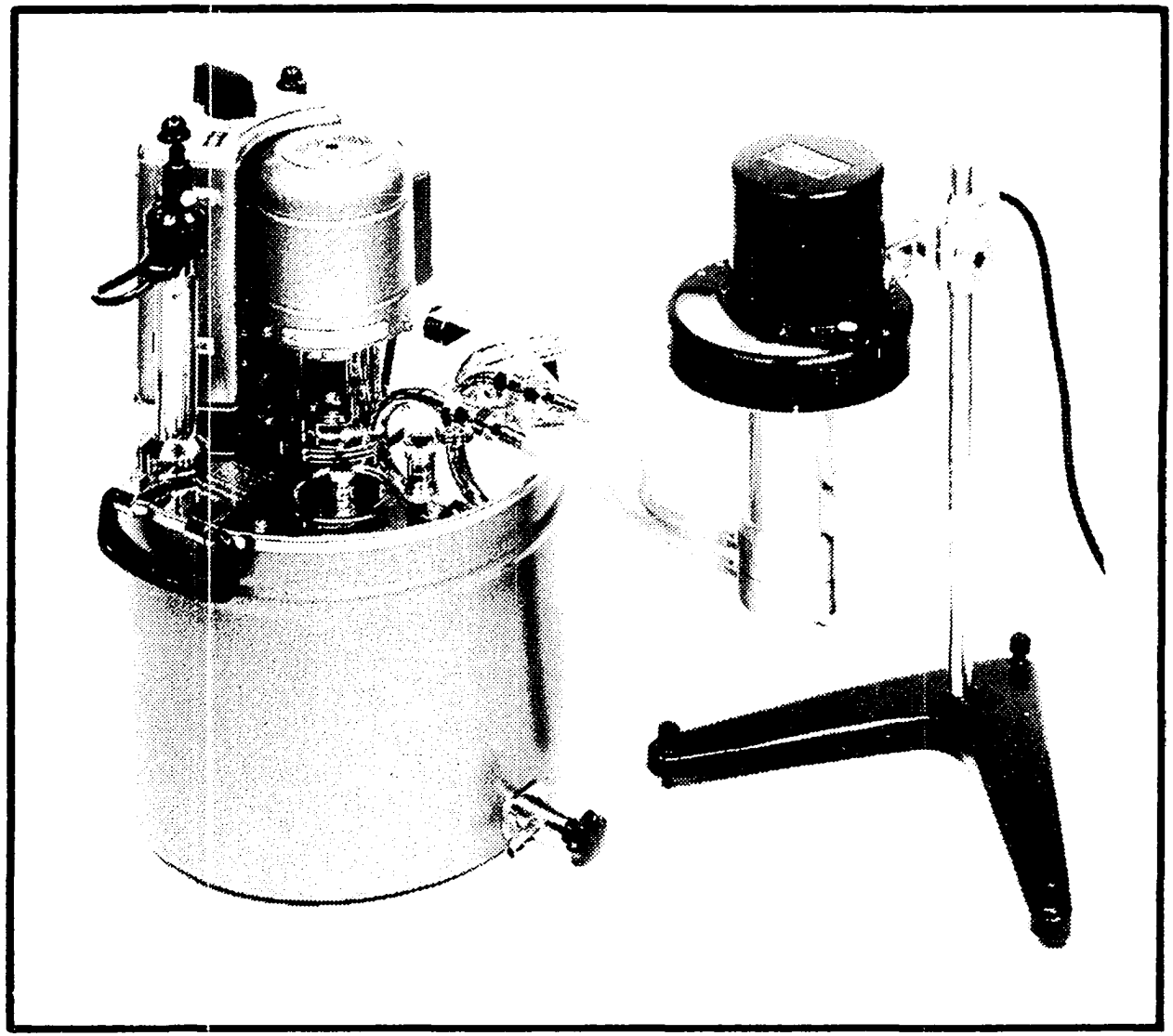

Figure IV-3. Model N Constant Temperature Bath with Wells-Brookfield Micro Viscometer (courtesy of Brookfield Laboratories, Inc.).

Pressure Measuring Devices

A pressure transducer, two master test pressure gauges, and a mercury manometer were used to record the pressure differential across the system.

The pressure transducer used in this investigation is a Model KP15 diaphragm type pressure transducer manufactured by Pace Wiancko Corporation of California. The diaphragm-type variable-reluctance pressure transducer is shown in simplified form in Figure IV-4. A diaphragm of magnetically-permeable material, supported between two symmetrical E core inductance assemblies, completes a magnetic circuit with each E core. The diaphragm reflects when there is a difference in pressure between the input lines. This increases the gap in the magnetic flux path of one core, and decreases the gap equally in the other.

The magnetic inductance varies with the gap, determining the inductance value, so that the overall effect of diaphragm motion is a change in inductance of two coils, (C_1 and C_2). The inductance ratio C_1/C_2 is conveniently measured in a bridge circuit, shown in Figure IV-5, which produces an output voltage proportional to the pressure difference. Two legs of the bridge are formed by the two E core coils (C_1 and C_2), the other two by resistances R_1 and R_2. The bridge is driven by an AC source.

The model KP15 provides multi-range capability with use of interchangeable diaphragms, (±1, ±5, ±25, ±100, ±500

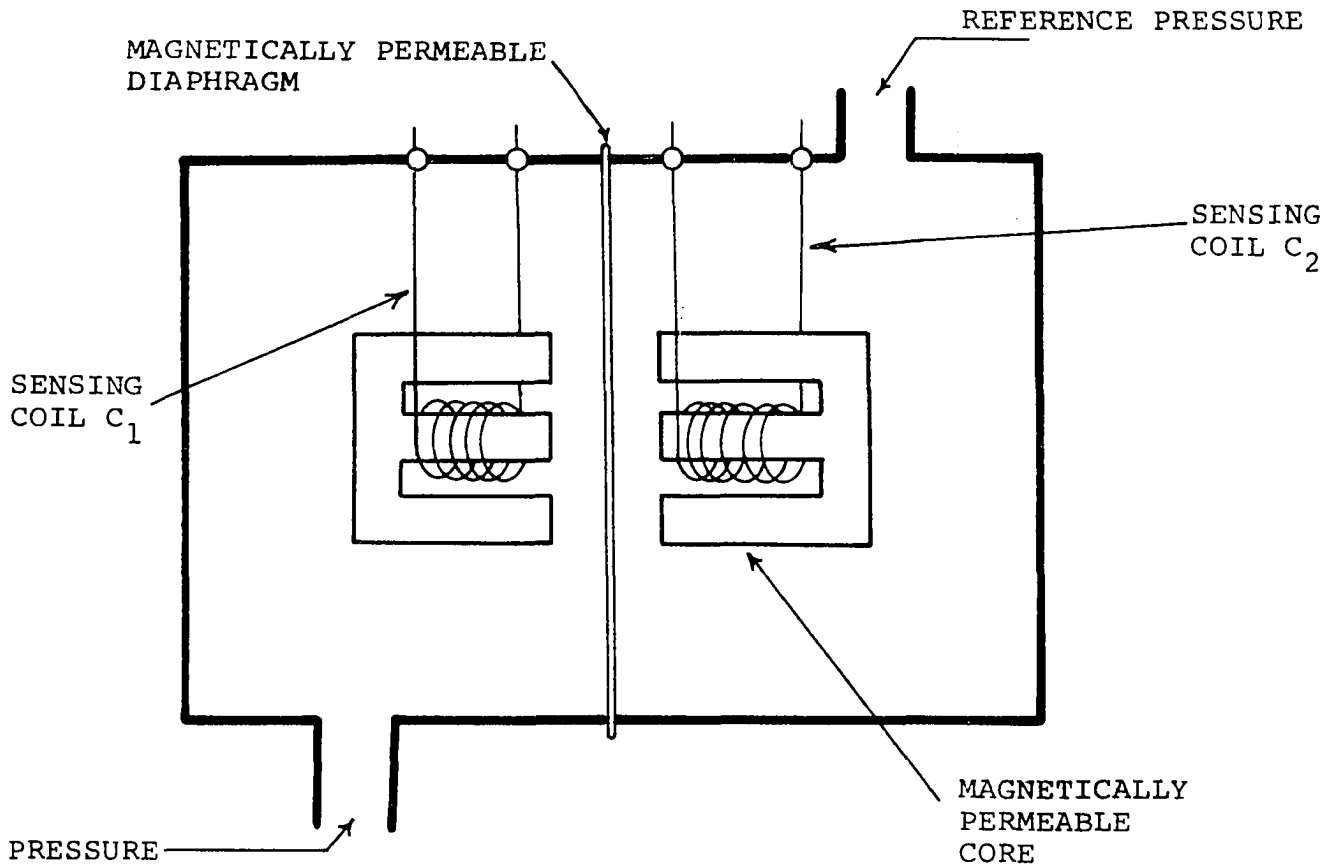

Figure IV-4. Schematic Diagram of the Diaphragm-Type Variable-Reluctance Pressure Transducer.

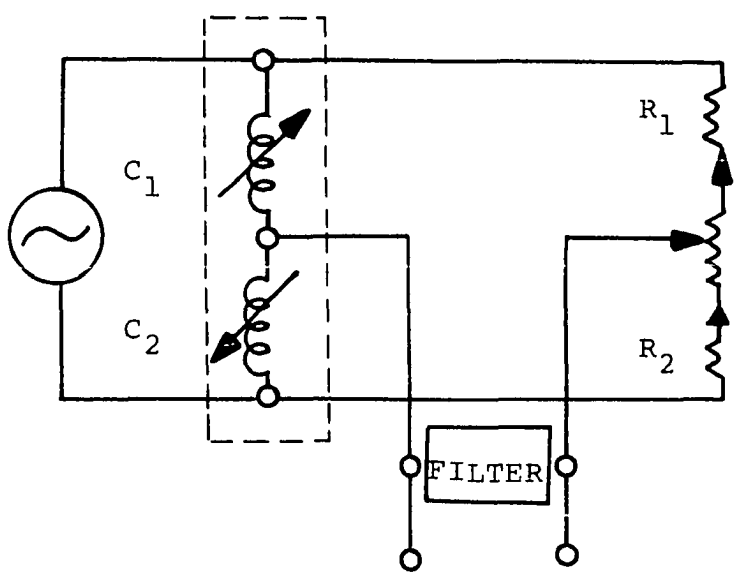

Figure IV-5. Schematic Diagram of the Bridge Circuit for Converting Coil Inductance Ratio to DC Output Voltage.

psi, gauge or differential). Stainless steel construction allows exposure to corrosive liquid and gases, both sides, for differential pressure measurements. It offers an accuracy of one percent of the reading over the range of 1-500 psi; it operates over an ambient temperature range of -65°F to 250°F at line pressure of up to 2,000 psi.

A model CD25 transducer indicator is also manufactured by the same corporation, which operates with the pressure transducer to provide a direct reading measurement system. The reading appears as a 5" meter indication with ±1 percent full scale accuracy or as a digit dial reading.

Two pressure gauges with maximum pressure readings of 600 and 1000 psi (manufactured by Marsh Instrument Company) were placed very close to the pressure transducer line to check the accuracy of the transducer at high pressure readings.

The mercury manometer was used in place of the pressure gauges to check the accuracy of the transducer at very low pressure readings. Expect for routine cleaning of the lines and the transducer diaphragm at the beginning of each series of runs the transducer performed very smoothly and with maximum accuracy. It should be also noted that a calibration check of the transducer was performed at the start of each series to prevent inaccuracy resulting from zero shift and drifting of the transducer indicator.

Preparation of Polymer Solutions

Fourteen different polymers, manufactured by five chemical companies, were used in this research. Their grade, type, and approximate molecular weight are given in the following table.

TABLE IV-1

SUMMARY OF THE WATER SOLUBLE POLYMERS USED

Polymer Grade	Polymer Type	Approximate Molecular Weight
Dow "Separan" NP-10	Polyacrylamide	1,000,000
Dow "Separan" NP-20	Polyacrylamide	3,100,000
Dow "Separan" AP-30	Polyacrylamide	3,500,000
Dow "Pusher" 700	Polyacrylamide	4-6,000,000
Union Carbide "Polyox" WSR-35	Polyethylene Oxide	200,000
Union Carbide "Polyox" WSR-205	Polyethylene Oxide	600,000
Union Carbide "Polyox" WSR-301	Polyethylene Oxide	4,000,000
Hercules "Reten" A-1	Polyacrylamide	- -
Hercules "Reten" A-5	Polyacrylamide	- -
Cyanamid RC-300	Polyacrylamide	5-7,000,000
Cyanamid RC-301	Polyacrylamide	10,000,000
Cyanamid RC-319	Polyacrylamide	4-6,000,000
Cyanamid RC-322	Polyacrylamide	14,000,000
Kelco "Kelzan" M	Polysaccharide	- -

The preparation of polymer solutions requires special attention. All polymer solutions were prepared carefully with the minimum degree of agitation to avoid mechanical degradation of the long chained polymer molecules. Sodium chloride was added to the distilled water to achieve the desired salt concentration of the solvent. Dry polymer

granules were initially wetted by the solvent and agitated by hand and allowed to set for about 30 minutes, after which they were mixed with the rest of the solvent. This method proved to be very efficient in obtaining the complete dispersion of the polymers. The solutions were then allowed to set for at least three days before the tests. It is believed that this period of three days is enough for complete mixing of the polymers. It was also noted that whenever the polymers were not completely dispersed in the solvent, a longer period of time was required for the polymer to dissolve. Some of the solutions were protected from auto-oxidation with addition of isopropanol and others with a very low concentration of formaldehyde.

Core Preparation

Sandstone cores used for the fluid flow displacement part of this research were Berea and Torpedo sands furnished by Cleveland Quarries Company of Ohio and U. S. Bureau of Mines respectively. (See Table IV-2 for detailed physical properties of the cores.) The cores were taped at both ends with regular masking tape, and painted with an epoxy base paint (manufactured by Zynalyte Products Company of California). A period of twelve hours was allowed for the paint to dry and seal after which the cores were placed inside two inch diameter extra heavy duty steel nipples, with the same length as the cores, vertically, and the empty space between

TABLE IV-2

SUMMARY OF PHYSICAL PROPERTIES OF POROUS MEDIA

Core No.	Type of Sandstone	Length (cm)	Diameter (cm)	Pore Volume (cm^3)	Porosity (% of Total Vol.)	Permeability (md)
1	Torpedo	8.676	3.710	21.272	22.7	618
2	Torpedo	8.390	3.703	23.160	25.6	276
3	Torpedo	8.490	3.706	21.272	23.2	824
4	Torpedo	8.110	3.713	21.272	24.2	244
5	Torpedo	8.873	3.717	24.055	25.0	656
6	Torpedo	8.790	3.710	24.751	26.0	112
7	Torpedo	8.893	3.710	21.569	22.4	595
8	Torpedo	8.036	3.706	21.570	24.9	560
9	Torpedo	8.190	3.773	15.805	17.3	891
10	Torpedo	9.000	3.703	25.953	26.8	349
11	Torpedo	8.900	3.696	18.588	19.5	256
12	Torpedo	9.006	3.548	15.320	17.2	286
13	Torpedo	8.870	3.780	19.383	19.6	246
14	Berea	8.800	3.700	18.706	19.8	658
15	Berea	8.780	3.776	18.507	18.8	416
16	Berea	8.953	3.673	22.763	24.0	534
17	Berea	8.803	3.803	21.492	21.5	534
18	Berea	8.840	3.796	19.999	19.9	516
19	Berea	8.890	3.806	19.004	18.8	439
20	Berea	8.900	3.773	19.203	19.3	640
21	Berea	5.051	3.653	6.268	11.8	247
22	Berea	5.060	3.680	7.860	14.6	309

the cores and the nipples were filled with a mixture of resins (50 percent Vesamid 140 "Polyamide" and 50 percent Genepox 190 "Epoxy") manufactured by the Chemical Division of General Mills of Illinois. A period of seven days was allowed for the resins to harden. The cores were then left in the oven and the oven temperature was slowly increased to 500°F and maintained at this temperature for 72 hours. These heat-treating processes were designed to further harden the epoxy resins, to stabilize clay content of the cores, and to prevent any plugging of the pores.

In order to determine permeability and porosity of the cores, a water permeability was run on each core after casting and heat-treating, and the core porosities were calculated by weighing the cores before and after saturation with a two percent NaCl solution. These values were then tested against the porosities determined by the Barne's Method, on small samples of the same cores. The two values were closely matched within one and one-half percent deviation.

Core Assembly

The core assembly consisted of the core encased in a two inch diameter, heavy duty pipe nipple and two heavy duty pipe caps. A quarter of an inch diameter hole was drilled in the center of each cap to accommodate the flow of fluids through the core. Two pressure taps were placed in the inlet and outlet lines, as close to the core as

possible, to insure the accurate measurement of pressure differential across the core. The pressure taps were then fed to the Variac pressure transducer (see Figure IV-6).

Fluid Reservoirs

The two fluid reservoirs used in this project were an open top five gallon tin tank and a relatively high pressure two gallon converted nitrogen tank with a high pressure liquid level indicator to indicate the liquid level at all times. The working pressure of the tank was specified at 1800 psi.

Pumping Equipment

Pumping equipment used included a one-quarter horsepower, General Electric vacuum pump to evacuate the cores at the beginning of each run, a 1500 rpm Cole-Palmer constant rate positive displacement pump to transfer the liquid from the open top reservoir to the high pressure tank, and a one-quarter horsepower, Wagner Electric Corporation positive displacement pump, equipped with a zero-max gear reducer and a Graham transmission to maintain a constant rate of flow through the cores for the low pressure oil displacement runs. This pump is capable of pumping fluids at a constant rate over a wide range of flow rate. One of the more important features of the pump is that it can operate at extremely low rates, about 1 cc/60 minutes. The rate of flow can be controlled by both the zero-max gear reducer and the transmission.

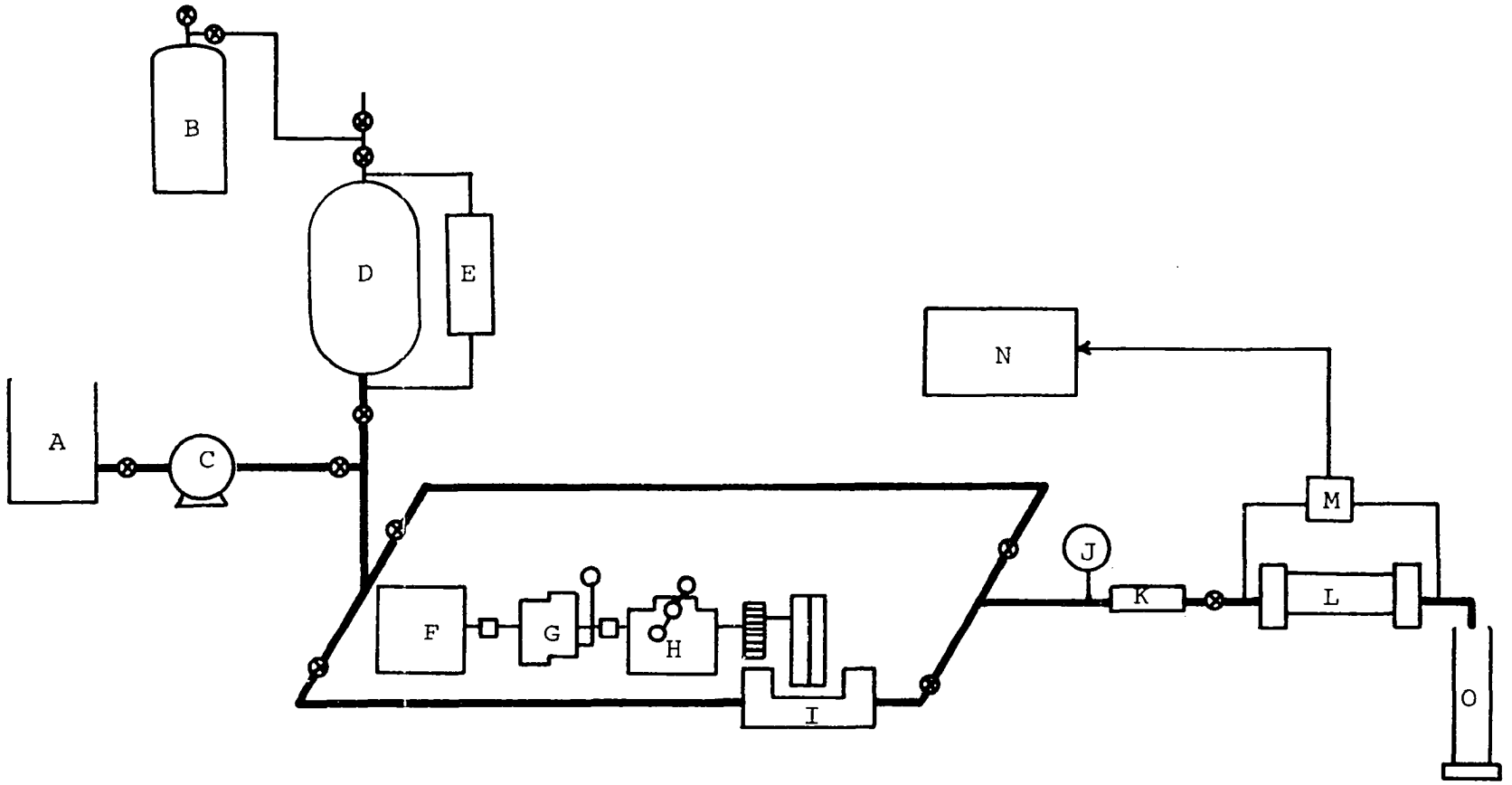

A. FLUID TANK
B. NITROGEN SOURCE
C. DISPLACEMENT PUMP
D. HIGH PRESSURE TANK
E. FLUID INDICATOR
F. 1/4 HP MOTOR
G. ZERO-MAX GEAR
H. TRANSMISSION
I. ZENITH PUMP
J. PRESSURE GAUGE
K. FILTER CELL
L. CORE
M. PRESSURE TRANSDUCER
N. TRANSDUCER INDICATOR
O. GRADUATED CYLINDER

Figure IV-6. Schematic Diagram of the Apparatus for Flow of Fluids Through Porous Media.

Valves, Flow Lines, and Filter

All valves were 1/4 inch steel valves with a maximum working pressure of 3000 psi. All flow lines were 1/4 inch heavy duty black steel pipe, and the filter was a 5 inch length by 1 inch in diameter stainless steel cell filed with a very fine glass wool (manufactured by W. H. Curtin and Company) and placed immediately before the core assembly.

Pressure Supply

The pressure source was a dry nitrogen bottle with a maximum pressure of 2500 psi equipped with a 3000 psi pressure regulator connected to the high pressure reservoir through a one-eighth inch diameter stainless steel tube.

CHAPTER V

EXPERIMENTAL PROCEDURE

All experimental runs were performed in a room in which the temperature was thermostatically controlled. The temperature was set at 75 $\pm$ 0.5°F and maintained there at all times. A schematic diagram of the apparatus, used for the flow of fluids through porous media is given in Figure IV-6.

Rheological Measurements

All rheological data were obtained with the cone and plate viscometer, "Wells-Brookfield Micro Viscometer" previously described in Chapter IV.

After calibrating the viscometer, the cup was removed, 1.0 to 1.5 cc of polymer solution was inserted, the cup was replaced and relocked, and the water circulation through the jacket was started. The water temperature was maintained at the same temperature as that of the room to assure the thermal stabilization of the solutions, and to prevent the temperature rise, resulting from shearing. At this point the sample was ready for rheological observation (shear stress-shear rate

measurements). Throughout this research readings were obtained over all the available speed ranges (0.30, 0.60, 1.50, 3.0, 6.0, 12.0, 30.0, 60.0 rpm) in descending order. At each level of speed enough time was allowed for the viscometer to stabilize after which the corresponding viscometer reading was recorded. For some of the samples the above procedure was reversed to check for the hysteresis effect and the repeatability of the data.

Using the viscometer reading, the shear stress, τ, was computed from Equation 5-1:

$$\tau = \frac{3T}{2\pi R^3} \tag{5-1}$$

Shear rate, γ, from Equation 5-2:

$$\gamma = \frac{2\pi\Omega}{\tan\theta} \tag{5-2}$$

and viscosity, μ, from Equation 5-3:

$$\mu = \frac{\tau 100}{\gamma} \tag{5-3}$$

where μ = viscosity, cps

τ = shear stress, dynes/cm^2

γ = shear rate, sec^{-1}

T = viscometer dial reading, percent full scale torque (full scale torque = 673.7 dynes-cm)

R = spindle radius, 2.40 cm (standard)

Ω = instrument speed, rpm

θ = cone angle, 1.57° (standard)

To study the effect of temperature on rheological behavior of polymer solutions, the desired temperature was set by means of a rotary magnet on the constant temperature bath. The bath liquid was allowed to circulate through the jacket. Enough time was allowed for the liquid temperature and the viscometer temperature to stabilize, after which a complete set of readings was recorded.

Fluid Flow Study

Having the cores encased and their permeabilities and porosities determined in the manner described earlier in Chapter IV, the cores were now ready for the fluid flow experiments. Two different types of tests were made, tests to study the polymer solutions behavior in consolidated porous media, and oil displacement tests to study and compare the effect of polymer-flood to that of the conventional water-flood.

1. Flow of polymer solutions:

In these series of tests, after assembling the core, the core was first evacuated for at least 30 minutes after which the upstream valve to the core was opened and a two percent NaCl brine allowed to flow through the core. The vacuum pump continued to run until core was completely saturated and brine came over into the trap on the vacuum line. The vacuum pump was then disconnected and pressure was applied to the pressure tank to force the brine through

the core. The pressure was allowed to stabilize and a few pore volumes of brine were allowed to pass through the core until a constant efflux rate was reached at which time the efflux rate and the pressure drop across the core were recorded. After recording the readings, the tank pressure was lowered, enough time was allowed for the pressure and the flow rate to stabilize and again the pressure drop and efflux rate were recorded. This procedure was continued until sufficient pressure drop-flow rate data were obtained.

After completion of the brine injection run pressure was removed, the brine contained in the pressure tank and the lines was completely drained and the tank was refilled with polymer solution. Again after evacuating the core for at least 30 minutes, this time, polymer solution was allowed to flow through the core and the same procedure as for brine injection was followed until adequate data were obtained.

It should be pointed out that in this part of the experiment, extra care was taken to make sure that a complete polymer flow rate and pressure drop stabilization has occurred, at each pressure step. For that reason a longer period of time was necessary for pressure drop-efflux rate to stabilize for polymer injection than that of brine injection process.

2. Oil displacement tests:

For oil displacement tests the cores were assembled as before and then a new method was used to study the oil

displacement processes. This method consisted of first saturating the core with a two percent NaCl solution, pumping the desired oil through the brine-saturated core until no more brine was recovered, and displacing the oil by continuously injecting a two percent NaCl solution. After displacing the oil with NaCl solution, the core was again resaturated with the same oil until the original or approximately original oil saturation was reached. The core was then flooded, this time, by continuously injecting the desired polymer solution. A constant injection rate was used, such that the superficial velocity was held constant at about 30 feet per day. It should be pointed out that a very long period of time was required for the complete oil saturation of the cores. This time period increased with oil viscosity and it was more than 24 hours for the most viscous oil.

CHAPTER VI

DISCUSSION AND RESULTS

1. POLYMER SOLUTIONS RHEOLOGICAL INVESTIGATION

Fluids categorized variously as plastics, Bingham plastics, pseudoplastics, and dilatants are the simplest types of non-Newtonian fluids. When complications due to the time of shear and strain are absent, a large number of mathematical relationships, empirical as well as theoretical, can be used to relate shear stress to shear rate for these materials. Some of the more important of these were reviewed in Chapter II. Through the work of a large number of investigators, (18,33,49,68) it has been evident that the rheological behavior of a large group of polymeric materials and their solutions can successfully be correlated through the use of one or more of these relationships. It has also been demonstrated that the power law model:

$$\tau_{xy} = - k\gamma^{n} \qquad (6\text{-}1)$$

which describes the shear stress-shear rate relationships in terms of two fluid property n and k, appears to be the most useful relationship proposed to date. This equation

is probably the simplest equation for relating shear stress to shear rate in non-Newtonian systems because it contains the minimum possible number of fluid property constants or parameters, has been shown to fit experimental data as well as other equations containing up to six constants (47,67), with only two exceptions. These exceptions occur at the very low shear rates at which fluids first begin to depart from Newtonian behavior and at the other extreme of very high shear rates at which the fluid behavior again reverts toward the Newtonian. The low shear region may be of importance in the processing of commercial thermoplastic polymers, while the high shear rate region may be reached under conditions of highly turbulent flow in a number of instances. The shear range of interest in non-Newtonian flow through porous media ranges from values on the order of one sec^{-1} for thechnological application related to oil recovery, to 10^{-5} sec^{-1} in problems related to naval architecture and bearing applications. Even under the two extreme conditions, however, the same equation may be used by allowing the constants n and k to become function of the shear rate. Thus while the empirical power law model has some definite limitations, it is always possible to employ it with only a reasonable amount of additional effort.

With the above idea in mind a total of 88 solutions of twelve different polymers, more frequently used by petroleum industry, was tested. The idea was first to correlate

the shear stress-shear rate data, indicated by the cone and plate viscometer, using the simplest non-Newtonian relationship, the power law equation. The Sisko (71) model:

$$\tau_{xy} = - a\gamma - b\gamma^{n} \qquad (6\text{-}2)$$

which is a very simple extension of the power law equation, or the Ellis (73) model could be used for those solutions which were not adequately expressed by the power law relationship. The results of these tests are shown in Figures VI-1 through VI-24 and summarized in Tables B-1 through B-88. The values of shear stress and shear rate calculated from the cone and plate viscometer are plotted on log-log coordinate, Figures VI-1 through VI-12, as points. The lines drawn on these figures are the least square representation of power law model using the viscometer data. The least square regressions were performed by a program written and run on an IMB time-sharing computer which aside from computing the best fit also calculated the standard error of estimation for some of the correlations.

As seen from Figures VI-1 through VI-12 for the viscometric data obtained over a broad range of polymer concentration and a much broader range of shear stress-shear rate than any other previous investigation, the two-parameter power law equation was found to give an excellent fit. The standard error of estimation was calculated from equation:

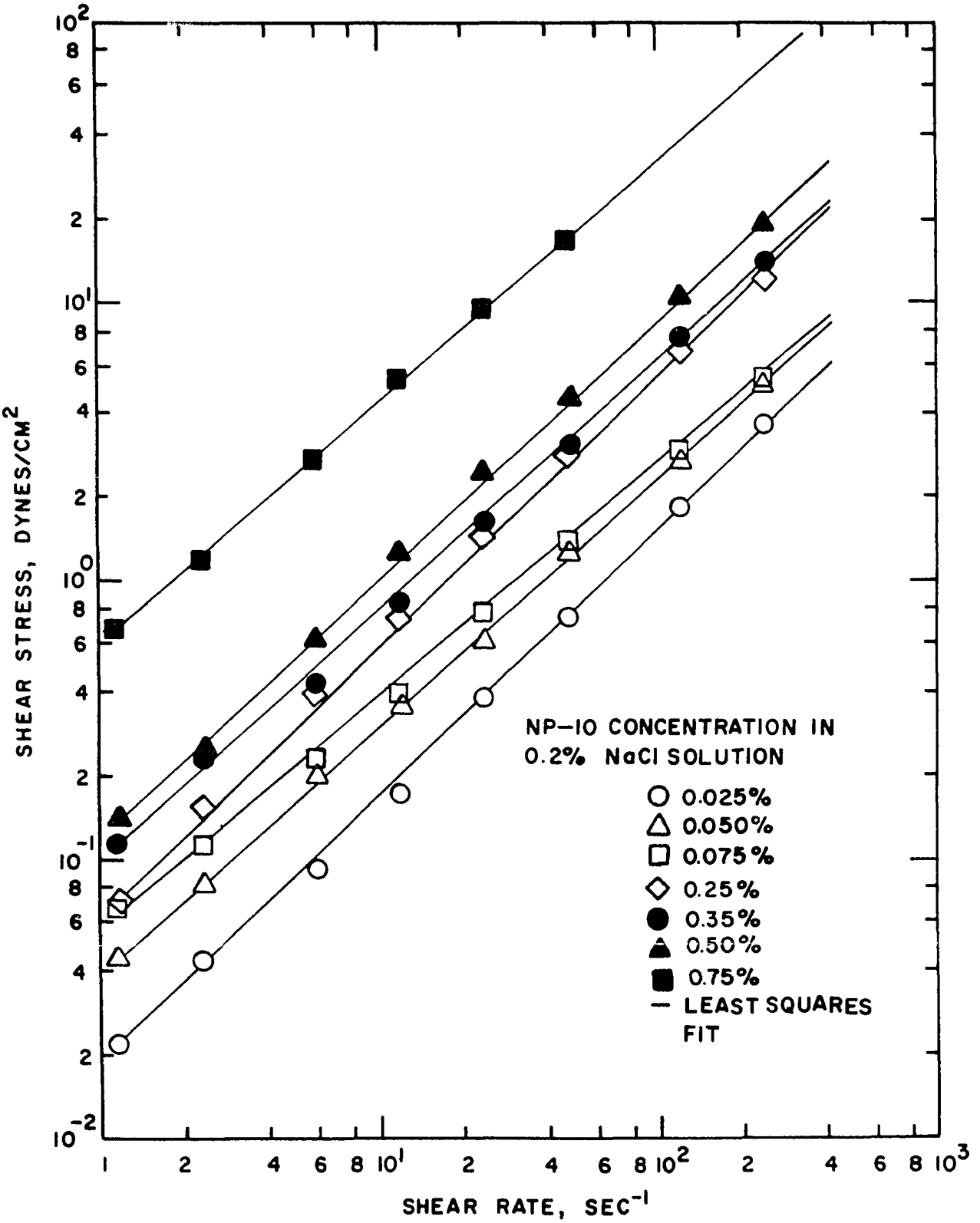

Figure VI-1. Shear Stress Versus Shear Rate for Various Concentrations of "Separan" NP-10.

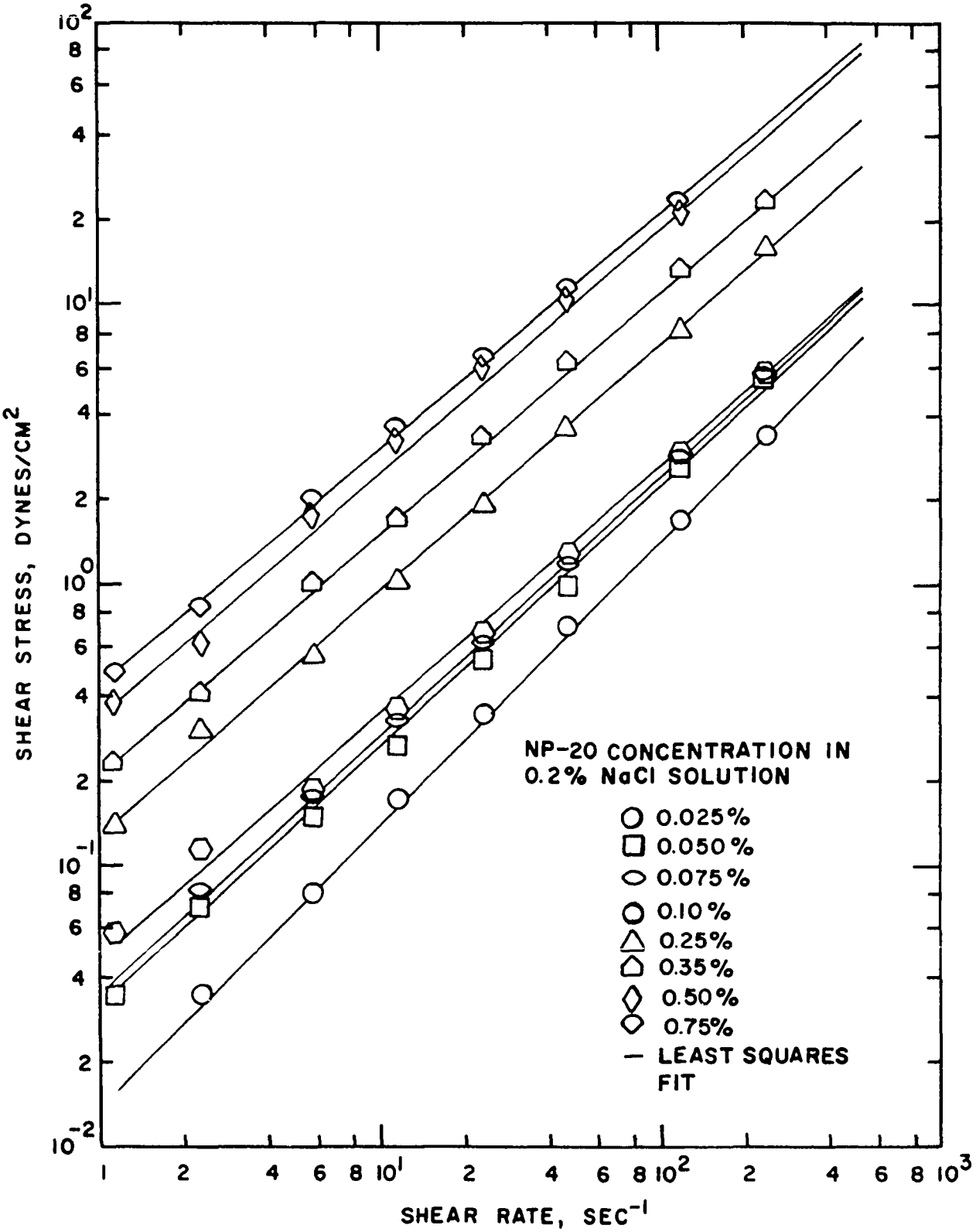

Figure VI-2. Shear Stress Versus Shear Rate for Various Concentrations of "Separan" NP-20.

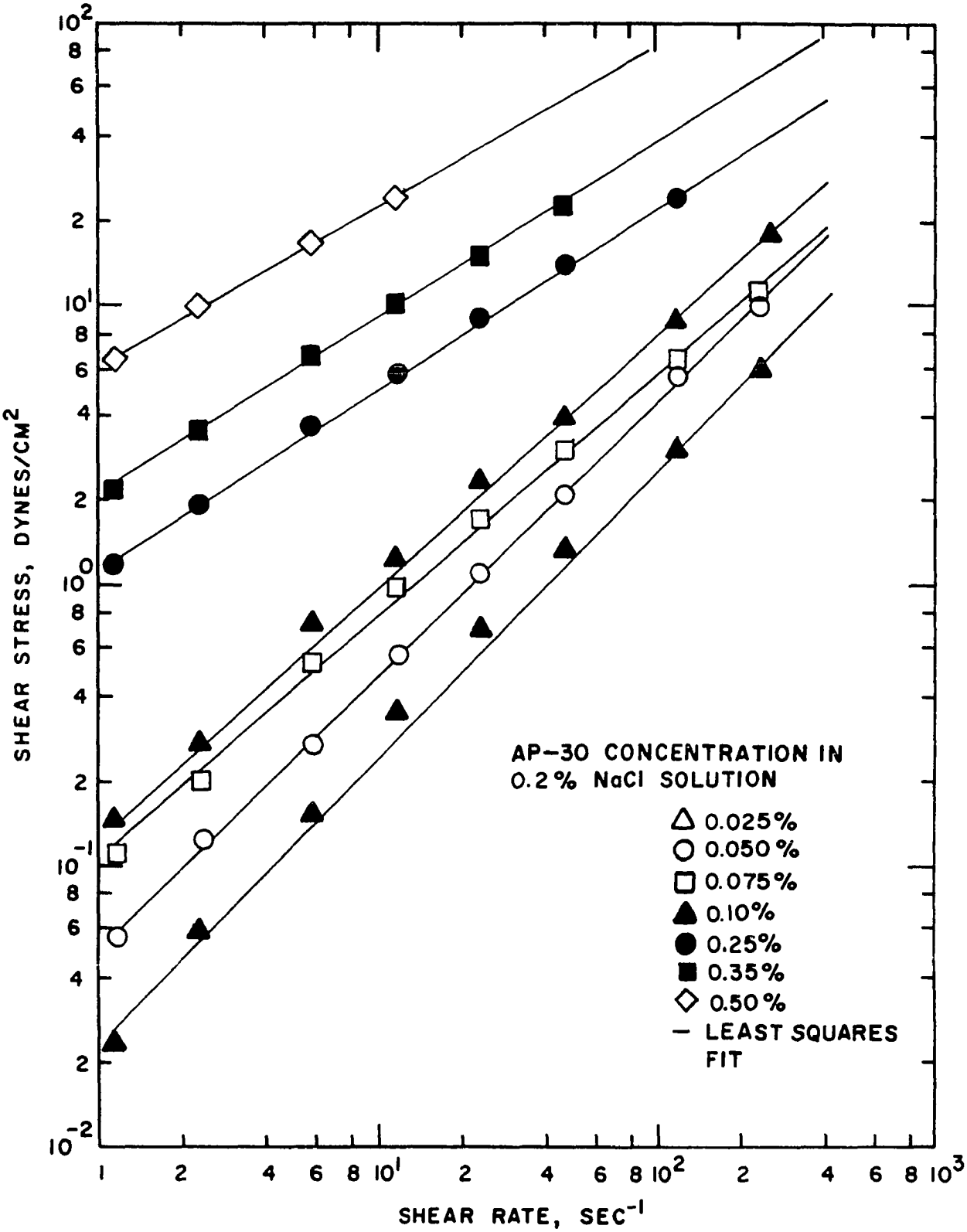

Figure VI-3. Shear Stress Versus Shear Rate for Various Concentrations of "Separan" AP-30.

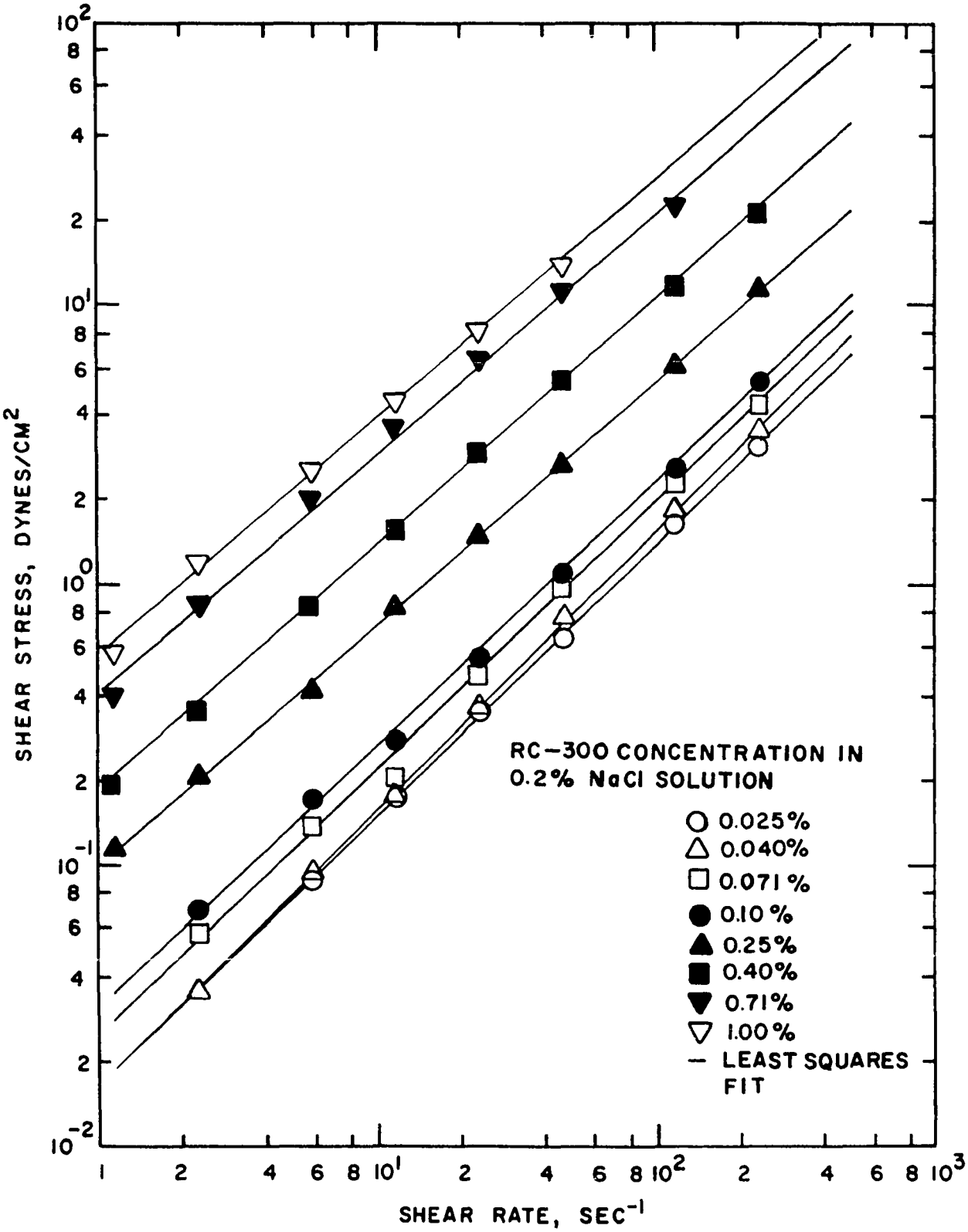

Figure VI-4. Shear Stress Versus Shear Rate for Various Concentrations of RC-300.

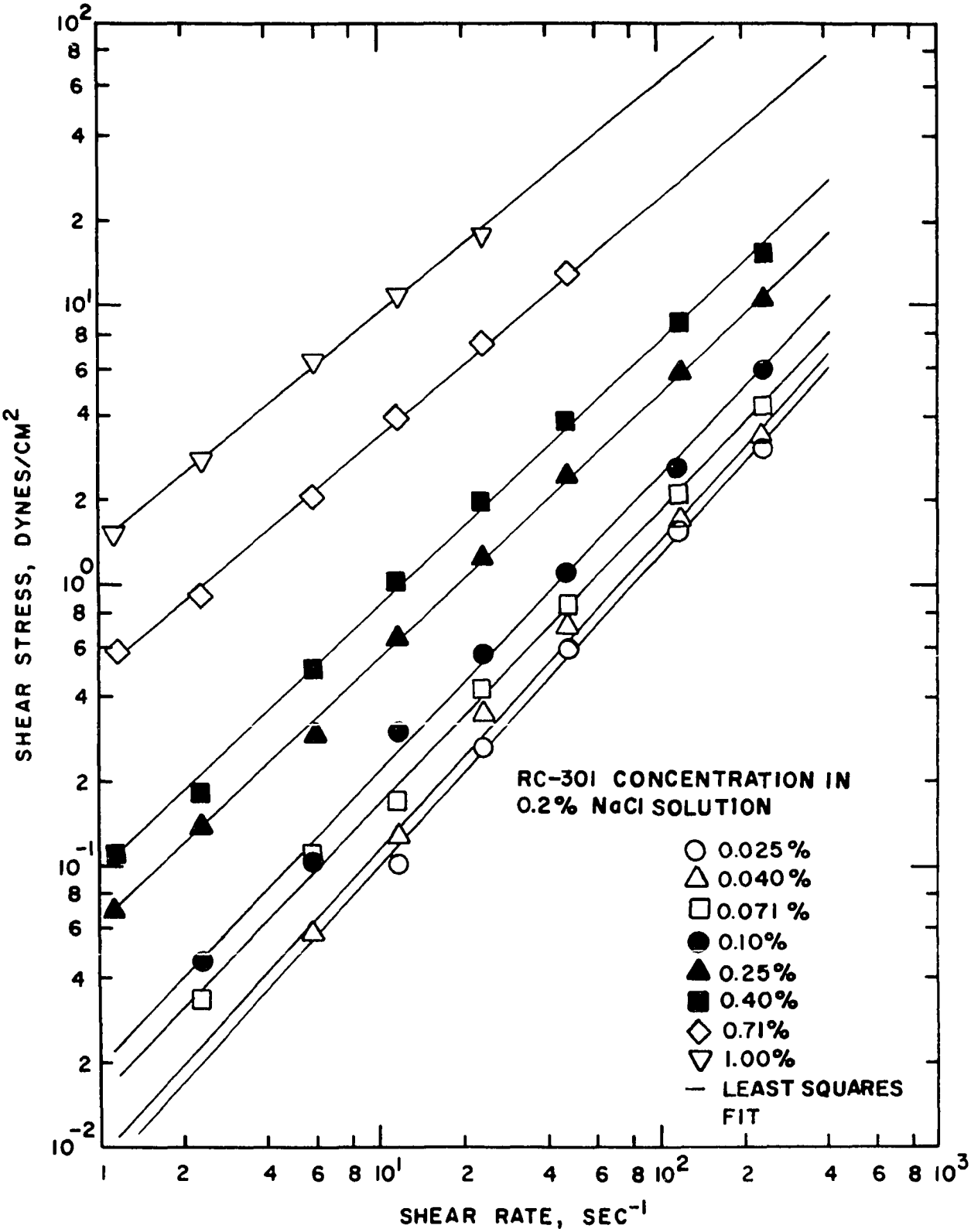

Figure VI-5. Shear Stress Versus Shear Rate for Various Concentrations of RC-301.

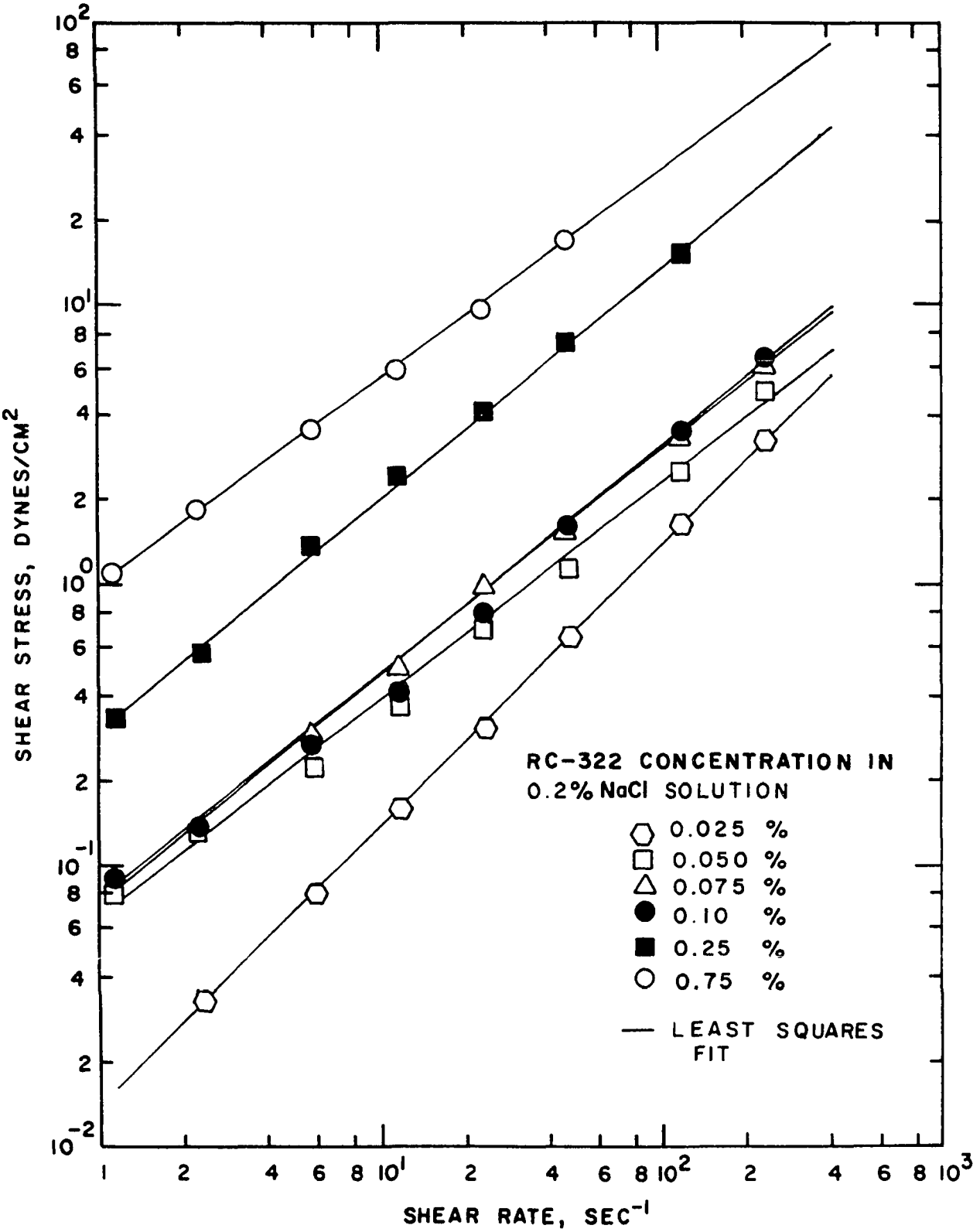

Figure VI-6. Shear Stress Versus Shear Rate for Various Concentrations of RC-322.

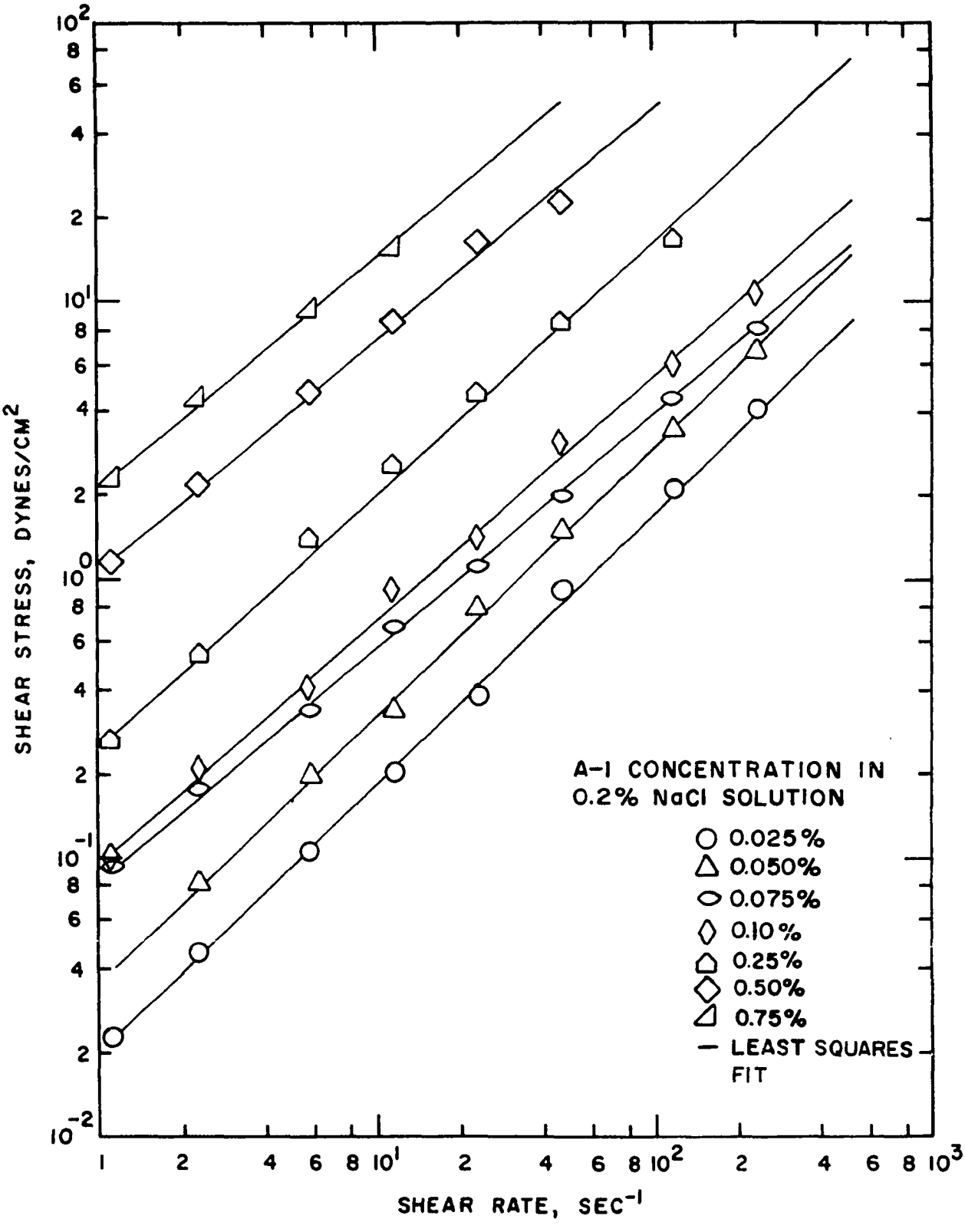

Figure VI-7. Shear Stress Versus Shear Rate for Various Concentrations of "Reten" A-1.

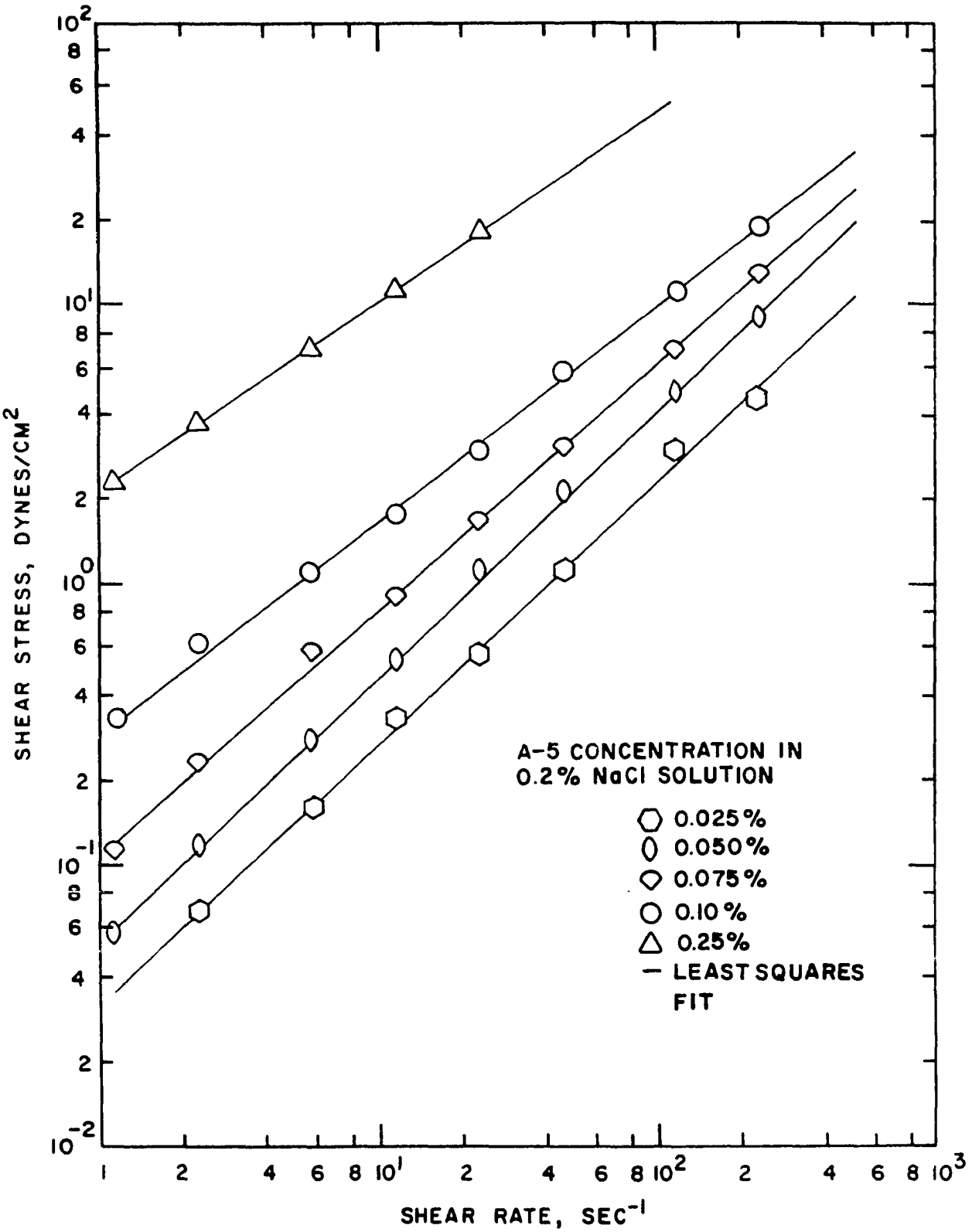

Figure VI-8. Shear Stress Versus Shear Rate for Various Concentrations of "Reten" A-5.

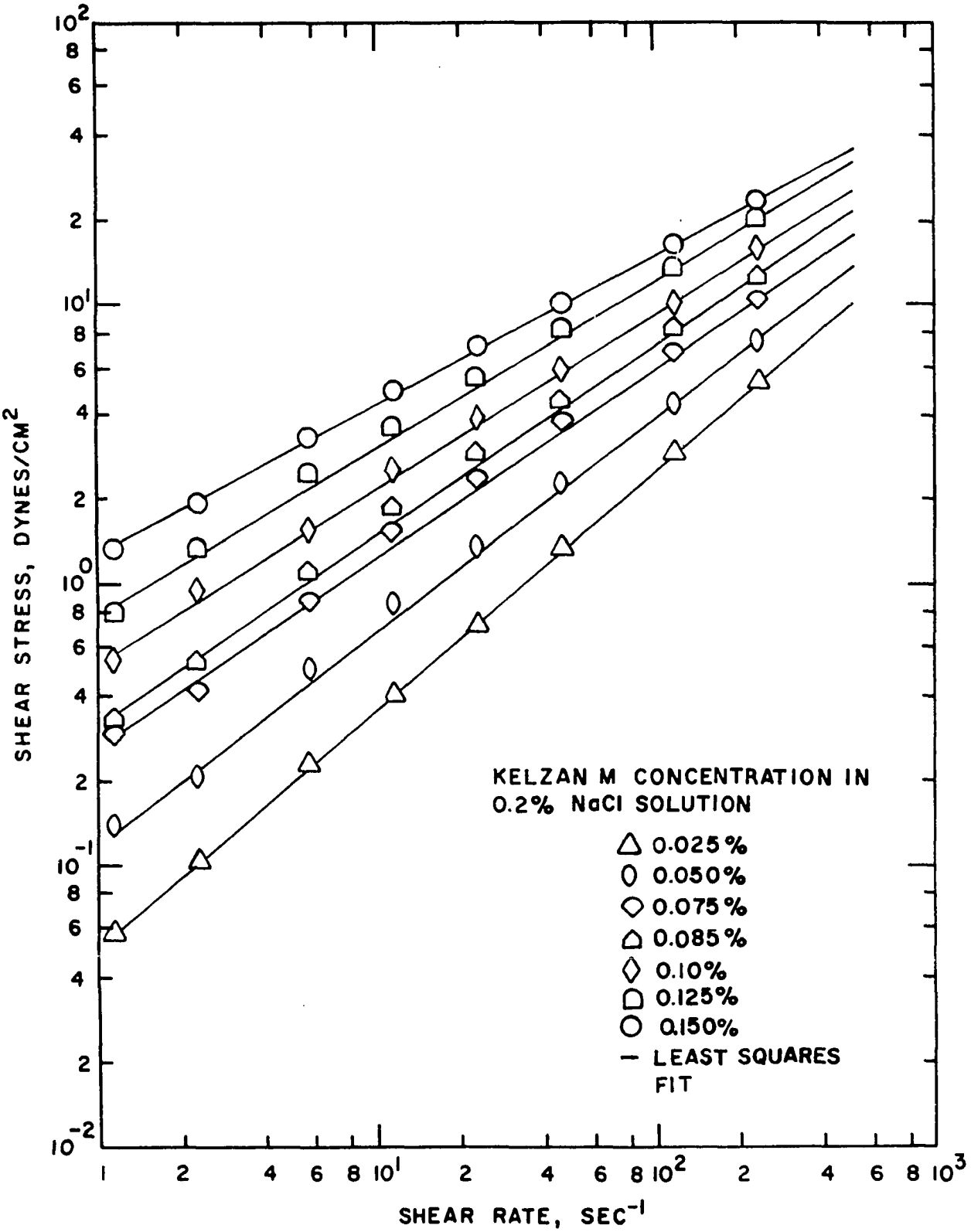

Figure VI-9. Shear Stress Versus Shear Rate for Various Concentrations of "Kelzan" M.

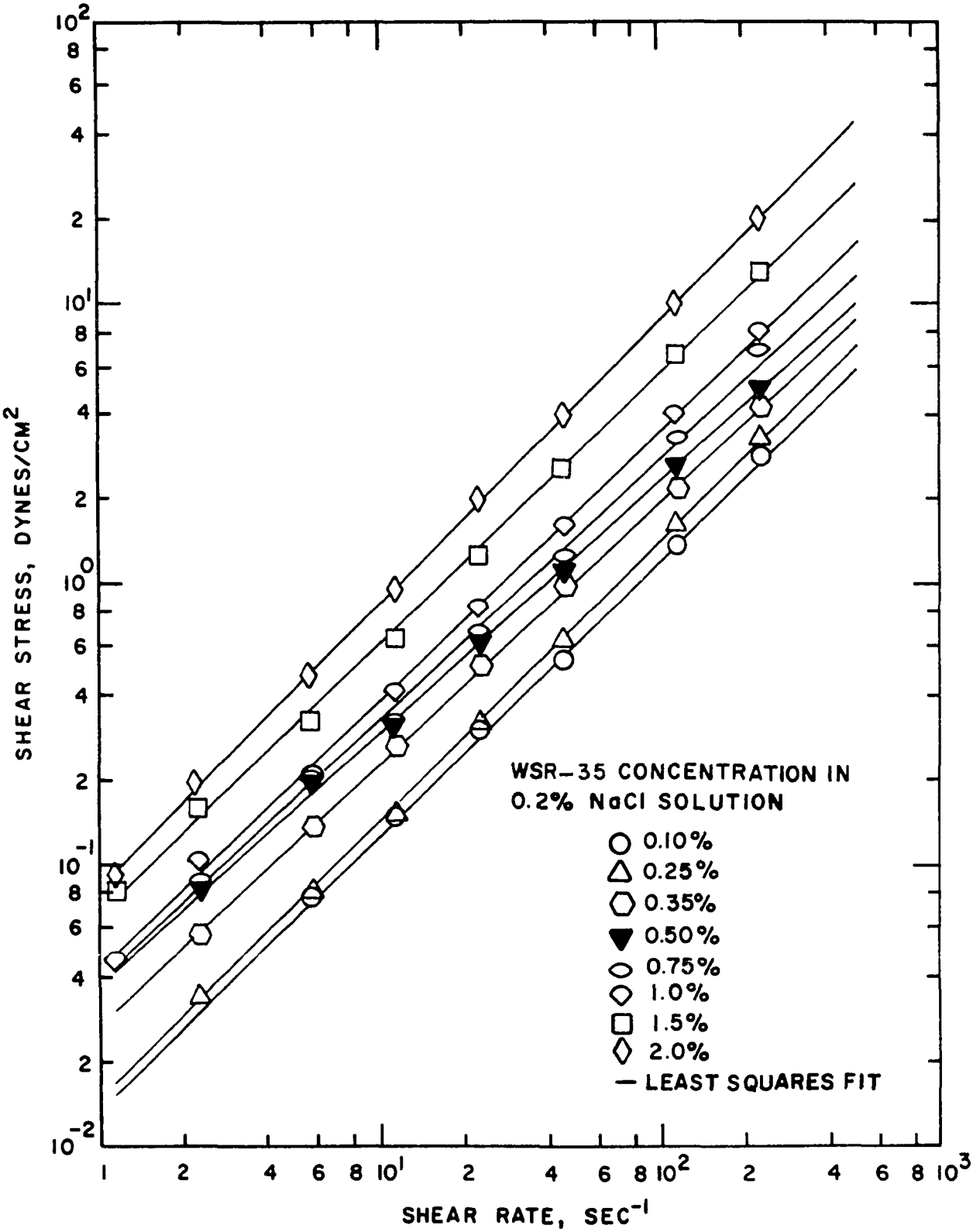

Figure VI-10. Shear Stress Versus Shear Rate for Various Concentrations of "Polyox" WSR-35.

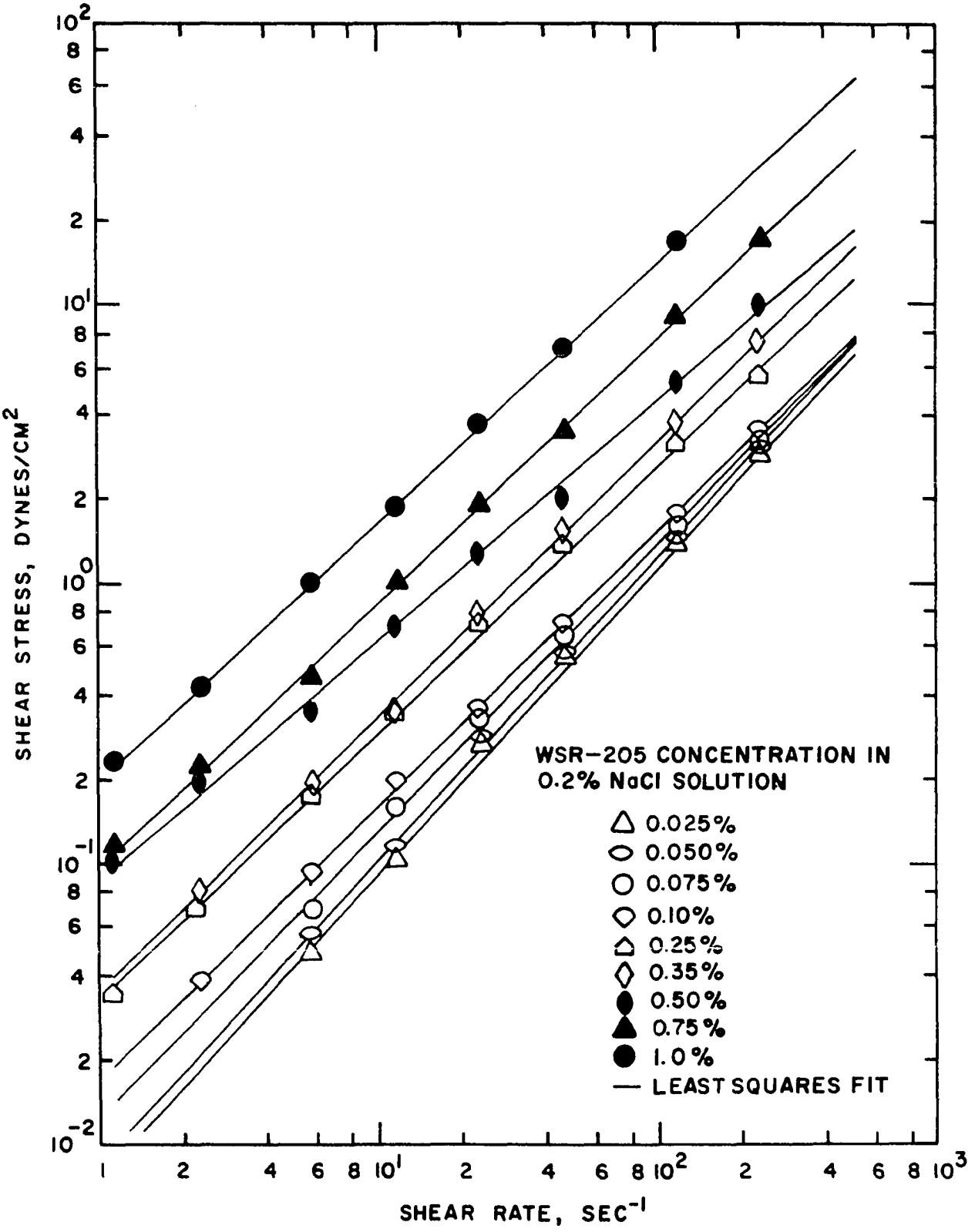

Figure VI-11. Shear Stress Versus Shear Rate for Various Concentrations of "Polyox" WSR-205.

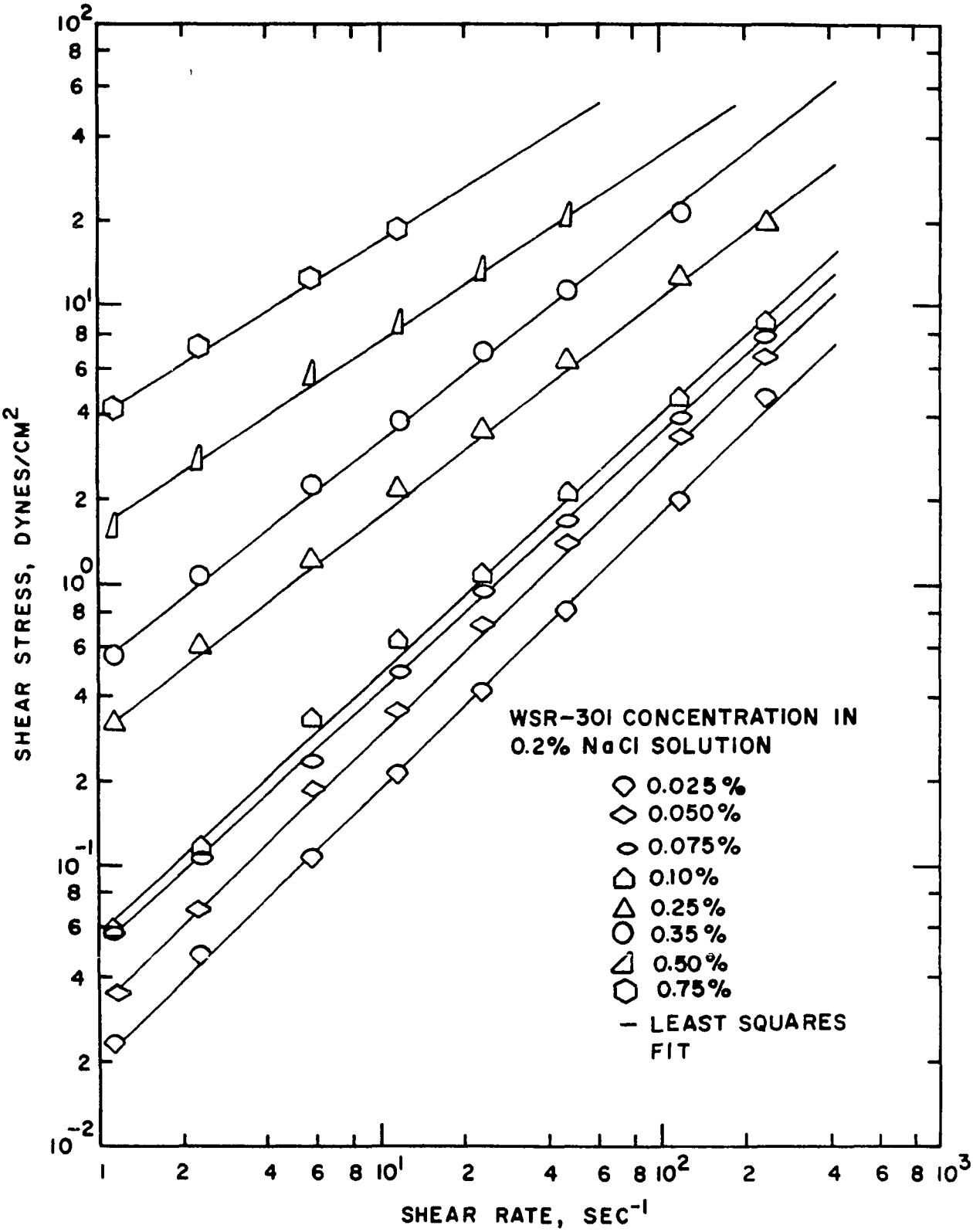

Figure VI-12. Shear Stress Versus Shear Rate for Various Concentrations of "Polyox" WSR-301.

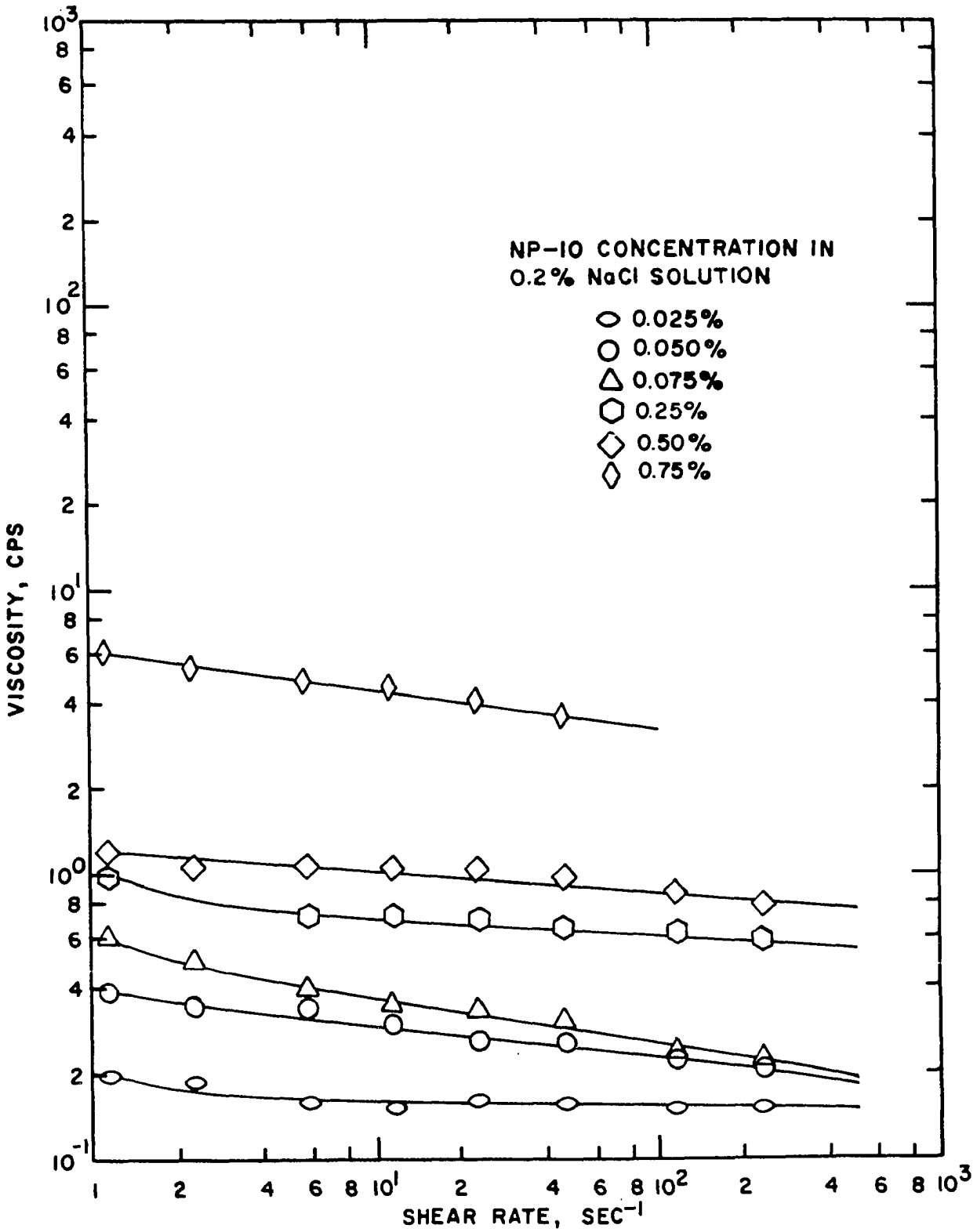

Figure VI-13. Viscosity-Shear Rate Relations of Various Concentrations of "Separan" NP-10.

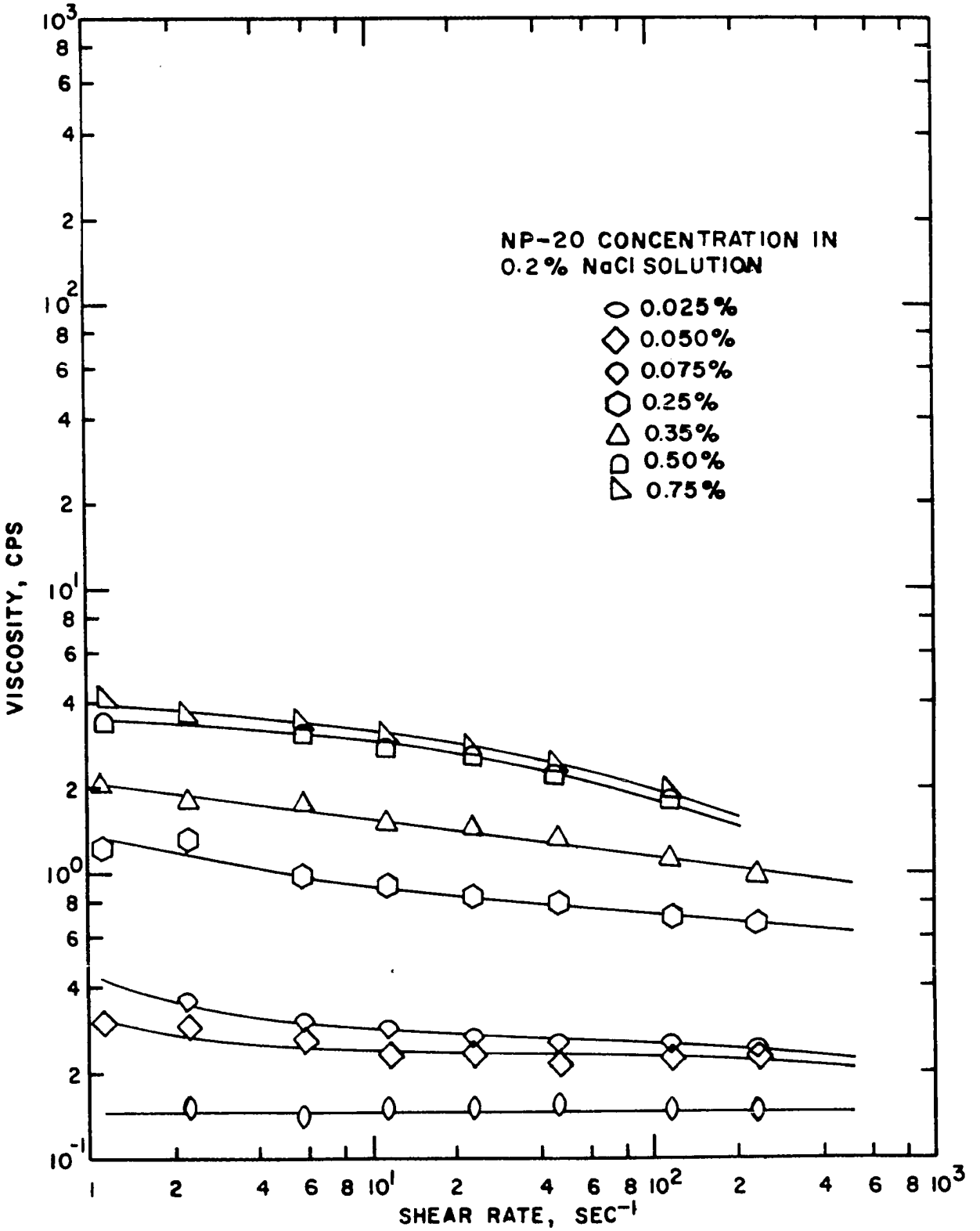

Figure VI-14. Viscosity-Shear Rate Relations of Various Concentrations of "Separan" NP-10.

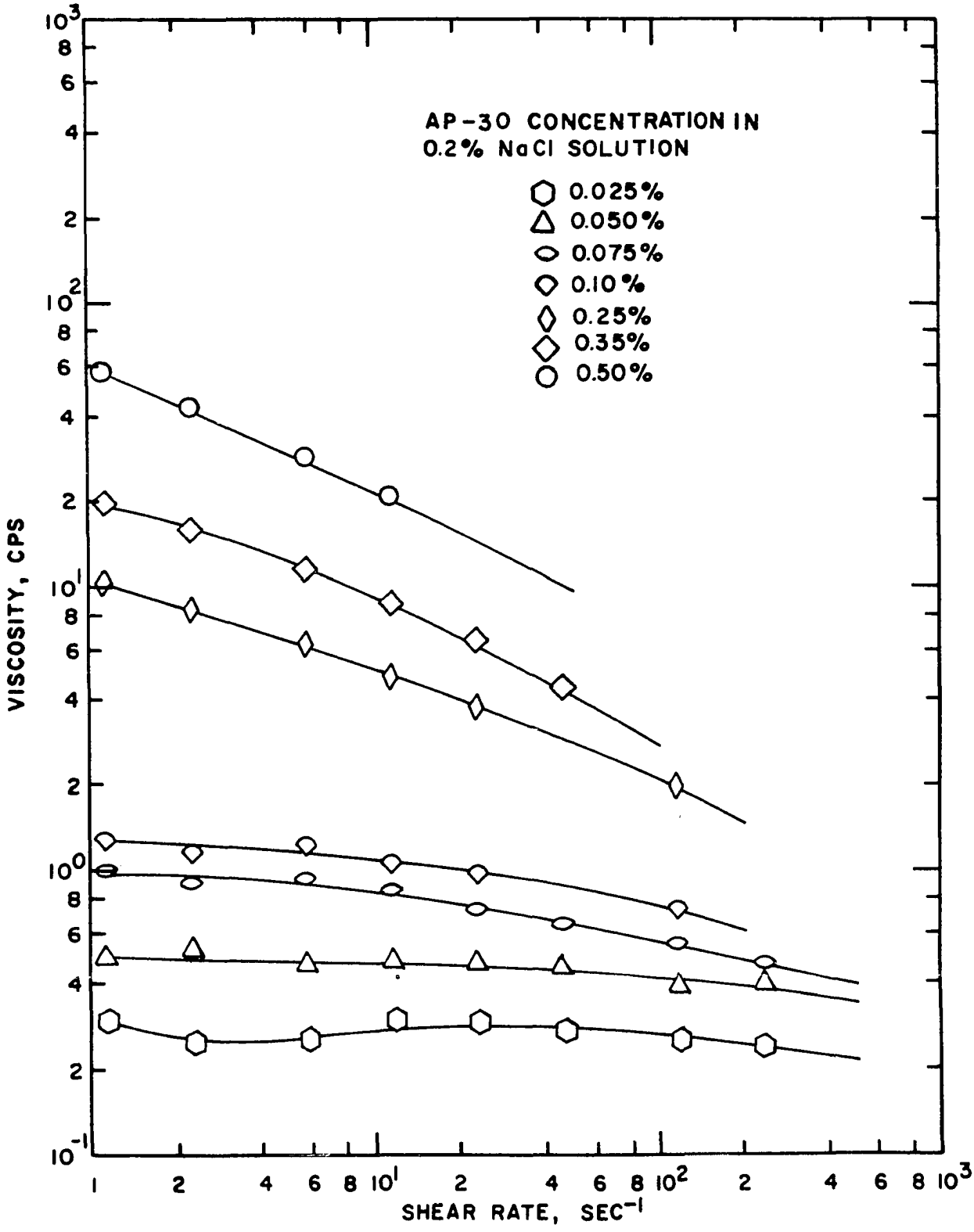

Figure VI-15. Viscosity-Shear Rate Relations of Various Concentrations of "Separan" AP-30.

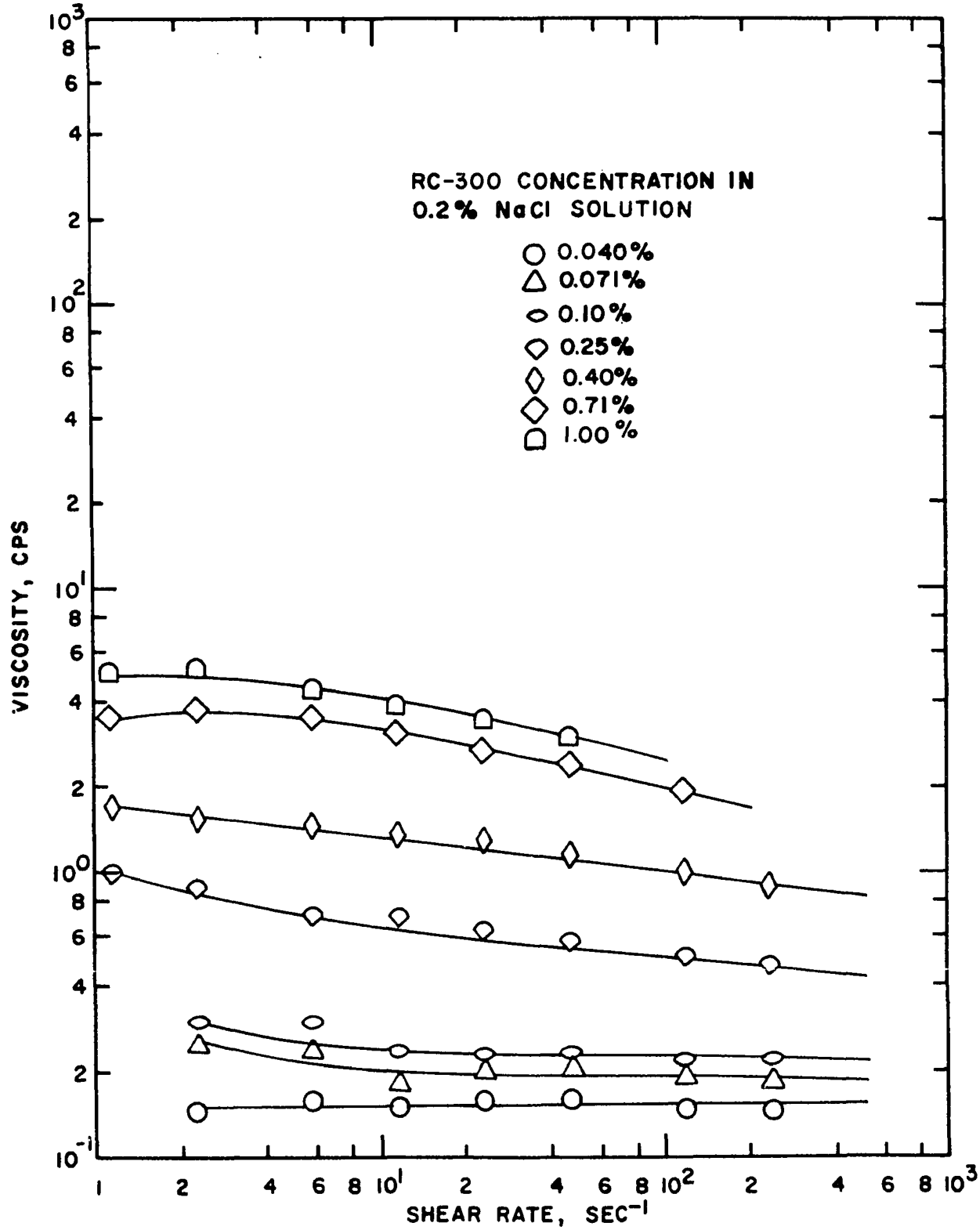

Figure VI-16. Viscosity Shear Rate Relations of Various Concentrations of RC-300.

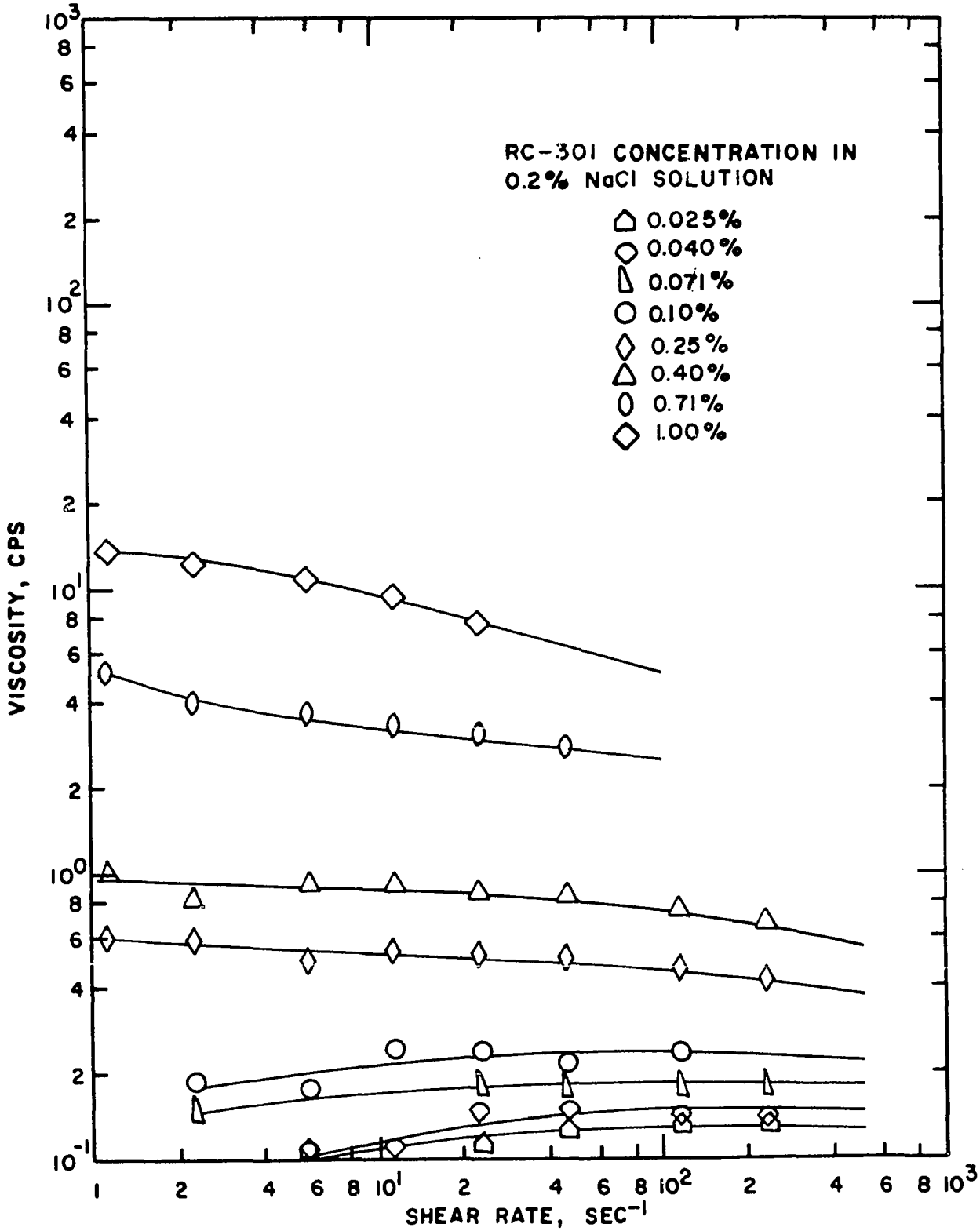

Figure VI-17. Viscosity-Shear Rate Relations of Various Concentrations of RC-301.

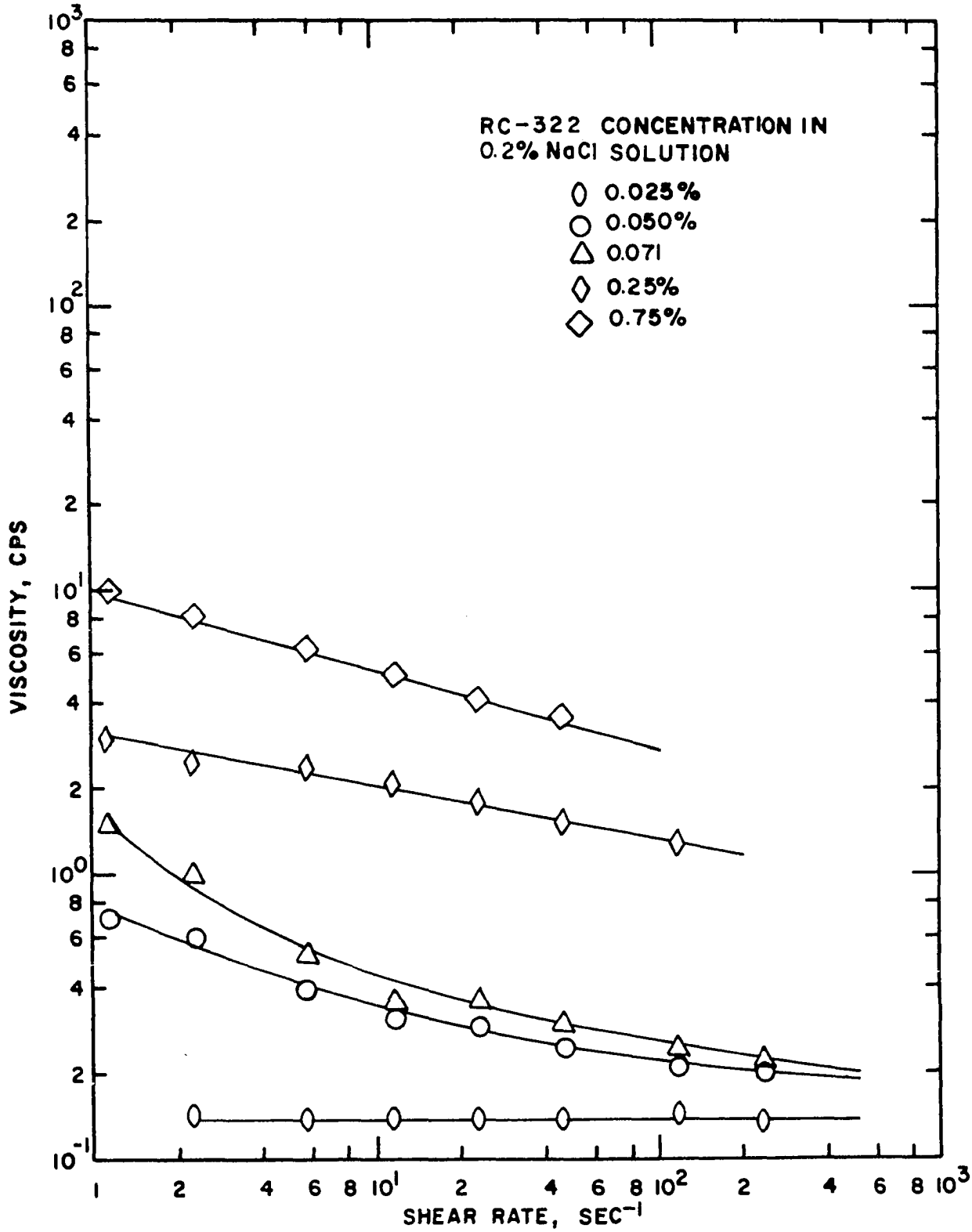

Figure VI-18. Viscosity-Shear Rate Relations of Various Concentrations of RC-322.

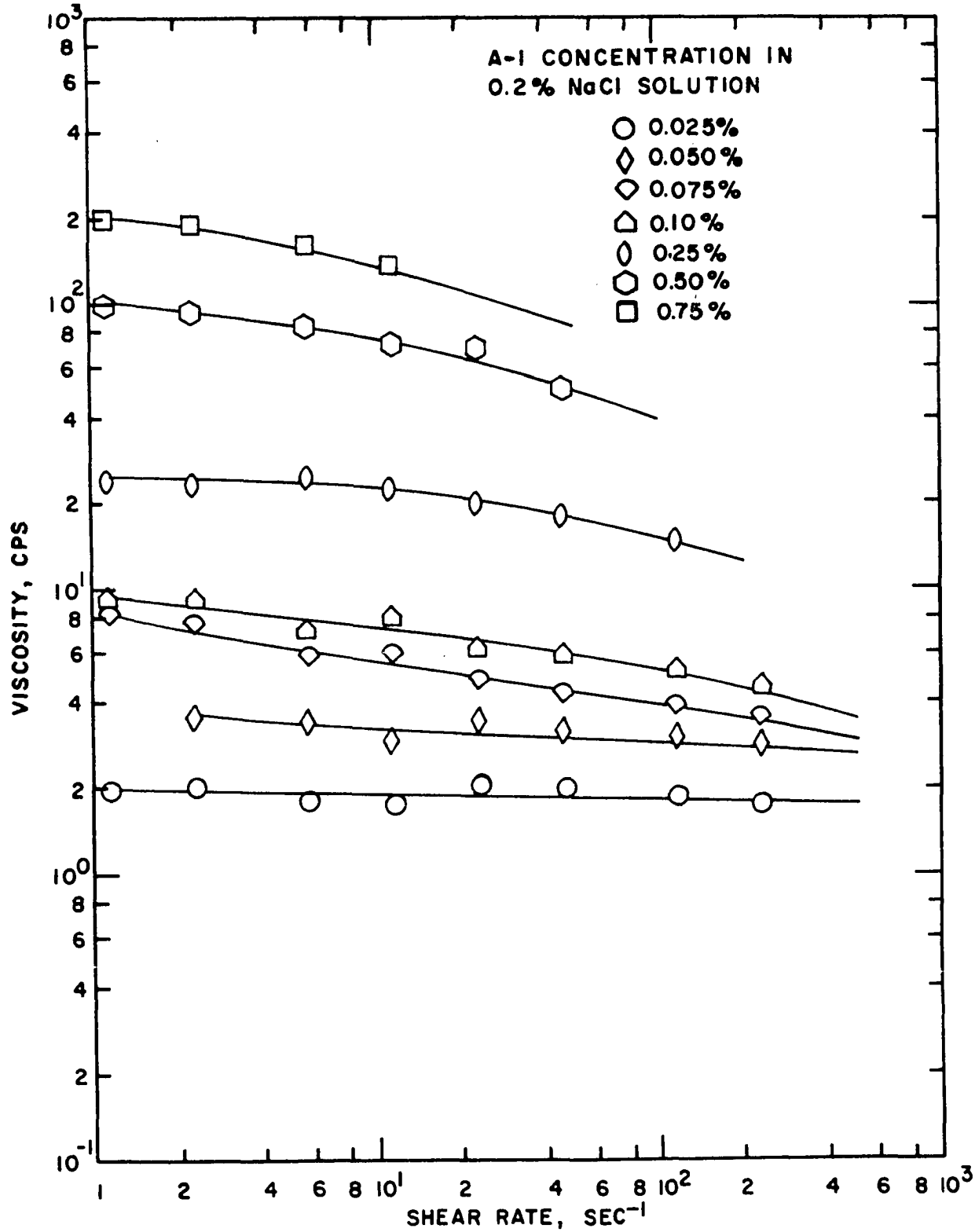

Figure VI-19. Viscosity-Shear Rate Relations of Various Concentrations of "Reten" A-1.

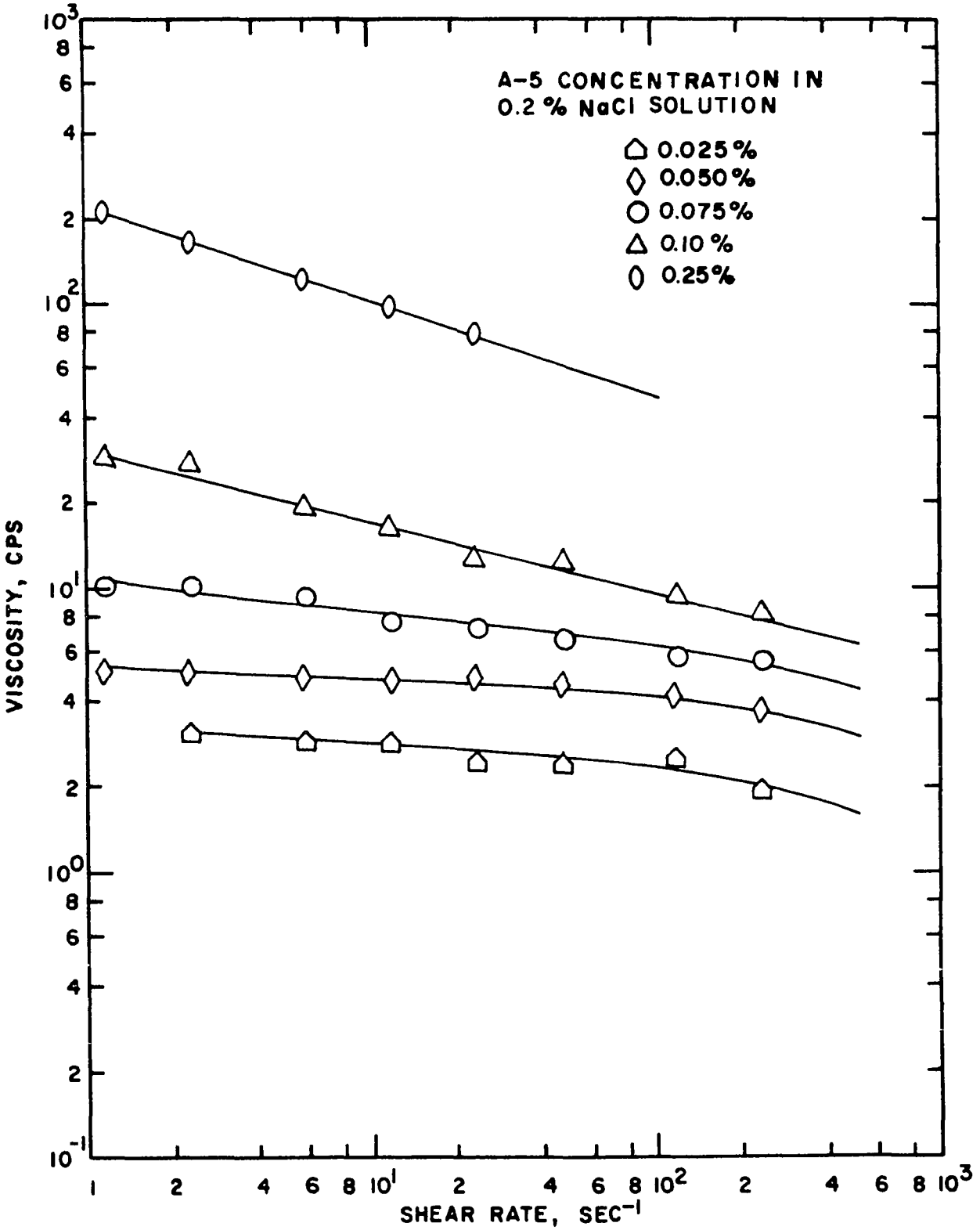

Figure VI-20. Viscosity-Shear Rate Relations of Various Concentrations of "Reten" A-5.

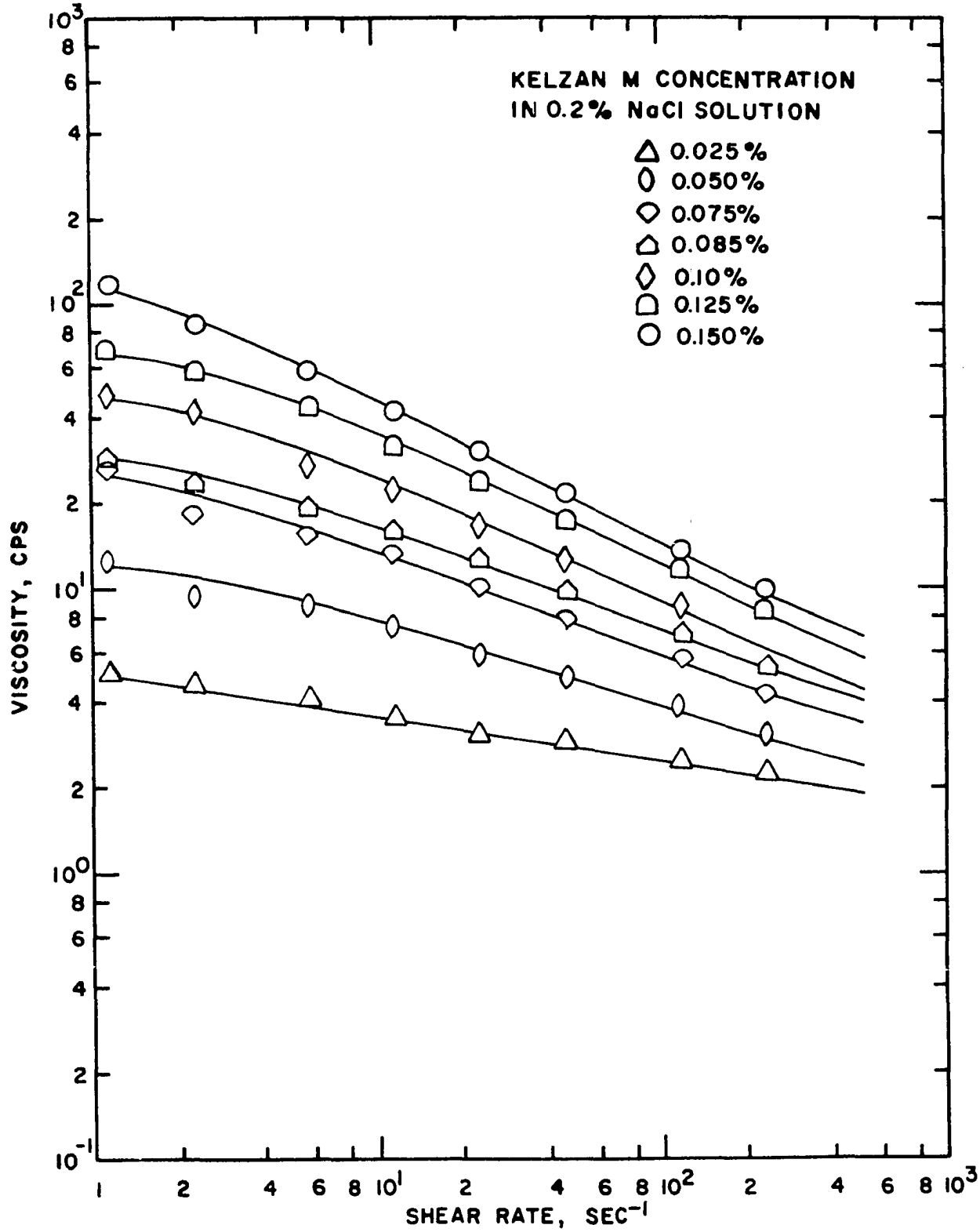

Figure VI-21. Viscosity-Shear Rate Relations of Various Concentrations of "Kelzan" M.

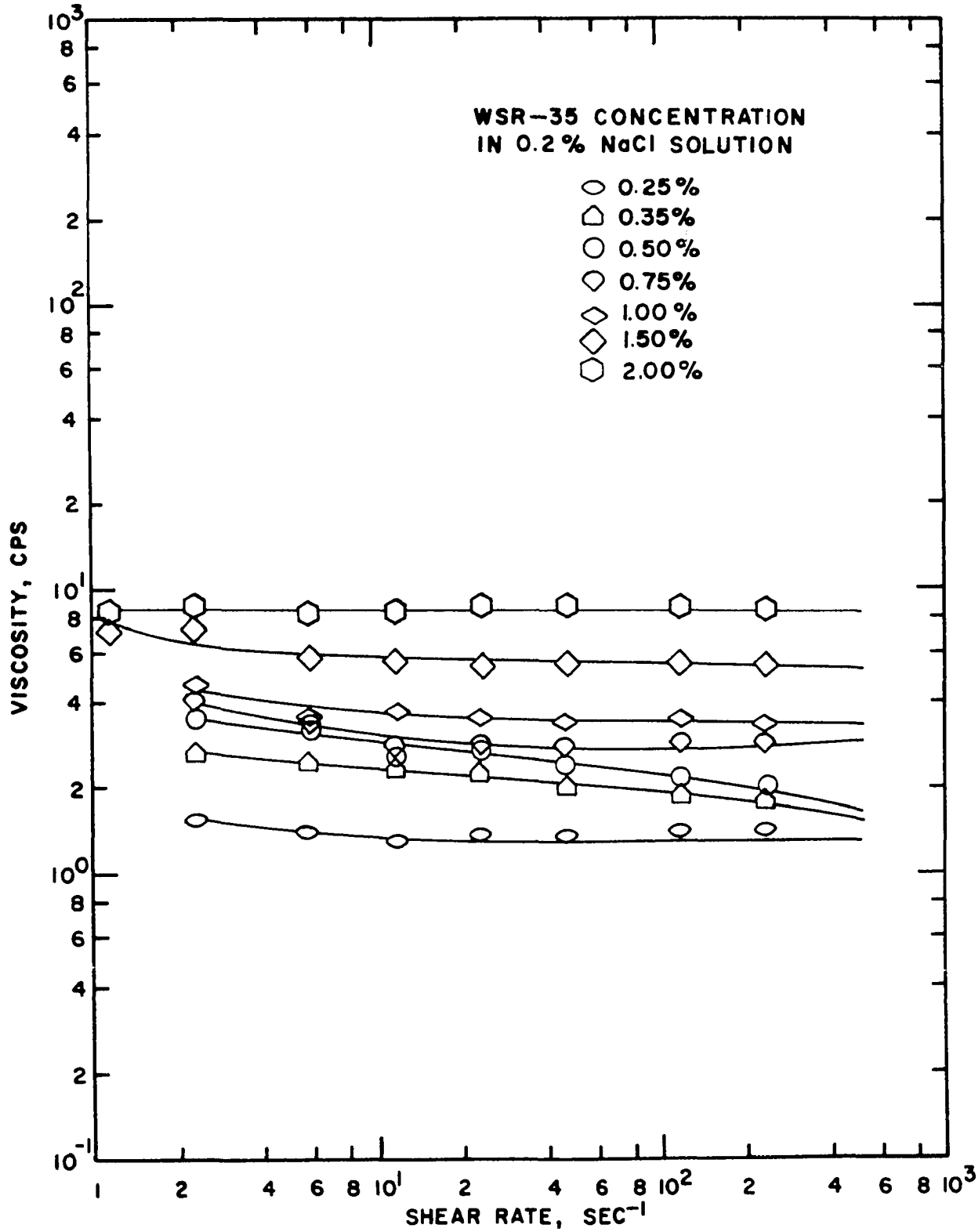

Figure VI-22. Viscosity-Shear Rate Relations of Various Concentrations of "Polyox" WSR-35.

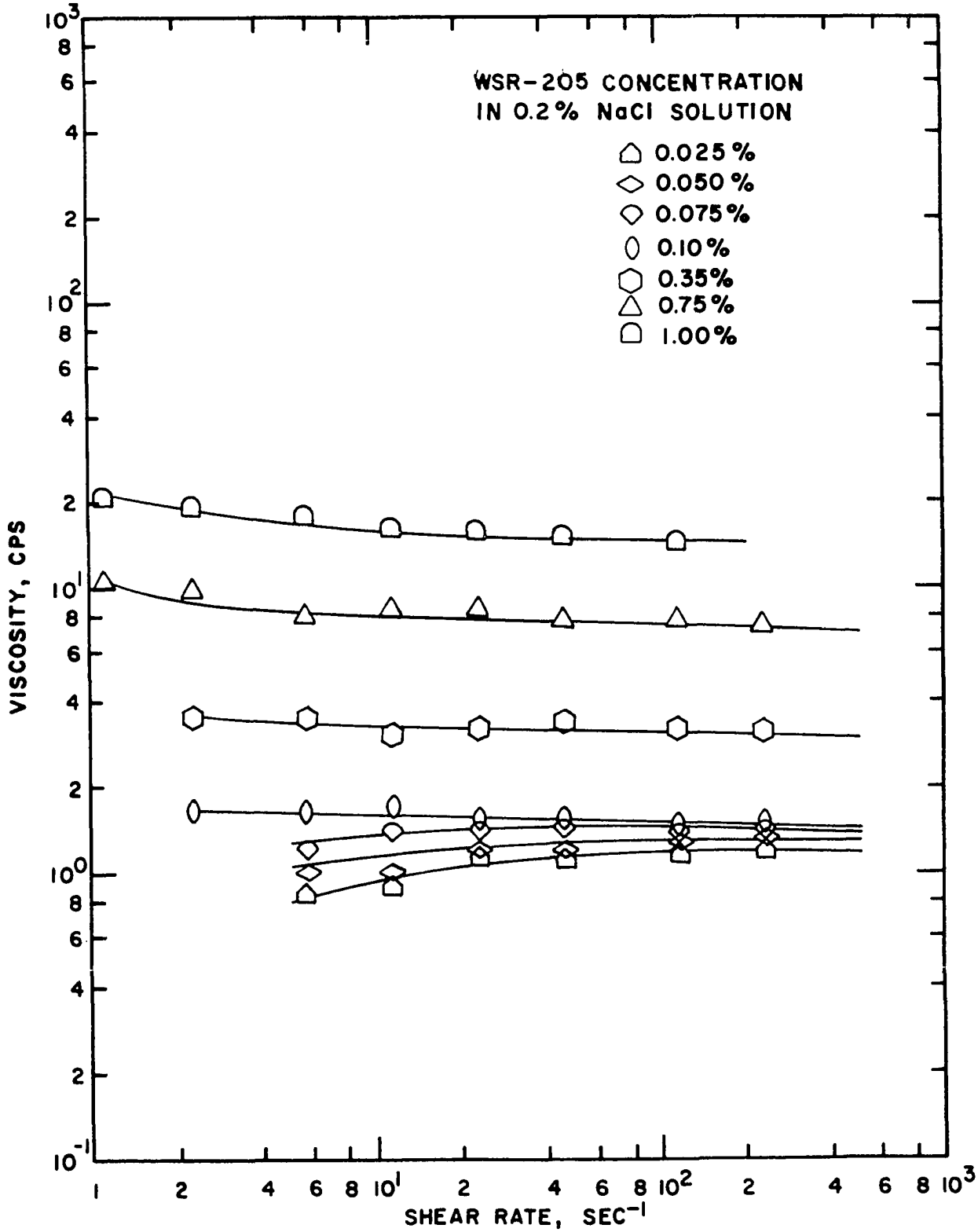

Figure VI-23. Viscosity-Shear Rate Relations of Various Concentrations of "Polyox" WSR-205.

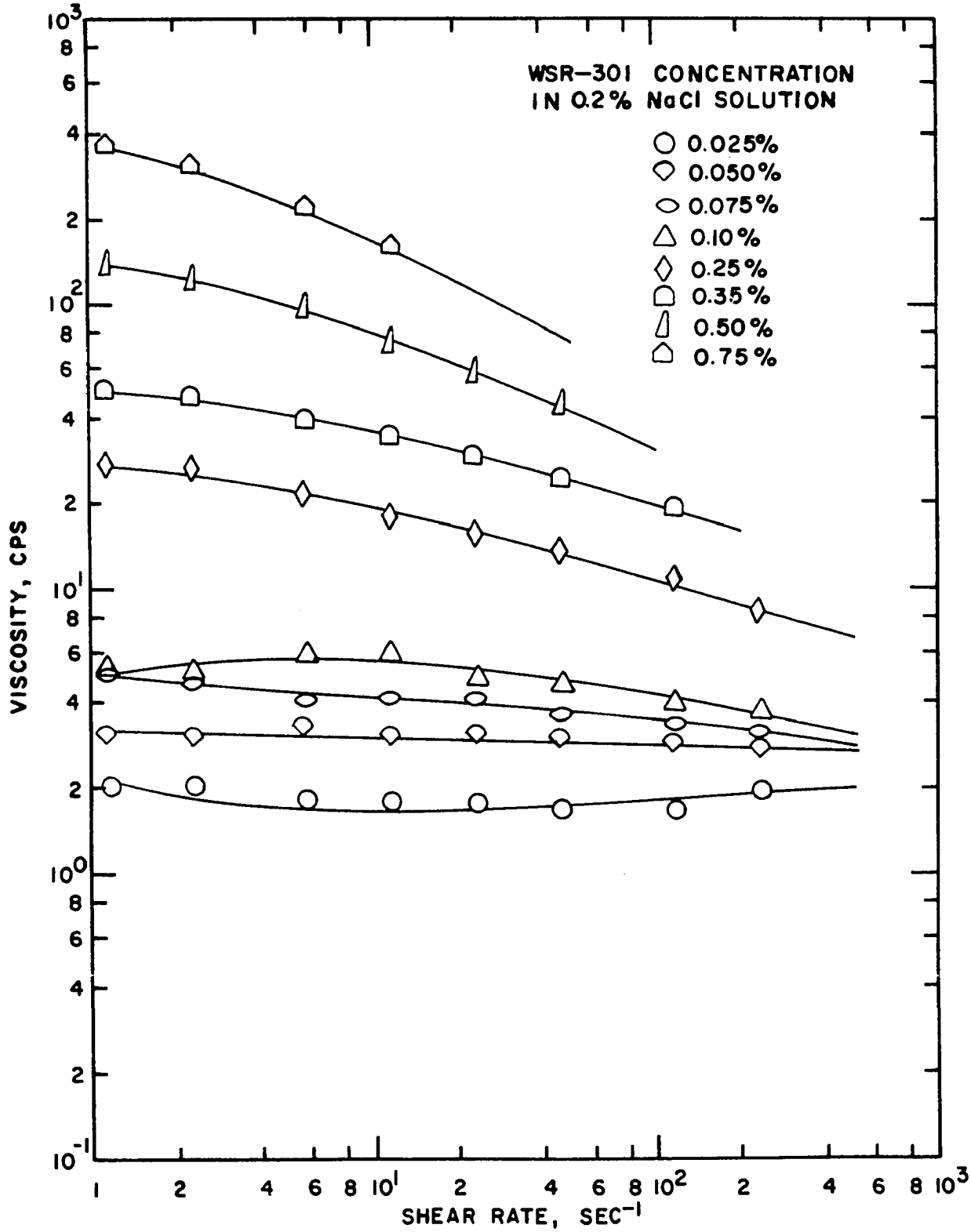

Figure VI-24. Viscosity-Shear Rate Relations of Various Concentrations of "Polyox" WSR-301.

$$S = \sqrt{\frac{\Sigma (\tau_M - \tau_E)^2}{N-2}} \qquad (6-3)$$

where S is the standard error of estimation, N is the number of data points, τ_M is the shear stress measured with the viscometer, and τ_E is the estimated value of shear stress from the power law equation. It ranged between 0.006 for 0.025 percent RC-322 to 0.125 for 0.05 percent AP-30. A tabulated values of parameter n and k are given in Table VI-1. From all the solutions tested, only the 0.025 percent solution of NP-20 and the 2 percent solution of WSR-35 were Newtonian (n = 1.0). The rest were non-Newtonian. Figures VI-13 through VI-24 give the individual viscosity-shear rate relationship for all the solutions tested. Except for a handful of non-Newtonian solutions, which were essentially dilatant (n>1.0), the rest appeared to be pseudoplastic (n<1.0).

Effect of Polymer Concentration on Solution Viscosity

Analysis of Table VI-1 clearly indicates that the value of constant k increased as the polymer concentration increased. Since, the higher the k value the more viscous the fluid; it can be concluded that the solution viscosity increases as the polymer concentration increases. This can also be noted from graphs of the solutions viscosity versus the polymer concentration in Figure VI-25 which indicates that everything else held constant the solution becomes more viscous as the polymer concentration is increased.

TABLE VI-1

TABULATED VALUES OF POWER LAW CONSTANTS n AND k
FOR VARIOUS POLYMER SOLUTIONS

Run No.	Polymer Brand	Concentration (Percent by Weight)	k	n
1	Separan NP-10	0.025	0.0212	0.9297
2	Separan NP-10	0.050	0.0396	0.8867
3	Separan NP-10	0.075	0.0587	0.8207
4	Separan NP-10	0.250	0.0621	0.9850
5	Separan NP-10	0.350	0.0988	0.8986
6	Separan NP-10	0.500	0.1210	0.9321
7	Separan NP-10	0.750	0.6005	0.8709
8	Separan NP-20	0.025	0.0140	1.0000
9	Separan NP-20	0.050	0.0320	0.9195
10	Separan NP-20	0.075	0.0355	0.9228
11	Separan NP-20	0.100	0.0465	0.8847
12	Separan NP-20	0.250	0.1270	0.8754
13	Separan NP-20	0.350	0.2060	0.8541
14	Separan NP-20	0.500	0.3300	0.8693
15	Separan NP-20	0.750	0.4320	0.8391
16	Separan AP-30	0.025	0.0247	1.0083
17	Separan AP-30	0.050	0.0518	0.9554
18	Separan AP-30	0.075	0.1097	0.9101
19	Separan AP-30	0.100	0.1222	0.8586
20	Separan AP-30	0.250	1.1233	0.9101
21	Separan AP-30	0.350	2.1006	0.6471
22	Separan AP-30	0.500	5.8653	0.6233
23	Kelzan M	0.025	0.0515	0.8451
24	Kelzan M	0.050	0.1200	0.7563
25	Kelzan M	0.075	0.2630	0.6694
26	Kelzan M	0.085	0.3160	0.6720
27	Kelzan M	0.100	0.5230	0.6176
28	Kelzan M	0.125	0.7700	0.5914
29	Kelzan M	0.150	1.2750	0.5250
30	Reten A-1	0.025	0.0202	0.9590
31	Reten A-1	0.050	0.0350	0.9590
32	Reten A-1	0.075	0.0820	0.8421
33	Reten A-1	0.100	0.0940	0.8751
34	Reten A-1	0.250	0.2430	0.9131
35	Reten A-1	0.500	1.0350	0.8332
36	Reten A-1	0.750	2.0630	0.8332

TABLE VI-1 (Continued)

Run No.	Polymer Brand	Concentration (Percent by Weight)	k	n
37	Reten A-5	0.025	0.0319	0.9195
38	Reten A-5	0.050	0.0527	0.9424
39	Reten A-5	0.075	0.1085	0.8693
40	Reten A-5	0.100	0.2868	0.9067
41	Reten A-5	0.250	2.1000	0.6745
42	Polyox WSR-35	0.100	0.0139	0.9623
43	Rolyox WSR-35	0.250	0.0155	0.9793
44	Polyox WSR-35	0.350	0.0286	0.9163
45	Polyox WSR-35	0.500	0.0380	0.8910
46	Polyox WSR-35	0.750	0.0405	0.9163
47	Polyox WSR-35	1.000	0.0433	0.9424
48	Polyox WSR-35	1.500	0.0682	0.9556
49	Polyox WSR-35	2.000	0.0850	1.0000
50	Polyox WSR-205	0.025	0.0076	1.0724
51	Polyox WSR-205	0.050	0.0088	1.0724
52	Polyox WSR-205	0.075	0.0128	1.0176
53	Polyox WSR-205	0.100	0.0173	0.9759
54	Polyox WSR-205	0.250	0.0335	0.9457
55	Polyox WSR-205	0.350	0.0355	0.9691
56	Polyox WSR-205	0.500	0.0885	0.8541
57	Polyox WSR-205	0.750	0.0960	0.9424
58	Polyox WSR-205	1.000	0.1940	0.9228
59	Polyox WSR-301	0.025	0.0200	0.9827
60	Polyox WSR-301	0.050	0.0310	0.9759
61	Polyox WSR-301	0.075	0.0500	0.9099
62	Polyox WSR-301	0.100	0.0555	0.9163
63	Polyox WSR-301	0.250	0.2950	0.7673
64	Polyox WSR-301	0.350	0.5190	0.7898
65	Polyox WSR-301	0.500	1.5440	0.6619
66	Polyox WSR-301	0.750	3.9150	0.6224
67	RC-300	0.025	0.0169	0.9544
68	RC-300	0.040	0.0170	0.9951
69	RC-300	0.071	0.0250	0.9449
70	RC-300	0.100	0.0315	0.9248
71	RC-300	0.250	0.0984	0.8593
72	RC-300	0.400	0.1890	0.8783
73	RC-300	0.710	0.4120	0.8565
74	RC-300	1.000	0.5610	0.8443

TABLE VI-1 (Continued)

Run No.	Polymer Brand	Concentration (Percent by Weight)	k	n
75	RC-301	0.025	0.0082	1.0985
76	RC-301	0.040	0.0095	1.0909
77	RC-301	0.071	0.0161	1.0306
78	RC-301	0.100	0.0200	1.0141
79	RC-301	0.250	0.0650	0.8226
80	RC-301	0.400	0.0984	0.9407
81	RC-301	0.710	0.4910	0.8479
82	RC-301	1.000	1.4000	0.8183
83	RC-322	0.025	0.0146	0.9924
84	RC-322	0.050	0.0670	0.7627
85	RC-322	0.075	0.0740	0.7954
86	RC-322	0.100	0.0697	0.8116
87	RC-322	0.250	0.3130	0.8224
88	RC-322	0.750	1.0000	0.7319

Effect of Molecular Weight on Viscosity of Polymer Solution

From the previous discussions (18,33,59,76) it would seem that the polymer molecular weight would be a factor affecting the viscosity of polymer solution. The results of runs 42, 53, and 62, with 0.1 percent concentration of polyethylene oxide WSR-35, WSR-205, and WSR-301, and runs 79 and 87, with 0.25 percent concentration of polyacrylamide RC-301 and RC-322, plotted on Figures VI-26 through VI-29, indicate that for the same concentration of a specific type of polymer, the viscosity increase with molecular weight. In practice, this could be a very important factor which must be considered in the design of a polymer flooding program. The use of a relatively small amount of high molecular weight

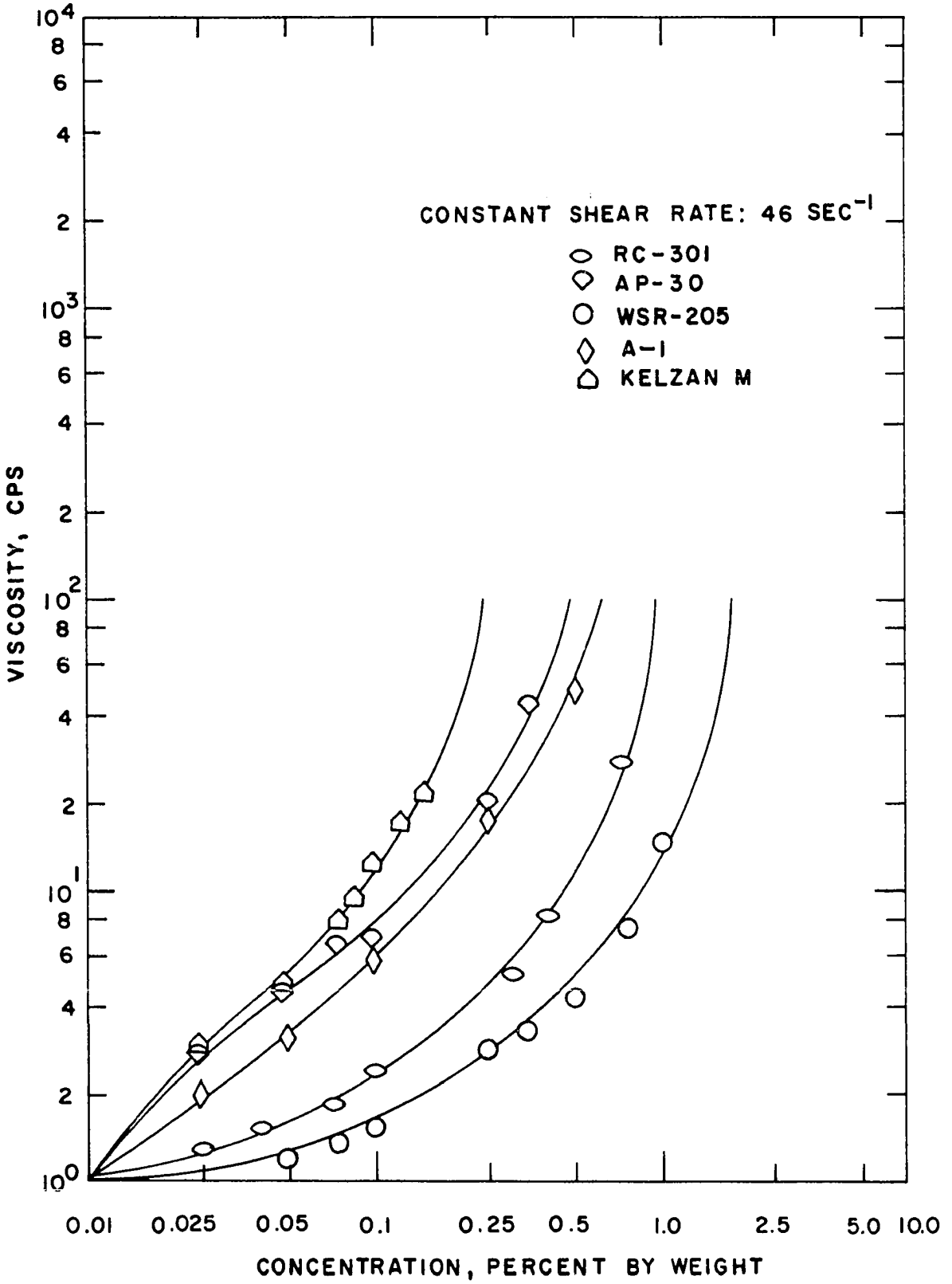

Figure VI-25. Influence of Polymer Concentrations on Solution Viscosity.

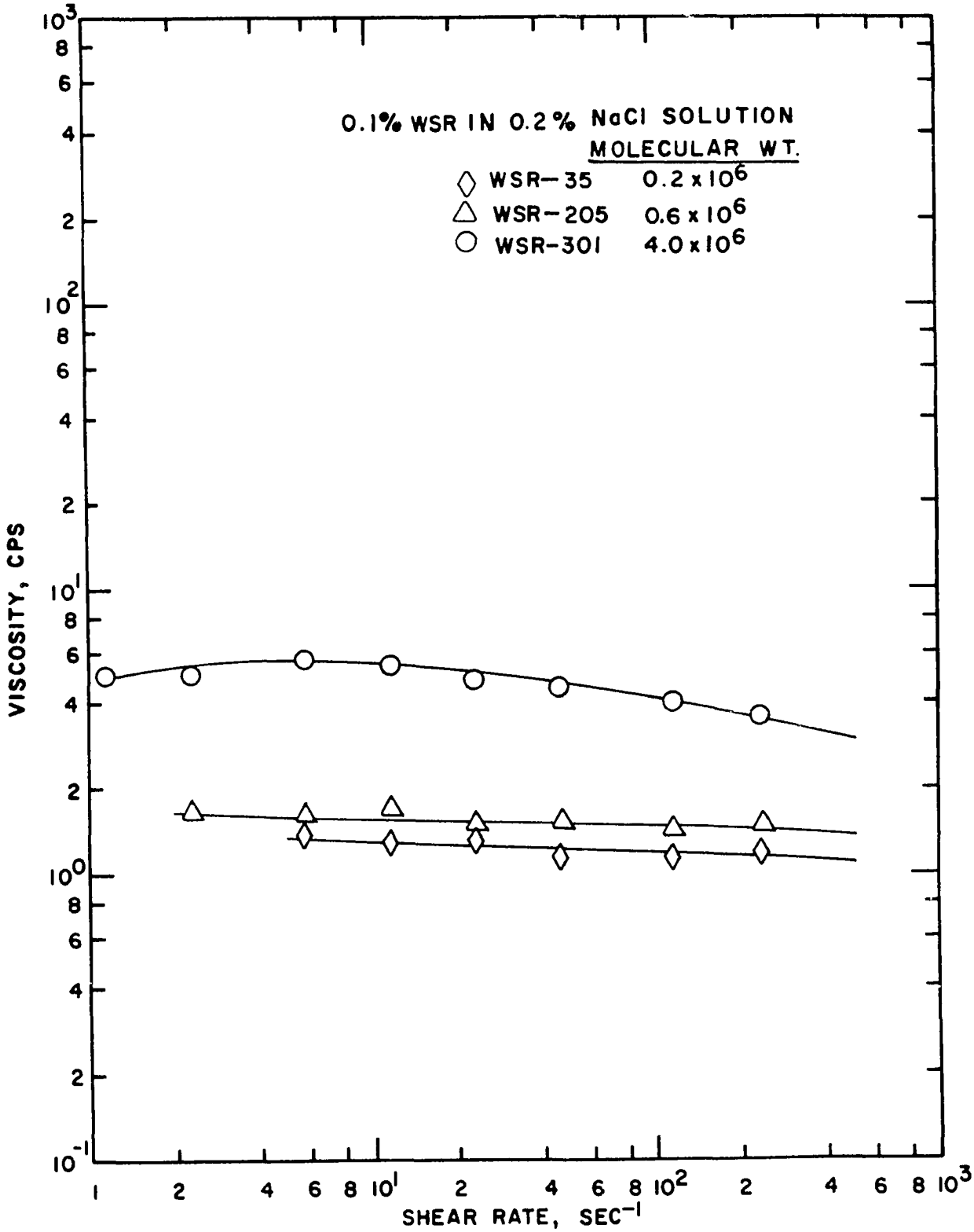

Figure VI-26. Viscosity-Shear Rate Relations of 1.0% "Polyox" WSR with Varying Molecular Weights.

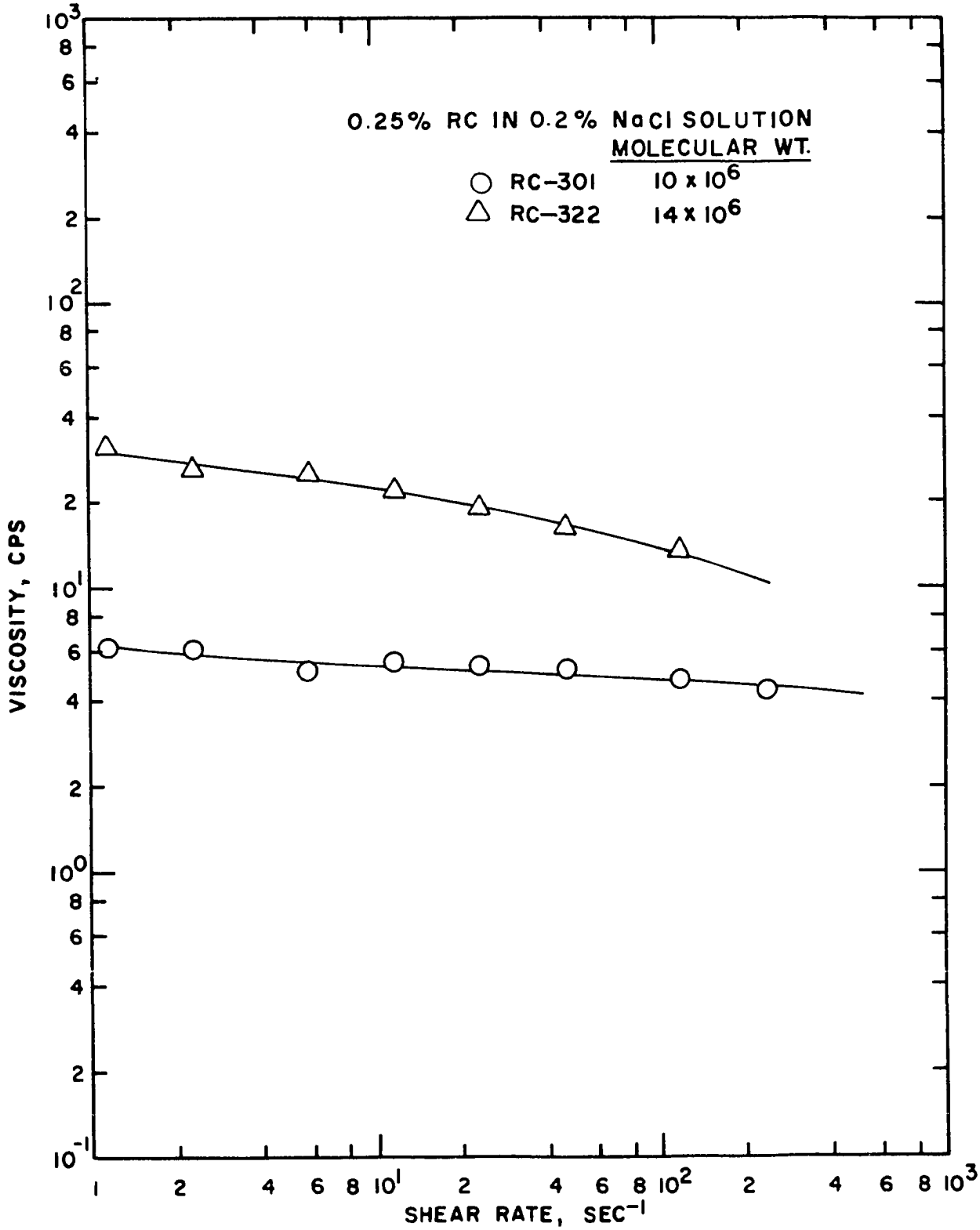

Figure VI-27. Viscosity-Shear Rate Relations of 0.25% RC with Varying Molecular Weights.

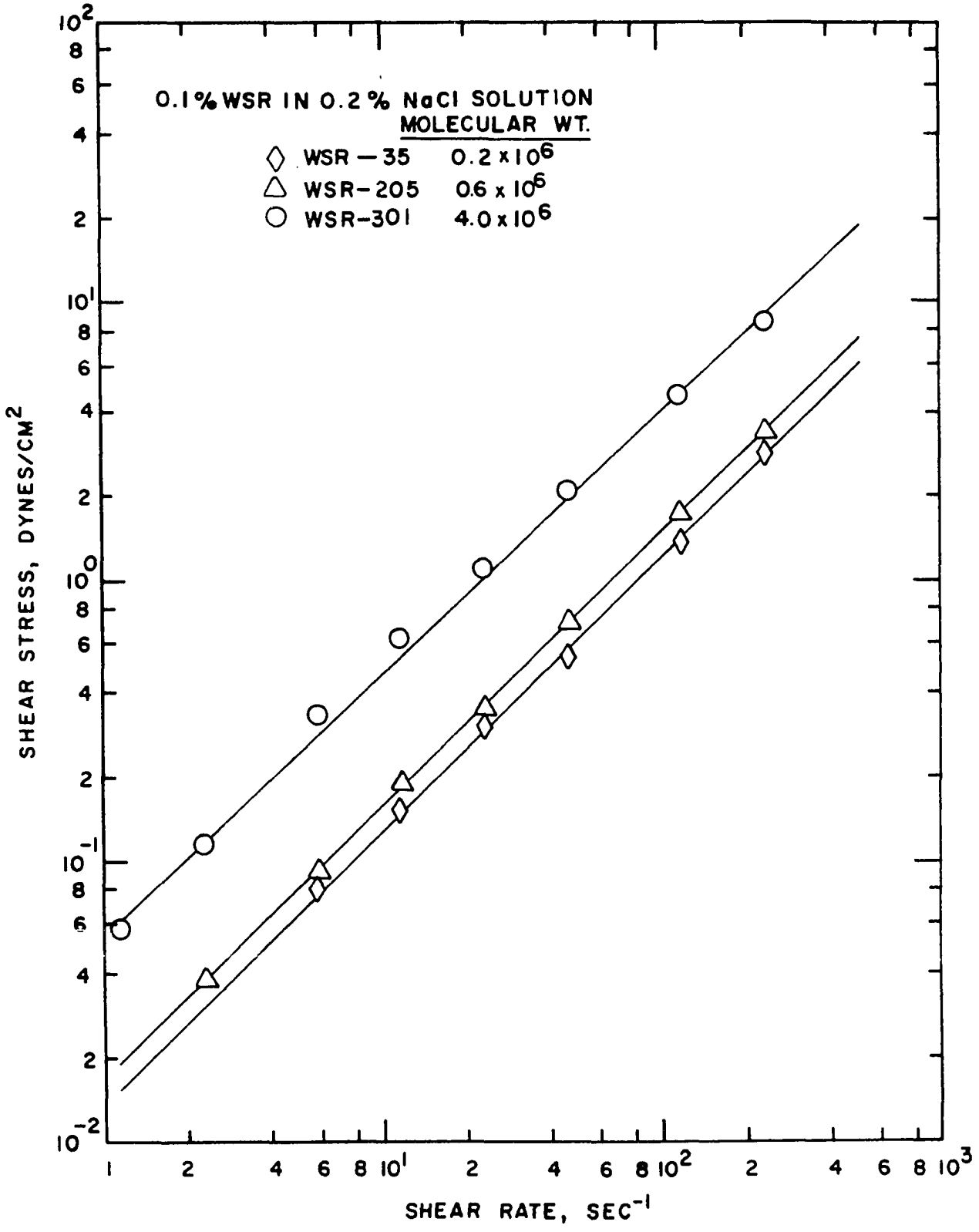

Figure VI-28. Shear Stress-Shear Rate Relations of 0.1% RC with Varying Molecular Weights.

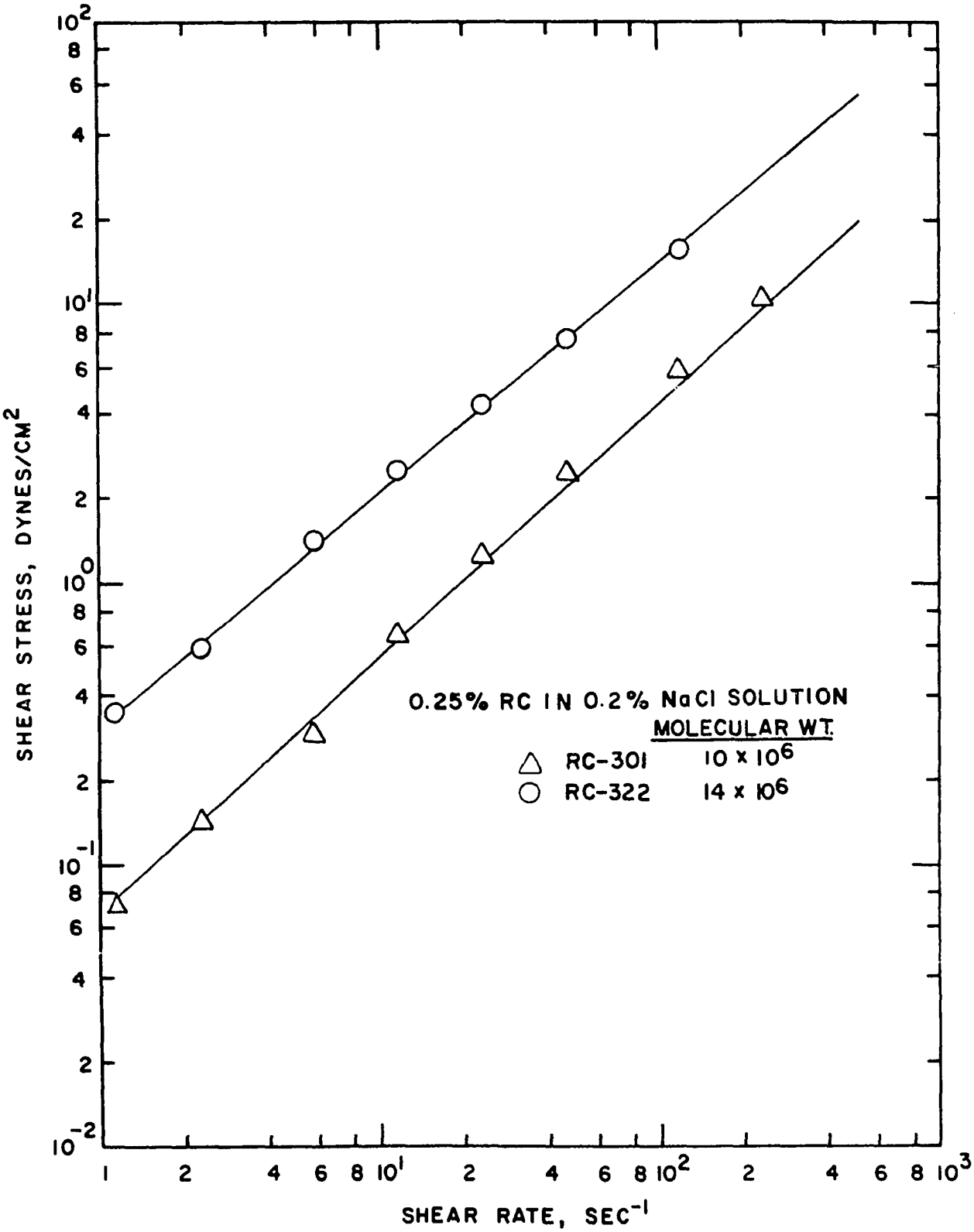

Figure VI-29. Shear Stress-Shear Rate Relations of 0.25% RC with Varying Molecular Weights.

polymer, in a flooding program, would undoubtedly be an economic advantage over that of using a considerable amount of low molecular weight polymer to achieve the desired viscosity.

Effect of Salinity on Polymer Solution Viscosity

The indirect effect of sodium chloride concentration on solution viscosity has been discussed previously (29,53, 76). It has been pointed out that, there exist some self-repelling electrical charges within the particles of the solutions of the ionic polymers (polyelectrolytes) which cause them to expand in rod-like or cylindrical configuration. The rod-like particles when entangled with one another give rise to high solution viscosity. Mungan (53) explained that addition of salt to the polyelectrolyle solutions would neutralize the electrical charge within the particles. As the net charge of the polymer molecules decreases, the self repelling forces within the molecules are diminished and the molecules assume a more nearly spherical shape. The change in shape and size of the particles in turn results in a lower solution viscosity. Gogarty (29), who has also studied the effect of salinity on molecular size, concludes that large increases in the viscosity of solution result from small changes in polymer particle size as NaCl concentration is lowered.

The results of the series of experimental runs made on solutions of three different polymers, with varying degrees

of salinity, are given in Figures VI-30 through VI-33 and summarized in Tables B-89 through B-109 of the Appendix B. For each series of runs the polymer concentration was kept constant, while NaCl concentration increased. As can be seen from these figures there appears to be an unusually sharp decrease in solution viscosity and its shear dependence with increasing NaCl concentration. This is specifically indicated by Figure VI-33 which also shows that, regardless of the type of polymer tested, the sharp decrease in viscosity of the solution appeared to reach a maximum limit, at about 4 percent NaCl concentration, after which a small increase in solution viscosity is observed. It is the author's opinion that the reversal and increase in solution viscosity at higher NaCl concentration could be essentially attributed to the high percentage of dissolved salt not the polymer behavior.

Effect of Temperature on Polymer Solution Viscosity

Although in practice the secondary recovery of oil by polymer flooding is performed under reservoir temperature, which is essentially much higher than the surface temperature, little experimental work on the effect of reservoir temperature on polymer solution behavior has been published.

To study the temperature effect, a total of five different polymer solutions (partially hydrolyzed polyacrylamide NP-10, A-1 and RC-301, polyethylene oxide WSR-301 and Polysaccharide "Kelzan" M) were tested. The results of

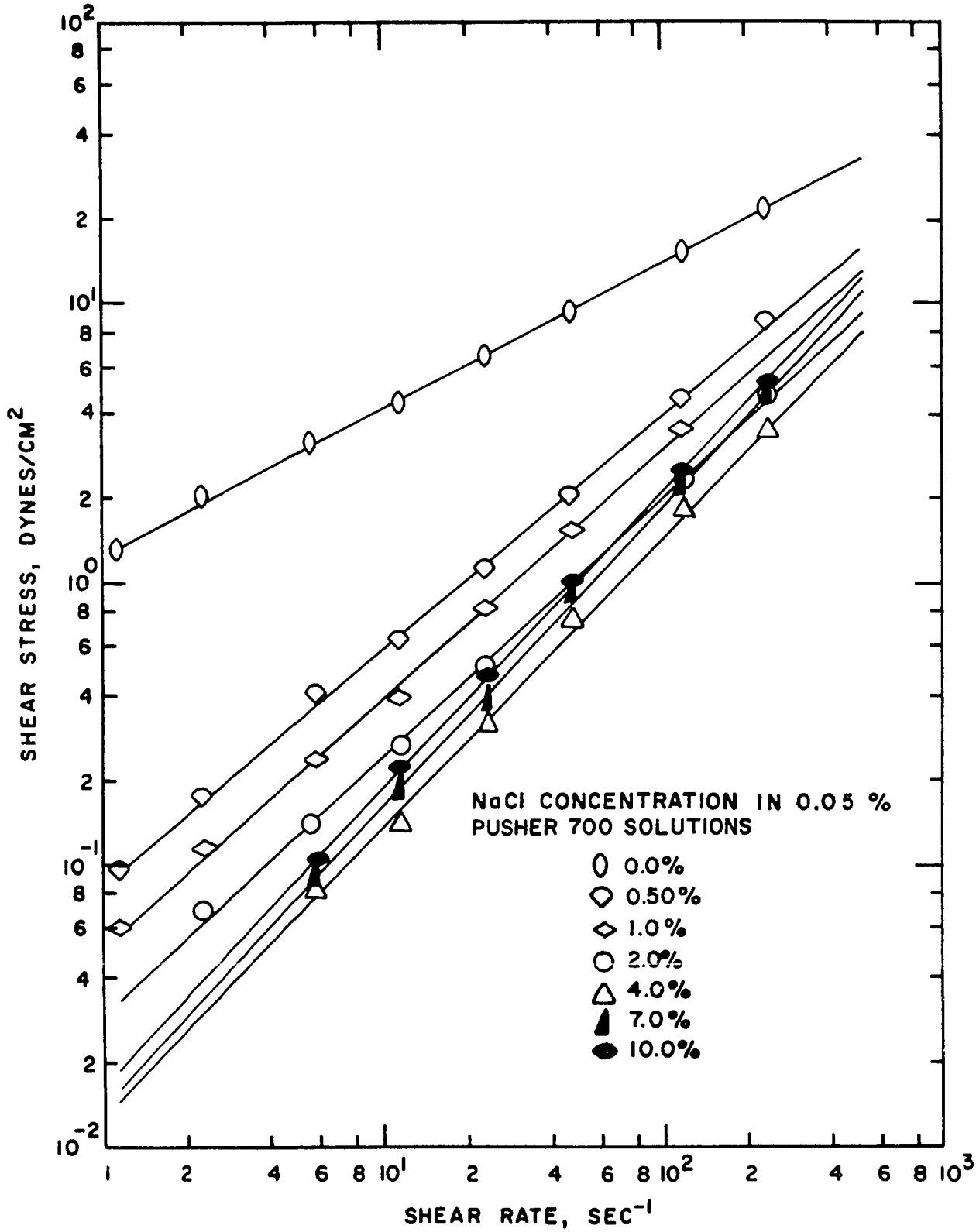

Figure VI-30. Shear Stress-Shear Rate Relations of 0.05% Pusher 700 in Varying NaCl Concentrations.

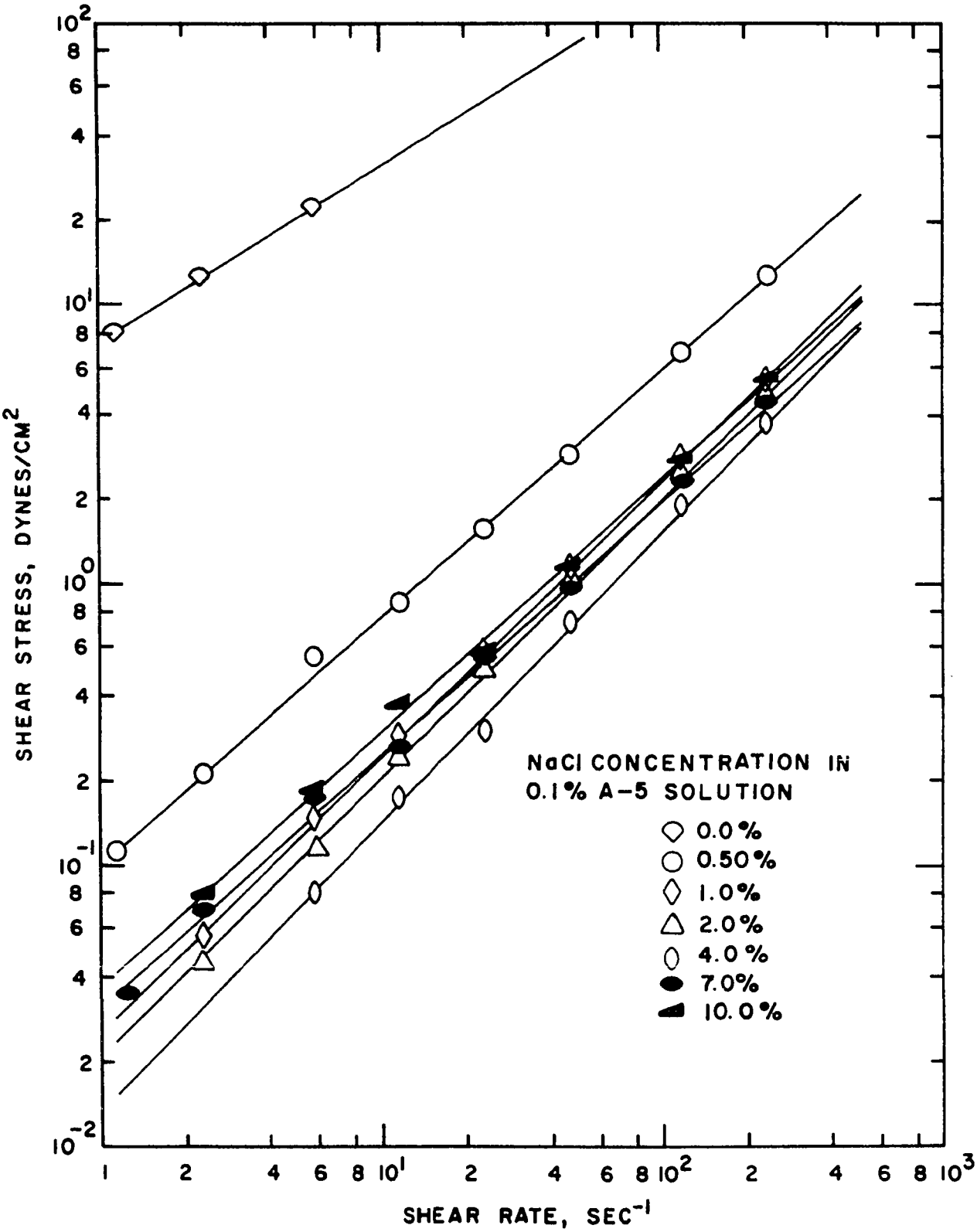

Figure VI-31. Shear Stress-Shear Rate Relations of 0.1% "Reten" A-5 in Varying NaCl Concentrations.

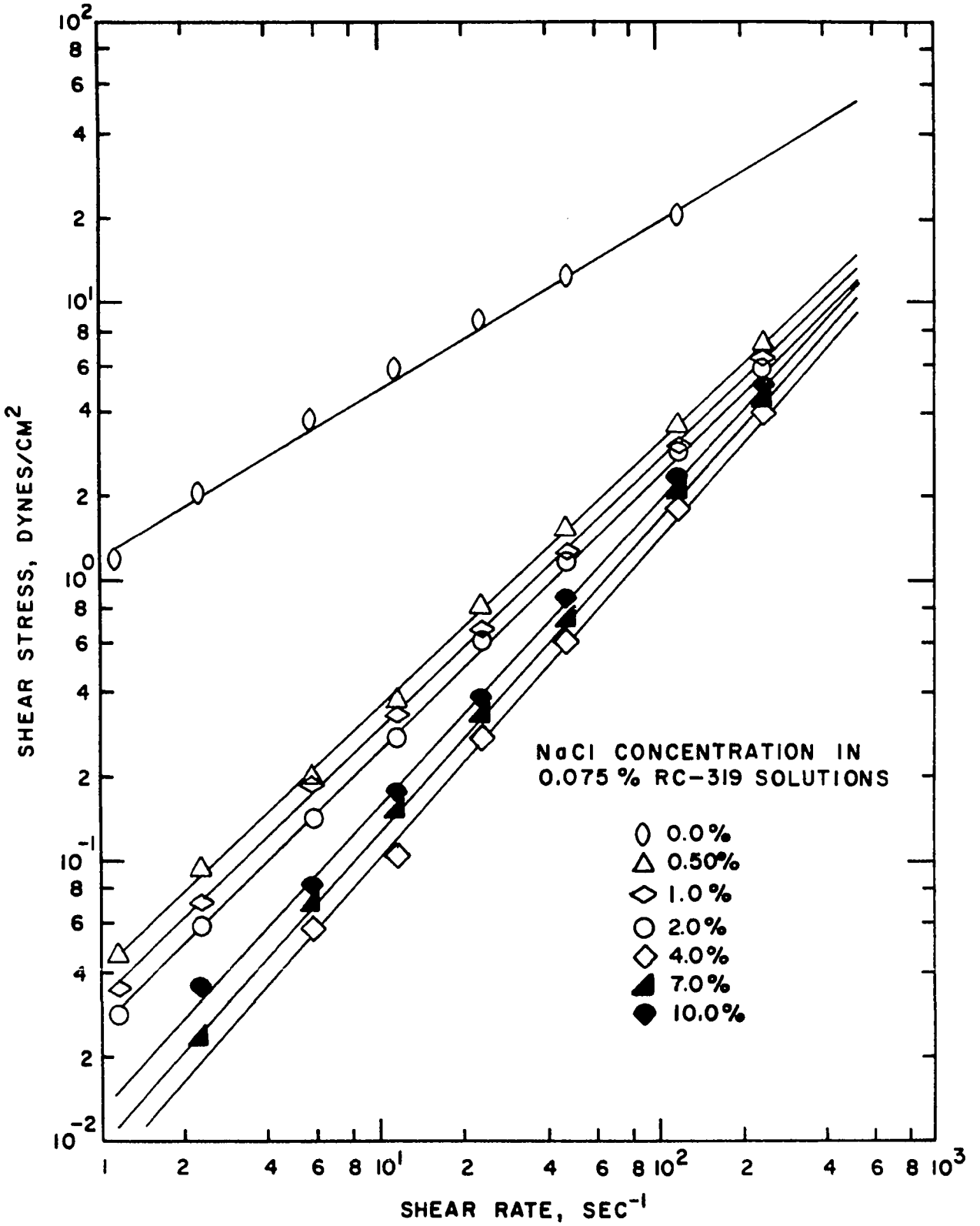

Figure VI-32. Shear Stress-Shear Rate Relations of 0.075% RC-319 in Varying NaCl Concentrations.

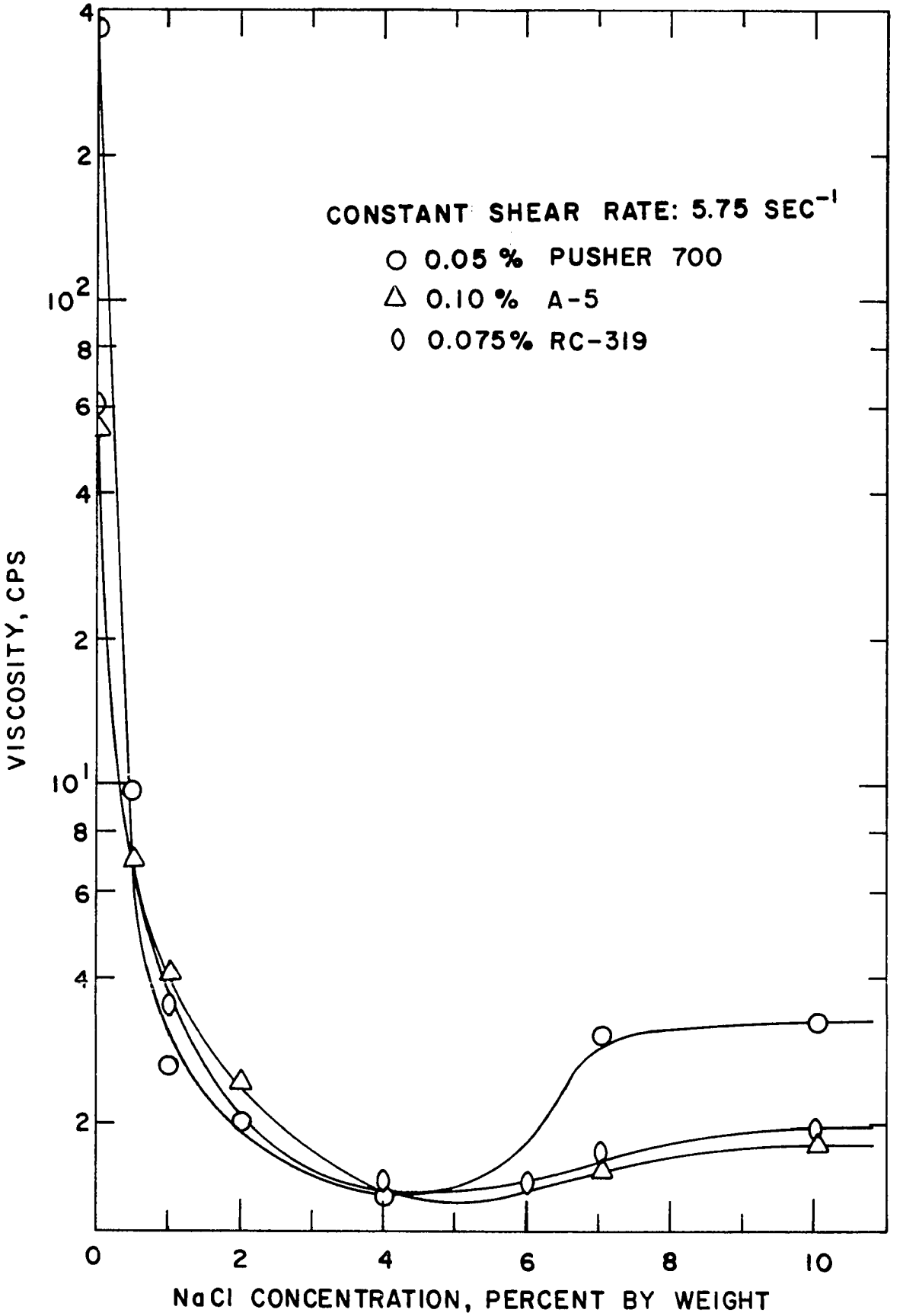

Figure VI-33. Influence of NaCl Concentration on Solution Viscosity.

these tests are shown in Figures VI-34 through VI-39 and tabulated in Tables B-110 through B-132 of Appendix B. As it can be seen from these results polymer solution viscosity and its shear dependence decrease with increasing temperature. Under the limited range of temperature tested, Figure VI-39 clearly indicates that, depending upon the nature of polymer, the degree of hydrolyzation, concentration and its molecular weight, the rheological behavior of each solution, due to the temperature rise, was found to be uniquely different from the others. The fact that the viscosity-temperature curves do not follow a specific pattern is a clear indication pointing to the fallacy of the conclusions drawn by Smith (76) who argued that the polymer contribution to flow resistance in porous media is nearly independent of temperature and by Mungan (53) who explained that the decrease in viscosity of a polymer solution is due simply to the decrease in the viscosity of water as the temperature is increased. Because, had the reduction in solution viscosities been due simply to the solution water, it was necessary for all the curves in Figure VI-39 to have the same shape which is not apparently the case in this investigation. Obviously reservoir temperature is a factor affecting the solution viscosity and must be certainly weighted among other factors such as polymer concentration, molecular weight, degree of hydrolyzation and the salt concentration.

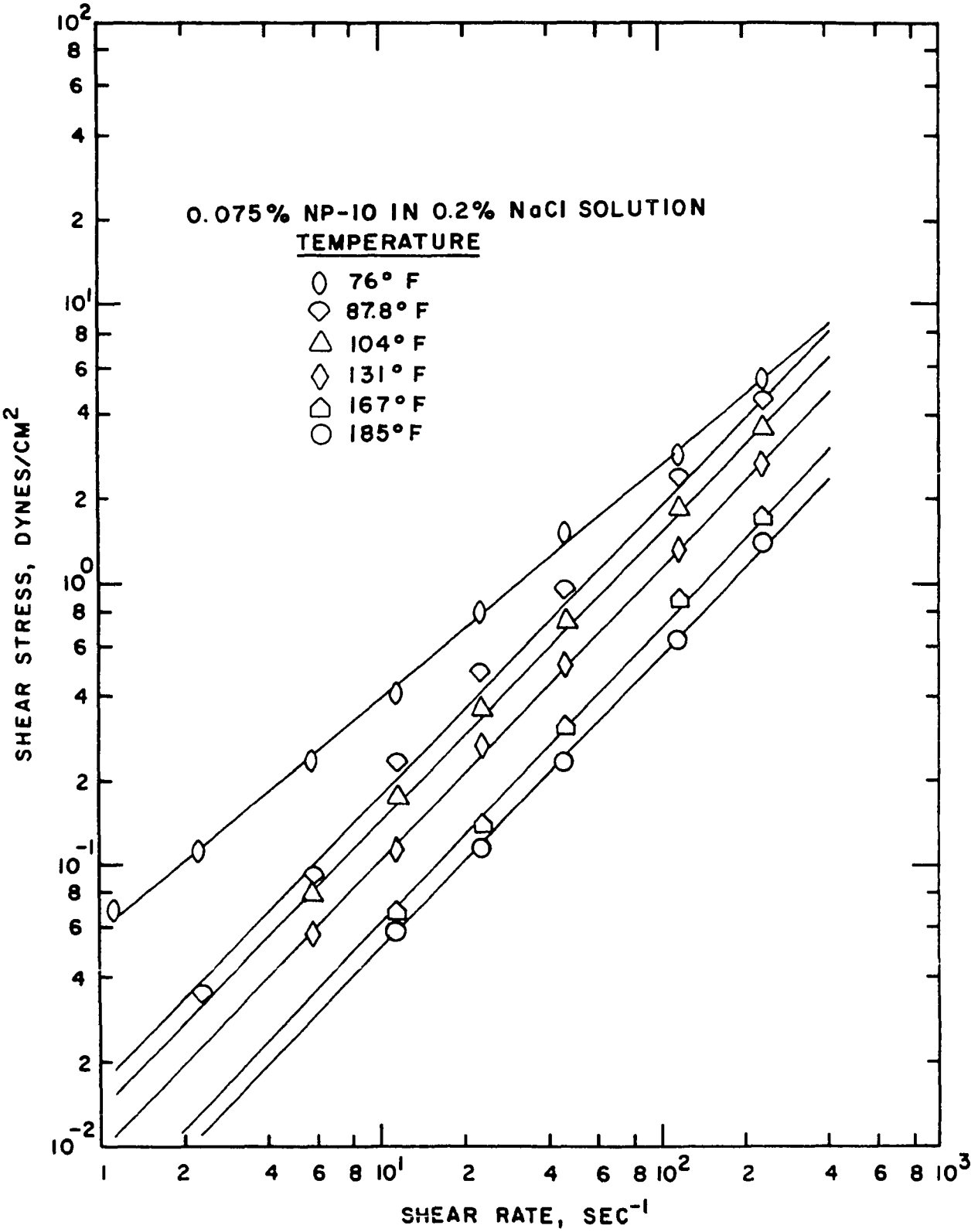

Figure VI-34. Shear Stress-Shear Rate Relations of 0.075% "Separan" NP-10 at Elevated Temperatures.

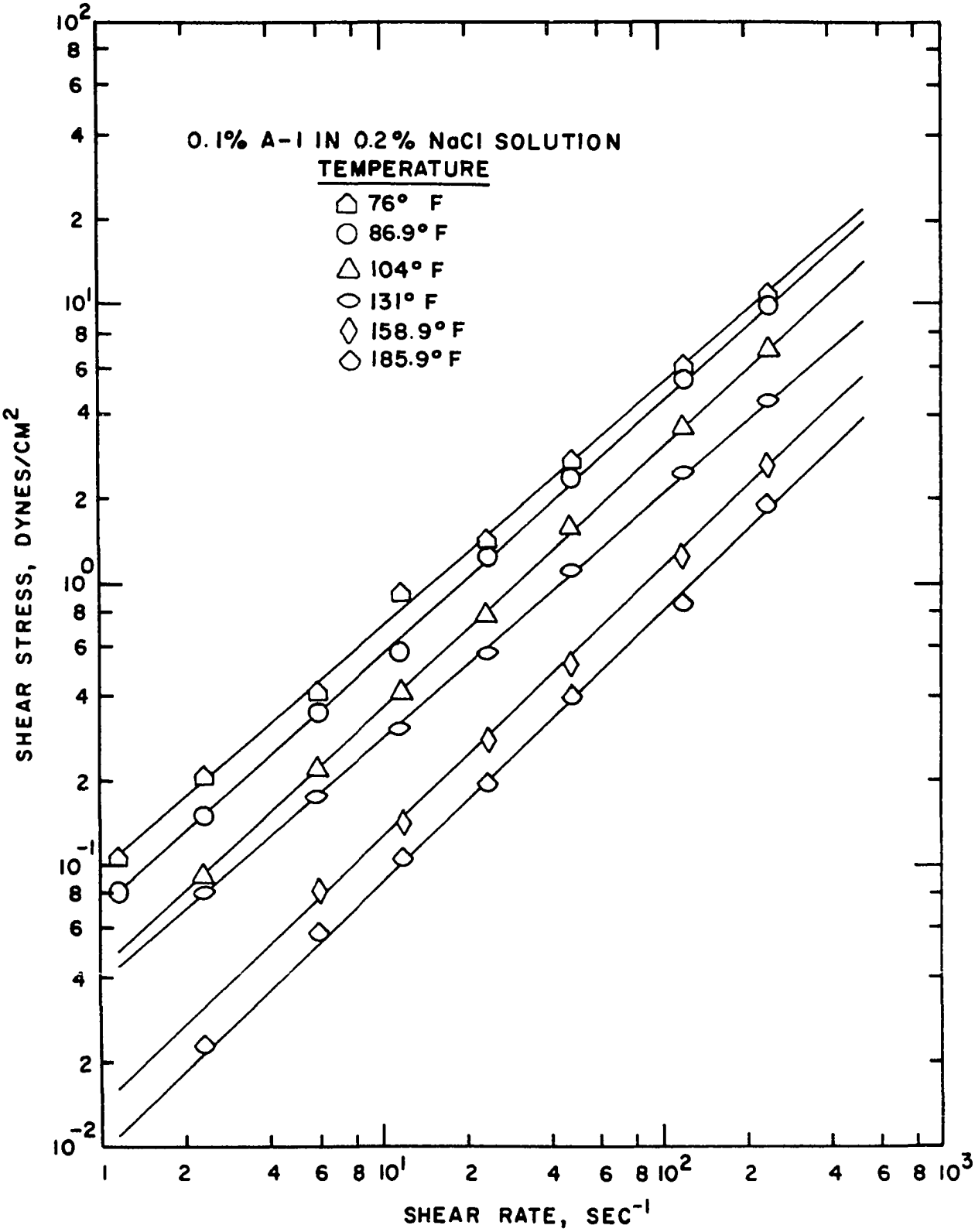

Figure VI-35. Shear Stress-Shear Rate Relations of 0.1% "Reten" A-1 at Elevated Temperatures.

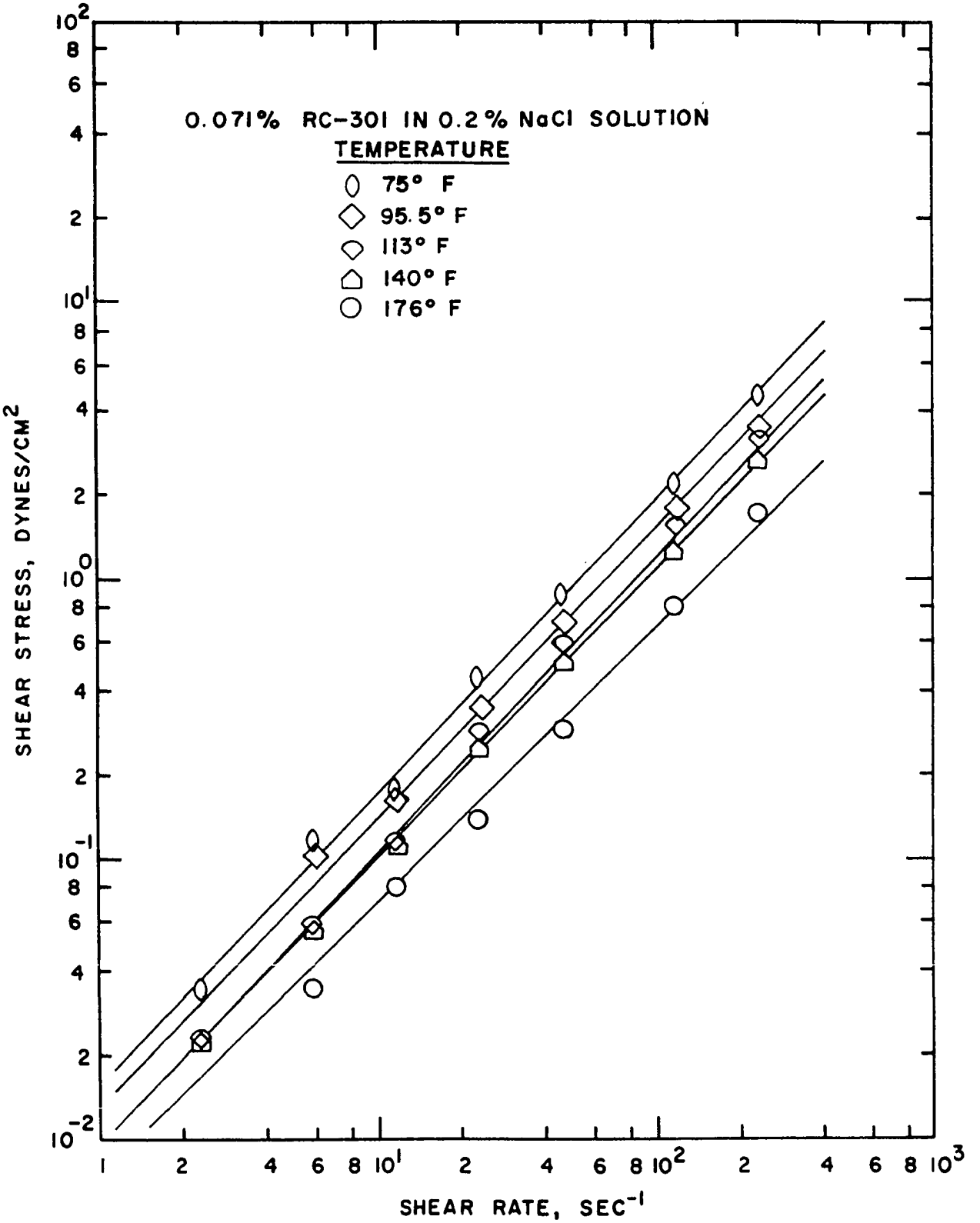

Figure VI-36. Shear Stress-Shear Rate Relations of 0.071% RC-301 at Elevated Temperatures.

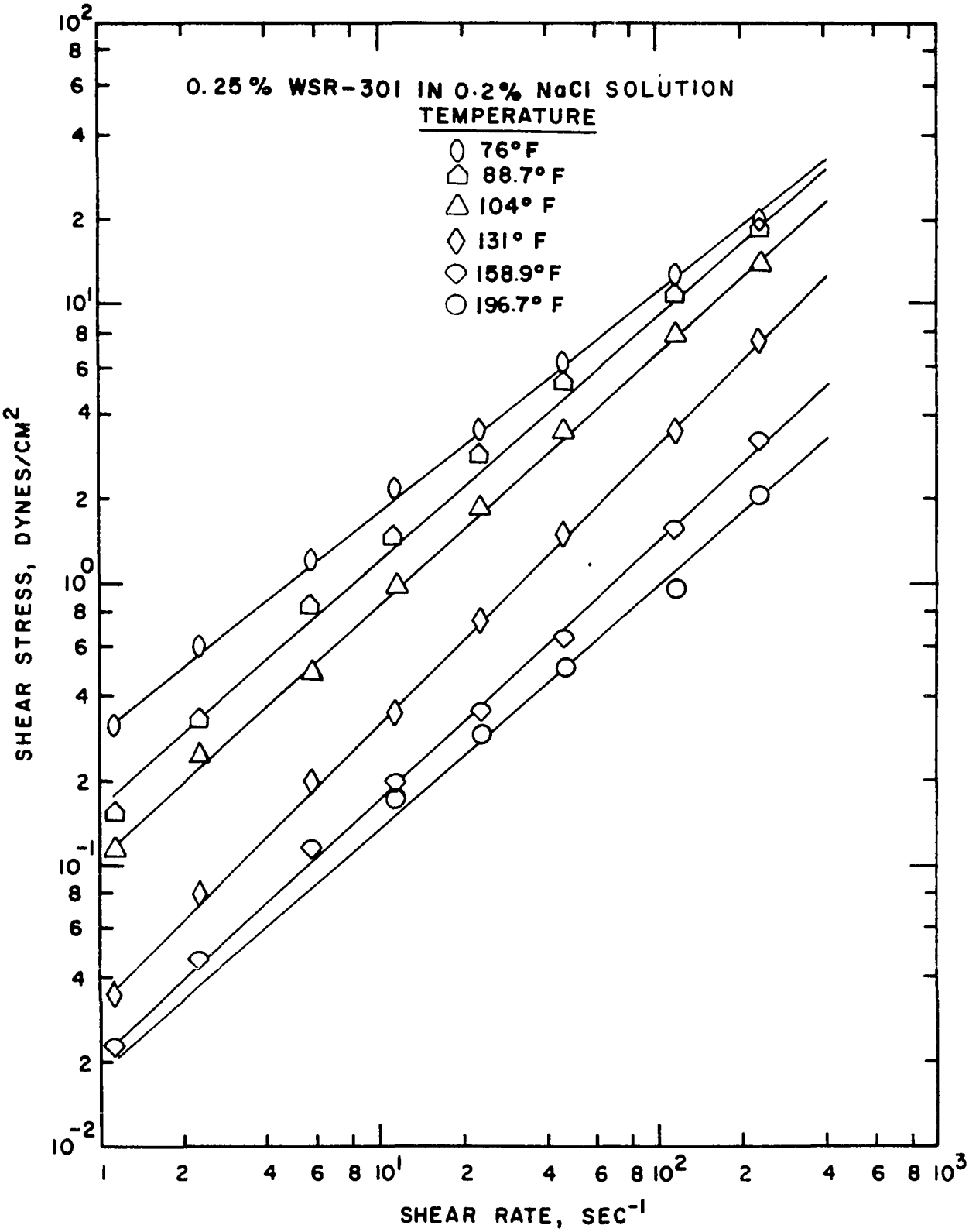

Figure VI-37. Shear Stress-Shear Rate Relations of 0.25% "Polyox" WSR-301 at Elevated Temperatures.

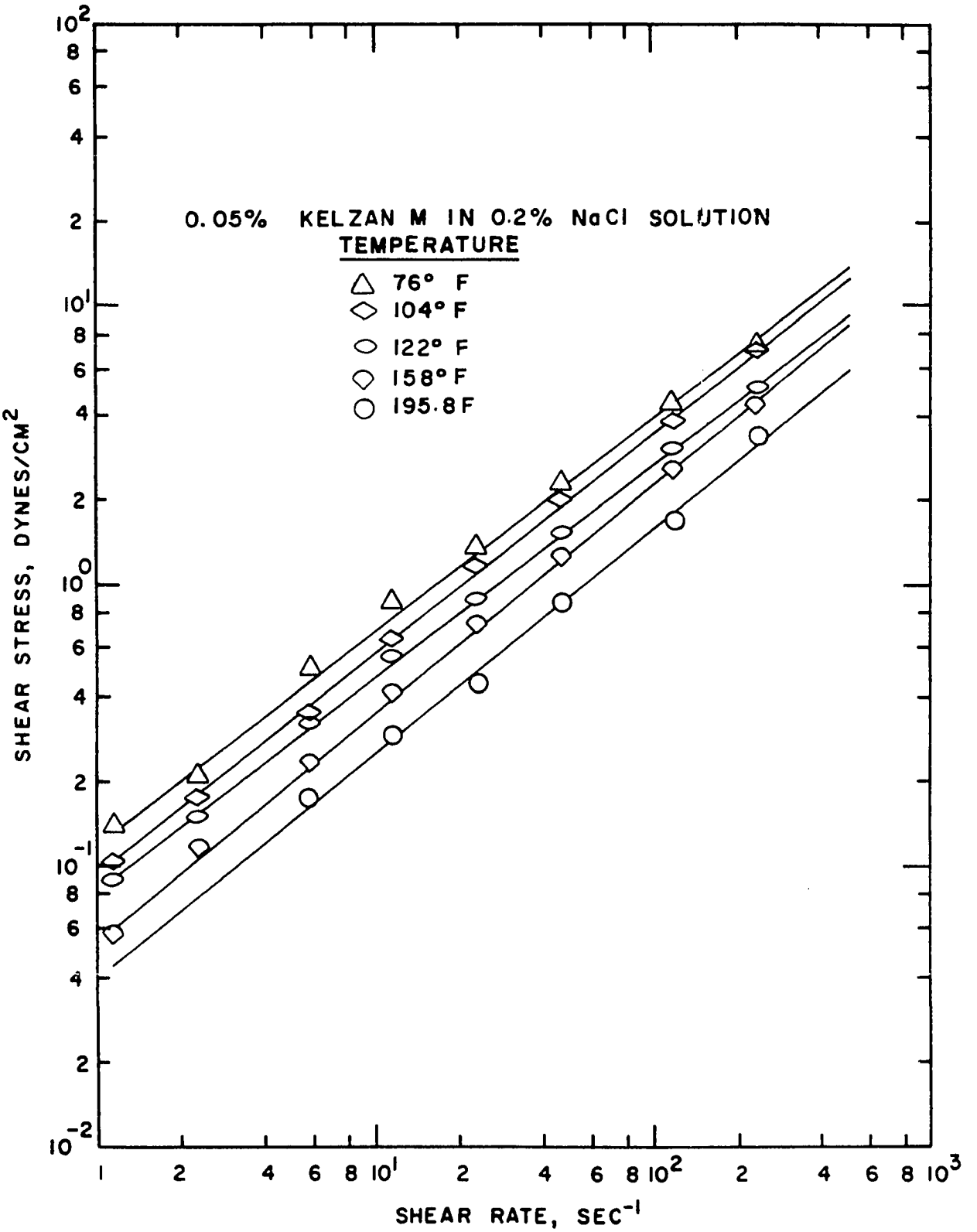

Figure VI-38. Shear Stress-Shear Rate Relations of 0.05% Kelzan M at Elevated Temperatures.

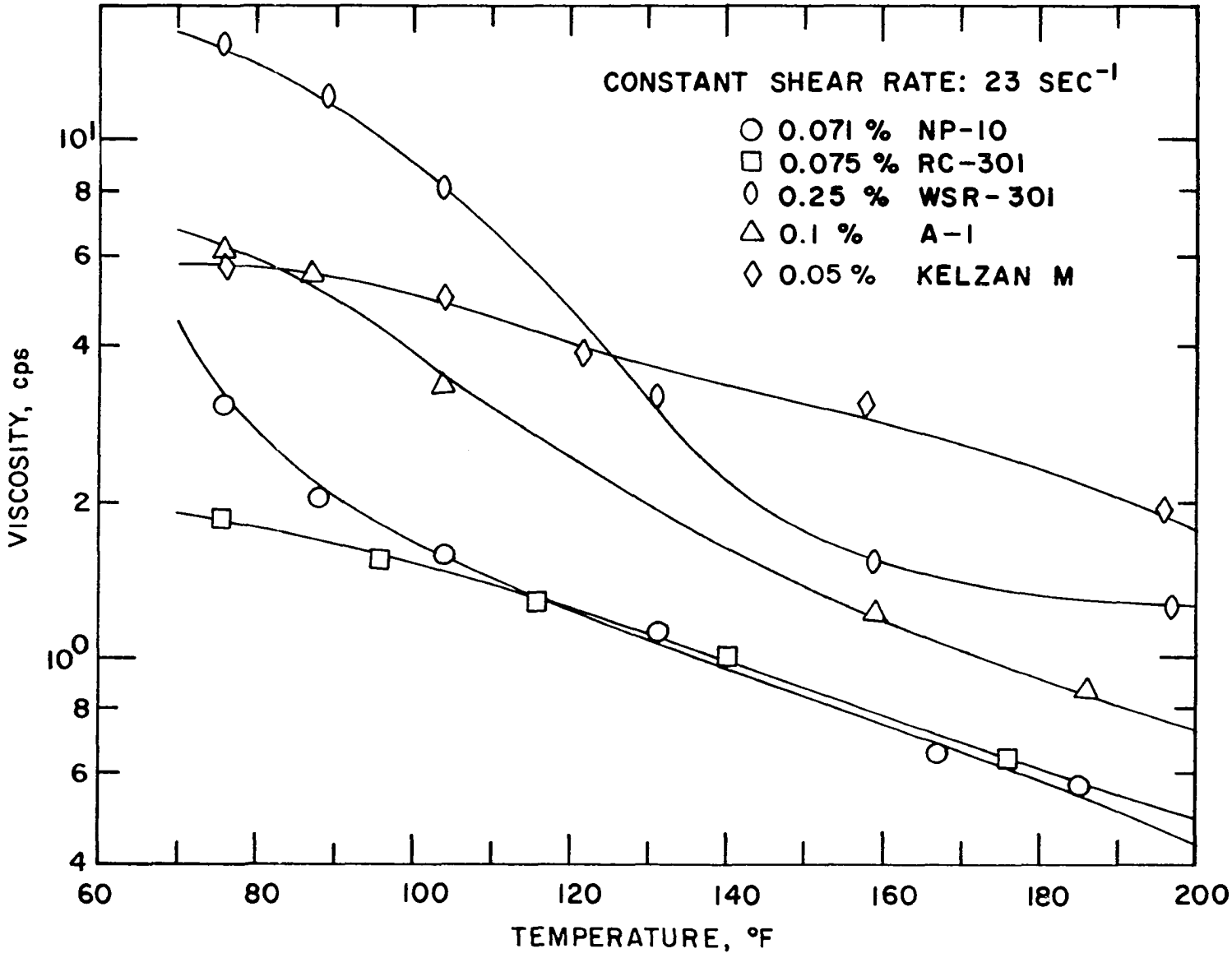

Figure VI-39. Effect of Temperature on Polymer Solution Viscosity.

A short review of literature (37) indicated that successful polymer floodings have been performed under reservoir temperature as high as 229°F. It is a general opinion that polymer flooding at higher reservoir temperatures is also possible, provided a maximum limit of 300°F is not reached. This is believed to be the temperature at which most of the polymer molecules decompose.

2. POLYMER SOLUTION DISPLACEMENT PROCESSES

Polymer Solution Behavior in Porous Media

The basic study of the flow of fluid through porous media was initiated by H. D'Arcy in 1856. He experimented on the flow of liquid through sand filters, which resulted in a basic equation of the flow of laminar fluid through porous media still used today. The D'Arcy's equation in its vector form, neglecting gravitational force, may be written as:

$$\bar{V}_o = - \lambda \Delta P \qquad (6\text{-}4)$$

where $\bar{V}_o$ is the fluid velocity vector, ΔP is the pressure gradient, and λ is the constant of proportionality. Through the extensive studies of the flow of laminar fluid through porous media, the constant λ was found to be dependent upon the properties of the fluid and the porous media. Consequently, it was replaced by the ratio $\frac{K}{\mu}$. Where K is the permeability, a property of the porous media, and μ is the fluid viscosity.

The Equation 6-4 then becomes:

$$\bar{V}_o = - \frac{K}{\mu} \frac{\Delta P}{L} \qquad (6\text{-}5)$$

For one dimensional flow of linear fluid through porous media of length L, the D'Arcy's equation may be expressed as:

$$V_o = - \frac{K}{\mu} \frac{\Delta P}{L} \qquad (6\text{-}6)$$

By replacing the velocity, V_o, by Q/A, where Q is the rate of flow of fluid, and A is the cross-sectional area of porous media, the Equation 6-6 results in a more familiar expression:

$$Q = - \frac{K}{\mu} \frac{A\Delta P}{L} \qquad (6\text{-}7)$$

For many years this simple form of D'Arcy's equation has been successfully used to describe the linear flow of Newtonian fluids through porous media. For non-Newtonian fluids, because of the viscosity variation with shear rate, Equation 6-7 has failed to accurately express the fluid flow behavior in porous media. So a number of modified D'Arcy equations, more applicable to the flow of non-Newtonian fluids through porous media, have been proposed. Some of the most important of them are reviewed elsewhere (18). A polymer solution, which is one of the most complicated non-Newtonian fluids presents still another difficulty, the permeability is

apparently altered. Lately it has been noted (11,18,53,62, 67) that some of the polymer will adsorb to the rock surfaces inside the porous matrix. Adsorption reduces the size of the pore openings which in turn reduces the original rock permeability. Therefore, in the case of the flow of non-Newtonian polymer solutions through porous media it is impossible to distinguish between a change in the solution viscosity and a reduction in the rock permeability. In recent years, the combined ratio $\frac{K}{\mu}$ (mobility) has been extensively used as a single parameter to characterize the flow properties of a particular polymer solution-porous system. In 1964 Pye (62) experienced a rather unusual response in flowing aqueous solutions of polyacrylamide polymer through porous media. He observed that the apparent viscosity of the polymer solutions calculated from D'Arcy's Equation 6-7 wher much higher than the viscosities determined with an Ostwald viscometer. He referred to this unusual departure from expected response as the resistance property of the polymer and defined it as the ratio of the brine mobility to the polymer solution mobility:

$$R = \frac{K_w/\mu_w}{K_p/\mu_p} = \frac{\lambda_w}{\lambda_p} \qquad (6\text{-}8)$$

Where R is the resistance factor, μ_p is the apparent viscosity of the polymer solution in the core and subscripts w and p refer to the brine and polymer solution respectively. In

doing so he has introduced a manner of expressing the effectiveness of the polymer additives in a secondary recovery program. An increase in resistance factor provides a more favorable mobility ratio which in turn results in a more efficient oil recovery.

In this investigation the resistivity concept proposed by Pye (62) was utilized to study and compare the flow behavior of five different types of polymer solutions through consolidated porous media. Two of these polymers have been used by other investigators. A solution of polyethylene oxide "polyox" WSR-301 used by Dauben (18) for flow through unconsolidated sands and a partially hydrolyzed polyacrylamide believed to be "pusher" 700 has been used by Burcik (7,8,9,10,11) for flow through the Berea discs. For each core two successive floods were conducted. Each core was first flooded with a 2 percent NaCl solution and the brine mobility was determined. The core was then flooded with a particular polymer soluiton over a wide range of pressure drop increments and the polymer solution mobility at each pressure increment was also calculated. (See Chapter V for more detailed description of the procedure.) The results of these experimental runs, presented in the form of resistance factor versus superficial velocity, are shown in Figures VI-40 through VI-52 and summarized in Tables C-1 through C-16 of Appendix C. As it is indicated by these figures, except for the solution of 0.05 percent partially

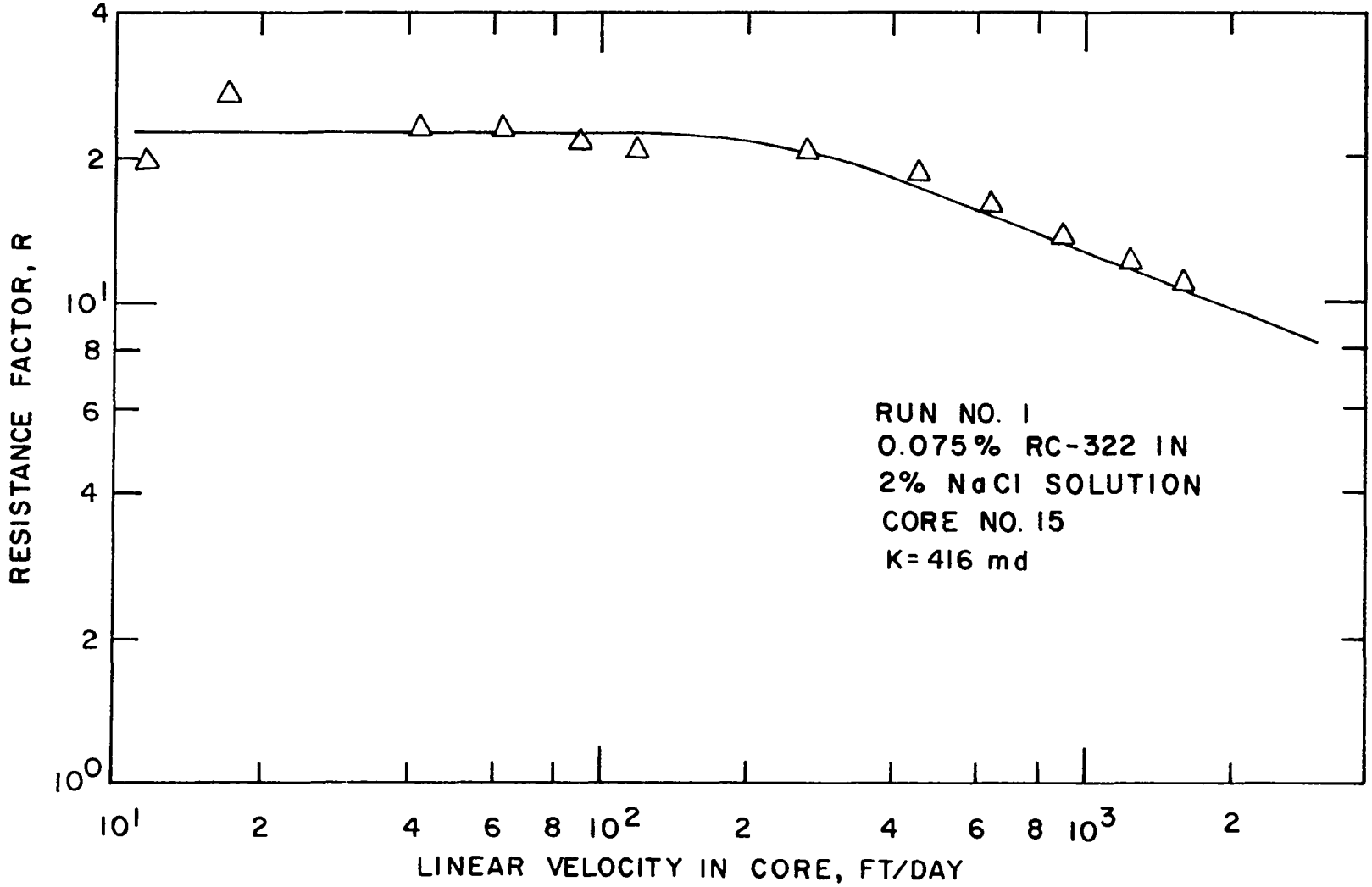

Figure VI-40. Influence of Flooding Velocity on Resistance Factor For 0.075% RC-322.

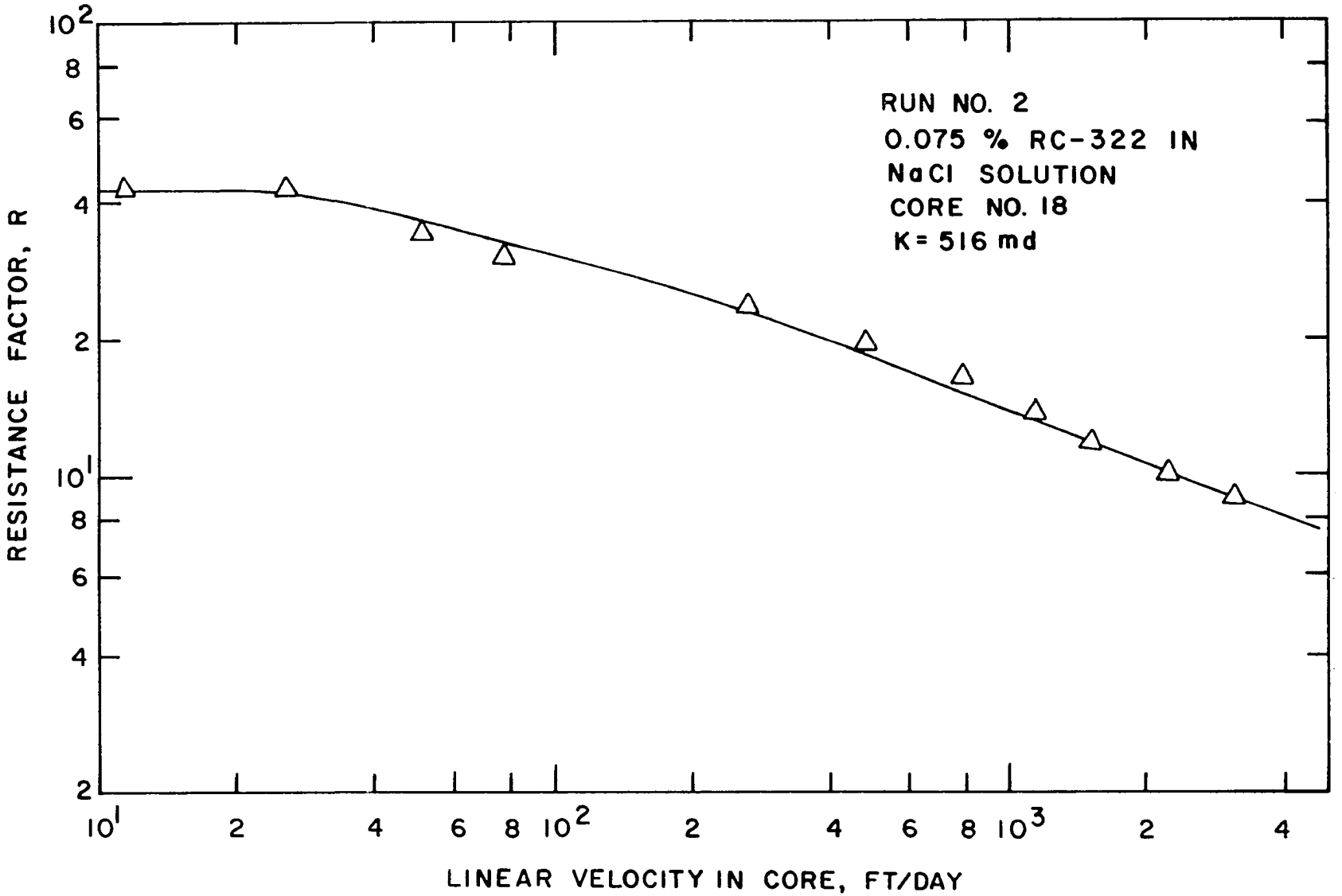

Figure VI-41. Influence of Flooding Velocity on Resistance Factor For 0.075% RC-322.

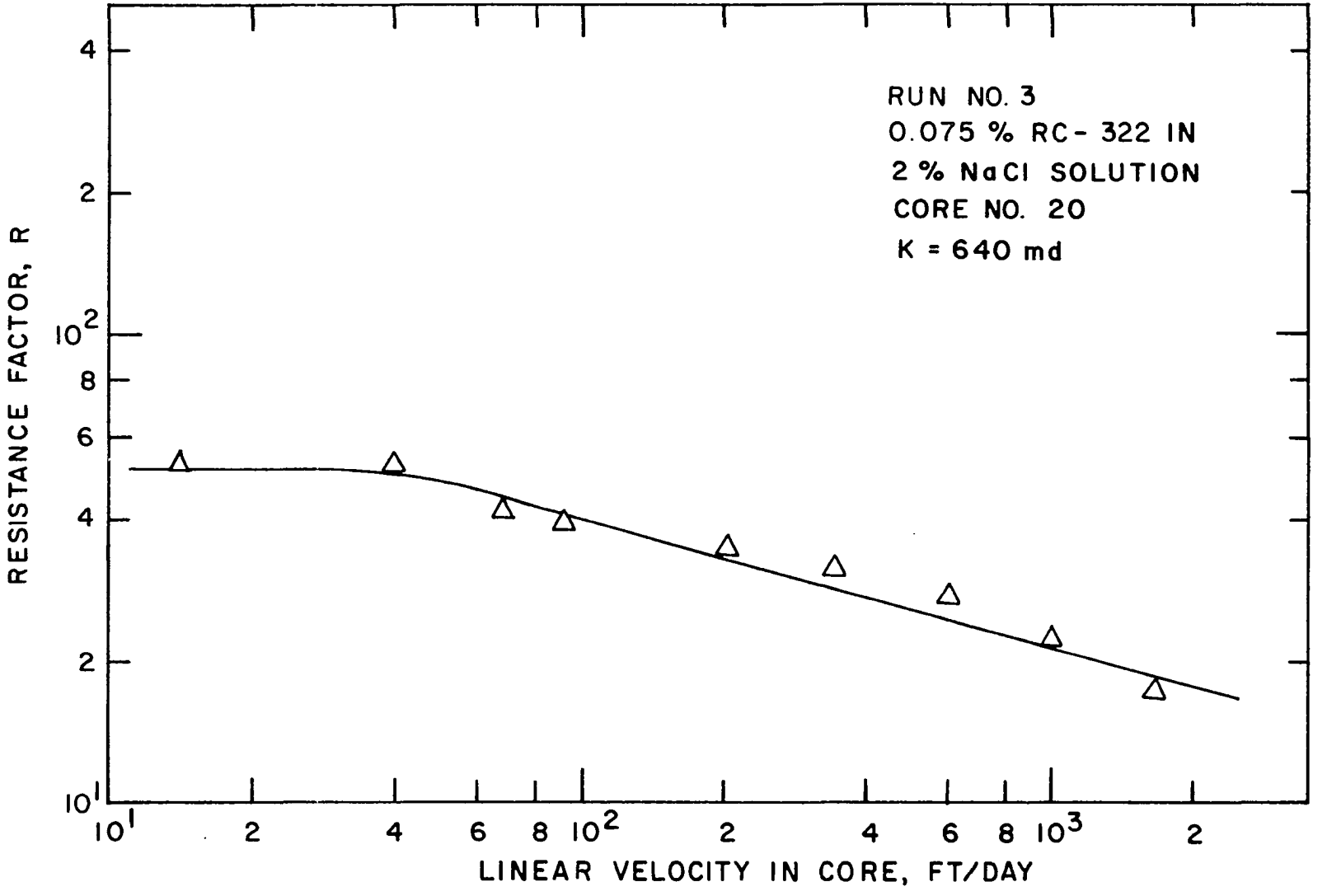

Figure VI-42. Influence of Flooding Velocity on Resistance Factor For 0.075% RC-322.

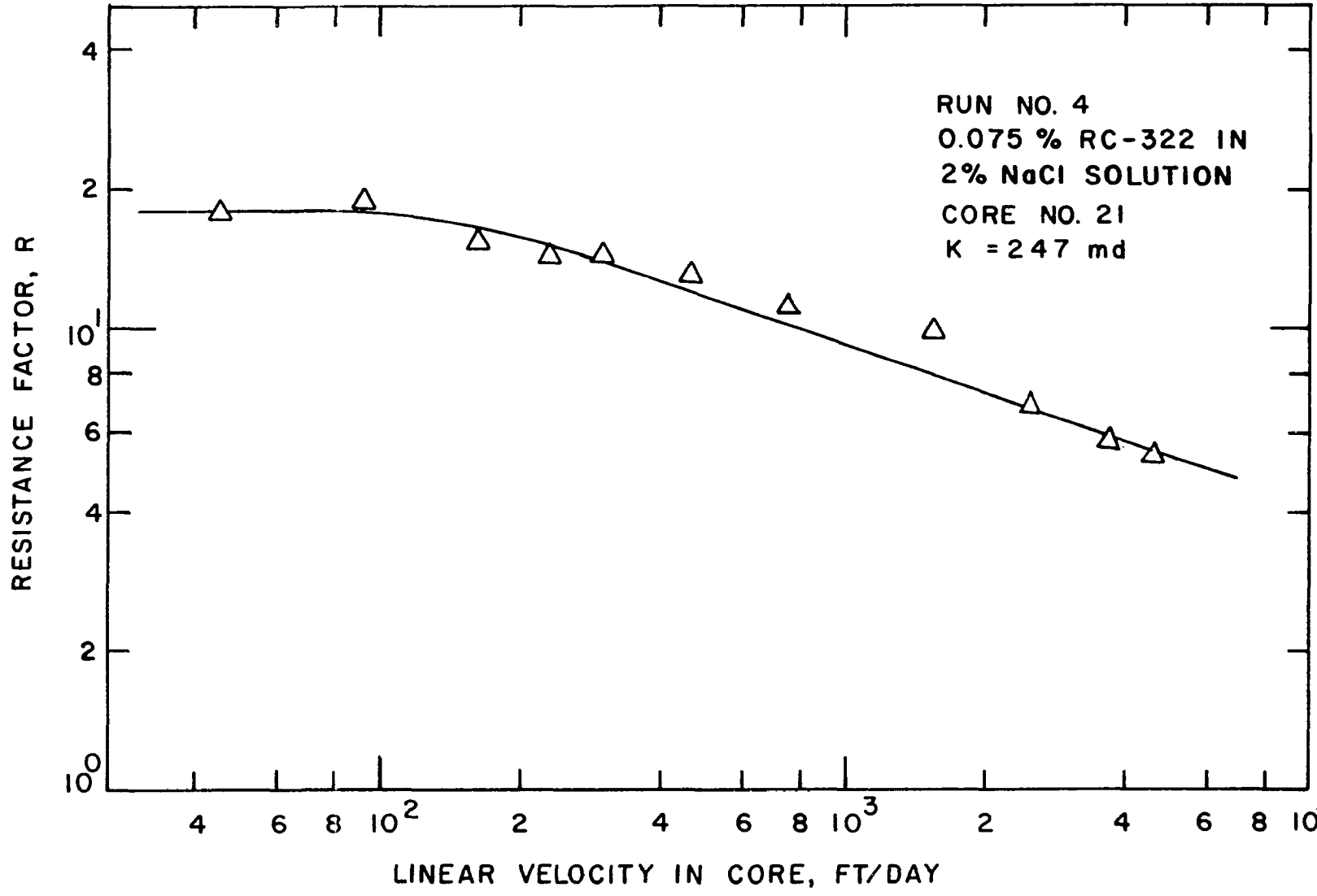

Figure VI-43. Influence of Flooding Velocity on Resistance Factor For 0.075% RC-322.

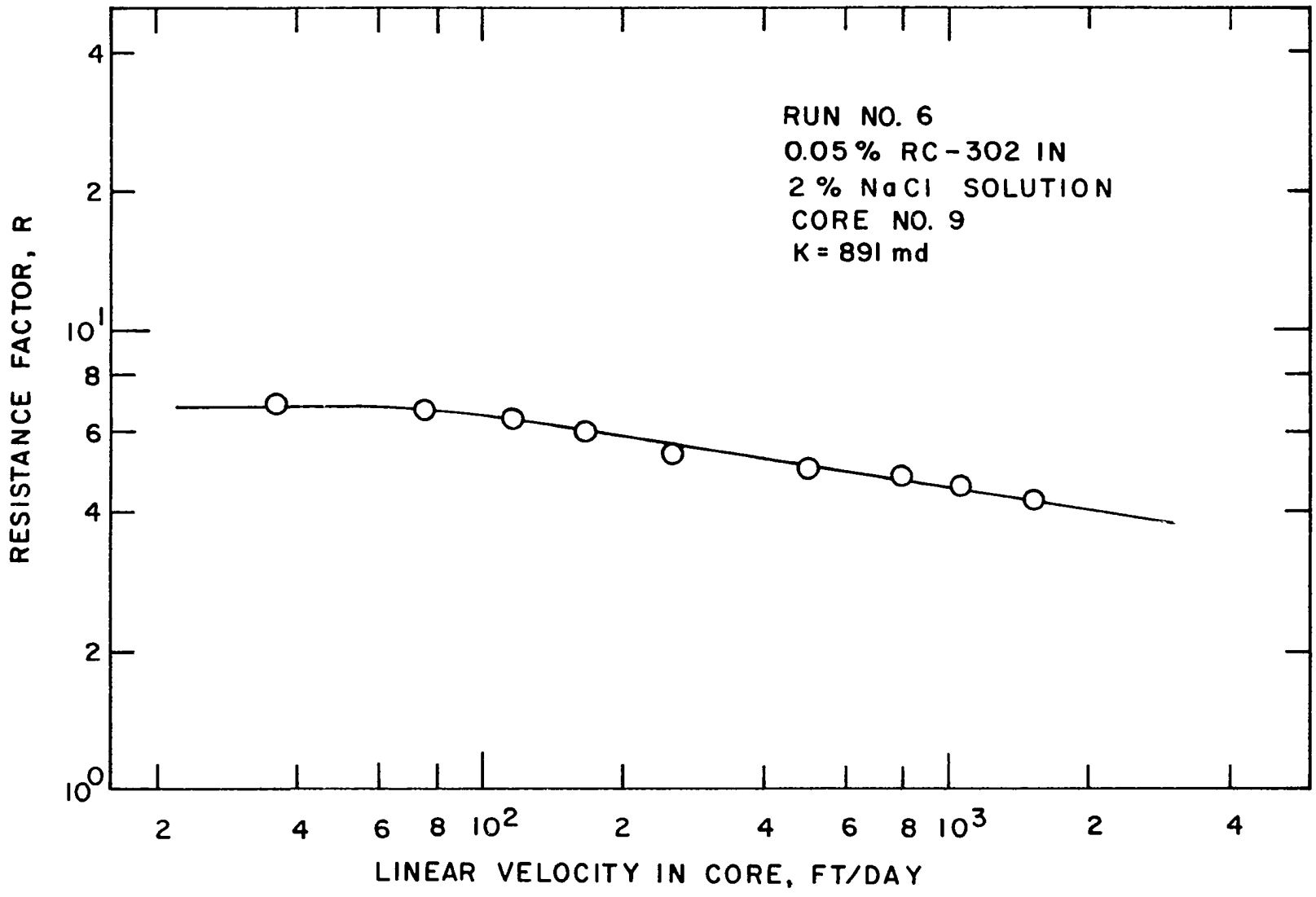

Figure VI-44. Influence of Flooding Velocity on Resistance Factor For 0.05% RC-302.

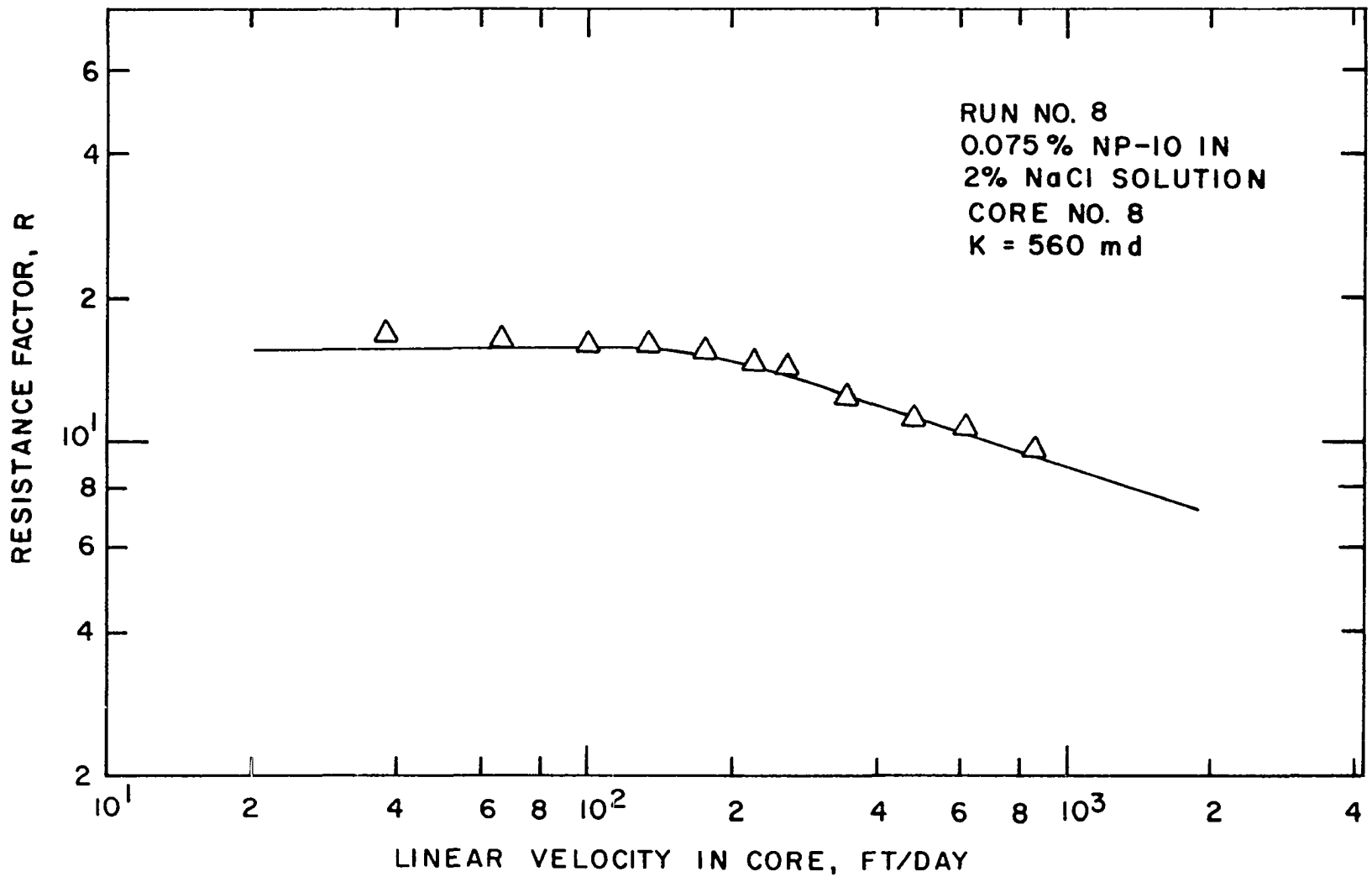

Figure VI-45. Influence of Flooding Velocity on Resistance Factor For 0.075% "Separan" NP-10.

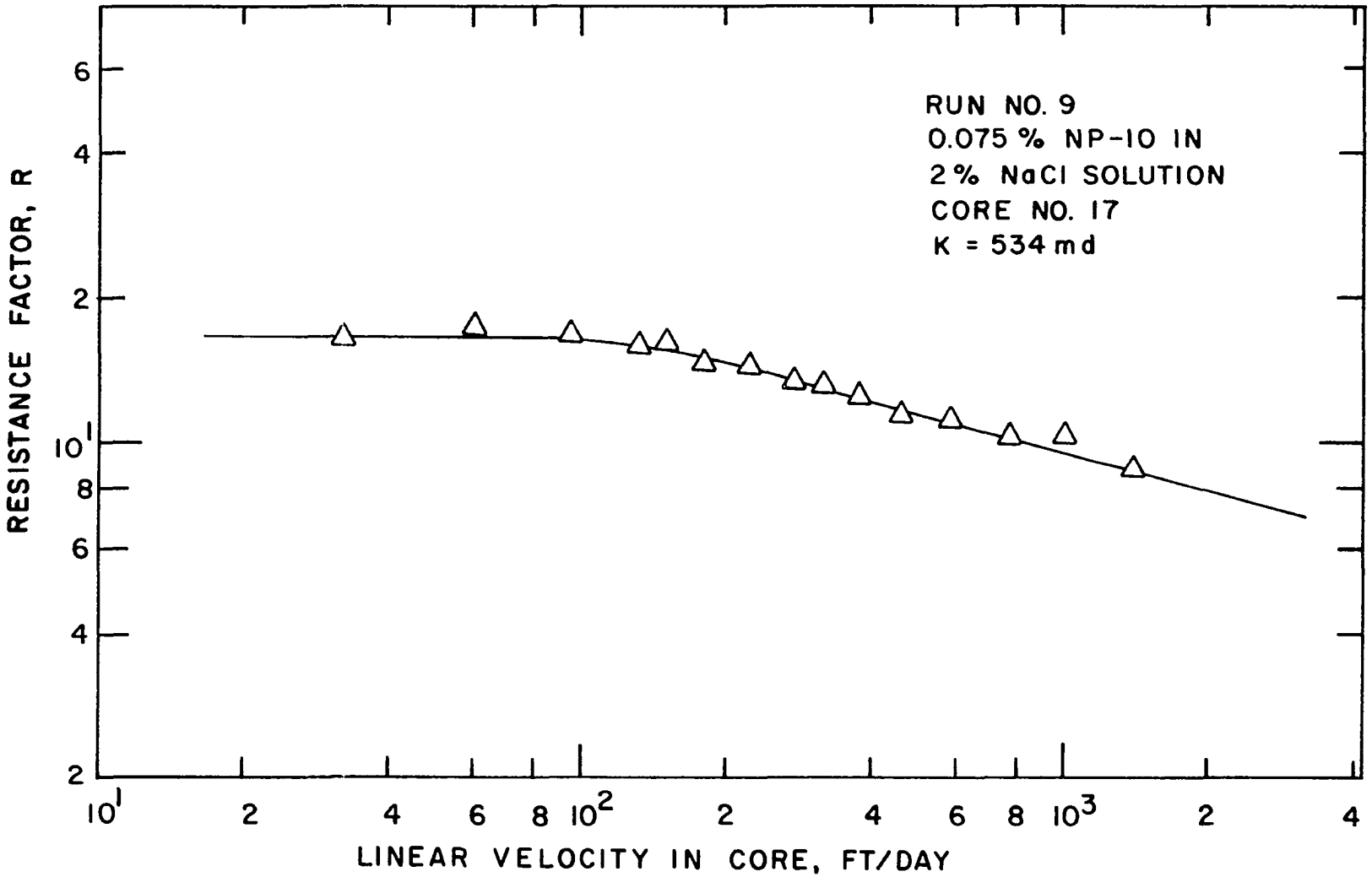

Figure VI-46. Influence of Flooding Velocity on Resistance Factor For 0.075% "Separan" NP-10.

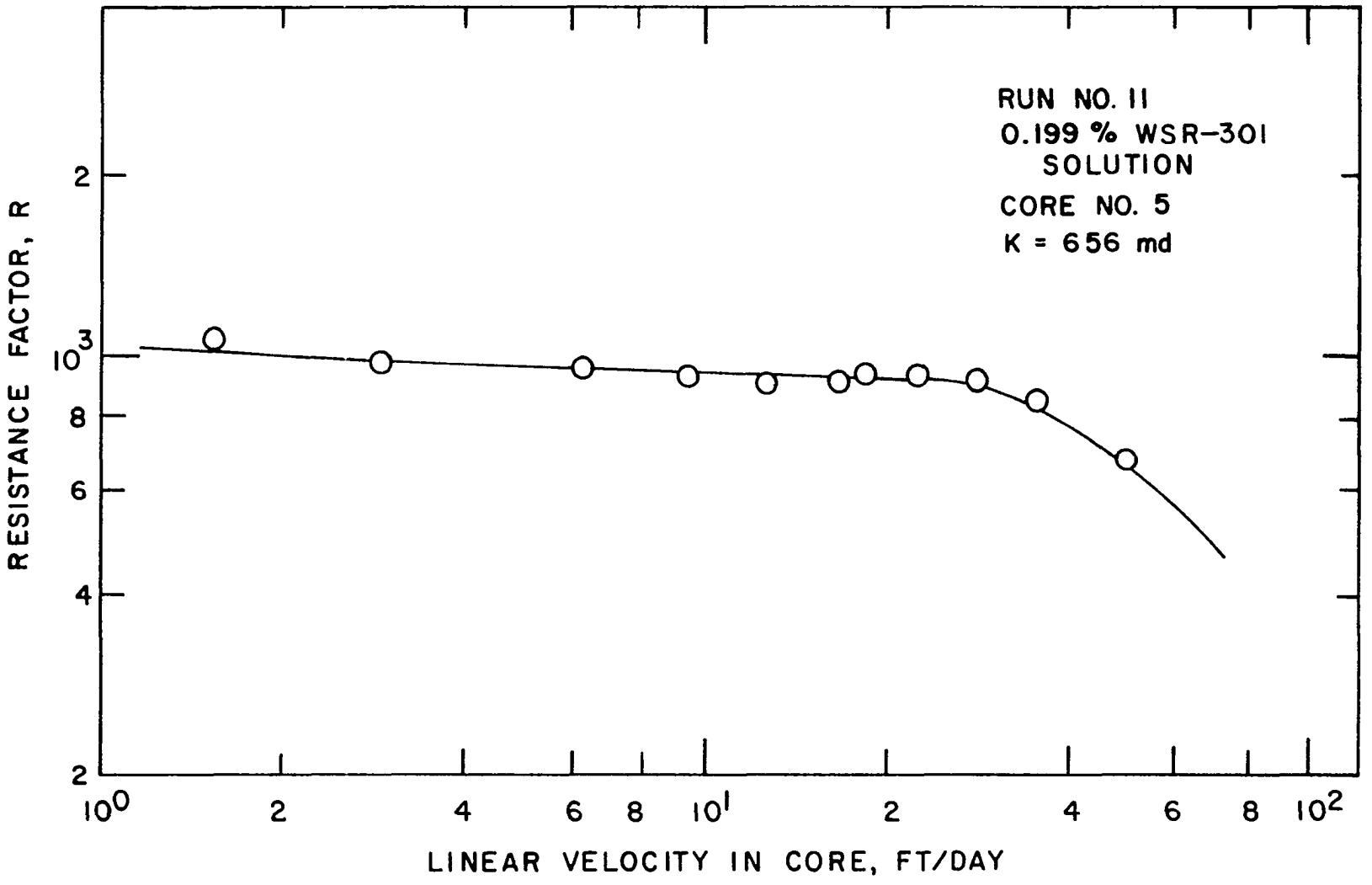

Figure VI-47. Influence of Flooding Velocity on Resistance Factor For 0.199% "Polyox" WSR-301.

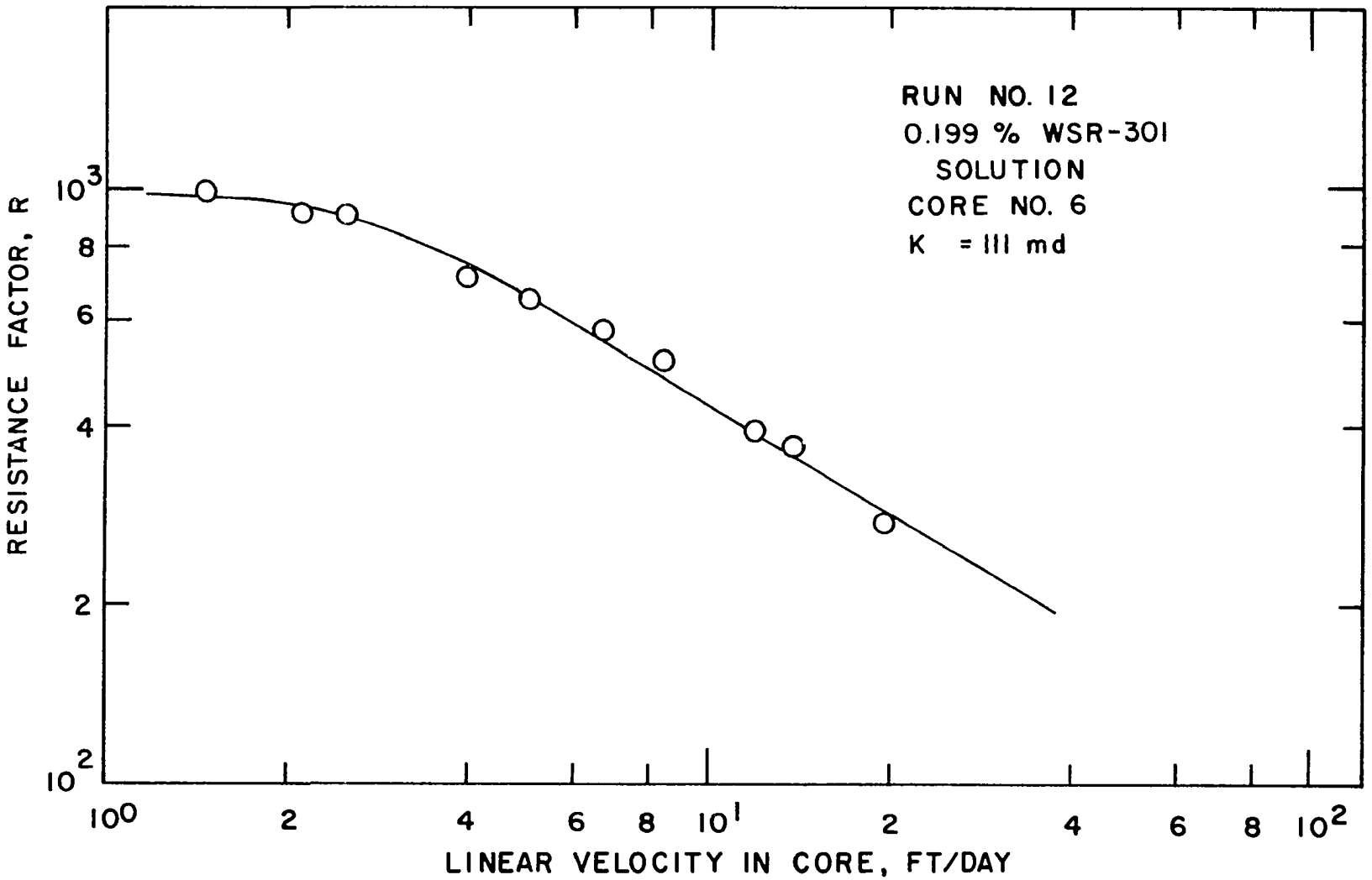

Figure VI-48. Influence of Flooding Velocity on Resistance Factor For 0.199% "Polyox" WSR-301.

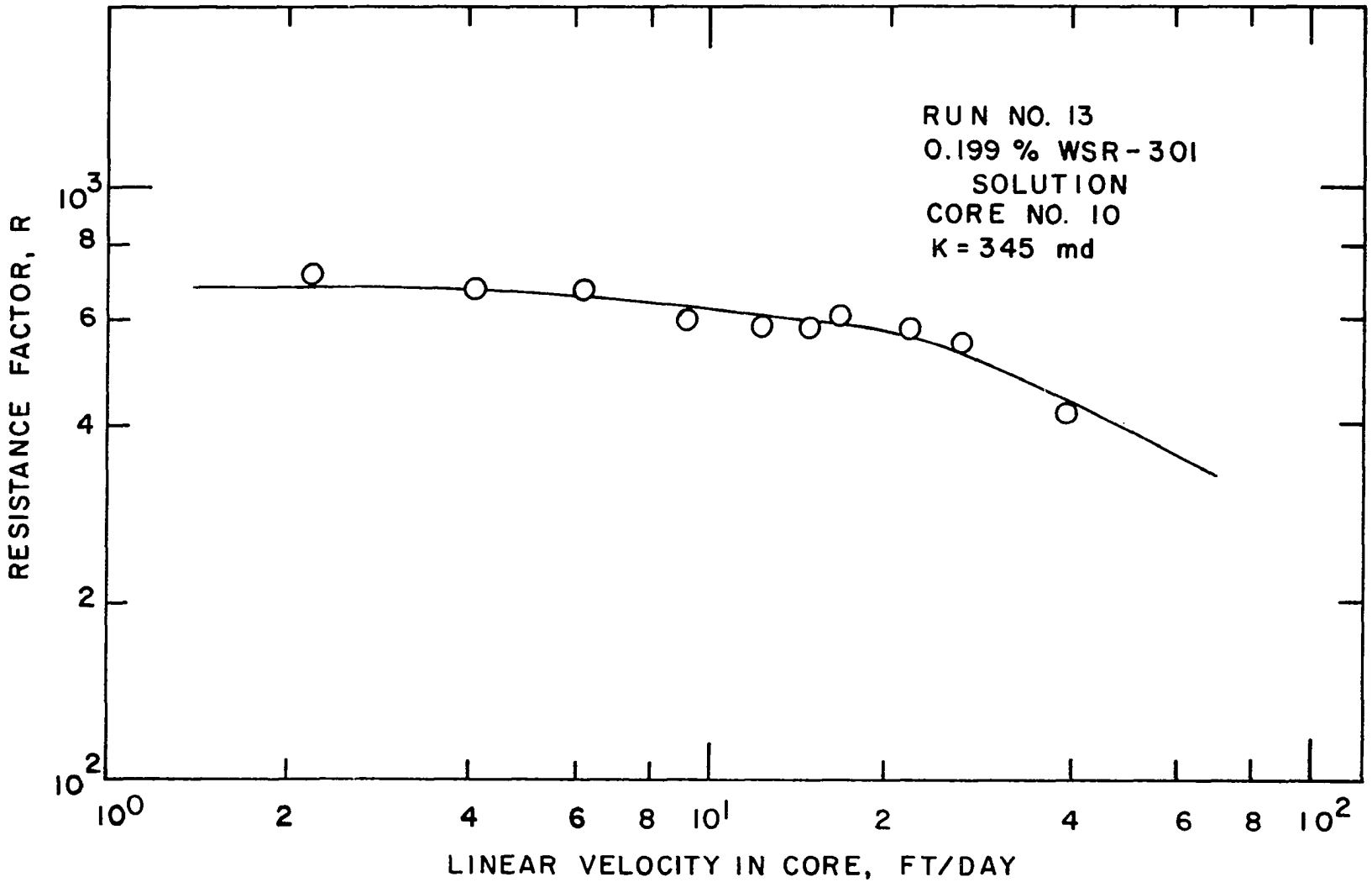

Figure VI-49. Influence of Flooding Velocity on Resistance Factor For 0.199% "Polyox" WSR-301.

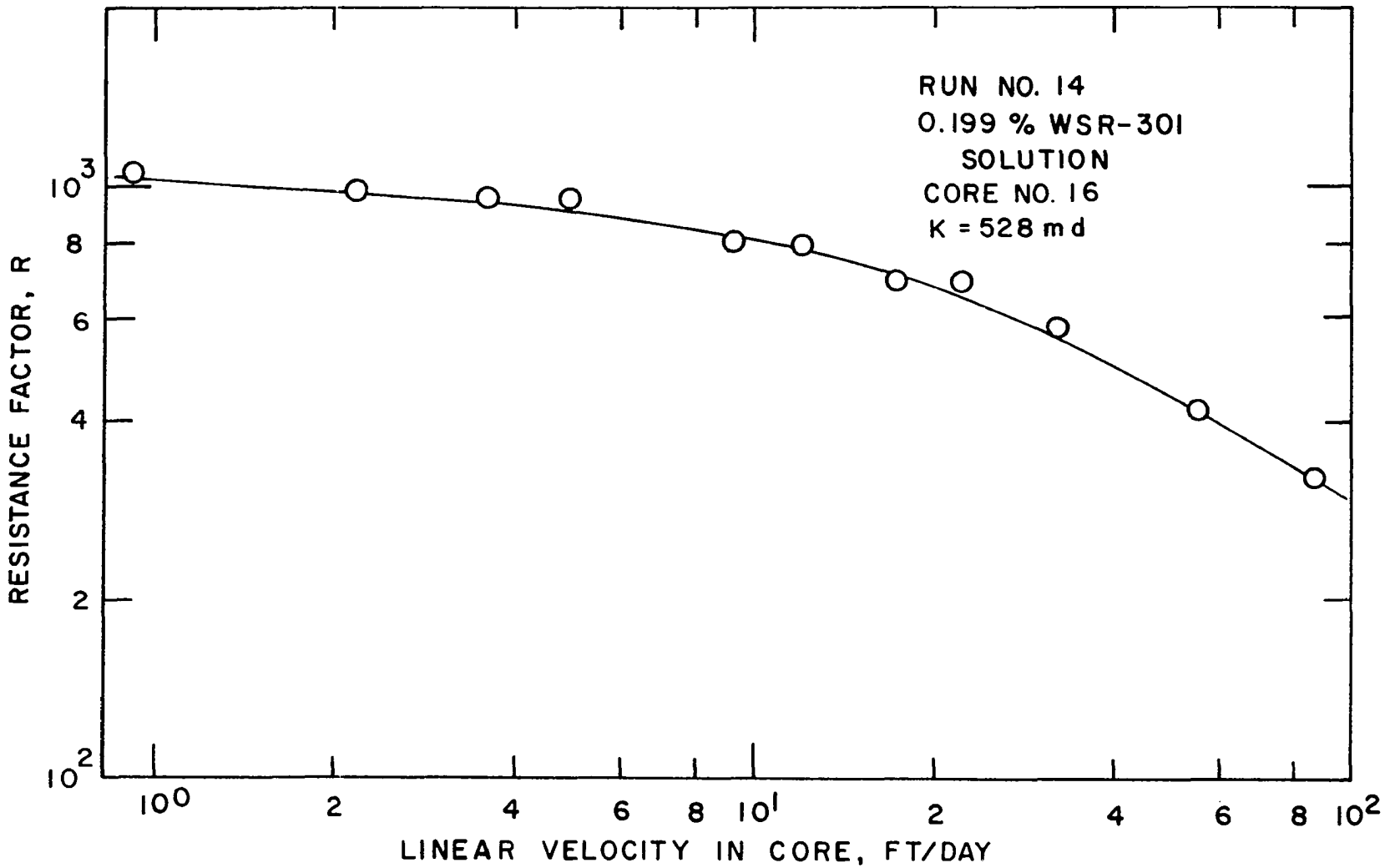

Figure VI-50. Influence of Flooding Velocity on Resistance Factor For 0.199% "Polyox" WSR-301.

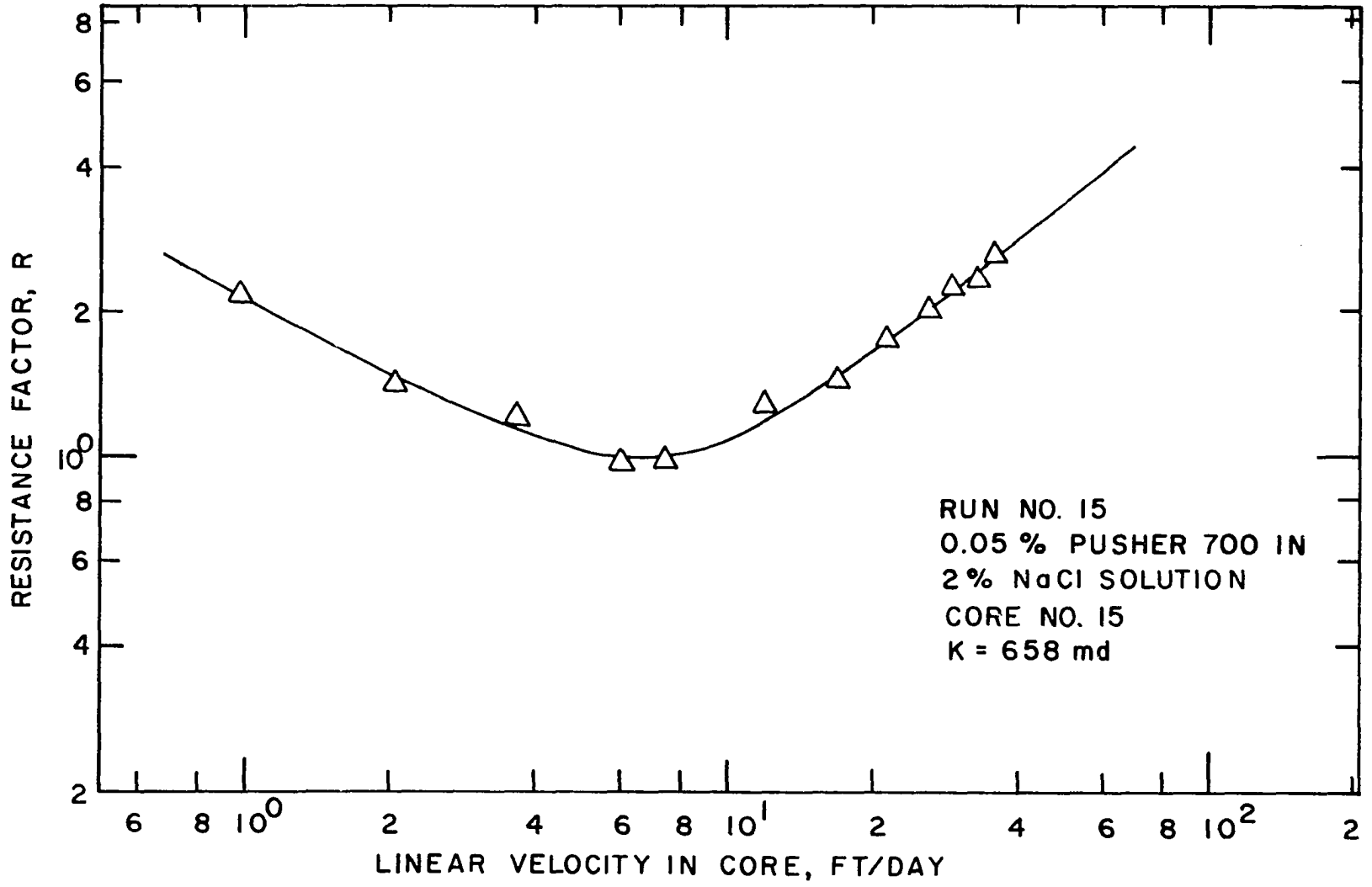

Figure VI-51. Influence of Flooding Velocity on Resistance Factor For 0.05% "Pusher" 700.

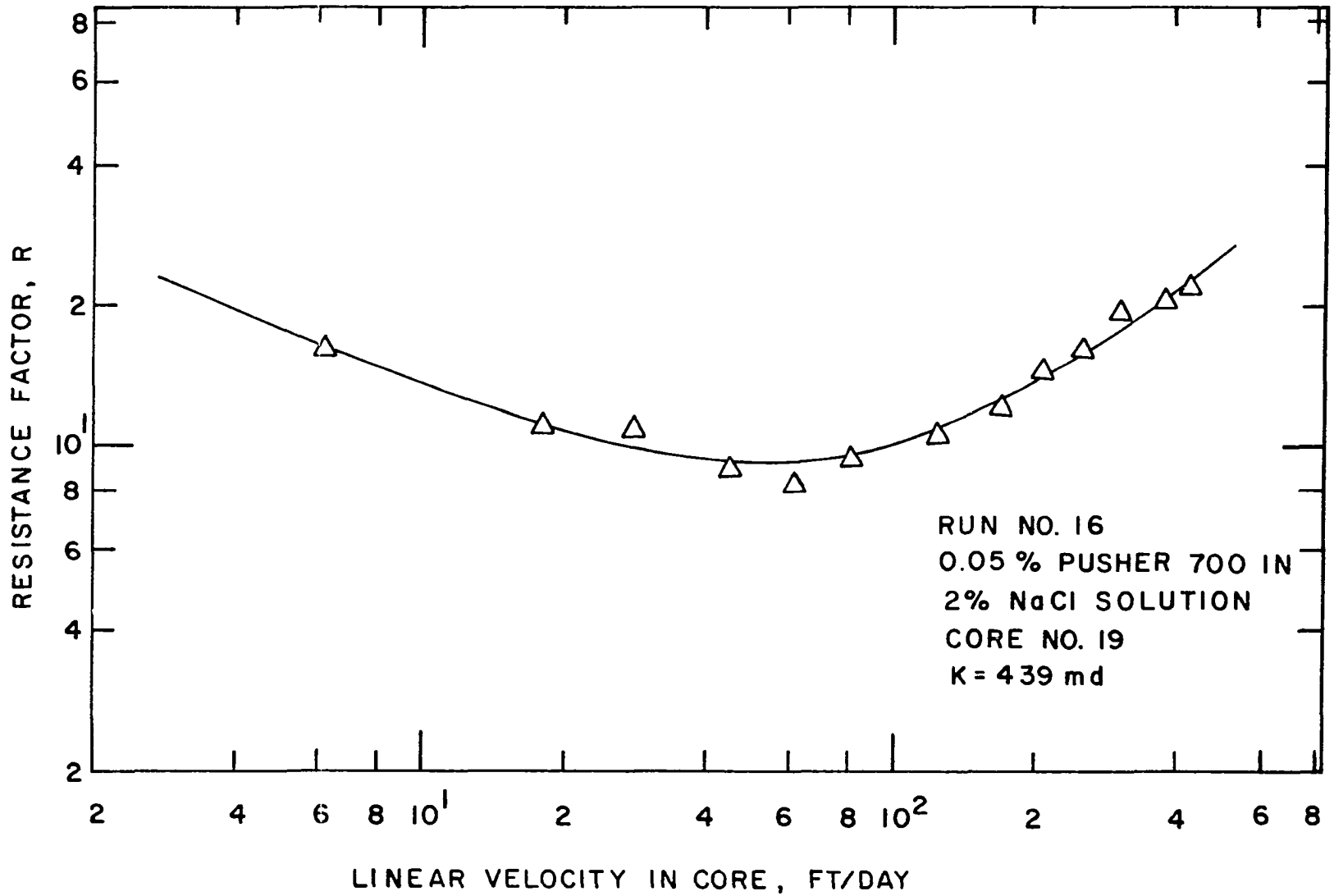

Figure VI-52. Influence of Flooding Velocity on Resistance Factor For 0.05% "Pusher" 700.

hydrolyzed polyacrylamide "pusher" 700, the resistance factor of all the other solutions appeared to be essentially at a maximum and substantially constant over a region of relatively low flow rates whereas at higher level of flow rates the resistance factor decreased with increasing velocity. The stabilization of the resistance factor at low flow rates may be attributed to the fact that at such low rates of flow velocity, with an equally low shear rates inside the porous media, polymer solutions may essentially behave as Newtonian fluids. It has been also suggested (67) that a dynamic equilibrium condition exists between the tendency of the polymer molecules to adsorb on the surfaces of the sands and the tendency of the fluid movement to disassociate and remove adsorbed polymers. At low rates of flow velocity the tendency of the adsorbed layer to be swept away is distinctively lowered. Consequently the tendency for adsorption is favored. The adsorbed molecules may further serve as attachment sites for other molecules from immediately adjacent surfaces and for the molecules still in the flow stream. Therefore a network of polymer molecules may be developed which would affect the bed permeability by the plugging of minute pores or filling of the pendular region. Under these conditions permeability reduction would probably be the only factor producing flow resistance. Thus a maximum polymer adsorption in the low region of flow velocity results in a maximum permeability reduction which in turn results in a maximum and somewhat stabilized resistance factor.

At higher flow velocity with relatively higher shear rates polymer solutions behave primarily as pseudoplastic non-Newtonian fluids. This behavior combined with the permeability reduction caused by polymer adsorption, which in this case is not as great as in the previous region because the tendency of the adsorption layer to be swept away is much higher, results in a decrease in resistance factor as the flow velocity is increased. In this region of higher flow velocity non-Newtonian behavior of the polymer solution is obviously a predominant factor affecting the behavior and the magnitude of the resistance factor.

For the experimental runs made with a 0.05 percent solution of polyacrylamide "pusher" 700, shown in Figures VI-51 and VI-52, the behavior differs greatly from that of the other polymers. Namely at low flow rates, the resistance factor decreases with increasing flow velocity whereas at higher flow rates the resistance factor increases as the flow velocity is increased. This unusual behavior of polyacrylamide "pusher" 700 solution can best be explained as follows: It has been suggested by Burcik (7,8,9,10,11) that some of the partially hydrolyzed polyacrylamide polymer solutions are dialtant in porous media that is the solution viscosity increases with increasing shear rate. He has referred to this phenomena as the pseudo-dilatancy behavior of a polymer solution since it can only be observed in porous media containing adsorbed polymer, but not in capillary

viscometers. The results of the experimental runs made with "pusher" 700 appeared to be in very good agreement with Burcik's results. To show this fact more clearly the results of four runs, made with a 2 percent NaCl solution and polymer solutions simultaneously and plotted in the form of flow rate versus pressure drop, are given in Figures VI-53 through VI-56. As shown in these figures, the departure between the 2 percent NaCl solution curves and the polymer solution curves clearly indicates the resistance effect caused by the adsorbed polymer solutions curves. They indicate at high velocities an increase in apparent viscosity with increasing shear rate for the 0.05 percent solution of "pusher" 700. On the other hand, a reversed curvature is observed over the entire velocity range for the solutions of 0.075 percent NP-10 and 0.075 percent RC-322 polymers which were previously found to have shown some pseudoplastic behavior in porous media. It has been also suggested (18,33) that the pseudo dilatancy behavior of polymer solution would greatly increase the efficiency of the displacement process from a porous media having a range of pore sizes or from hetrogeneous porous media. That is because in a conventional displacement process the linear flow rate through the more permeable bed would exceed that of the less permeable bed. Therefore when breakthrough occurs, considerable oil will still remain in the less permeable bed. When the displacing phase is a dilatant fluid, the higher rate of flow in the more permeable

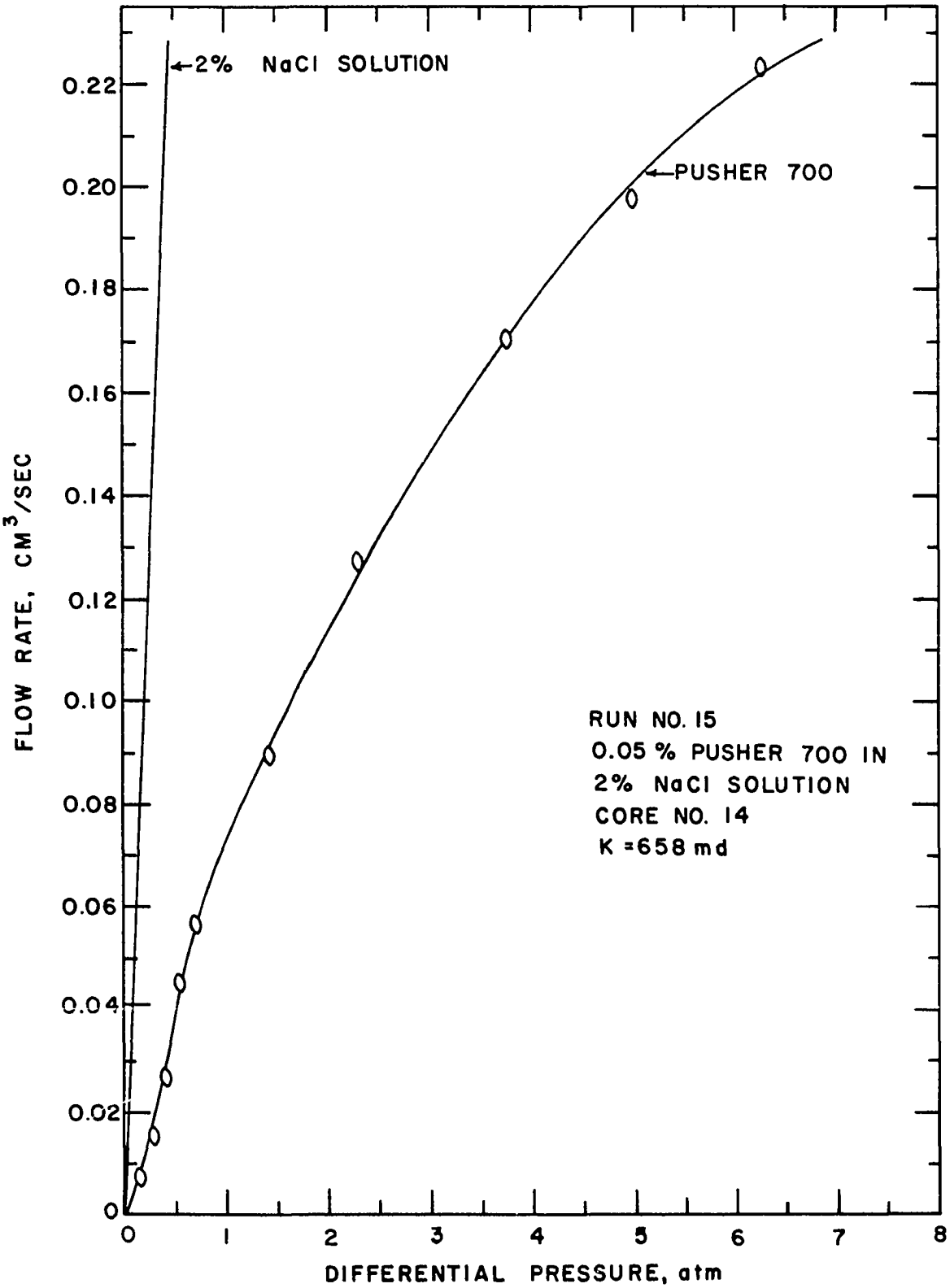

Figure VI-53. Rate of Flow Versus Differential Pressure.

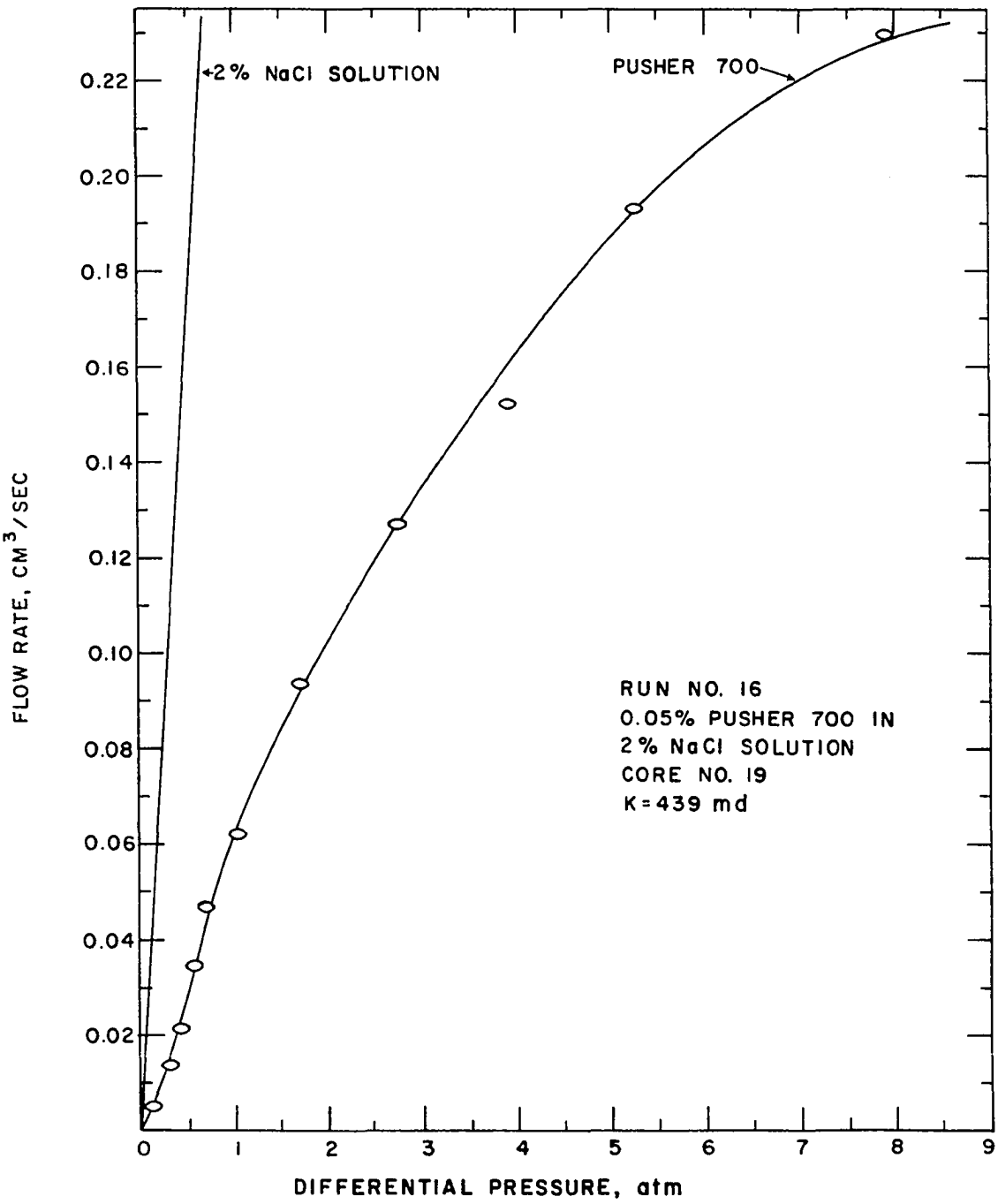

Figure VI-54. Rate of Flow Versus Differential Pressure.

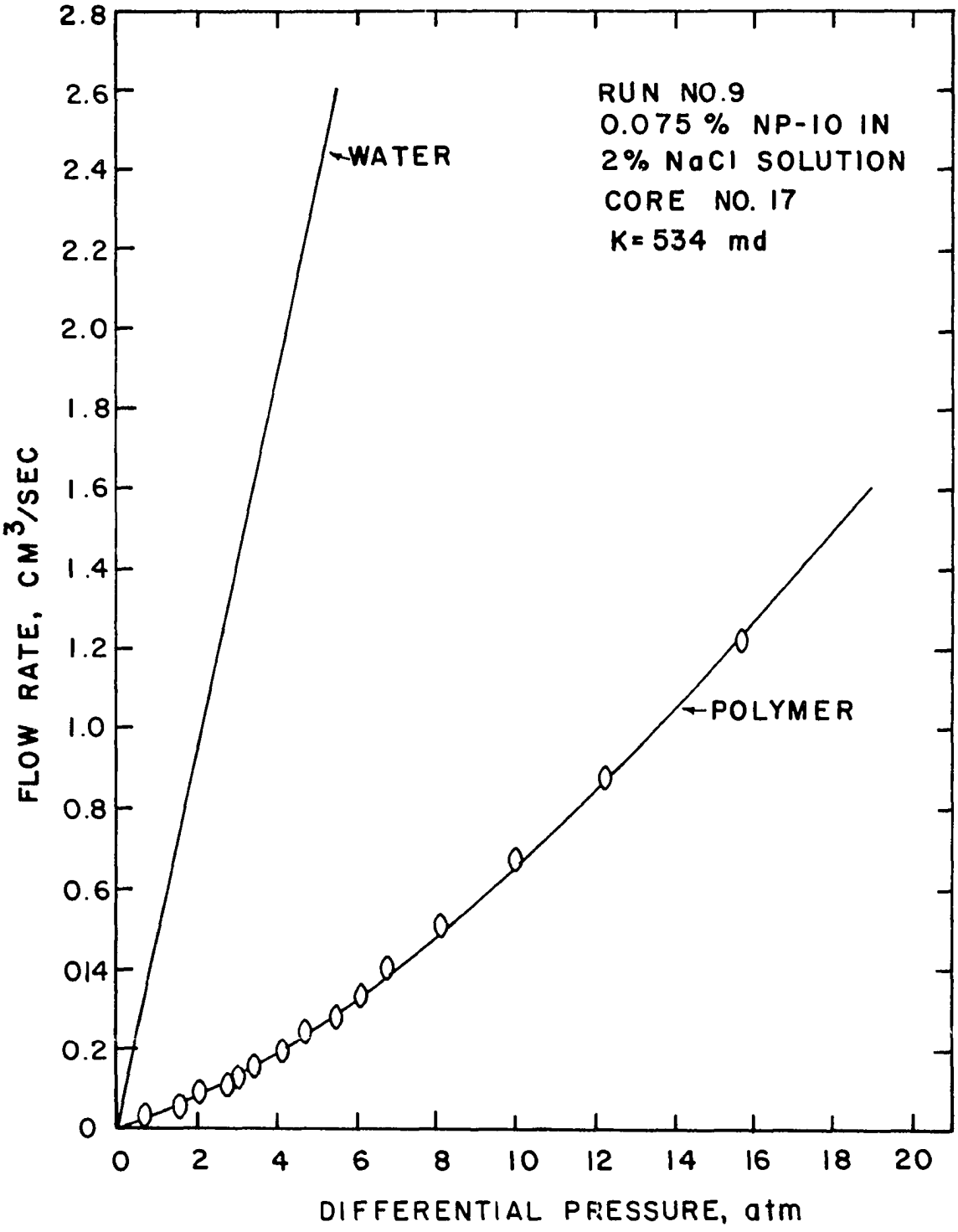

Figure VI-55. Rate of Flow Versus Differential Pressure.

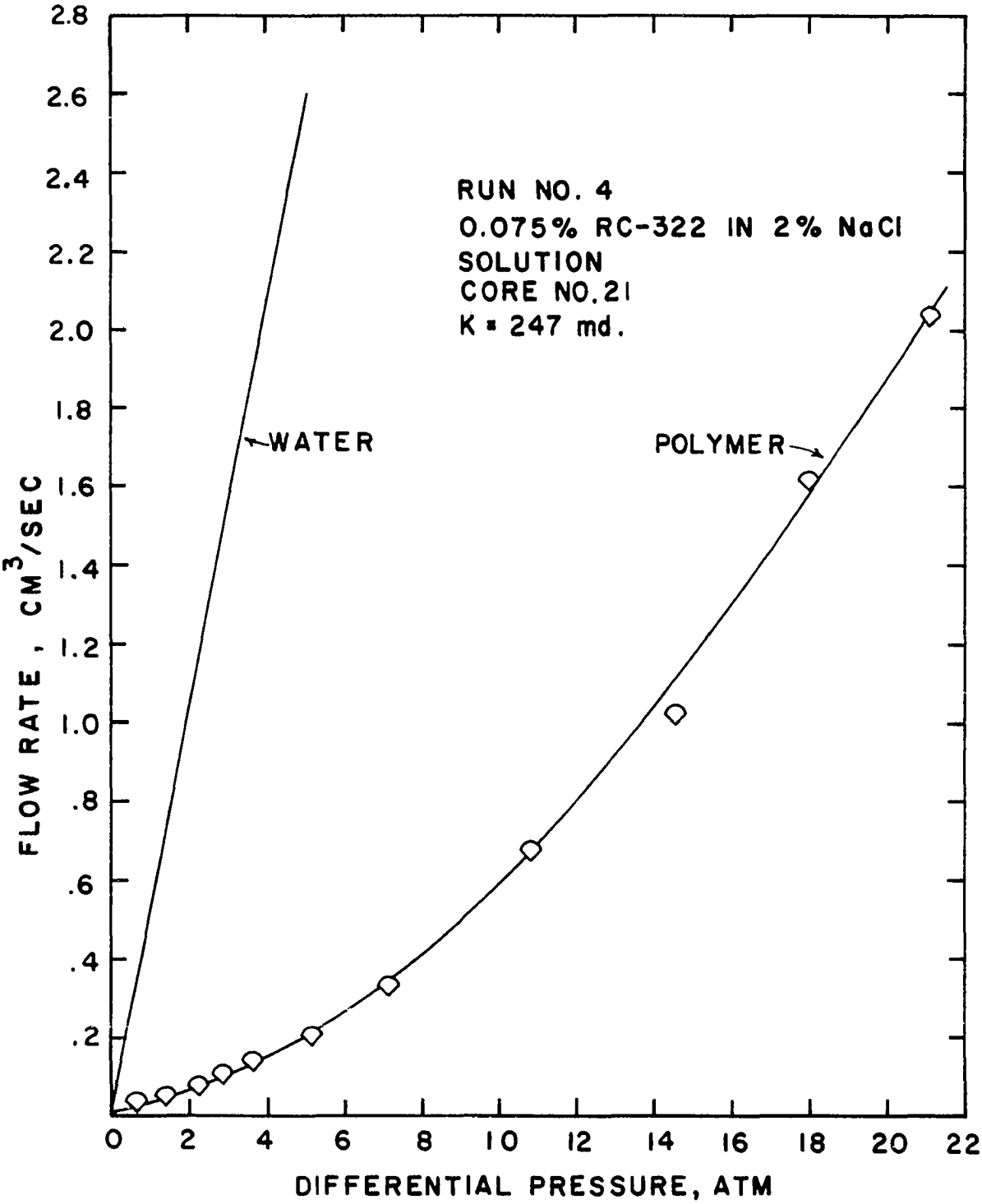

Figure VI-56. Rate of Flow Versus Pressure Differential Pressure.

bed will cause an increase in solution viscosity which will retard the flow and result in a more even flood and a more efficient oil displacement processes.

It is very important to note at this point that at no time was there any indication of gel formation on the surface of the cores nor was there ever a complete plugging of any core throughout these tests. This is supported by the fact that the flow rate and the pressure drop stabilized at each and every pressure increment.

Development of a Reduced Friction Factor-Reynolds Number Correlative Equation

Lately it is customary to present results of the flow in porous media in terms of a Reynolds number and a friction factor. A number of attempts have been made (14,17, 33,67) to define these factors in terms of various hydraulic radius theories which are essentially more suitable to the flow of fluids through unconsolidated porous beds. A general form of the friction factor-Reynolds number for the flow of fluids through porous media, as defined by Muskat (54) with analogy to the flow of fluids in a pipe, is as follows:

$$R_e = \frac{DV_o\rho}{\mu} \tag{6-9}$$

$$f = \frac{D\Delta P}{2L\rho V_o^2} \tag{6-10}$$

where f is the friction factor, R_e is the Reynolds number, ρ is the fluid density, μ is the fluid viscosity, L is the length of the porous media, ΔP is the pressure drop across the bed, V_o is the average flow velocity, and D is the average sand grain diameter. The term D which should physically represent the average pore diameter has been vigorously used as sand grain diameter, simply, because it is much easier to measure the sand grain diameter by direct microscopic examination of a cross section of the porous media.

It is very important to a reservoir engineer to be able to correlate the results of fluid flow through a particular consolidated bed by means of a Reynolds number-friction factor relationship. By having such a relationship he can easily predict the flow velocity of the bed for a given pressure drop.

Muskat (54), by using Fancher's friction factor chart for flow of fluids through porous sands, has shown that, regardless of the physical significance of the definition of term D and irrespective of the type of porous medium used, up to a Reynolds number of the order of one Fancher's data strictly obeyed the following relationship:

$$\log f = \log \alpha - \log R_e \qquad (6\text{-}11)$$

which expresses the fact that, up to the Reynolds number of the order of one, a plot of friction factor versus Reynolds number is a straight line on log-log paper with its intercept,

$f = \alpha$, at $\log R_e = 0$. Having the above relationship in mind and noting the difficulties involved in the accurate estimation of an average sand grain diameter in consolidated porous sands a method was proposed to correlate the results of the flow of a number of polymer solutions through consolidated porous cores in terms of a reduced friction factor-Reynolds number equation. The correlation method which relates the properties of the fluid to the flow characteristics, implicit of the rock properties, is as follows:

The equation 6-11 can also be written as:

$$\log f = \log \frac{\alpha}{R_e} \tag{6-12}$$

or

$$f = \frac{\alpha}{R_e} = \alpha \ (R_e)^{-1} \tag{6-13}$$

Substituting the values of f and R_e from Equations 6-9 and 6-10 in to the Equation 6-13, the Equation 6-13 then becomes:

$$\frac{D\Delta P}{2L\rho V_o^2} = \alpha\left(\frac{DV_o\rho}{\mu}\right)^{-1} = \alpha D^{-1}\left(\frac{V_o\rho}{\mu}\right)^{-1} \tag{6-14}$$

or

$$\frac{D\Delta P}{2L\rho V_o^2} = \frac{\alpha}{D}\left(\frac{V_o\rho}{\mu}\right)^{-1} \tag{6-15}$$

Dividing the both sides of the Equation 6-15 by D, the Equation 6-15 then reduces to:

$$\frac{\Delta P}{2L\rho V_o^2} = \frac{\alpha}{D^2}\left(\frac{V_o\rho}{\mu}\right)^{-1} \tag{6-16}$$

Defining a reduced friction factor as:

$$f_r = \frac{\Delta P}{2L\rho V_o^2} \tag{6-17}$$

and a reduced Reynolds number as:

$$R_r = \frac{V_o\rho}{\mu} \tag{6-18}$$

the Equation 6-16 now becomes:

$$f_r = \left(\frac{\alpha}{D^2}\right) R_r^{-1} \tag{6-19}$$

taking logarithm of both sides of the Equation 6-19, the final correlative equation then takes the form:

$$\log f_r = \log\left(\frac{\alpha}{D^2}\right) - \log R_r \tag{6-20}$$

As for the Muskat's Equation 6-11, the reduced friction factor, f_r, and the reduced Reynolds number, R_r, of the above equation when plotted on log-log paper should also result in a straight line with its intercept, $f = \frac{\alpha}{D^2}$, at $R_r = 1.0$.

The primary advantage of presenting the results of flow of fluid data in this way is that one can predict the flow velocity or the pressure drop in a given system without determining an average sand grain diameter, D, or any other physical properties of the rock.

To verify, the above proposed reduced friction factor-Reynolds number correlation. The correlation was first applied to the flow of a 2 percent NaCl solution through a total of ten different cores. As expected, the results of these tests, given in the form of the reduced friction factor versus Reynolds number in Figures VI-57 and VI-58, clearly confirmed the applicability of the proposed correlation; since the data appeared to fit the Equation 6-20 quite well.

The application of the correlation to the flow of polymer solutions was also tested by flowing four different polymer solutions through the same cores. The results of these runs are presented in Figures VI-59 through VI-63 and summarized in Tables C-27 through C-36 of Appendix C. As can be seen from these figures, except for the 0.05 percent solution of partially hydrolyzed polyacrylamide "pusher" 700 which has apparently shown some dilatancy behavior at higher flow velocities, the rest of the polymer solutions appeared to follow the correlation quite well. On the reduced friction factor-Reynolds number plot for the flow of a 0.05 percent polyacrylamide "pusher" 700 solution through a consolidated core dilatancy shows the same way as turbulence

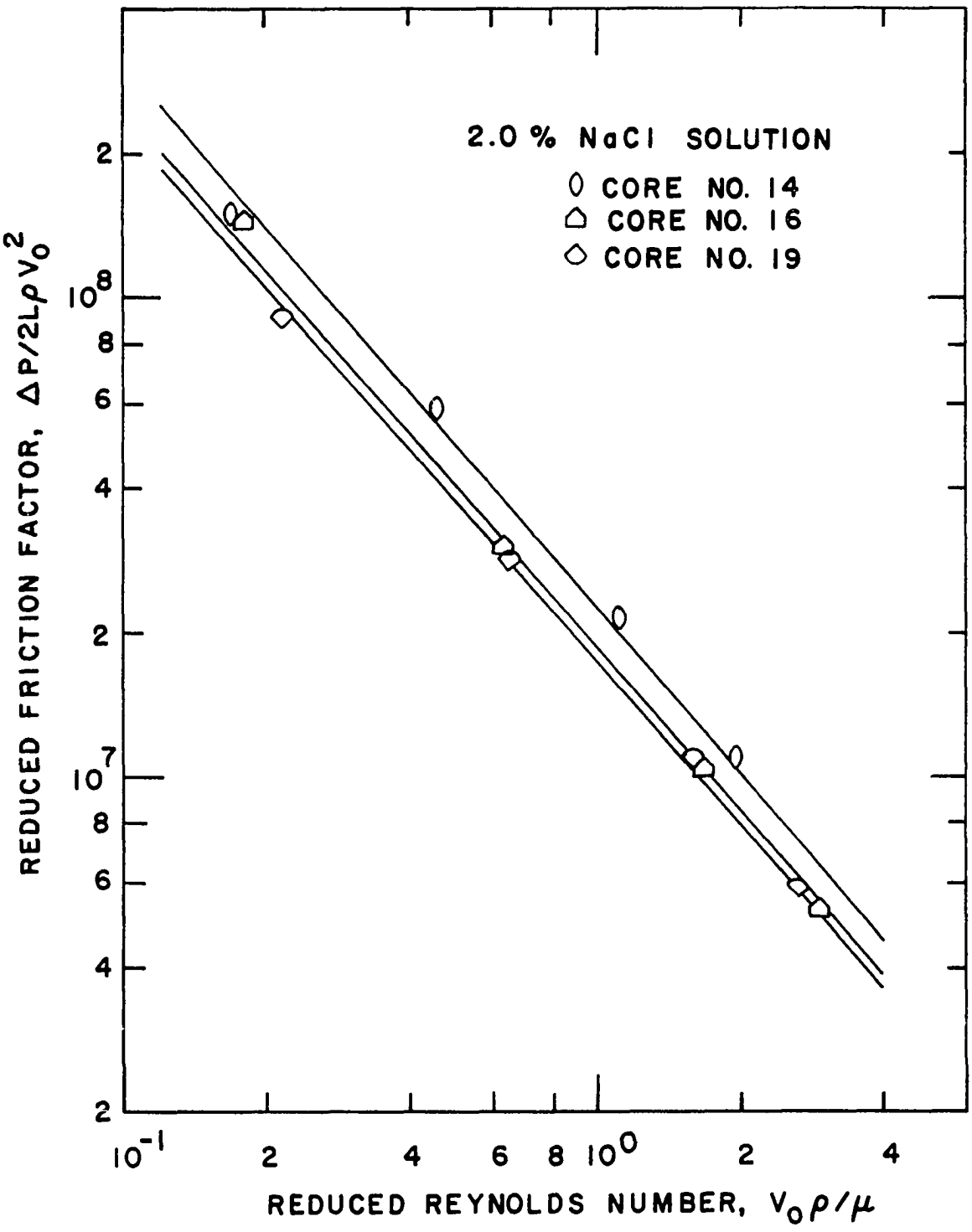

Figure VI-57. Correlation of Flow of 2% NaCl Solution Through Berea Cores Data Based on Equation 6-20.

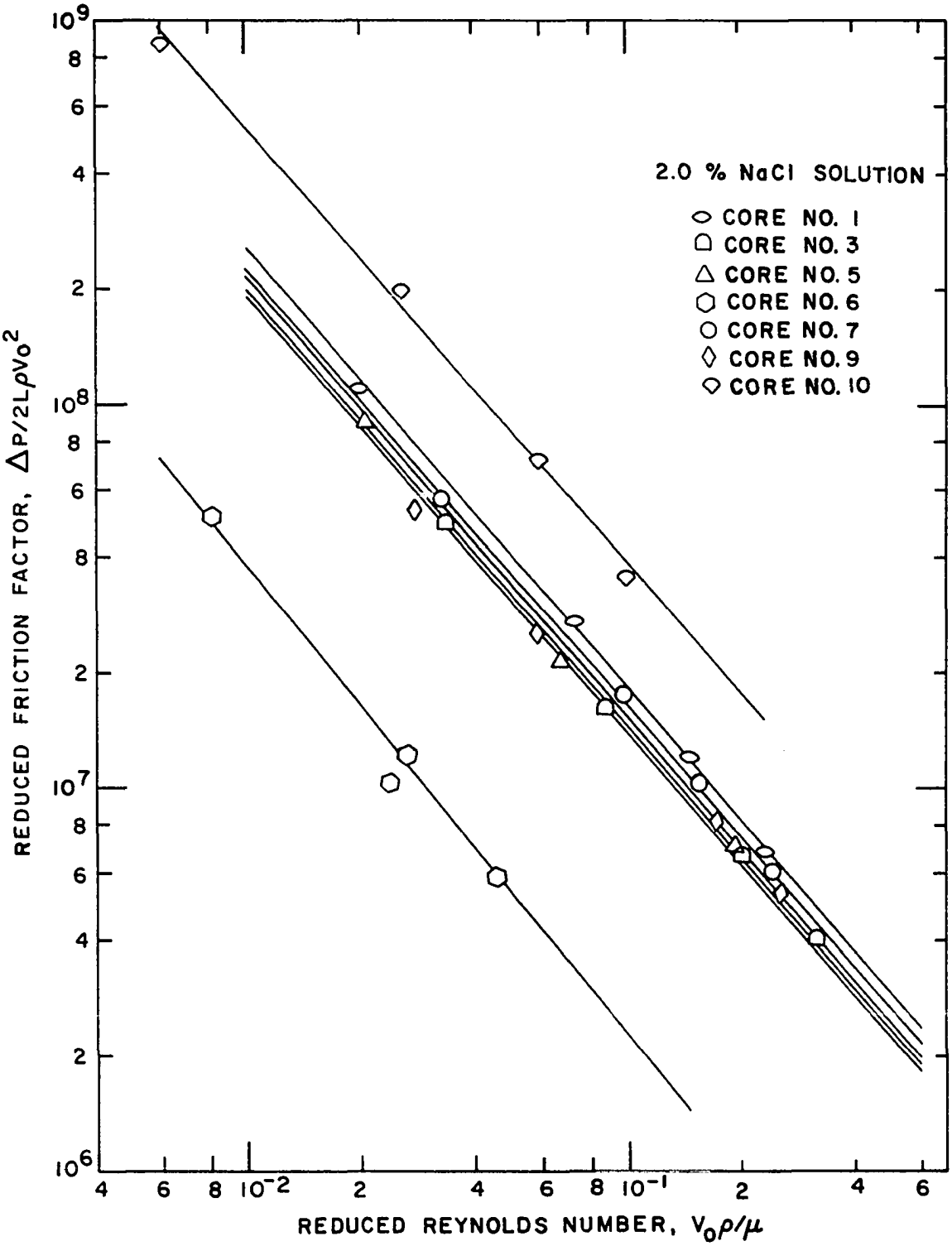

Figure VI-58. Correlation of Flow of 2% NaCl Solution through Torpedo Cores Data Based on Equation (6-20).

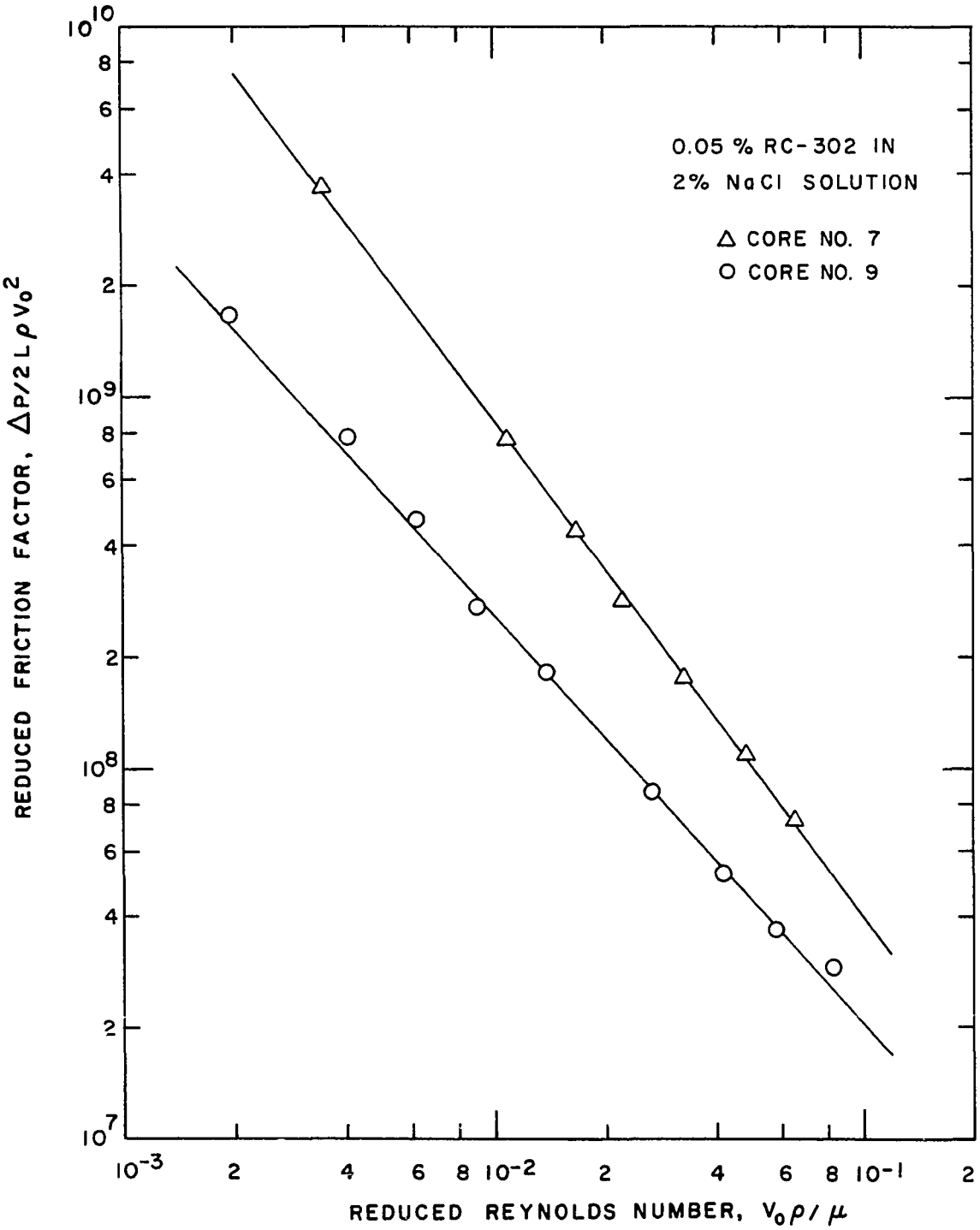

Figure VI-59. Correlation of Flow of 0.05% RC-302 Data Based on Equation (6-20) Run 28 and 29.

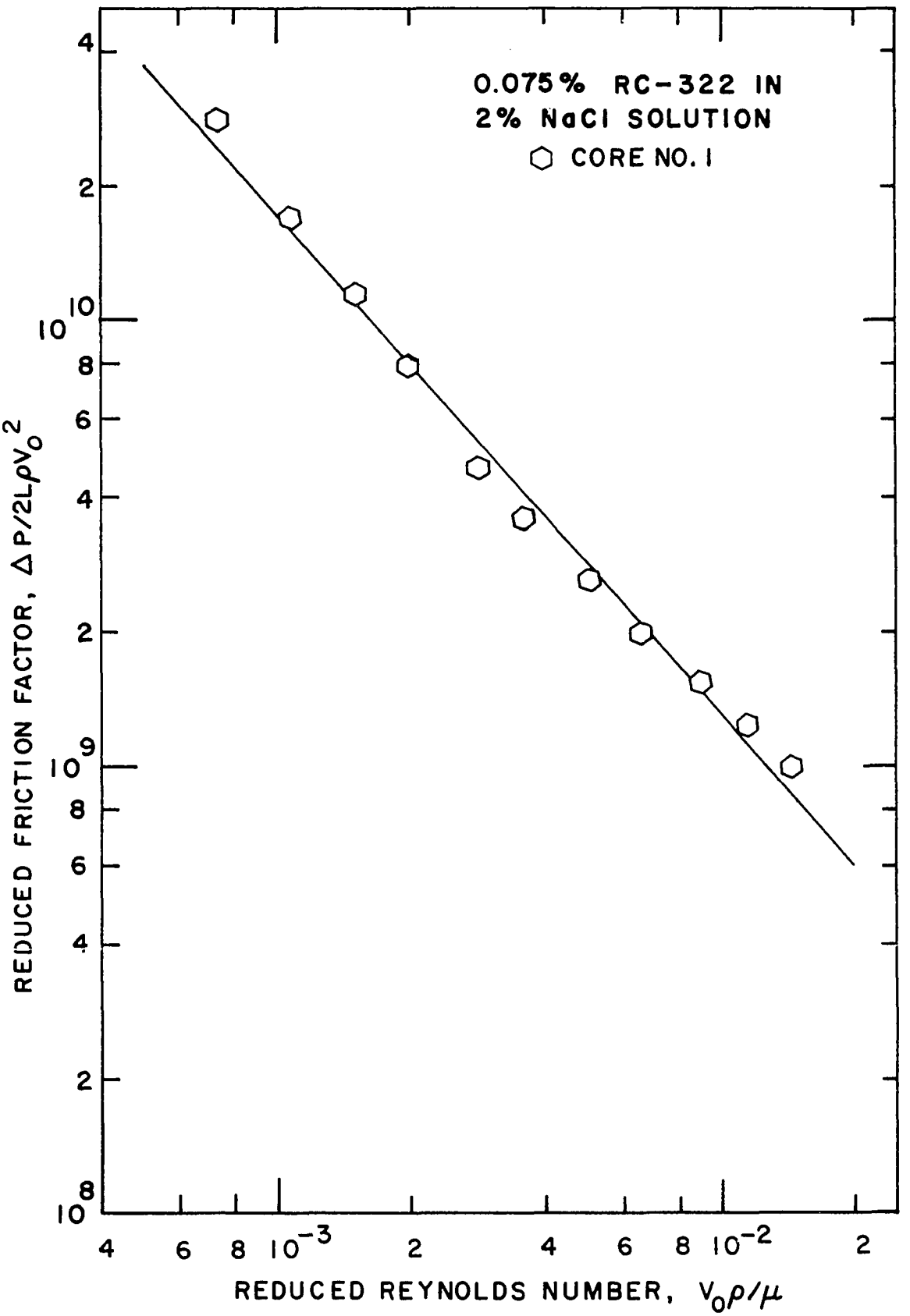

Figure VI-60. Correlation of Flow of 0.075% RC-322 Data Based on Equation 6-20, Run 29.

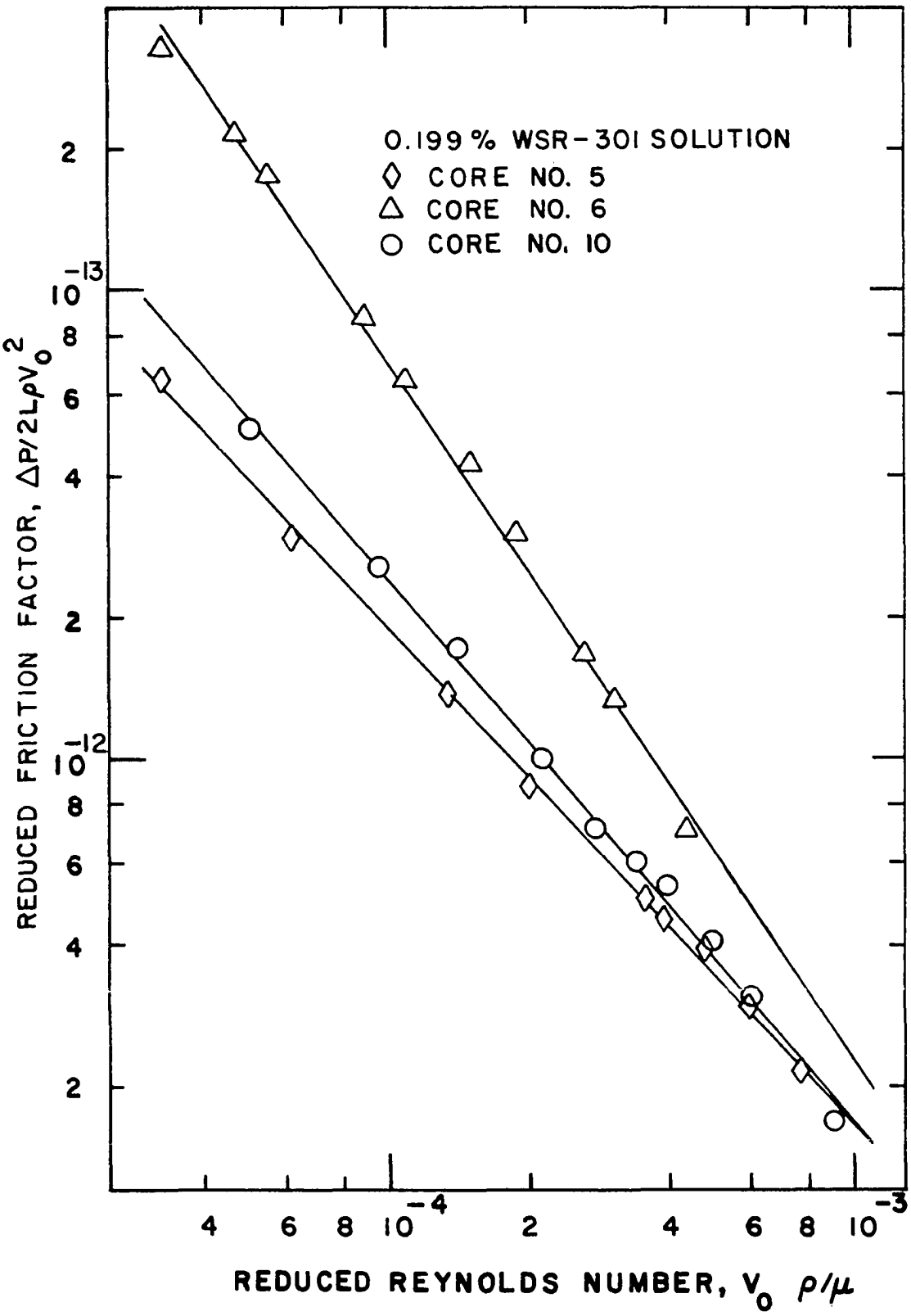

Figure VI-61. Correlation of Flow of 0.199% "Polyox" WSR-301 Data Based on Equation 6-20, Run 31, 32 and 33.

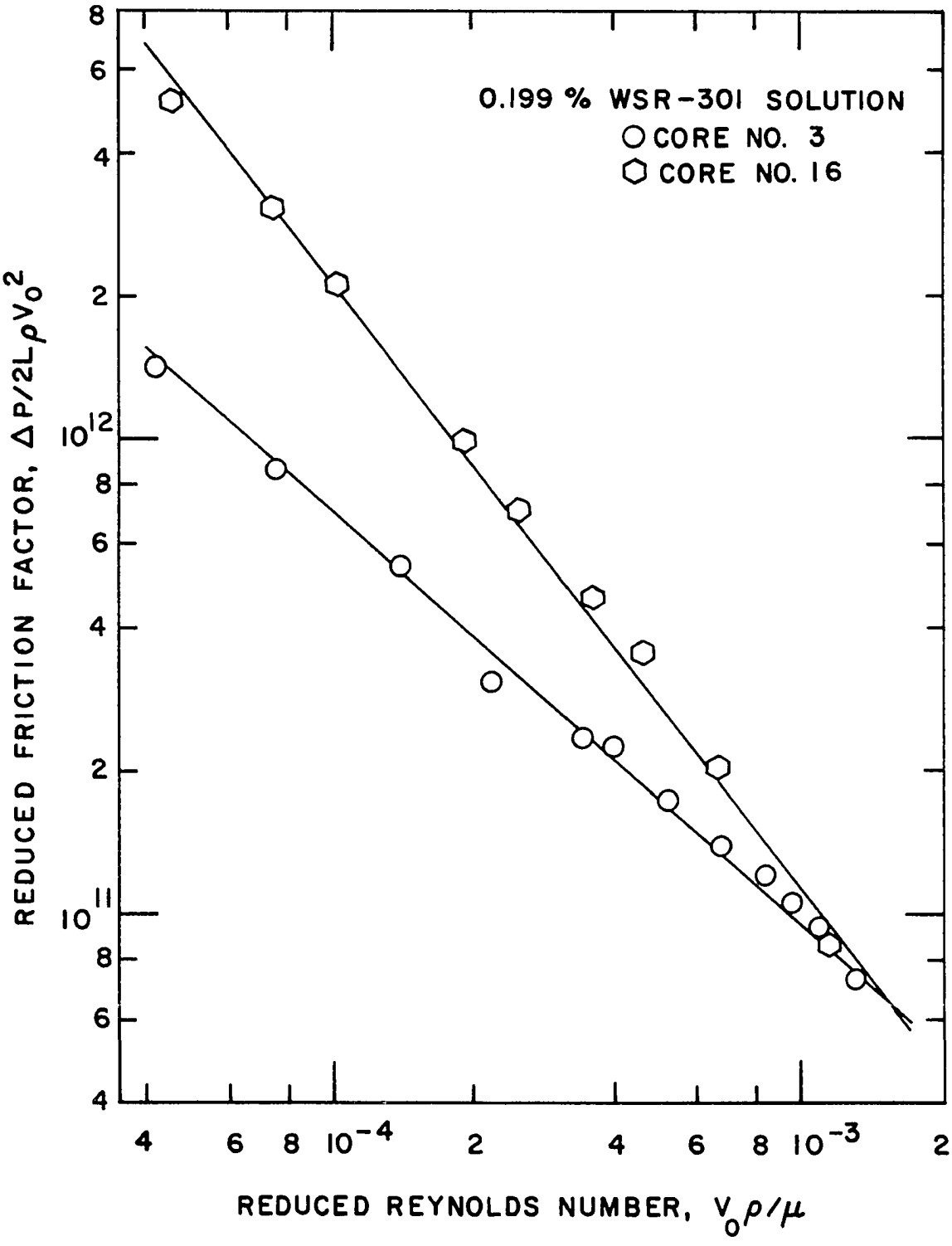

Figure VI-62. Correlation of Flow of 0.199% "Polyox" WSR-301 Data Based on Equation 6-20, Run 30 and 34.

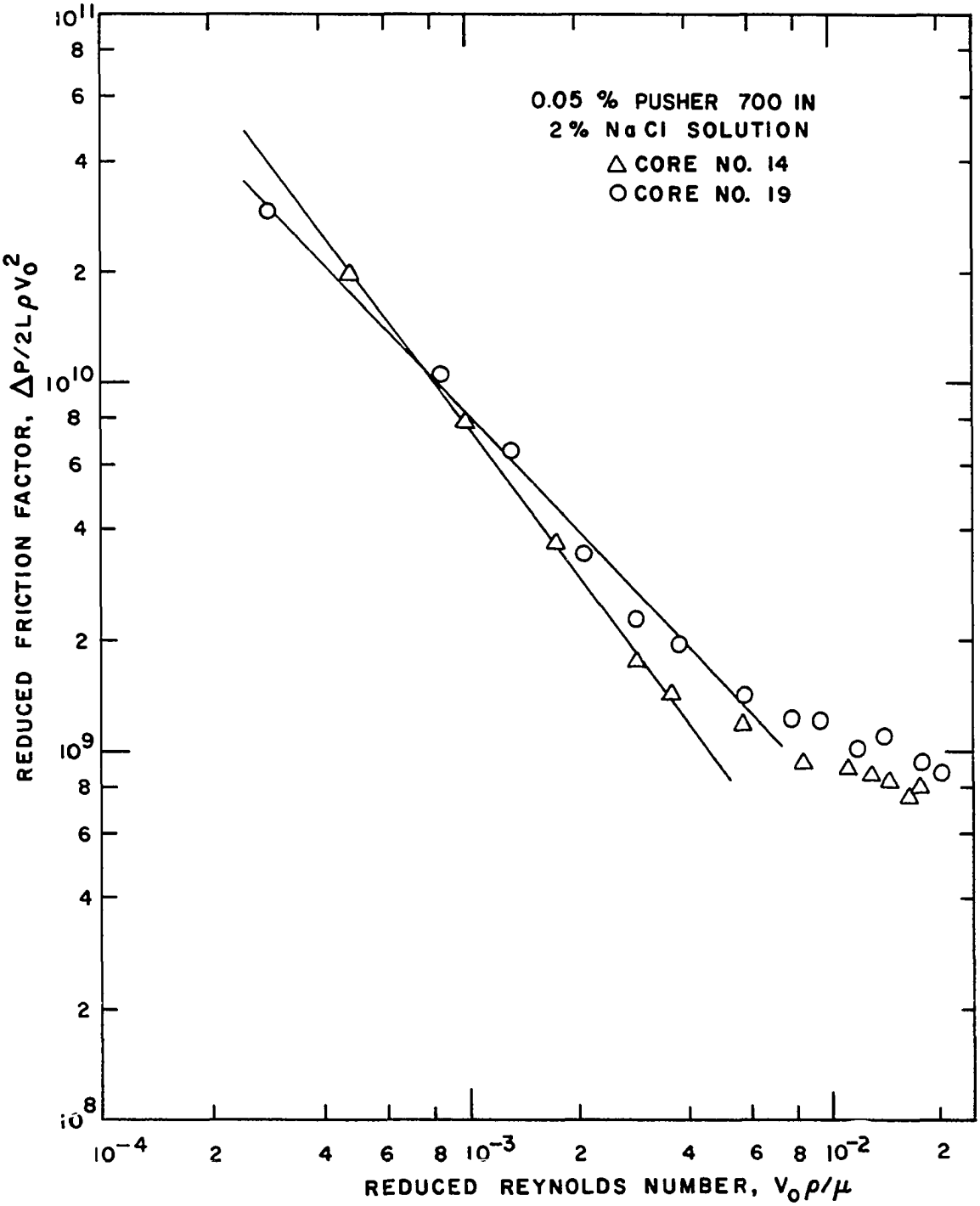

Figure VI-63. Correlation of Flow of 0.05% Pusher 700 Data Based on Equation (6-20) Run 35 and 36.

in the flow of a non-Newtonian fluid. The graphs are given here both to emphasize the applicability of the correlation to the flow of various polymer solutions through consolidated sands and to serve as a basis for prediction of the flow velocity when the pressure drop is known.

Mobility Ratio Concept in Oil Displacement Processes

The concept of mobility ratio has long been recognized by the reservoir engineers. Mobility, λ, of a fluid, in a porous medium, is defined as the ratio of its effective permeability to its viscosity and it is included in all the fluid flow models describing the flow of single-phase fluid in porous media. The mobility ratio, when one fluid displaces another with which it is immiscible, is defined as the ratio of the mobility of the displacing fluid to that of the displaced fluid:

$$M = \frac{(K/\mu)\ \text{displacing}}{(K/\mu)\ \text{displaced}} = \frac{\lambda\ \text{displacing}}{\lambda\ \text{displaced}} \qquad (6\text{-}21)$$

Where M is the mobility ratio, λ the mobility, K the effective permeability, and μ the fluid viscosity. The mobility ratio is a very important factor in all secondary recovery predictions governing both the displacement and the volumetric sweep efficiency of the oil displacement process. A mobility ratio of greater than one will result in an uneven displacement and a poor oil recovery (15,18), thereby a less efficient displacement process. On the other hand a mobility

ratio of one or less will result in a more piston-like displacement process, a higher oil recovery, and a more efficient process. It has been shown (62,69) that, the mobility ratio is even more significant in hetrogeneous reservoirs, where the rate of fluid advance is proportional to its effective permeability. In the past few years some attempts have been made to increase the viscosity of the injection water by addition of a small amount of high molecular weight water soluble polymers. An increase in the viscosity of the displacing fluid will provide a more favorable mobility ratio, and therefore an improved oil recovery.

Two different concentrations of polyethylene oxide WSR-301 water soluble polymer, five consolidated cores, and four different oils (see Table VI-2) were used to study the process of displacing the oil from cores, both by a 2 percent NaCl water and a polymer solution, and dependency of the oil recovery on oil polymer solution viscosity ratio. The results of these runs are shown in Figures VI-64 through VI-73 and are summarized in Tables C-37 through C-41 of Appendix C. It can be seen from these figures that:

1. There is an increase in oil recovery by polymer injection over water injection.
2. The increase in oil recovery at breakthrough is much higher for oils with low viscosities than those with higher viscosities.
3. The increase in oil recovery varied between 4 to 6 percent of the initial oil in place.

TABLE VI-2

PROPERTIES OF OIL USED

Oil Name	Viscosity (cps) (25°C)	Specific Gravity (25°C)	Manufacturer
Soltrol 130	1.51	.747	Phillips Petroleum Company
Soltrol 170	2.72	.768	Phillips Petroleum Company
Drakel 13	26.39	.869	Pennsylvania Refining Company
Drakel 21	44.16	.874	Pennsylvania Refining Company

This increase in oil recovery by polymer injection can be attributed to the improved mobility ratio of the system resulting from addition of 0.05 percent "polyox" WSR-301 polymer to the 2 percent NaCl injection water. The viscosity of injection fluid was raised to 1.84 cps. which in turn resulted in a lower mobility ratio:

$$M = \frac{K_p/\mu_p}{K_o/\mu_o} \qquad (6\text{-}22)$$

A lower mobility ratio than that provided by water injection process, resulted in a more piston-like displacement process and an increase in oil recovery. This concept can be more clearly understood by referring to the run No. 46 Figure VI-72. In this run the same kind of oil as that of run No.

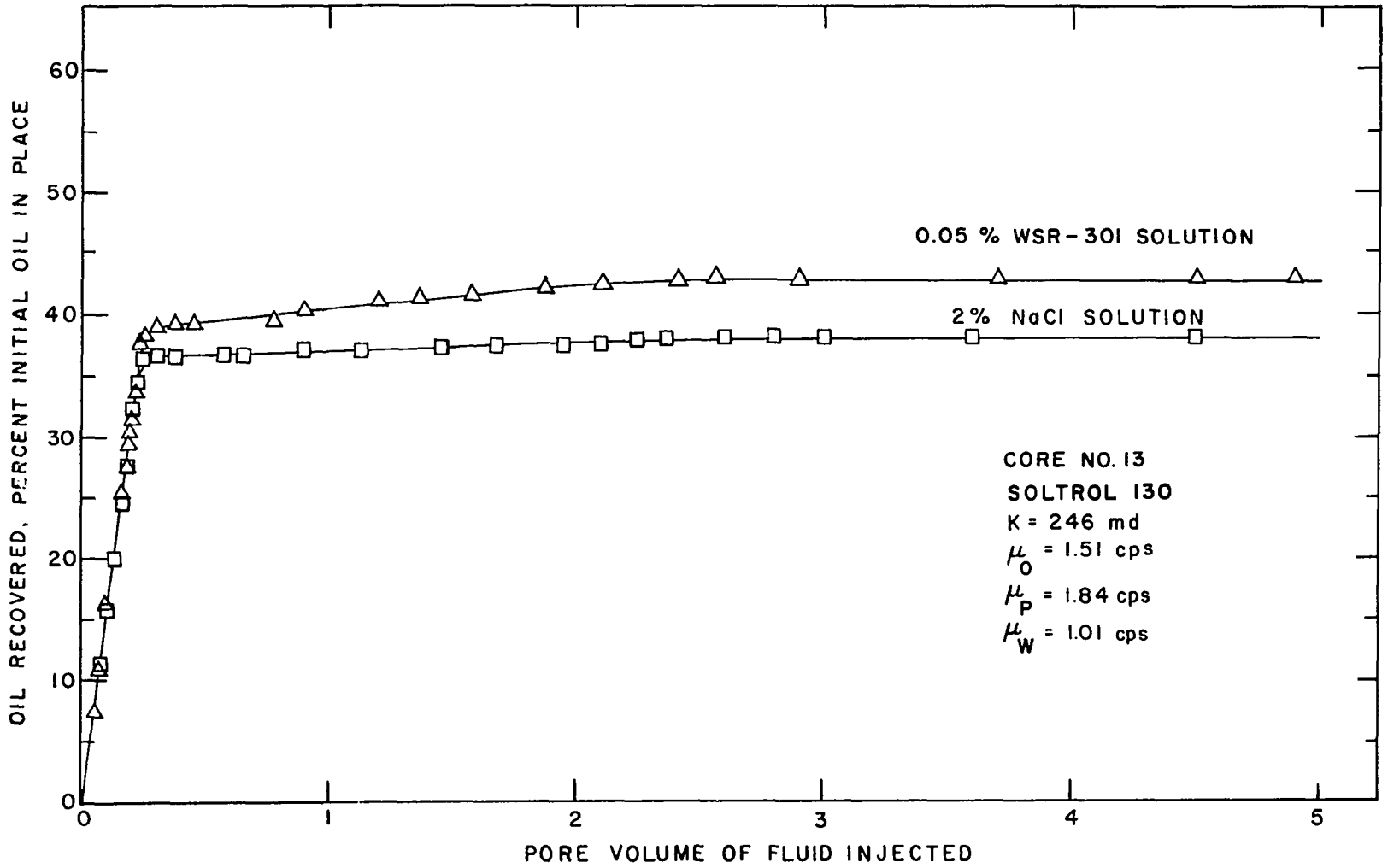

Figure VI-64. Oil Displacement from Core by Brine and 0.05% "Polyox" WSR-301 Solution Run 37 and 38.

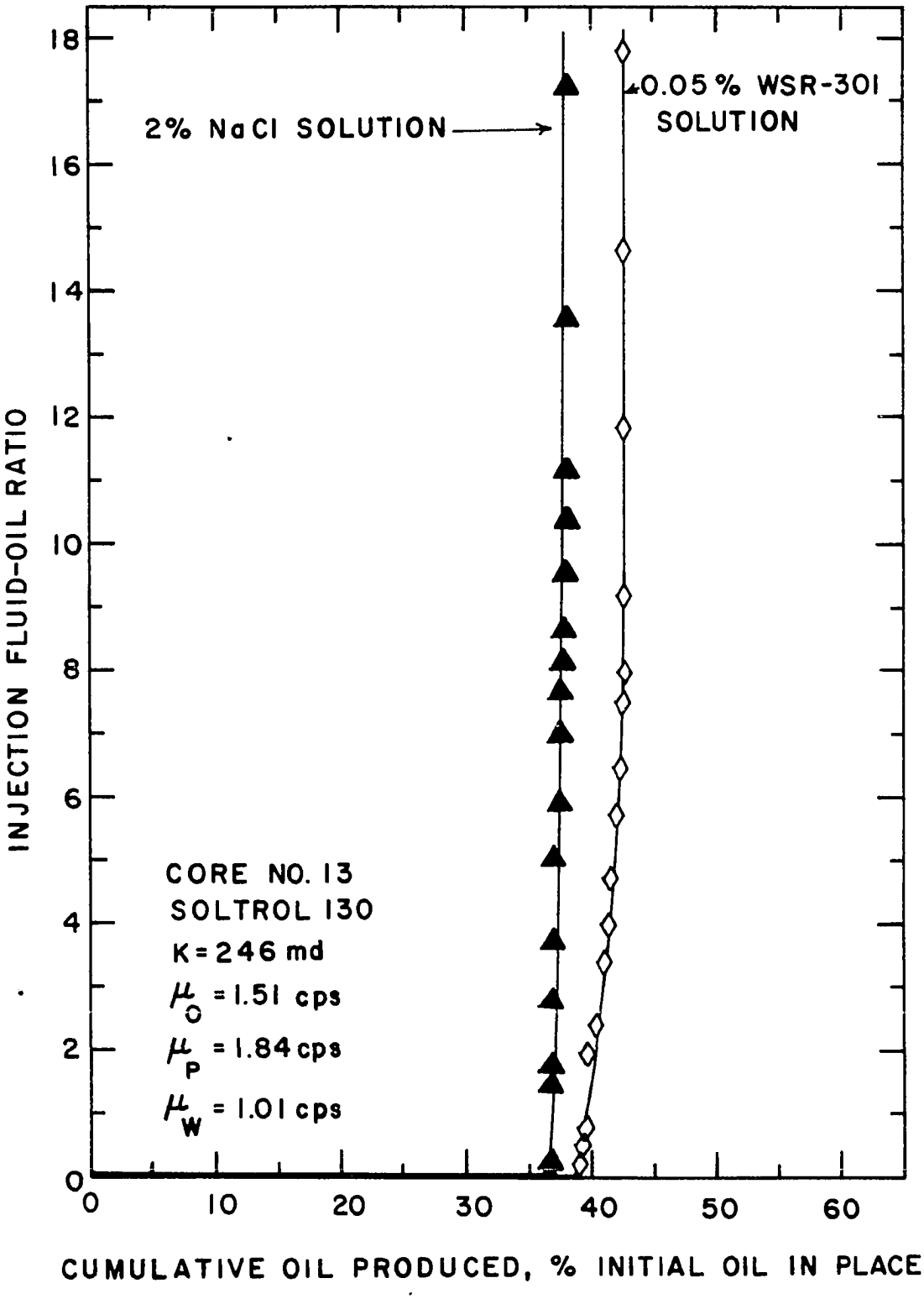

Figure VI-65. Injection Fluid-Oil Ratio Versus Cumulative Oil Produced.

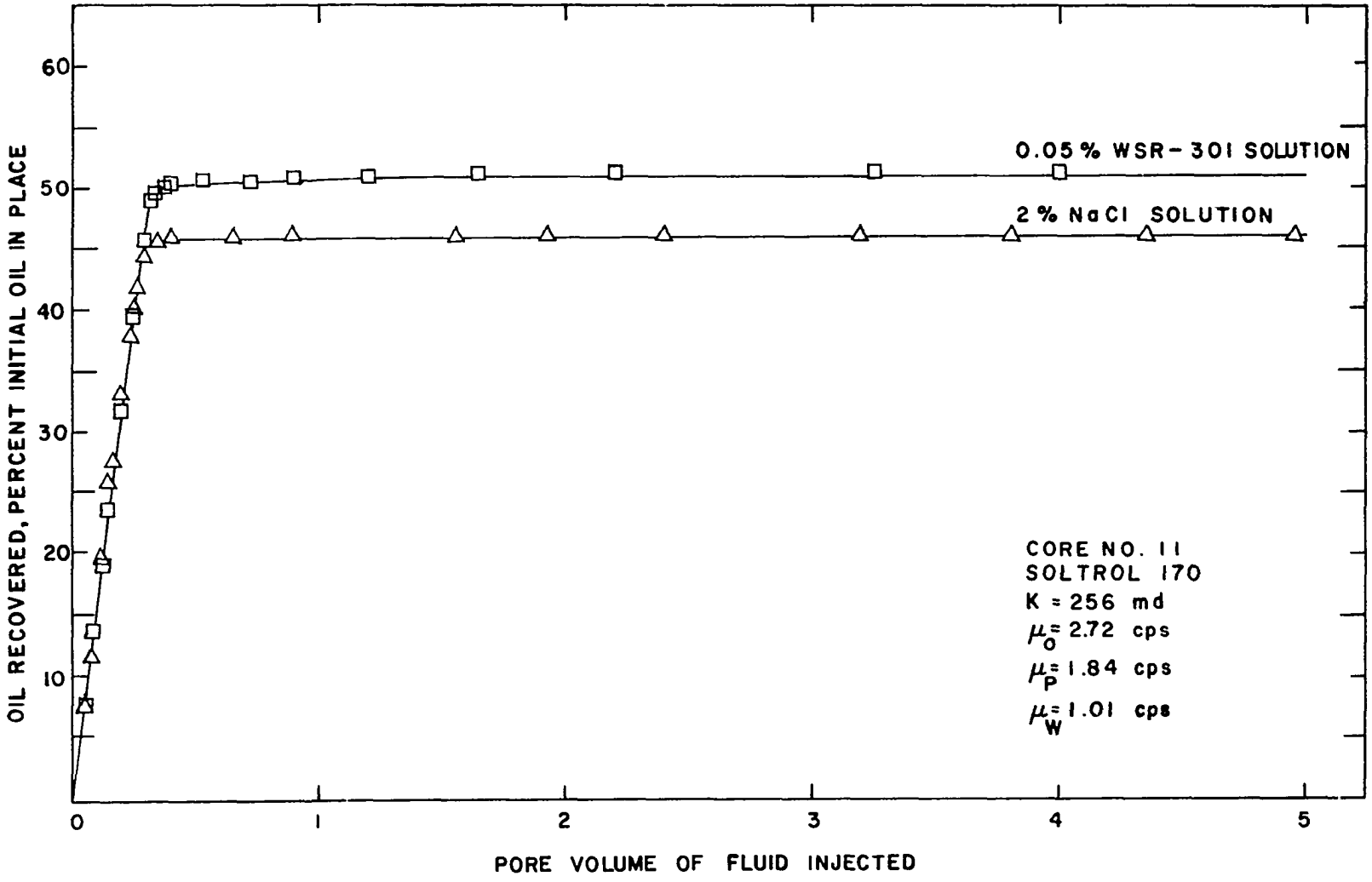

Figure VI-66. Oil Displacement from Core by Brine and 0.05% "Polyox" WSR-301 Solution Run 39 and 40.

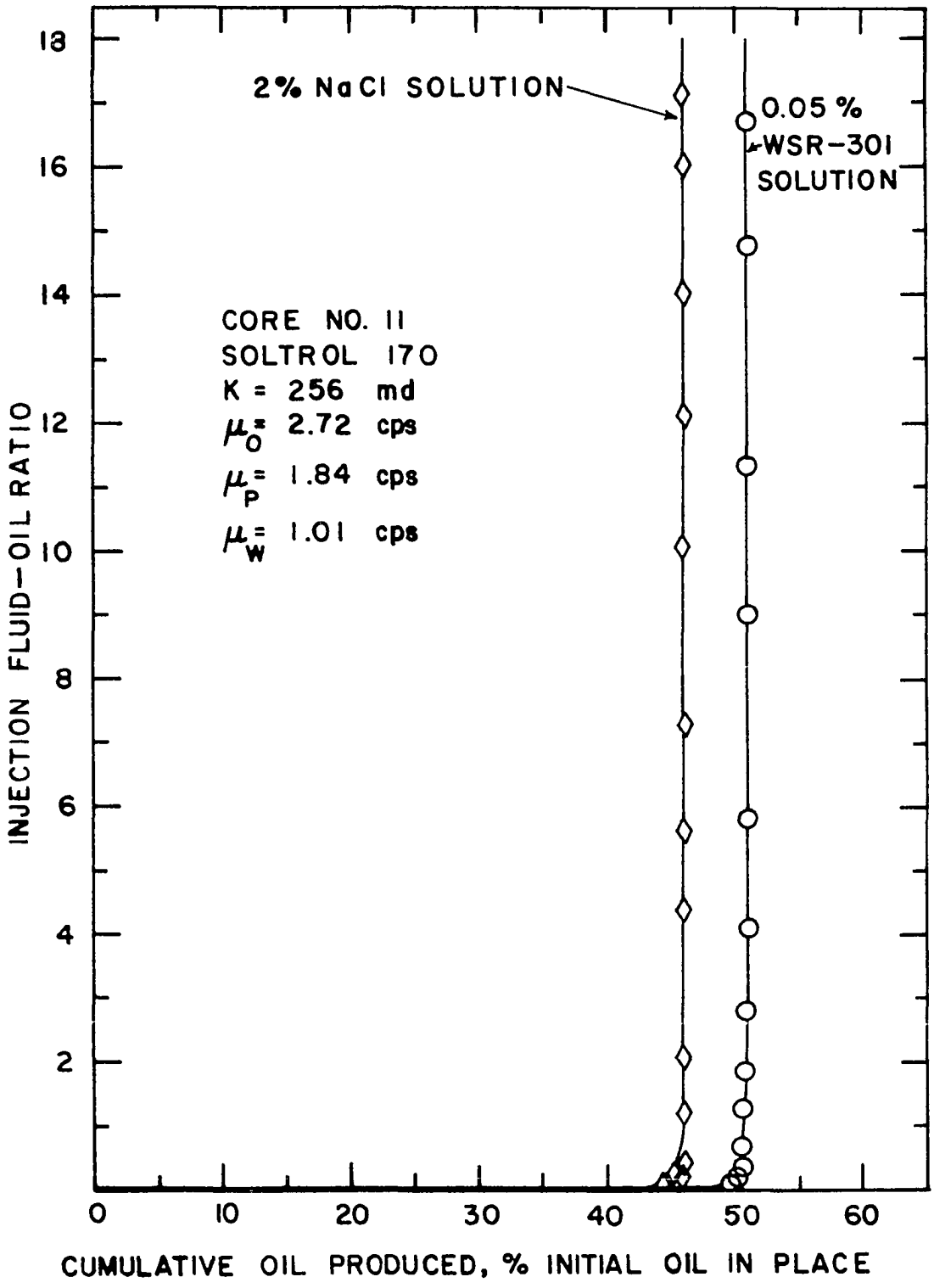

Figure VI-67. Injection Fluid-Oil Ratio Versus Cumulative Oil Produced.

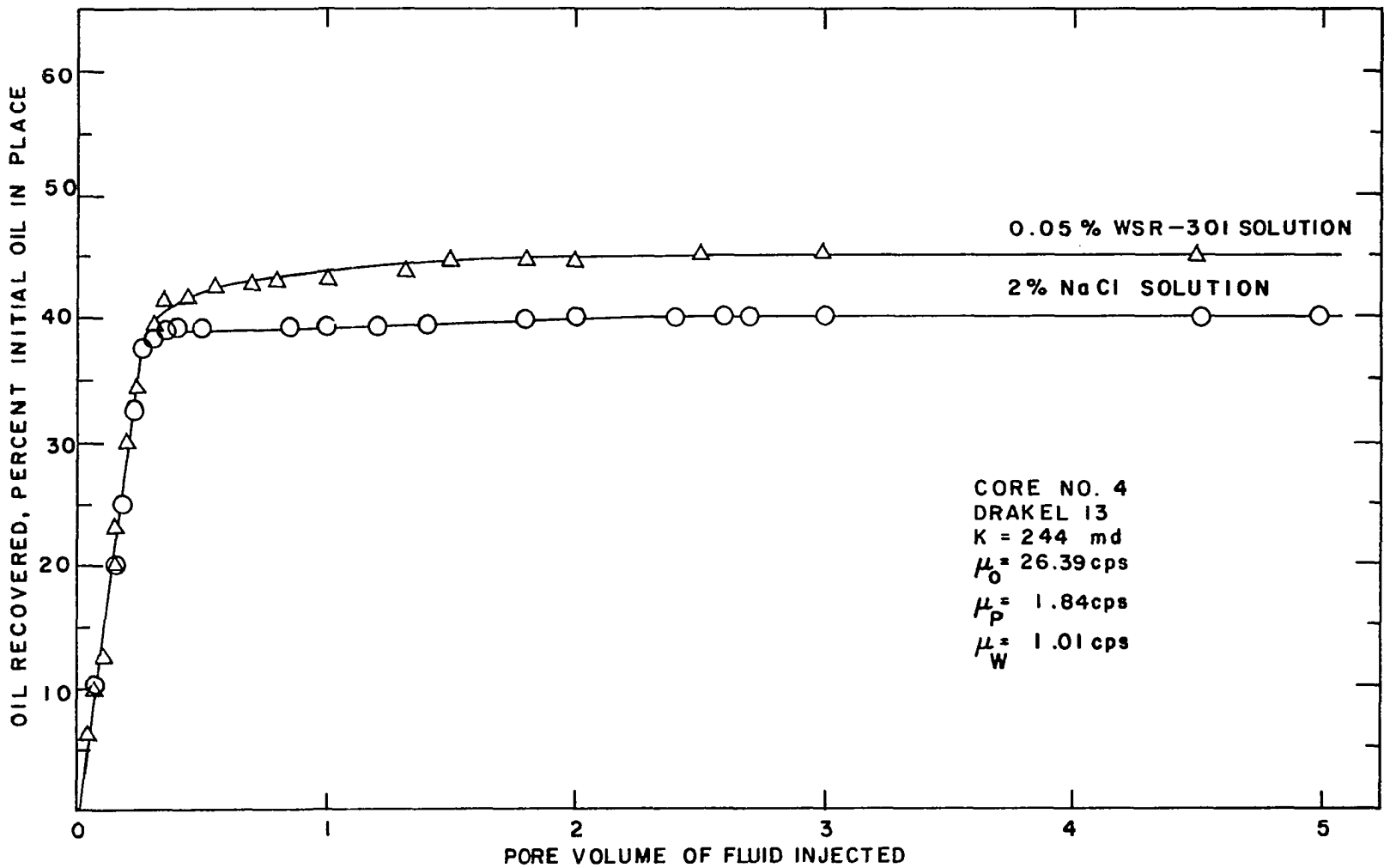

Figure VI-68. Oil Displacement from Core by Brine and 0.05% "Polyox" WSR-301 Solution Run 41 and 42.

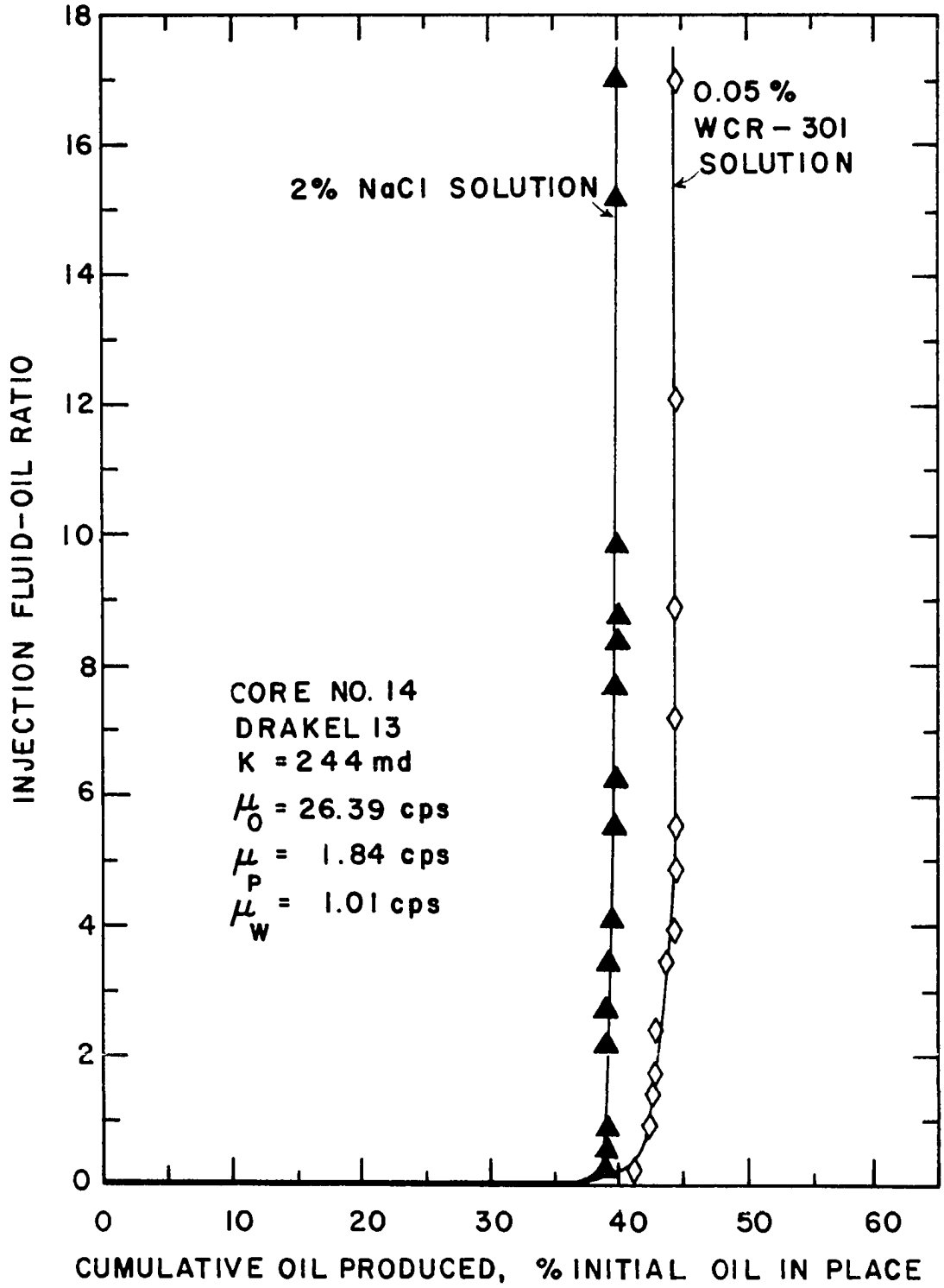

Figure VI-69. Injection Fluid-Oil Ratio Versus Cumulative Oil Produced.

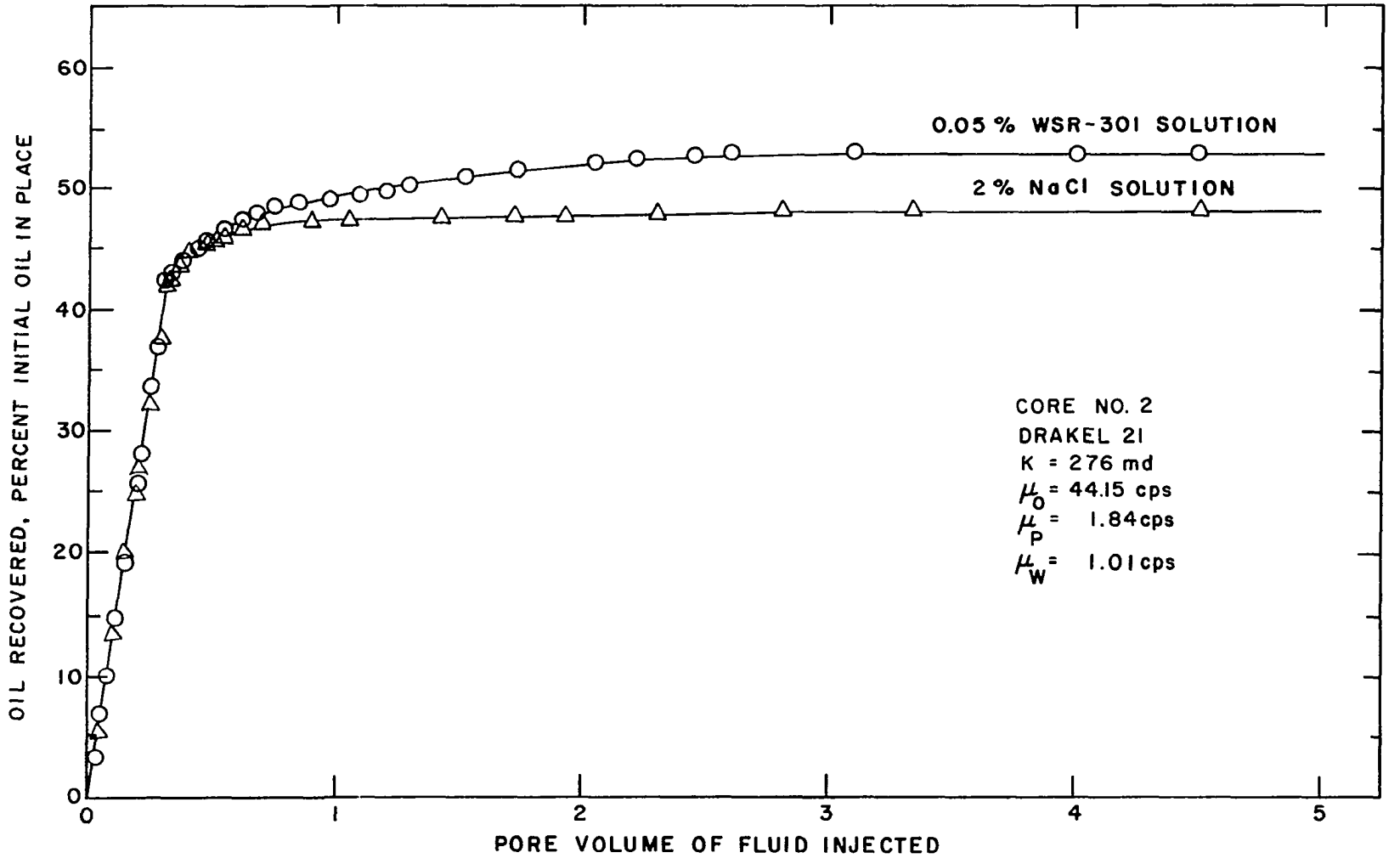

Figure VI-70. Oil Displacement from Core by Brine and 0.05% "Polyox" WSR-301 Solution Run 43 and 44.

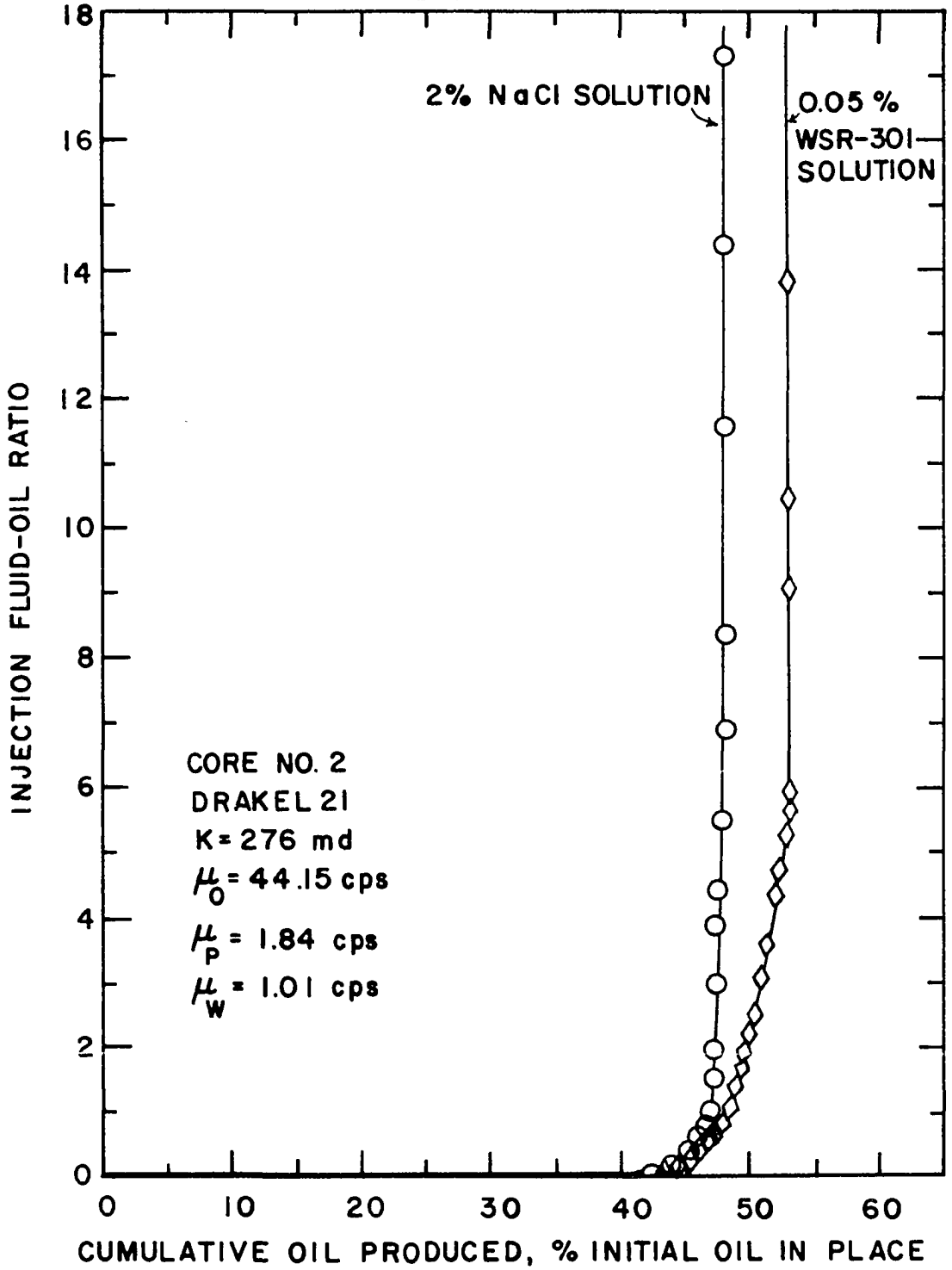

Figure VI-71. Injection Fluid-Oil Ratio Versus Cumulative Oil Produced.

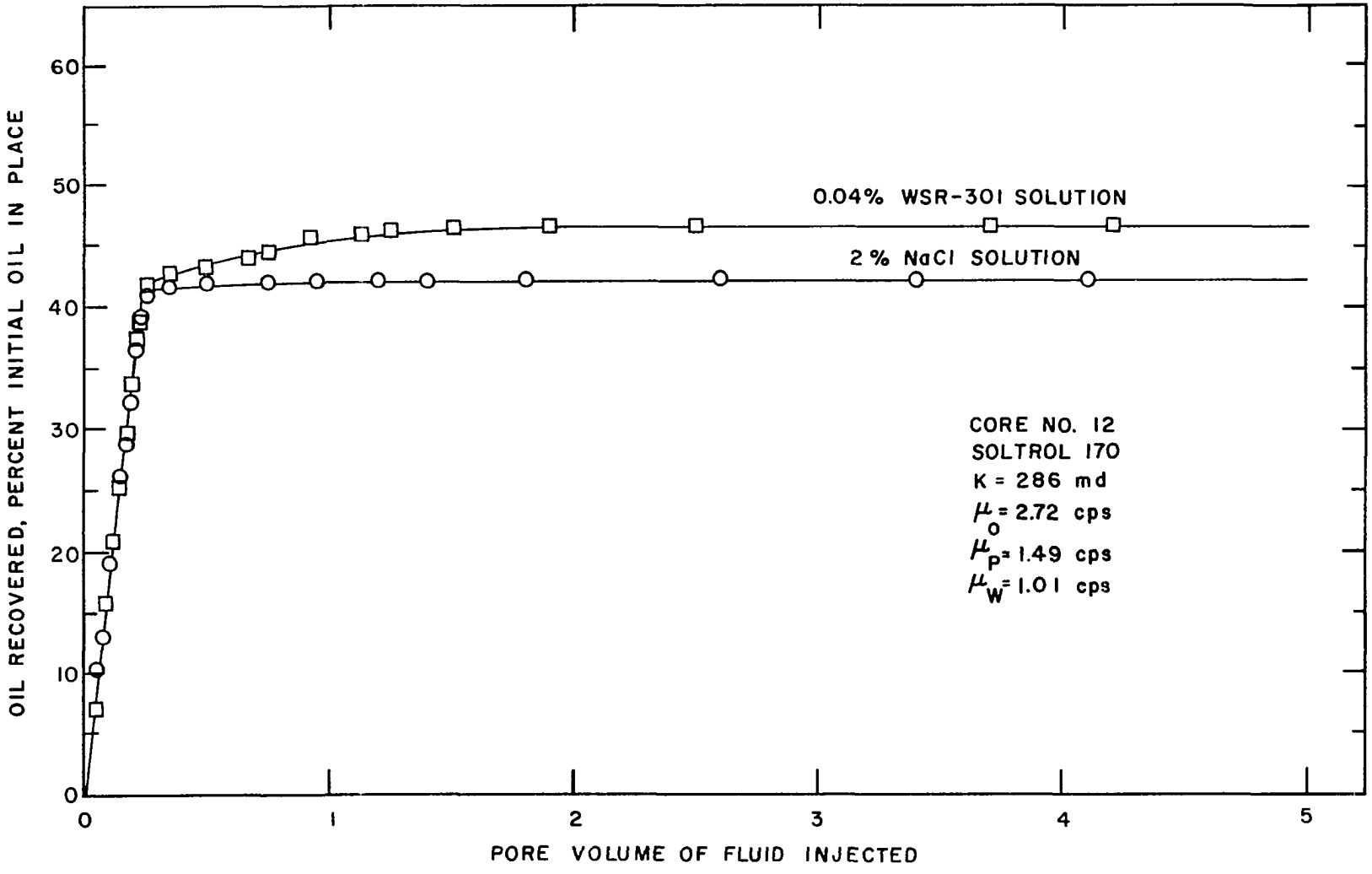

Figure VI-72. Oil Displacement from Core by Brine and 0.04% "Polyox" WSR-301 Solution Run 45 and 46.

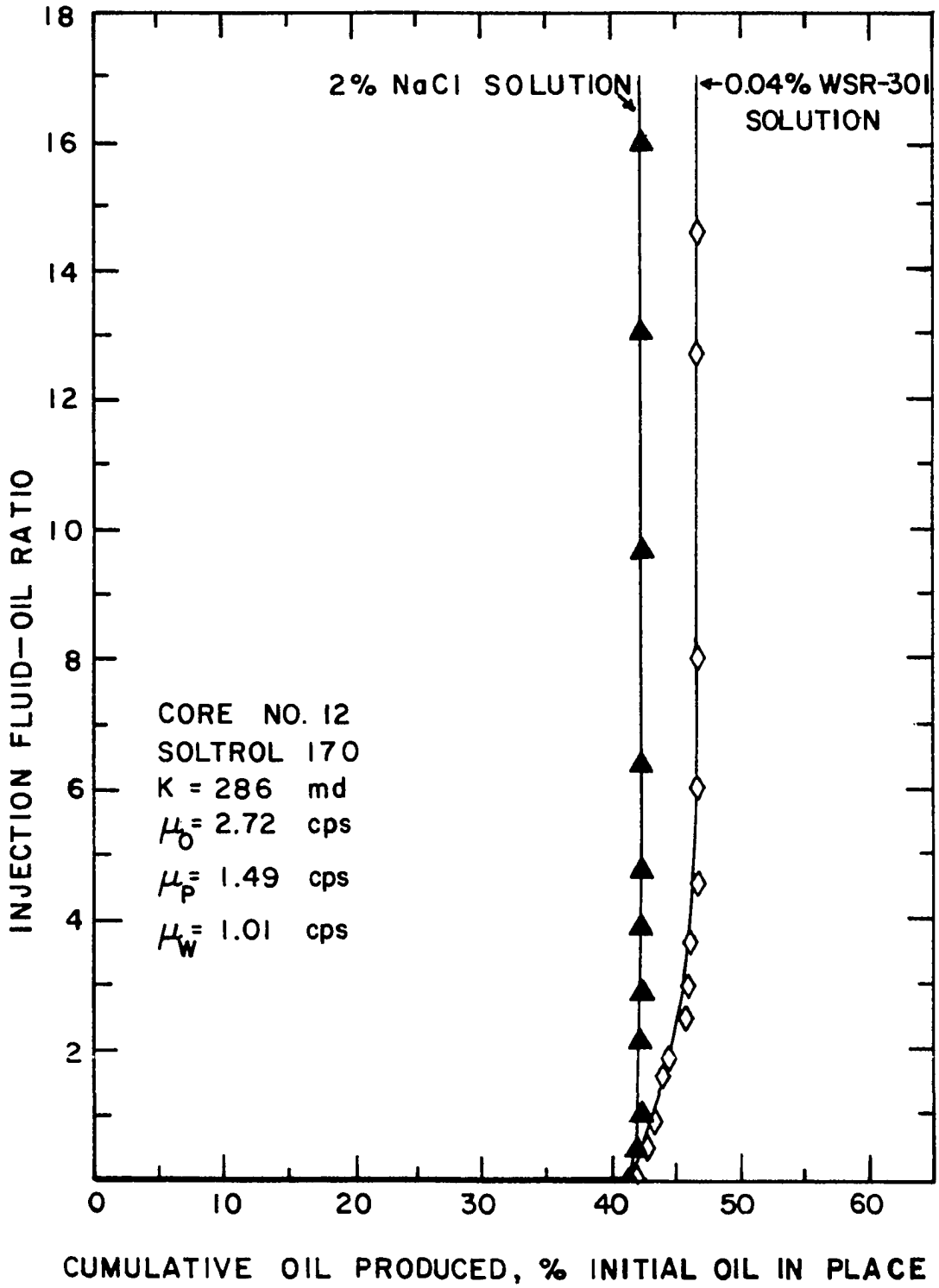

Figure VI-73. Injection Fluid-Oil Ratio Versus Cumulative Oil Produced.

40 Figure VI-66 was used, but the polymer concentration was reduced to .04 percent for which the solution viscosity was only 1.49 cps. It can be seen from Figure VI-72 that, also the same kind of oil as the run No. 40 was used, the increase in oil recovery is much lower than that of the run with the 1.84 cps polymer solution. This result clearly indicates that also an improvement in the mobility ratio of the system was achieved through the use of .04 percent "polyox" WSR-301 polymer. The polymer concentration and consequently the solution viscosity was not high enough to provide a comparable mobility ratio to that of the previous run. Obviously, the result is a lower displacement efficiency and a poorer oil recovery.

Effect of Viscosity Ratio on Displacement Processes

The effect of viscosity ratio on displacement process can best be demonstrated by comparing the Figures VI-64 through VI-71. These figures are the results of displacement runs made with four different viscosity oils (1.51, 2.72, 26.39, 44.16 cps), and a polymer solution with the viscosity of 1.84 cps. As it can be seen from these figures, in low viscosity oils most of the increase in oil recovery was obtained at breakthrough, while in high viscosity oils two to three pore volumes of polymer solution has to be injected, after breakthrough, in order to achieve a comparable result. The results of these runs as expected are in agreement with

the well known Buckley-Leverett fractional flow relationship. They proposed that in the absence of gravitational and capillary pressure effects, f_d, the fraction of displacing fluid in the flowing stream, is related to the properties of the system as follows:

$$f_d = \frac{1}{1 + \frac{K_o}{K_d}\frac{\mu_d}{\mu_o}} \qquad (6\text{-}23)$$

Where μ_o and μ_d are the viscosities of the oil and the displacing fluid, and K_o and K_d are the effective permeabilities of the sand to the oil and the displacing fluid respectively. In the case of a polymer solution displacing oil, Equation 6-23 can be written as:

$$f_p = \frac{1}{1 + \frac{K_o}{K_p}\frac{\mu_p}{\mu_o}} \qquad (6\text{-}24)$$

Where f_p is the fraction of polymer solution in the effluent stream, K_p the effective permeability to polymer, and μ_p the viscosity of the polymer solution. Rearranging Equation 6-24 one obtains:

$$1 = f_p\left(1 + \frac{K_o}{K_p}\frac{\mu_p}{\mu_o}\right) \qquad (6\text{-}25)$$

Dividing the both sides of the Equation 6-25 by f_p

$$\frac{1}{f_p} - 1 = \frac{K_o}{K_p}\frac{\mu_p}{\mu_o} \tag{6-26}$$

or

$$\frac{K_o}{K_p}\frac{\mu_p}{\mu_o} = \frac{1 - f_p}{f_p} \tag{6-27}$$

Let $f_o = \frac{q_o}{q_o + q_p}$ and $f_p = 1 - f_o$, Equation 6-27 can be written as: (6-28)

$$\frac{K_o}{K_p}\frac{\mu_p}{\mu_o} = \frac{1 - 1 + f_o}{1 - f_o} = \frac{f_o}{1 - f_o} = \frac{q_o/(q_o + q_p)}{1 - q_o/(q_o + q_p)}$$

$$\frac{K_o}{K_p}\frac{\mu_p}{\mu_o} = \frac{q_o}{q_p} \tag{6-29}$$

The reciprocal of the Equation 6-29 will be:

$$\frac{K_p}{K_o}\frac{\mu_o}{\mu_p} = M = \frac{q_p}{q_o} \tag{6-30}$$

It can be seen from Equation 6-30 that the producing polymer oil ratio, q_p/q_o, is a function of the product of the oil-polymer viscosity ratio and the ratio of their effective permeability. Since the effective permeability is primarily a function of the average fluid saturation in the core (15), any change in the right hand side of the Equation 6-30 will be a result of a change in the viscosity ratio. Thus, an

increase in polymer-oil ratio at a particular saturation in a core may be anticipated from a decrease in polymer viscosity or an increase in the oil viscosity that was essentially the case with this investigation. A high viscosity oil, resulted in a lower oil recovery, and a higher polymer production, at breakthrough. The result was that a higher volume of polymer solution had to be injected, and consequently a longer period of time had to be devoted to achieve the ultimate oil recovery.

In order to obtain a successful oil recovery through the process of polymer injection, the process should at least achieve one of two things:

1. Improve the volumetric sweep efficiency of the reservoir.
2. Reduce the average oil saturation of the swept volume.

The results of this study clearly indicates that only a very small, if any, reduction in residual oil saturation can be expected from polymer injection. Therefore, polymer injection must essentially recover more oil by improving volumetric efficiency.

CHAPTER VII

CONCLUSIONS

Based on the experimental work, the following conclusions were drawn, subject, of course, to the limitations of the experimental work and applicable only to the specified system:

1. The viscometer data obtained for a total of 88 solutions of twelve different polymers, over a broader range of shear stress-shear rate than any other previous investigation, appeared to fit the power law equation quite well. The standard error of estimation ranged between 0.006 for 0.025 percent RC-322 to 0.125 for 0.05 percent AP-30 solution.

2. Of all the solutions tested, only the 2 percent solution of WSR-35 and the 0.025 percent solution of NP-20 were found to be Newtonian the rest appeared to be non-Newtonian.

3. Furthermore, except for a handful of non-Newtonian solutions, which exhibited dilatancy, the rest appeared to be pseudoplastics.

4. Based upon the rheological data it was concluded that the polymer solution viscosity increased as the molecular weight and polymer concentration increased.

5. The data also indicates that polymer solution viscosity and its shear dependence decreased with increasing sodium chloride concentration. However, an unusual increase in solution viscosity at NaCl concentrations greater than 4 percent may be attributed to the high percentage of dissolved salt not to the polymer behavior.

6. The solution viscosity decreased as the solution temperature increased. The fact that the viscosity-temperature curves of five different polymer solutions did not follow a specific pattern, has led to the rejection of the previously reported concept that the decrease in the viscosity of polymer solution is due only to the decrease in the viscosity of water as the temperature is increased.

7. The flow behavior of polymer solutions through porous media was successfully expressed by the resistance factor-velocity relationship.

8. The resistance to flow, for most of the solutions tested, exhibited its maximum value and it was essentially constant over a region of relatively low flow rates whereas at higher level of flow rates the resistance to flow decreased as the flow velocity increased.

9. The resistance to flow, in porous media, is due both to the change in solution viscosity and to the reduction

in the core permeability. At low rates of flow velocity, the polymer solution essentially behaves as a Newtonian fluid therefore permeability reduction is probably the only factor causing the flow resistance. While at higher rates of flow the polymer solution behaves as a pseudoplastic fluid. This behavior combined with the reduction in the core permeability results in a decrease in the resistance factor, as the flow velocity is increased. In this region of higher flow velocities, no doubt, non-Newtonian behavior of the polymer solution is the predominant factor influencing the resistance to flow.

10. A reduced friction factor-Reynolds number, which relates the fluid properties to the flow characteristics, was developed to predict the flow of non-Newtonian polymer solutions through consolidated porous media. The correlation was successfully tested both for flow of a 2 percent NaCl solution and flow of four different polymer solutions.

11. Except for the 0.05 percent solution of partially hydrolyzed polyacrylamide "pusher" 700 which has apparently shown some dilatancy behavior, the rest appeared to follow the correlation quite well. On the reduced friction factor-Reynolds number plot for the flow of a 0.05 percent polyacrylamide "pusher" 700 solution through a consolidated core dilatancy shows up in the same way as turbulence in the flow of a non-Newtonian fluid.

12. Based upon the oil displacement from consolidated core data it was concluded that 1) There is an increase in oil recovery by polymer injection over water injection. The increase in oil recovery varied between 4 to 6 percent of the initial oil in place. 2) The increase in oil recovery at breakthrough is much higher for oils with low viscosities than those with higher viscosities. 3) Only a small, if any, reduction in residual oil saturation can be expected from polymer injection. Therefore, polymer injection must essentially recover more oil by improving volumetric sweep efficiency.

REFERENCES

1. Baily, F. E., Powell, G. M., and Smith, K. L., "High Molecular Weight Polymers of Ethylene Oxide: Solution Properties," Industrial and Engineering Chemistry, 50 (1):8-11. January 1958.

2. Billmeyer, F. W., Jr., Textbook of Polymer Chemistry, (New York: Interscience Publishers, Inc., 1965).

3. Bird, R. B., Stewart, W. E., and Lightfoot, E. N., Transport Phenomena, (New York: John Wiley and Sons, Inc., 1965).

4. Bird, R. B., "Unsteady Pseudoplastic Flow Near a Moving Wall," A.I.Ch.E. Journal, 5:1959.

5. Bogur, D. C., "An Explicit Constitutive Equation Based on an Integrated Strain History," Industrial and Engineering Chemistry Fundamentals, 5:253. May 1966.

6. Bueche, F., Physical Properties of Polymer, (New York: Interscience Publishers, Inc., 1962).

7. Burcik, Emil J., "A Note on the Flow Behavior of Polyacrylamide Solutions in Porous Media," Producers Monthly, June 1965, 14-17.

8. Burcik, Emil J., "Pseudo Dialatant Flow of Polyacrylamide Solutions in Porous Media," Producers Monthly, March, 1967.

9. Burcik, Emil J., and Ferrer, Jose, "The Mechanism of Pseudo Dialatant Flow," Producers Monthly, March, 1968, 7-8.

10. Burcik, Emil J., and Walrond, Kermitt W., "Microgel in Polyacrylamide Solutions and its Role in Mobility Control," Producers Monthly, September 1968, 12-14.

11. Burcik, Emil J., "The Mechanism of Microgel Formation in Partially Hydrolyzed Polyacrylamide," Journal of Petroleum Technology, April 1969, 373-374.

12. Carothers, W. H., Transactions of Faraday Society, 32:39. 1936.

13. Carpenter, N. F., and Ernst, E. A., "Acidizing with Swellable Polymers," Journal of Petroleum Technology, 295:1041. September 1962.

14. Christopher, Robert H., and Middleman, Stanley, "Power-Law Flow through a Packed Tube," Industrial and Engineering Chemistry Fundamentals, 4(4):422-425. November 1965.

15. Clay, Trell Dane, The Effect of Polymer Additives on Oil Recovery in Conventional Waterflooding, Master of Science Thesis, Department of Petroleum Engineering, University of Oklahoma, 1965.

16. Collier, John R., "Polymer Deformation and Orientation," Industrial and Engineering Chemistry, 61(10):72-85. October 1969.

17. Collins, Royal Eugene, Flow of Fluid through Porous Materials, (New York: Reinhold Publishing Corporation, 1961).

18. Dauben, Dwight L., Non-Newtonian Flow through Porous Media, Ph.D. Dissertation, Department of Petroleum Engineering, University of Oklahoma, 1966.

19. Dauben, Dwight L., and Menzie, D. E., "Flow of Polymer Solutions through Porous Media," Journal of Petroleum Technology, August 1967, 1065-1072.

20. Drew, Thomas B., and Hoopee, Jr., John W., Advances in Chemical Engineering, (New York: New York Academic Press, Inc., 1956). Vol. 1.

21. Ergun, S., "Fluid Flow through Packed Columns," Chemical Engineering Progress, 1952. Vol. 48.

22. Eyring, J., "Viscosity, Plasticity, and Diffusion as Examples of Absolute Reaction Rates," Journal of Chemistry and Physics, 1963. Vol. 4.

23. Ferry, John D., Viscoelastic Properties of Polymers, (New York: John Wiley and Sons, Inc., 1961).

24. Flory, Paul J., Principles of Polymer Chemistry, (New York: Cornell University Press, 1953).

25. Frederickson, Arnold G., Principles and Application of Rheology, Englewood Cliffs, New Jersey: Prentice-Hall, Inc., 1964).

26. Frederickson, A. G., "Viscoelastic Phenomena in Thick Liquids," Modern Chemical Engineering, Edited by Andreas Acrivos. 1:197-259.

27. Gee, R. E., and Lyon, J. B., "Nonisothermal Flow of Viscous Non-Newtonian Fluids," Industrial and Engineering Chemistry,1957. Vol. 49.

28. Gogarty, W. G., "Rheological Properties of Pseudo-plastic Fluids in Porous Media," paper presented at the 41st Annual Fall Meeting of the Society of Petroleum Engineers of AIME, Dallas, Texas, October 2-5, 1966, SPE No. 1566-A.

29. Gogarty, W. B., "Mobility Control with Polymer Solutions," Society of Petroleum Engineers Journal, June 1967, 161-170.

30. Gogarty, W. B., Meabon, H. P., and Milton, H. W., Jr., "Mobility Control Design for Miscible-Type Waterfloods using Micellar Solutions," Journal of Petroleum Technology, February 1970, 141-147.

31. Gregg, S. J., The Surface Chemistry of Solids, (New York: Reinhold Publishing Corporation,1961). Second Edition.

32. Harries, C., Annules der Chemie und Pharmacie, 1914. Vol. 406.

33. Harvey, A. Herbert, An Investigation of the Flow of Polymers Solutions Through Porous Media, Ph.D. Dissertation, Department of Petroleum Engineering, University of Oklahoma, 1967.

34. Hill, F. N., Bailey, F. E., and Fitzpatrick, J. T., "High Molecular Weight Polymers of Ethylene Oxide: Polymerization with Alkaline Earth Carbonate Catalysts," Industrial and Engineering Chemistry, 50(1):5-7. January 1958.

35. Hlasiwetz, H, and Haberman, J., Annules der Chemie und Pharmacie, 1871. Vol. 159.

36. Jargon, J. R., and Van Poollen, H. K., "Unsteady-state Flow of Non-Newtonian Fluids through Porous Media," paper presented at the 41st annual fall meeting of the Society of Petroleum Engineers of AIME, Dallas, Texas, October 2-5, 1966, SPE No. 1567.

37. Jewett, R. L. and Schurz, G. F., "Polymer Flooding-A Current Appraisal," Paper presented at the 44th annual fall meeting of Society of the Petroleum Engineers of AIME, Denver, Colorado, Sept. 28-October 1, 1969, SPE No. 2545.

38. Jones, Merrill A., "Waterflood Mobility Control: A Case History," Journal of Petroleum Technology, September, 1966, 1151-1156.

39. Ladyzhenskaya, O. A., The Mathematical Theory of Viscous Incompressible Flow, (New York: Gordon & Breach, 1966). Second Edition.

40. Leigh, D. C., "Non-Newtonian Fluids and the Second Law of Thermodynamics," Physics of Fluids, 1962. Vol. 5.

41. Lourenco, A. V., Annales de Chemie et de Physique, 1863. Vol. 67.

42. Lynch, E. J. and MacWilliams, D. C. "Mobility Control with Partially Hydrolyzed Polyacrylamide," Journal of Petroleum Technology, April 1969, 1247-1248.

43. Mark, H. and Whitby, G. S. eds., Collected Papers of Wallace Hume Carothers, (New York: Interscience Publishers, 1940).

44. Mark, Herman F., "The Nature of Polymeric Materials," Scientific American, 217(3):149-156. September 1967

45. McKinley, R. M., Jahns, H. O., Harris, W. W., and Greenhorn, R. A., "Non-Newtonian Flow in Porous Media," A.I.Ch.E. Journals, 12(1):17-20. January 1966.

46. Meter, D. and Brid, R. B., "Tube Flow of Non-Newtonian Polymer Solution: Part I. Laminar Flow and Rheological Models," American Institute of Chemical Engineers Journal, 10:878. 1964.

47. Metzner, A. B., "Recent Developments in the Engineering Aspects of Rheology," Rheological Acta, Band 1, August 1958, 205.

48. Metzner, A. B., Houghton, W. T., Sailor, R. A. and White, J. L., "A Method for Measurement of Normal Stresses in Simple Shearing Flow," Transactions of the Society of Rheology, 5:133-147, 1961.

49. Metzner, A. B., and White, J. L., "Flow Behavior of Viscoelastic Fluids in the Inlet Region of a Channel," A.I.Ch.E Journal, 11(6):989-995. 1965.

50. Metzner, A. B., White, J. L., and Denn, M. M., "Constitution Equations for Viscoelastic Fluids for Short Deformation Period and for Rapidly Changing Flows: Significance of the Deborah Number," A.I.Ch.E. Journal, 12(5). 1966.

51. Middleman, Stanley, The Flow of High Polymers, (New York: Interscience Publishers, 1968).

52. Mooney, Melvin, "Explicit Formulas for Slip and Fluidity," Journal of Rheology, April 1931, 210-222.

53. Mungan, N., Smith, F. W., and Thompson, J. L., "Some Aspects of Polymer Floods," Journal of Petroleum Technology, September 1966, 1143-1150.

54. Muskat, M., The Flow of Homogeneous Fluids Through Porous Media, (Michigan: J. W. Edwards, 1946). Second Printing.

55. Muskat, M., Physical Principles of Oil Production, (New York: McGraw-Hill Book Company, Inc., 1949).

56. Pao, Y. H., Journal of Polymer Science, 1962. Vol. 61.

57. Pasini, III, J., "Initial Results of Oil Recovery Tests on Cow Run Sandstone Core using Polymer Solutions," Producers Monthly, March 1966, 2-3.

58. Patent No. 3,039,529. Secondary Recovery of Petroleum, Keith M. McKennon, June 19, 1962.

59. Patton, J. T. and Coats, K. H., "Prediction of Polymer Flood Performance," paper presented at the 44th annual fall meeting of the Society of Petroleum Engineers of AIME, Denver, Colorado, September 28, October 1, 1969. SPE No. 2546.

60. Powell, R. E. and Eyring, H., "Mechanism of the Relaxation Theory of Viscosity," Nature, 1944. Vol. 154.

61. Pranger, S., "Viscous Flow through Porous Media," Physics of Fluids, 1961. Vol. 4.

62. Pye, David J., "Improved Secondary Recovery by Control of Water Mobility," Journal of Petroleum Technology, August 1964, 911-916.

63. Rathna, S. L., "Slow Motion of a Non-Newtonian Liquid Past a Sphere," Journal of Mechanics and Applied Mathematics, 1962. Vol. 15.

64. Ree, T. and Eyring, H., The Relaxation Theory of Transport Phenomena, Chapter 3, (New York: Academic Press, 1958).

65. Reiner, M., Deformation of Flow, (London: H. K. Lewis Company, 1949).

66. Reiner, M., Deformation, Strain, and Flow, (New York: Interscience, 1960).

67. Sadowski, T. J. and Bird, R. B., "Non-Newtonian Flow through Porous Media," I. Theoretical, Transaction of the Society of Rheology, 1965. Vol. 9.

68. Sadowski, T. J., "Non-Newtonian Flow through Porous Media," II. Experimental, Transaction of the Society of Rheology, 1965. Vol. 9.

69. Sandiford, B. B., "Laboratory and Field Studies of Water Floods using Polymer Solutions to Increase Oil Recoveries," Journal of Petroleum Technology, August 1964, 917-22.

70. Severs, Edward T., Rheology of Polymers. (New York: Reinhold Publishing Corporation, 1962).

71. Sisko, A. W., "The Flow of Lubricating Greases," Industrial and Engineering Chemistry, 1958. Vol. 50.

72. Sitaramiah, Gullapalli, and Smith, Charles L., "Turbulent Drag Reduction by Polyacrylamide and Other Polymers," Society of Petroleum Engineers Journal, June 1969, 183-188.

73. Skelland, A. H. P., Non-Newtonian Flow and Heat Transfer, (New York: John Wiley and Sons, Inc., 1967).

74. Slater, George E. and Faroug Ali, S. M., "Prediction of Sweep Efficiency in Polymer Flooding," Producers Monthly, October 1968, 22-27.

75. Slattery, J. C. and Bird, R. B., "Non-Newtonian Flow Past a Sphere," Chemical Engineering Science, 1961. Vol. 16.

76. Smith, Frank W., "The Behavior of Partially Hydrolyzed Polyacrylamide Solutions in Porous Media," Journal of Petroleum Technology, February 1970, 148-156.

77. Snell, Gene W. and Schurz, George F., "Polymer Chemicals Aid in Unique Recovery Process," Petroleum Engineers, February 1966, 53-59.

78. Stille, John K., Introduction to Polymer Chemistry, (New York: John Wiley and Sons, Inc., 1962).

79. Tamura, Mikio, Kurata, Mikio and Kotaka, Tado, "Normal Stress Effect in Polymer Solutions, Measurements in a Parallel Plate Instrument," Bulletin Chemical Society of Japan, 37(32). 1959.

80. Union Carbide Corporation Information Bulletin No. F-41101 A, How to Dissolve Polyox Water Soluble Resins, December 1964.

81. Union Carbide Corporation Application Bulletin No. F-41350 A, POLYOX Friction Reducing Agent FRA, December 1966.

82. Union Carbide Corporation Information Bulletin No. F-42506, POLYOX--Water-Soluble Resins, June 1969.

83. Van Wazer, J. R., Lyons, J. W., Kim, K. Y., and Caldwell, R. E., Viscosity and Flow Measurement, (New York: Interscience Publishers, 1963).

84. Wattenbarger, Robert A., "A Rapid Method for Determining Characteristics of Liquid Flow in Porous Media," Journal of Petroleum Technology, November 1968, 1219-1221.

85. Weissenberge, K., "A Continuum Theory of Rheological Phenomena," Nature, 1948. Vol. 159.

86. Weissenberge, K., "Abnormal Substances and Abnormal Phenomena of Flow," Proceedings of International Congress of Rheology, 1948. 1:29.

APPENDIX A

NOMENCLATURE

APPENDIX A

NOMENCLATURE

Upper Case Letters

A = Cross sectional area

A_o = Fluid parameter, defined by Equation 3-14

A_1 = Fluid parameter, defined by Equation 3-14

a = Constant, defined by Equation 3-13

b = Constant, defined by Equation 3-13

c = Fluid parameter, defined by Equation 3-17

D = Average sand grain diameter

D = Capillary diameter

D_P = Mean particle diameter

d = Constant, defined by Equation 2-10

F = Ergun's friction factor

F = Constant, defined by Equation 2-18

f = Friction factor

f_d = Fraction of displacing fluid in the flowing stream

f_p = Fraction of polymer in the flowing stream

f_r = Reduced friction factor

G = Mass flow rate, ρV

g = Gravitational acceleration

I_1, I_2, I_3 = Scalar invariant of the $\bar{\bar{\gamma}}$ tensor

K = Permeability

K_o = Effective permeability to oil

K_P = Effective permeability to polymer

K_W = Effective permeability to water

k = Constant, defined by Equation 3-12

L = Length

M = Mobility ratio, defined by Equation 1-1

N = Number of data points

n = Constant, defined by Equation 3-12

ΔP = Pressure drop

Q = Volumetric flow rate

q = Volumetric flow rate

q_o = Oil flow rate

q_p = Polymer flow rate

R = Resistance factor, defined by Equation 6-8

R = Spindle radius associated with cone and plate viscometer

R_e = Reynolds number

R_h = Hydralic radius

R_r = Reduced Reynolds number

s = Constant, defined by Equation 2-11

T = Torque

t = Constant defined by Equation 2-11

V = Superficial velocity V_o/ϕ

V_o = Velocity, Q/A

$\bar{V}_o$ = Velocity vector

$\bar{V}$ = Average velocity in capillary model

Greek Symbols

α = Constant, defined by Equation 6-11

β = Constant, defined by Equation 2-4

γ = Shear rate, = $\frac{du}{dy}$

γ_{ij} = Cortesian components of the rate of deformation tensor

$\bar{\bar{\gamma}}$ = Rate of deformation tensor

$\bar{\gamma}$ = Average shear rate

λ = Mobility, K/μ

λ_o = Oil mobility

λ_p = Polymer mobility

λ_w = Water mobility

μ = Fluid viscosity

μ_c = Cross viscosity

μ_e = Effective viscosity

μ_o = Oil viscosity

μ_o = Lower limiting viscosity (Newtonian viscosity)

μ_p = Polymer viscosity

μ_w = Water viscosity

μ_∞ = Upper limiting viscosity

ρ = Fluid density

σ = Potential

τ = Shear stress

τ_E = Shear stress measured with viscometer

τ_{ij} = Cortesian components of shear stress tensor

τ_M = Shear stress estimated from power law model

τ_{yx} = Shear stress acting in the x-direction on a surface normal to the y-direction

$\bar{\bar{\tau}}$ = Shear stress tensor

θ = Cone angle associated with cone and plate viscometer

ϕ = Porosity

Ω = Rotation speed associated with viscometer

APPENDIX B

POLYMER SOLUTION RHEOLOGICAL DATA

TABLE B-1

VISCOMETRIC DATA

0.025 Percent Polyacrylamide NP-10 In 0.2 Percent NaCl Solution

Run Number	1
Solution Temperature	76°F
Solution Density	0.990 gm/cm^3
Cannon-Fenske Viscosity	1.228 cps
Power Law Exponent, n	0.9297
Power Law Coefficient, k	0.0212
Standard Error of Estimation	0.0640

Viscometer Speed (rpm)	Shear Rate (sec^{-1})	Percent Full Scale Torque	Shear Stress ($dynes/cm^2$)	Viscosity (cps)
0.3	1.15	0.10	0.023	2.000
0.6	2.30	0.20	0.044	1.913
1.5	5.75	0.40	0.093	1.617
3.0	11.50	0.75	0.175	1.522
6.0	23.00	1.65	0.384	1.669
12.0	46.00	3.15	0.733	1.594
30.0	115.00	7.75	1.803	1.567
60.0	230.00	15.45	3.595	1.564

TABLE B-2

VISCOMETRIC DATA

0.05 Percent Polyacrylamide NP-10 In 0.2 Percent NaCl Solution

Run Number	2
Solution Temperature	76°F
Solution Density	0.990 gm/cm^3
Cannon-Fenske Viscosity	1.492 cps
Power Law Exponent, n	0.8867
Power Law Coefficient, k	0.0396
Standard Error of Estimation	0.0201

Viscometer Speed (rpm)	Shear Rate (sec^{-1})	Percent Full Scale Torque	Shear Stress ($dynes/cm^2$)	Viscosity (cps)
0.3	1.15	0.19	0.045	3.913
0.6	2.30	0.35	0.081	3.522
1.5	5.75	0.85	0.198	3.443
3.0	11.50	1.50	0.349	3.035
6.0	23.00	2.55	0.593	2.578
12.0	46.00	5.20	1.210	2.631
30.0	115.00	11.25	2.618	2.275
60.0	230.00	21.55	5.014	2.181

TABLE B-3

VISCOMETRIC DATA

0.075 Percent Polyacrylamide NP-10 In 0.2 Percent NaCl Solution

Run Number	3
Solution Temperature	76°F
Solution Density	0.990 gm/cm^3
Cannon-Fenske Viscosity	1.748 cps
Power Law Exponent, n	0.8207
Power Law Coefficient, k	0.0587
Standard Error of Estimation	0.0219

Viscometer Speed (rpm)	Shear Rate (sec^{-1})	Percent Full Sclae Torque	Shear Stress ($dynes/cm^2$)	Viscosity (cps)
0.3	1.15	0.30	0.070	6.087
0.6	2.30	0.50	0.116	5.043
1.5	5.75	1.00	0.233	4.052
3.0	11.50	1.75	0.407	3.539
6.0	23.00	3.35	0.780	3.391
12.0	46.00	6.10	1.419	3.085
30.0	115.00	12.05	2.804	2.437
60.0	230.00	22.55	5.247	2.282

TABLE B-4

VISCOMETRIC DATA

0.25 Percent Polyacrylamide NP-10 In 0.2 Percent NaCl Solution

Run Number	4
Solution Temperature	76°F
Solution Density	0.993 gm/cm^3
Cannon-Fenske Viscosity	4.074 cps
Power Law Exponent, n	0.9850
Power Law Coefficient, k	0.0621
Standard Error of Estimation	0.0500

Viscometer Speed (rpm)	Shear Rate (sec^{-1})	Percent Full Scale Torque	Shear Stress ($dynes/cm^2$)	Viscosity (cps)
0.3	1.15	0.31	0.072	6.261
0.6	2.30	0.65	0.151	6.565
1.5	5.75	1.70	0.395	6.869
3.0	11.50	3.15	0.733	6.373
6.0	23.00	6.10	1.419	6.168
12.0	46.00	11.95	2.781	6.046
30.0	115.00	27.95	6.503	5.651
60.0	230.00	51.30	11.937	5.192

TABLE B-5

VISCOMETRIC DATA

0.35 Percent Polyacrylamide NP-10 In 0.2 Percent NaCl Solution

Run Number	5
Solution Temperature	76°F
Solution Density	0.990 gm/cm^3
Cannon-Fenske Viscosity	4.819 cps
Power Law Exponent, n	0.8986
Power Law Coefficient, k	0.0988
Standard Error of Estimation	0.0341

Viscometer Speed (rpm)	Shear Rate (sec^{-1})	Percent Full Scale Torque	Shear Stress ($dynes/cm^2$)	Viscosity (cps)
0.3	1.15	0.50	0.116	10.087
0.6	2.30	1.00	0.233	10.130
1.5	5.75	1.80	0.419	7.280
3.0	11.50	3.60	0.838	7.286
6.0	23.00	6.95	1.617	7.029
12.0	46.00	13.00	3.020	6.565
30.0	115.00	31.70	7.376	6.410
60.0	230.00	58.20	13.540	5.890

TABLE B-6

VISCOMETRIC DATA

0.50 Percent Polyacrylamide NP-10 In 0.2 Percent NaCl Solution

Run Number	6
Solution Temperature	76°F
Solution Density	0.993 gm/cm^3
Cannon-Fenske Viscosity	6.826 cps
Power Law Expoennt, n	0.9321
Power Law Coefficient, k	0.1210
Standard Error of Estimation	0.0215

Viscometer Speed (rpm)	Shear Rate (sec^{-1})	Percent Full Scale Torque	Shear Stress ($dynes/cm^2$)	Viscosity (cps)
0.3	1.15	0.60	0.139	12.086
0.6	2.30	1.05	0.244	10.608
1.5	5.75	2.65	0.616	10.713
3.0	11.50	5.30	1.233	10.720
6.0	23.00	10.25	2.385	10.367
12.0	46.00	19.05	4.433	9.637
30.0	115.00	43.10	10.029	8.715
60.0	230.00	78.00	18.150	7.895

TABLE B-7

VISCOMETRIC DATA

0.75 Percent Polyacrylamide NP-10 In 0.2 Percent NaCl Solution

Run Number	7
Solution Temperature	76°F
Solution Density	0.993 gm/cm^3
Cannon-Fenske Viscosity	28.844 cps
Power Law Exponent, n	0.8709
Power Law Coefficient, k	0.6006
Standard Error of Estimation	0.0118

Viscometer Speed (rpm)	Shear Rate (sec^{-1})	Percent Full Scale Torque	Shear Stress ($dynes/cm^2$)	Viscosity (cps)
0.3	1.15	2.95	0.684	59.477
0.6	2.30	5.20	1.210	52.610
1.5	5.75	11.75	2.734	47.550
3.0	11.50	22.45	5.224	45.420
6.0	23.00	20.20	9.354	40.660
12.0	46.00	70.45	16.414	35.688

TABLE B-8

VISCOMETRIC DATA

0.025 Percent Polyacrylamide NP-20 In 0.2 Percent NaCl Solution

Run Number	8
Solution Temperature	76°F
Solution Density	0.993 gm/cm^3
Cannon-Fenske Viscosity	1.155 cps
Power Law Exponent, n	1.0000
Power Law Coefficient, k	0.0140

Viscometer Speed (rpm)	Shear Rate (sec^{-1})	Percent Full Scale Torque	Shear Stress ($dynes/cm^2$)	Viscosity (cps)
0.6	2.30	0.15	0.035	1.522
1.5	5.75	0.35	0.081	1.409
3.0	11.50	0.75	0.174	1.513
6.0	23.00	1.50	0.349	1.517
12.0	46.00	3.05	0.710	1.543
30.0	115.00	7.30	1.698	1.475
60.0	230.00	14.50	3.374	1.467

TABLE B-9

VISCOMETRIC DATA

0.05 Percent Polyacrylamide NP-20 In 0.2 Percent NaCl Solution

Run Number	9
Solution Temperature	76°F
Solution Density	0.991 gm/cm^3
Cannon-Fenske Viscosity	1.451 cps
Power Law Exponent, n	0.9195
Power Law Coefficient, k	0.0320

Viscometer Speed (rpm)	Shear Rate (sec^{-1})	Percent Full Scale Torque	Shear Stress (dynes/cm^2)	Viscosity (cps)
0.3	1.15	0.15	0.035	3.043
0.6	2.30	0.30	0.698	2.933
1.5	5.75	0.65	0.151	2.626
3.0	11.50	1.15	0.267	2.321
6.0	23.00	2.30	0.535	2.326
12.0	46.00	4.25	0.989	2.150
30.0	115.00	11.30	2.629	2.285
60.0	230.00	22.85	5.317	2.313

TABLE B-10

VISCOMETRIC DATA

0.075 Percent Polyacrylamide NP-20 In 0.2 Percent NaCl Solution

Run Number	10
Solution Temperature	76°F
Solution Density	0.991 gm/cm^3
Cannon-Fenske Viscosity	1.730 cps
Power Law Exponent, n	0.9228
Power Law Coefficient, k	0.0355

Viscometer Speed (rpm)	Shear Rate (sec^{-1})	Percent Full Scale Torque	Shear Stress ($dynes/cm^2$)	Viscosity (cps)
0.6	2.30	0.35	0.082	3.565
1.5	5.75	0.75	0.174	3.026
3.0	11.50	1.40	0.326	2.834
6.0	23.00	2.65	0.617	2.683
12.0	46.00	5.05	1.175	2.554
30.0	115.00	12.30	2.862	2.487
60.0	230.00	23.55	5.480	2.384

TABLE B-11

VISCOMETRIC DATA

0.10 Percent Polyacrylamide NP-20 In 0.2 Percent NaCl Solution

Run Number	11
Solution Temperature	76°F
Solution Density	0.990 gm/cm^3
Cannon-Fenske Viscosity	2.264 cps
Power Law Exponent, n	0.8845
Power Law Coefficient, k	0.0465

Viscometer Speed (rpm)	Shear Rate (sec^{-1})	Percent Full Scale Torque	Shear Stress ($dynes/cm^2$)	Viscosity (cps)
0.3	1.15	0.25	0.058	5.043
0.6	2.30	0.50	0.116	5.043
1.5	5.75	0.75	0.174	3.026
3.0	11.50	1.55	0.361	3.138
6.0	23.00	2.90	0.675	2.936
12.0	46.00	5.55	1.291	2.807
30.0	115.00	12.85	2.990	2.599
60.0	230.00	24.10	5.608	2.439

TABLE B-12

VISCOMETRIC DATA

0.25 Percent Polyacrylamide NP-20 In 0.2 Percent NaCl Solution

Run Number	12
Solution Temperature	76°F
Solution Density	0.990 gm/cm^3
Cannon-Fenske Viscosity	4.788 cps
Power Law Exponent, n	0.8754
Power Law Coefficient, k	0.1270

Viscometer Speed (rpm)	Shear Rate (sec^{-1})	Percent Full Scale Torque	Shear Stress ($dynes/cm^2$)	Viscosity (cps)
0.3	1.15	0.60	0.139	12.087
0.6	2.30	1.30	0.302	13.130
1.5	5.75	2.40	0.558	9.704
3.0	11.50	4.40	1.024	8.904
6.0	23.00	8.25	1.919	8.344
12.0	46.00	15.40	3.583	7.789
30.0	115.00	34.45	8.016	6.966
60.0	230.00	66.55	15.485	6.736

TABLE B-13

VISCOMETRIC DATA

0.35 Percent Polyacrylamide NP-20 In 0.2 Percent NaCl Solution

Run Number	13
Solution Temperature	76°F
Solution Density	0.988 gm/cm^3
Cannon-Fenske Viscosity	8.539 cps
Power Law Exponent, n	0.8541
Power Law Coefficient, k	0.2060

Viscometer Speed (rpm)	Shear Rate (sec^{-1})	Percent Full Scale Torque	Shear Stress ($dynes/cm^2$)	Viscosity (cps)
0.3	1.15	1.00	0.233	20.261
0.6	2.30	1.75	0.407	17.695
1.5	5.75	4.35	1.012	17.599
3.0	11.50	7.40	1.722	14.973
6.0	23.00	14.15	3.292	14.314
12.0	46.00	26.00	6.049	13.150
30.0	115.00	55.90	13.007	11.303
60.0	230.00	96.45	22.443	9.763

TABLE B-14

VISCOMETRIC DATA

0.50 Percent Polyacrylamide NP-20 In 0.2 Percent NaCl Solution

Run Number	14
Solution Temperature	76°F
Solution Density	0.993 gm/cm^3
Cannon-Fenske Viscosity	16.079 cps
Power Law Exponent, n	0.8693
Power Law Coefficient, k	0.3300

Viscometer Speed (rpm)	Shear Rate (sec^{-1})	Percent Full Scale Torque	Shear Stress ($dynes/cm^2$)	Viscosity (cps)
0.3	1.15	1.65	0.384	33.391
0.6	2.30	2.65	0.617	26.391
1.5	5.75	7.50	1.740	30.260
3.0	11.50	13.85	3.216	27.963
6.0	23.00	25.00	5.817	25.292
12.0	46.00	43.35	10.087	21.929
30.0	115.00	87.80	20.430	17.753

TABLE B-15

VISCOMETRIC DATA

0.75 Percent Polyacrylamide NP-20 In 0.2 Percent NaCl Solution

Run Number	15
Solution Temperature	76°F
Solution Density	0.993 gm/cm^3
Power Law Exponent, n	0.8391
Power Law Coefficient, k	0.4320

Viscometer Speed (rpm)	Shear Rate (sec^{-1})	Percent Full Scale Torque	Shear Stress ($dynes/cm^2$)	Viscosity (cps)
0.3	1.15	2.05	0.477	41.478
0.6	2.30	3.55	0.826	35.913
1.5	5.75	8.50	1.978	34.400
3.0	11.50	15.00	3.490	30.345
6.0	23.00	26.90	6.259	27.214
12.0	46.00	45.95	10.685	23.229
30.0	115.00	92.00	21.407	18.607

TABLE B-16

VISCOMETRIC DATA

0.025 Percent Polyacrylamide AP-30 In 0.2 Percent NaCl Solution

Run Number	16
Solution Temperature	76°F
Solution Density	0.990 gm/cm^3
Cannon-Fenske Viscosity	1.758 cps
Power Law Exponent, n	1.0084
Power Law Coefficient, k	0.0247
Standard Error of Estimation	0.0706

Viscometer Speed (rpm)	Shear Rate (sec^{-1})	Percent Full Scale Torque	Shear Stress ($dynes/cm^2$)	Viscosity (cps)
0.3	1.15	0.15	0.035	3.043
0.6	2.30	0.25	0.058	2.522
1.5	5.75	0.65	0.151	2.626
3.0	11.50	1.50	0.349	3.035
6.0	23.00	2.90	0.675	2.935
12.0	46.00	5.50	1.280	2.783
30.0	115.00	12.60	2.932	2.550
60.0	230.00	24.15	5.619	2.443

TABLE B-17

VISCOMETRIC DATA

0.05 Percent Polyacrylamide AP-30 In 0.2 Percent NaCl Solution

Run Number	17
Solution Temperature	76°F
Solution Density	0.988 gm/cm^3
Cannon-Fenske Viscosity	2.626 cps
Power Law Exponent, n	0.9554
Power Law Coefficient, k	0.0517
Standard Error of Estimation	0.1253

Viscometer Speed (rpm)	Shear Rate (sec^{-1})	Percent Full Scale Torque	Shear Stress ($dynes/cm^2$)	Viscosity (cps)
0.3	1.15	0.25	0.057	4.954
0.6	2.30	0.55	0.125	5.435
1.5	5.75	1.16	0.270	4.696
3.0	11.50	2.40	0.558	4.852
6.0	23.00	4.70	1.094	4.756
12.0	46.00	9.05	2.106	4.578
30.0	115.00	19.40	4.514	3.925
60.0	230.00	40.00	9.300	4.044

TABLE B-18

VISCOMETRIC DATA

0.075 Percent Polyacrylamide AP-30 In 0.2 Percent NaCl Solution

Run Number	18
Solution Temperature	76°F
Solution Density	0.990 gm/cm^3
Cannon-Fenske Viscosity	3.506 cps
Power Law Exponent, n	0.8585
Power Law Coefficient, k	0.1097
Standard Error of Estimation	0.0307

Viscometer Speed (rpm)	Shear Rate (sec^{-1})	Percent Full Scale Torque	Shear Stress ($dynes/cm^2$)	Viscosity (cps)
0.3	1.15	0.50	0.116	10.087
0.6	2.30	0.90	0.209	9.087
1.5	5.75	2.30	0.535	9.304
3.0	11.50	4.15	0.966	8.661
6.0	23.00	7.30	1.699	7.387
12.0	46.00	12.85	2.990	6.500
30.0	115.00	27.05	6.294	5.473
60.0	230.00	46.90	10.913	4.745

TABLE B-19

VISCOMETRIC DATA

0.10 Percent Polyacrylamide AP-30 In 0.2 Percent NaCl Solution

Run Number	19
Solution Temperature	76°F
Solution Density	0.988 gm/cm^3
Cannon-Fenske Viscosity	4.131 cps
Power Law Exponent, n	0.9101
Power Law Coefficient, k	0.1222
Standard Error of Estimation	0.0495

Viscometer Speed (rpm)	Shear Rate (sec^{-1})	Percent Full Scale Torque	Shear Stress ($dynes/cm^2$)	Viscosity (cps)
0.3	1.15	0.60	0.145	12.608
0.6	2.30	1.15	0.268	11.652
1.5	5.75	3.05	0.710	12.348
3.0	11.50	5.15	1.198	10.417
6.0	23.00	9.75	2.269	9.865
12.0	46.00	16.40	3.816	6.816
30.0	115.00	36.30	8.447	7.345
60.0	230.00	72.90	16.963	7.375

TABLE B-20

VISCOMETRIC DATA

0.25 Percent Polyacrylamide AP-30 In 0.2 Percent NaCl Solution

Run Number	20
Solution Temperature	76°F
Solution Density	0.986 gm/cm^3
Cannon-Fenske Viscosity	21.857 cps
Power Law Exponent, n	0.6471
Power Law Coefficient, k	1.1233
Standard Error of Estimation	0.0164

Viscometer Speed (rpm)	Shear Rate (sec^{-1})	Percent Full Scale Torque	Shear Stress ($dynes/cm^2$)	Viscosity (cps)
0.3	1.15	5.05	1.175	102.173
0.6	2.30	8.25	1.920	83.478
1.5	5.75	15.55	3.618	62.921
3.0	11.50	24.05	5.596	48.661
6.0	23.00	37.75	8.784	38.191
12.0	46.00	57.30	13.438	20.254
30.0	115.00	99.25	23.094	20.082

TABLE B-21

VISCOMETRIC DATA

0.35 Percent Polyacrylamide AP-30 In 0.2 Percent NaCl Solution

Run Number	21
Solution Temperature	76°F
Solution Density	0.984 gm/cm^3
Cannon-Fenske Viscosity	39.850 cps
Power Law Exponent, n	0.6233
Power Law Coefficient, k	2.1006
Standard Error of Estimation	0.0152

Viscometer Speed (rpm)	Shear Rate (sec^{-1})	Percent Full Scale Torque	Shear Stress ($dynes/cm^2$)	Viscosity (cps)
0.3	1.15	9.45	2.199	191.216
0.6	2.30	15.40	3.583	155.782
1.5	5.75	27.85	6.480	112.694
3.0	11.50	42.45	9.878	85.894
6.0	23.00	63.90	14.764	64.191
12.0	46.00	95.15	22.140	42.394

TABLE B-22

VISCOMETRIC DATA

0.50 Percent Polyacrylamide AP-30 In 0.2 Percent NaCl Solution

Run Number	22
Solution Temperature	76°F
Solution Density	0.986 gm/cm^3
Power Law Exponent, n	0.5656
Power Law Coefficient, k	5.8652
Standard Error of Estimation	0.0086

Viscometer Speed (rpm)	Shear Rate (sec^{-1})	Percent Full Scale Torque	Shear Stress ($dynes/cm^2$)	Viscosity (cps)
0.3	1.15	26.90	6.259	544.258
0.6	2.30	40.95	9.529	414.302
1.5	5.75	68.75	15.997	278.204
3.0	11.50	98.95	23.025	200.216

TABLE B-23

VISCOMETRIC DATA

0.025 Percent Polysaccharide "Kelzan" M in 0.2 Percent NaCl Solution

Run Number	23
Solution Temperature	76°F
Solution Density	0.993 gm/cm^3
Cannon-Fenske Viscosity	1.464 cps
Power Law Exponent, n	0.8451
Power Law Coefficient, k	0.0515

Viscometer Speed (rpm)	Shear Rate (sec^{-1})	Percent Full Scale Torque	Shear Stress ($dynes/cm^2$)	Viscosity (cps)
0.3	1.15	0.25	0.058	5.043
0.6	2.30	0.45	0.105	4.565
1.5	5.75	1.00	0.233	4.052
3.0	11.50	1.75	0.407	3.539
6.0	23.00	3.05	0.710	3.087
12.0	46.00	5.70	1.326	2.883
30.0	115.00	12.30	2.862	2.487
60.0	230.00	22.20	5.166	2.247

TABLE B-24

VISCOMETRIC DATA

0.05 Percent Polysaccharide "Kelzan" M in 0.2 Percent NaCl Solution

Run Number	24
Solution Temperature	76°F
Solution Density	0.993 gm/cm^3
Cannon-Fenske Viscosity	2.271 cps
Power Law Exponent, n	0.7563
Power Law Coefficient, k	0.1200

Viscometer Speed (rpm)	Shear Rate (sec^{-1})	Percent Full Scale Torque	Shear Stress ($dynes/cm^2$)	Viscosity (cps)
0.3	1.15	0.60	0.140	12.174
0.6	2.30	0.90	0.209	9.087
1.5	5.75	2.15	0.500	8.087
3.0	11.50	3.65	0.849	7.382
6.0	23.00	5.75	1.329	5.765
12.0	46.00	9.60	2.234	4.857
30.0	115.00	18.50	4.305	3.741
60.0	230.00	30.20	7.027	3.057

TABLE B-25

VISCOMETRIC DATA

0.075 Percent Polysaccharide "Kelzan" M in 0.2 Percent NaCl Solution

Run Number	25
Solution Temperature	76°F
Solution Density	0.993 gm/cm^3
Cannon-Fenske Viscosity	3.417 cps
Power Law Exponent, n	0.6694
Power Law Coefficient	0.2630

Viscometer Speed (rpm)	Shear Rate (sec^{-1})	Percent Full Scale Torque	Shear Stress ($dynes/cm^2$)	Viscosity (cps)
0.3	1.15	1.25	0.291	25.530
0.6	2.30	1.75	0.407	17.695
1.5	5.75	3.70	0.861	14.974
3.0	11.50	6.45	1.501	13.051
6.0	23.00	9.85	2.292	9.966
12.0	46.00	15.65	3.641	7.915
30.0	115.00	27.90	6.492	5.641
60.0	230.00	43.10	10.029	4.363

TABLE B-26

VISCOMETRIC DATA

0.085 Percent Polysaccharide "Kelzan" M in 0.2 Percent NaCl Solution

Run Number	26
Solution Temperature	76°F
Solution Density	0.993 gm/cm^3
Cannon-Fenske Viscosity	3.265 cps
Power Law Exponent, n	0.6720
Power Law Coefficient, k	0.3160

Viscometer Speed (rpm)	Shear Rate (sec^{-1})	Percent Full Scale Torque	Shear Stress ($dynes/cm^2$)	Viscosity (cps)
0.3	1.15	1.40	0.326	28.348
0.6	2.30	2.30	0.535	23.261
1.5	5.75	4.65	1.082	18.817
3.0	11.50	7.75	1.803	15.677
6.0	23.00	12.30	2.862	12.444
12.0	46.00	19.00	4.421	9.611
30.0	115.00	34.05	7.923	6.885
60.0	230.00	52.30	12.170	5.294

TABLE B-27

VISCOMETRIC DATA

0.10 Percent Polysaccharide "Kelzan" M in 0.2 Percent NaCl Solution

Run Number	27
Solution Temperature	76°F
Solution Density	0.993 gm/cm^3
Cannon-Fenske Viscosity	4.338 cps
Power Law Exponent, n	0.6176
Power Law Coefficient, k	0.5230

Viscometer Speed (rpm)	Shear Rate (sec^{-1})	Percent Full Scale Torque	Shear Stress ($dynes/cm^2$)	Viscosity (cps)
0.3	1.15	2.30	0.535	46.521
0.6	2.30	4.05	0.942	40.956
1.5	5.75	6.55	1.524	26.504
3.0	11.50	10.75	2.501	21.746
6.0	23.00	16.40	3.816	16.592
12.0	46.00	24.45	5.687	12.363
30.0	115.00	42.30	9.843	8.553
60.0	230.00	65.75	15.300	5.294

TABLE B-28

VISCOMETRIC DATA

0.125 Percent Polysaccharide "Kelzan" M in 0.2 Percent NaCl Solution

Run Number	28
Solution Temperature	76°F
Solution Density	0.993 gm/cm^3
Cannon-Fenske Viscosity	6.157 cps
Power Law Exponent, n	0.5914
Power Law Coefficient, k	0.7700

Viscometer Speed (rpm)	Shear Rate (sec^{-1})	Percent Full Scale Torque	Shear Stress ($dynes/cm^2$)	Viscosity (cps)
0.3	1.15	3.30	0.768	66.782
0.6	2.30	5.60	1.303	56.652
1.5	5.75	10.35	2.408	41.877
3.0	11.50	15.30	3.560	30.954
6.0	23.00	22.80	5.305	23.066
12.0	46.00	33.80	7.865	17.098
30.0	115.00	55.90	13.007	11.303
60.0	230.00	84.35	19.627	8.538

TABLE B-29

VISCOMETRIC DATA

0.15 Percent Polysaccharide "Kelzan" M in 0.2 Percent NaCl Solution

Run Number	29
Solution Temperature	76°F
Solution Density	0 993 gm/cm^3
Cannon-Fenske Viscosity	8.708 cps
Power Law Exponent, n	0.5250
Power Law Coefficient, k	1.2750

Viscometer Speed (rpm)	Shear Rate (sec^{-1})	Percent Full Scale Torque	Shear Stress (dynes/cm^2)	Viscosity (cps)
0.3	1.15	5.65	1.315	114.347
0.6	2.30	8.25	1.920	83.477
1.5	5.75	14.15	3.292	57.251
3.0	11.50	20.55	4.782	41.579
6.0	23.00	29.70	6.911	30.049
12.0	46.00	42.40	9.866	21.448
30.0	115.00	67.55	15.718	13.659
60.0	230.00	96.45	22.443	9.763

TABLE B-30

VISCOMETRIC DATA

0.025 Percent Polyacrylamide "Reten" A-5 In 0.2 Percent NaCl Solution

Run Number	30
Solution Temperature	76°F
Solution Density	0.994 gm/cm^3
Cannon-Fenske Viscosity	1.371 cps
Power Law Exponent, n	0.9590
Power Law Coefficient, k	0.0202

Viscometer Speed (rpm)	Shear Rate (sec^{-1})	Percent Full Scale Torque	Shear Stress ($dynes/cm^2$)	Viscosity (cps)
0.3	1.15	0.10	0.023	2.000
0.6	2.30	0.20	0.047	2.043
1.5	5.75	0.45	0.105	1.826
3.0	11.50	0.90	0.204	1.774
6.0	23.00	2.05	0.477	2.074
12.0	46.00	3.90	0.907	1.972
30.0	115.00	9.10	2.117	1.840
60.0	230.00	17.35	4.037	1.756

TABLE B-31

VISCOMETRIC DATA

0.05 Percent Polyacrylamide "Reten" A-1 In 0.2 Percent NaCl Solution

Run Number	31
Solution Temperature	76°F
Solution Density	0.994 gm/cm^3
Cannon-Fenske Viscosity	2.074 cps
Power Law Exponent, n	0.9590
Power Law Coefficient, k	0.0350

Viscometer Speed (rpm)	Shear Rate (sec^{-1})	Percent Full Scale Torque	Shear Stress ($dynes/cm^2$)	Viscosity (cps)
0.6	2.30	0.35	0.081	3.522
1.5	5.75	0.85	0.196	3.409
3.0	11.50	1.45	0.337	2.931
6.0	23.00	3.40	0.791	3.439
12.0	46.00	6.20	1.443	3.137
30.0	115.00	14.60	3.397	2.952
60.0	230.00	28.00	6.515	2.834

TABLE B-32

VISCOMETRIC DATA

0.075 Percent Polyacrylamide "Reten" A-1 In 0.2 Percent NaCl Solution

Run Number	32
Solution Temperature	76°F
Solution Density	0.994 gm/cm^3
Cannon-Fenske Viscosity	2.513 cps
Power Law Exponent, n	0.8421
Power Law Coefficient, k	0.0820

Viscometer Speed (rpm)	Shear Rate (sec^{-1})	Percent Full Scale Torque	Shear Stress ($dynes/cm^2$)	Viscosity (cps)
0.3	1.15	0.40	0.093	8.087
0.6	2.30	0.75	0.175	7.609
1.5	5.75	1.45	0.335	5.826
3.0	11.50	2.90	0.675	5.870
6.0	23.00	4.65	1.082	4.705
12.0	46.00	8.45	1.966	4.274
30.0	115.00	18.90	4.398	3.822
60.0	230.00	34.20	7.958	3.462

TABLE B-33

VISCOMETRIC DATA

0.10 Percent Polyacrylamide "Reten" A-1 In 0.2 Percent NaCl Solution

Run Number	33
Solution Temperature	76°F
Solution Density	0.996 gm/cm^3
Cannon-Fenske Viscosity	3.297 cps
Power Law Exponent, n	0.8754
Power Law Coefficient, k	0.0940

Viscometer Speed (rpm)	Shear Rate (sec^{-1})	Percent Full Scale Torque	Shear Stress ($dynes/cm^2$)	Viscosity (cps)
0.3	1.15	0.45	0.105	9.130
0.6	2.30	0.90	0.209	9.087
1.5	5.75	1.75	0.407	7.078
3.0	11.50	3.90	0.907	7.887
6.0	23.00	6.05	1.408	6.122
12.0	46.00	11.35	2.641	5.742
30.0	115.00	25.15	5.852	5.085
60.0	230.00	45.00	10.471	4.555

TABLE B-34

VISCOMETRIC DATA

0.25 Percent Polyacrylamide "Reten" A-1 In 0.2 Percent NaCl Solution

Run Number	34
Solution Temperature	76°F
Solution Density	0.996 gm/cm^3
Cannon-Fenske Viscosity	10.793 cps
Power Law Exponent, n	0.9131
Power Law Coefficient, k	0.2430

Viscometer Speed (rpm)	Shear Rate (sec^{-1})	Percent Full Scale Torque	Shear Stress ($dynes/cm^2$)	Viscosity (cps)
0.3	1.15	1.15	0.268	23.304
0.6	2.30	2.30	0.535	23.261
1.5	5.75	5.95	1.385	24.087
3.0	11.50	10.85	2.525	21.087
6.0	23.00	19.50	4.537	19.727
12.0	46.00	34.70	8.074	17.553
30.0	115.00	70.15	16.323	14.185

TABLE B-35

VISCOMETRIC DATA

0.50 Percent Polyacrylamid "Reten" A-1 In 0.2 Percent NaCl Solution

Run Number	35
Solution Temperature	76°F
Solution Density	0.996 gm/cm^3
Cannon-Fenske Viscosity	43.486 cps
Power Law Exponent, n	0.8332
Power Law Coefficient, k	1.0350

Viscometer Speed (rpm)	Shear Rate (sec^{-1})	Percent Full Scale Torque	Shear Stress ($dynes/cm^2$)	Viscosity (cps)
0.3	1.15	4.80	1.117	97.130
0.6	2.30	9.10	2.117	92.043
1.5	5.75	19.90	4.631	80.538
3.0	11.50	34.80	8.098	70.470
6.0	23.00	68.65	15.974	69.455
12.0	46.00	94.95	22.094	48.032

TABLE B-36

VISCOMETRIC DATA

0.75 Percent Polyacrylamide "Reten" A-1 In 0.2 Percent NaCl Solution

Run Number	36
Solution Temperature	76°F
Solution Density	0.996 gm/cm^3
Power Law Exponent, n	0.8332
Power Law Coefficient, k	2.0630

Viscometer Speed (rpm)	Shear Rate (sec^{-1})	Percent Full Scale Torque	Shear Stress ($dynes/cm^2$)	Viscosity (cps)
0.3	1.15	9.65	2.211	192.260
0.6	2.30	18.30	4.258	185.129
1.5	5.75	38.30	8.912	154.989
3.0	11.50	63.90	14.869	129.301

TABLE B-37

VISCOMETRIC DATA

0.025 Percent Polyacrylamide "Reten" A-5 In 0.2 Percent NaCl Solution

Run Number	37
Solution Temperature	76°F
Solution Density	0.996 gm/cm^3
Cannon-Fenske Viscosity	1.604 cps
Power Law Exponent, n	0.9195
Power Law Coefficient, k	0.0319

Viscometer Speed (rpm)	Shear Rate (sec^{-1})	Percent Full Scale Torque	Shear Stress ($dynes/cm^2$)	Viscosity (vps)
0.6	2.30	0.30	0.070	3.043
1.5	5.75	0.70	0.163	2.835
3.0	11.50	1.40	0.326	2.835
6.0	23.00	2.40	0.558	2.426
12.0	46.00	4.70	1.094	2.378
30.0	115.00	12.45	2.897	2.517
60.0	230.00	19.05	4.433	1.928

TABLE B-38

VISCOMETRIC DATA

0.05 Percent Polyacrylamide "Reten" A-5 In 0.2 Percent NaCl Solution

Run Number	38
Solution Temperature	76°F
Solution Density	0.996 gm/cm^3
Cannon-Fenske Viscosity	2.648 cps
Power Law Exponent, n	0.9424
Power Law Coefficient, k	0.0527

Viscometer Speed (rpm)	Shear Rate (sec^{-1})	Percent Full Scale Torque	Shear Stress ($dynes/cm^2$)	Viscosity (cps)
0.3	1.15	0.25	0.058	5.043
0.6	2.30	0.50	0.116	5.043
1.5	5.75	1.20	0.279	4.852
3.0	11.50	2.30	0.535	4.652
6.0	23.00	4.70	1.094	4.757
12.0	46.00	8.85	2.059	4.476
30.0	115.00	20.40	4.747	4.125
60.0	230.00	37.25	8.668	3.771

TABLE B-39

VISCOMETRIC DATA

0.075 Percent Polyacrylamide "Reten" A-5 In 0.2 Percent NaCl Solution

Run Number	39
Solution Temperature	76°F
Solution Density	0.996 gm/cm^3
Cannon-Fenske Viscosity	3.697 cps
Power Law Exponent, n	0.8693
Power Law Coefficient, k	0.1085

Viscometer Speed (rpm)	Shear Rate (sec^{-1})	Percent Full Scale Torque	Shear Stress ($dynes/cm^2$)	Viscosity (cps)
0.3	1.15	0.50	0.116	10.087
0.6	2.30	1.00	0.233	10.130
1.5	5.75	2.30	0.535	9.304
3.0	11.50	3.80	0.884	7.696
6.0	23.00	7.05	1.640	7.131
12.0	46.00	12.95	3.013	6.550
30.0	115.00	28.50	6.632	5.763
60.0	230.00	53.95	12.554	5.461

TABLE B-40

VISCOMETRIC DATA

0.10 Percent Polyacrylamide "Reten" A-5 In 0.2 Percent NaCl Solution

Run Number	40
Solution Temperature	76°F
Solution Density	0.996 gm/cm^3
Cannon-Fenske Viscosity	5.350 cps
Power Law Exponent, n	0.9067
Power Law Coefficient, k	0.2865

Viscometer Speed (rpm)	Shear Rate (sec^{-1})	Percent Full Scale Torque	Shear Stress ($dynes/cm^2$)	Viscosity (cps)
0.3	1.15	1.40	0.326	28.348
0.6	2.30	2.65	0.617	26.826
1.5	5.75	4.65	1.082	18.817
3.0	11.50	7.45	1.734	15.079
6.0	23.00	12.45	2.897	12.596
12.0	46.00	24.20	5.631	12.242
30.0	115.00	46.15	10.739	9.332
60.0	230.00	79.80	18.568	8.077

TABLE B-41

VISCOMETRIC DATA

0.25 Percent Polyacrylamide "Reten" A-5 In 0.2 Percent NaCl Solution

Run Number	41
Solution Temperature	76°F
Solution Density	0.995 gm/cm^3
Cannon-Fenske Viscosity	39.115 cps
Power Law Exponent, n	0.6745
Power Law Coefficient, k	2.1000

Viscometer Speed (rpm)	Shear Rate (sec^{-1})	Percent Full Scale Torque	Shear Stress ($dynes/cm^2$)	Viscosity (cps)
0.3	1.15	9.95	2.315	201.303
0.6	2.30	15.65	3.642	158.347
1.5	5.75	29.15	6.783	117.963
3.0	11.50	46.75	10.878	94.595
6.0	23.00	75.75	17.626	76.638

TABLE B-42

VISCOMETRIC DATA

0.1 Percent Polyethylene Oxide WSR-35 In 0.2 Percent NaCl Solution

Run Number	42
Solution Temperature	76°F
Solution Density	0.996 gm/cm^3
Cannon-Fenske Viscosity	1.129 cps
Power Law Exponent, n	0.9623
Power Law Coefficient, k	0.0139

Viscometer Speed (rpm)	Shear Rate (sec^{-1})	Percent Full Scale Torque	Shear Stress ($dynes/cm^2$)	Viscosity (cps)
1.5	5.75	0.35	0.081	1.409
3.0	11.50	0.65	0.151	1.313
6.0	23.00	1.30	0.302	1.313
12.0	46.00	2.30	0.535	1.163
30.0	115.00	5.80	1.350	1.173
60.0	230.00	12.10	2.815	1.224

TABLE B-43

VISCOMETRIC DATA

0.25 Percent Polyethylene Oxide WSR-35 in 0.2 Percent NaCl Solution

Run Number	43
Solution Temperature	76°F
Solution Density	0.996 gm/cm^3
Cannon-Fenske Viscosity	1.396 cps
Power Law Exponent, n	0.9793
Power Law Coefficient, k	0.0155

Viscometer Speed (rpm)	Shear Rate (sec^{-1})	Percent Full Scale Torque	Shear Stress ($dynes/cm^2$)	Viscosity (cps)
0.6	2.30	0.15	0.035	1.522
1.5	5.75	0.35	0.081	1.409
3.0	11.50	0.65	0.151	1.313
6.0	23.00	1.40	0.326	1.417
12.0	46.00	2.70	0.628	1.365
30.0	115.00	7.05	1.633	1.419
60.0	230.00	14.15	3.292	1.432

TABLE B-44

VISCOMETRIC DATA

0.35 Percent Polyethylene Oxide WSR-35 in 0.2 Percent NaCl Solution

Run Number	44
Solution Temperature	76°F
Solution Density	0.996 gm/cm^3
Cannon-Fenske Viscosity	1.579 cps
Power Law Exponent, n	0.9163
Power Law Coefficient, k	0.0286

Viscometer Speed (rpm)	Shear Rate (sec^{-1})	Percent Full Scale Torque	Shear Stress ($dynes/cm^2$)	Viscosity (cps)
0.6	2.30	0.25	0.058	2.522
1.5	5.75	0.60	0.140	2.435
3.0	11.50	1.15	0.267	2.321
6.0	23.00	2.20	0.512	2.226
12.0	46.00	3.90	0.907	1.972
30.0	115.00	9.20	2.141	1.860
60.0	230.00	18.00	4.188	1.822

TABLE B-45

VISCOMETRIC DATA

0.5 Percent Polyethylene Oxide WSR-35 in 0.2 Percent NaCl Solution

Run Number	45
Solution Temperature	76°F
Solution Density	0.996 gm/cm^3
Cannon-Fenske Viscosity	1.918 cps
Power Law Exponent, n	0.8910
Power Law Coefficient, k	0.0380

Viscometer Speed (rpm)	Shear Rate (sec^{-1})	Percent Full Scale Torque	Shear Stress ($dynes/cm^2$)	Viscosity (cps)
0.6	2.30	0.35	0.081	3.522
1.5	5.75	0.85	0.981	3.443
3.0	11.50	1.30	0.302	2.626
6.0	23.00	2.70	0.628	2.730
12.0	46.00	4.70	1.094	2.378
30.0	115.00	10.95	2.548	2.214
60.0	230.00	20.70	4.814	2.095

TABLE B-46

VISCOMETRIC DATA

0.75 Percent Polyethylene Oxide WSR-35 in 0.2 Percent NaCl Solution

Run Number	46
Solution Temperature	76°F
Solution Density	0.998 gm/cm^3
Cannon-Fenske Viscosity	2.598 cps
Power Law Exponent, n	0.9163
Power Law Coefficient, k	0.0405

Viscometer Speed (rpm)	Shear Rate (sec^{-1})	Percent Full Scale Torque	Shear Stress ($dynes/cm^2$)	Viscosity (cps)
0.6	2.30	0.40	0.093	4.043
1.5	5.75	0.87	0.202	3.513
3.0	11.50	1.35	0.314	2.730
6.0	23.00	2.80	0.651	2.830
12.0	46.00	5.40	1.256	2.730
30.0	115.00	13.90	3.234	2.812
60.0	230.00	28.55	6.643	2.888

TABLE B-47

VISCOMETRIC DATA

1.00 Percent Polyethylene Oxide WSR-35 in 0.2 Percent NaCl Solution

Run Number	47
Solution Temperature	76°F
Solution Density	0.996 gm/cm^3
Cannon-Fenske Viscosity	3.308 cps
Power Law Exponent, n	0.9424
Power Law Coefficient, k	0.0433

Viscometer Speed (rpm)	Shear Rate (sec^{-1})	Percent Full Scale Torque	Shear Stress ($dynes/cm^2$)	Viscosity (cps)
0.3	1.15	0.20	0.047	4.087
0.6	2.30	0.45	0.105	4.565
1.5	5.75	0.90	0.209	3.635
3.0	11.50	1.85	0.430	3.739
6.0	23.00	3.45	0.803	3.491
12.0	46.00	6.70	1.559	3.389
30.0	115.00	16.85	3.921	3.410
60.0	230.00	33.70	7.842	3.410

TABLE B-48

VISCOMETRIC DATA

1.50 Percent Polyethylene Oxide WSR-35 in 0.2 Percent NaCl Solution

Run Number	48
Solution Temperature	76°F
Solution Density	0.998 gm/cm^3
Cannon-Fenske Viscosity	5.470 cps
Power Law Exponent, n	0.9556
Power Law Coefficient, k	0.0682

Viscometer Speed (rpm)	Shear Rate (sec^{-1})	Percent Full Scale Torque	Shear Stress ($dynes/cm^2$)	Viscosity (cps)
0.3	1.15	0.35	0.081	7.043
0.6	2.30	0.70	0.163	7.048
1.5	5.75	1.40	0.326	5.669
3.0	11.50	2.70	0.628	5.461
6.0	23.00	5.30	1.233	5.361
12.0	46.00	10.85	2.528	5.489
30.0	115.00	27.15	6.318	5.494
60.0	230.00	53.65	12.484	5.428

TABLE B-49

VISCOMETRIC DATA

2.00 Percent Polyethylene Oxide WSR-35 in 0.2 Percent NaCl Solution

Run Number	49
Solution Temperature	76°F
Solution Density	0.999 gm/cm^3
Cannon-Fenske Viscosity	8.667 cps
Power Law Exponent, n	1.0000
Power Law Coefficient, k	0.0850

Viscometer Speed (rpm)	Shear Rate (sec^{-1})	Percent Full Scale Torque	Shear Stress ($dynes/cm^2$)	Viscosity (cps)
0.3	1.15	0.40	0.093	8.087
0.6	2.30	0.85	0.198	8.609
1.5	5.75	2.00	0.465	8.087
3.0	11.50	4.05	0.942	8.191
6.0	23.00	8.50	1.978	8.600
12.0	46.00	16.75	3.898	8.474
30.0	115.00	41.80	9.726	8.457
60.0	230.00	82.95	19.302	8.392

TABLE B-50

VISCOMETRIC DATA

0.025 Percent Polyethylene Oxide WSR-205 in 0.2 Percent NaCl Solution

Run Number	50
Solution Temperature	76°F
Solution Density	0.993 gm/cm^3
Cannon-Fenske Viscosity	1.056 cps
Power Law Exponent, n	1.0724
Power Law Coefficient, k	0.0076

Viscometer Speed (rpm)	Shear Rate (sec^{-1})	Percent Full Scale Torque	Shear Stress ($dynes/cm^2$)	Viscosity (cps)
1.5	5.75	0.20	0.049	0.850
3.0	11.50	0.45	0.105	0.913
6.0	23.00	1.15	0.267	1.161
12.0	46.00	2.30	0.535	1.163
30.0	115.00	5.80	1.350	1.173
60.0	230.00	12.15	2.827	1.229

TABLE B-51

VISCOMETRIC DATA

0.05 Percent Polyethylene Oxide WSR-205 in 0.2 Percent NaCl Solution

Run Number	51
Solution Temperature	76°F
Solution Density	0.991 gm/cm^3
Cannon-Fenske Viscosity	1.142 cps
Power Law Exponent, n	1.0724
Power Law Coefficient, k	0.0088

Viscometer Speed (rpm)	Shear Rate (sec^{-1})	Percent Full Scale Torque	Shear Stress ($dynes/cm^2$)	Viscosity (cps)
1.5	5.75	0.25	0.058	1.009
3.0	11.50	0.50	0.116	1.009
6.0	23.00	1.20	0.279	1.213
12.0	46.00	2.40	0.558	1.213
30.0	115.00	5.95	1.384	1.203
60.0	230.00	13.15	3.060	1.331

TABLE B-52

VISCOMETRIC DATA

0.075 Percent Polyethylene Oxide WSR-205 in 0.2 Percent NaCl Solution

Run Number	52
Solution Temperature	76°F
Solution Density	0.990 gm/cm^3
Cannon-Fenske Viscosity	1.235 cps
Power Law Exponent, n	1.0176
Power Law Coefficient, k	0.0128

Viscometer Speed (rpm)	Shear Rate (sec^{-1})	Percent Full Scale Torque	Shear Stress (dynes/cm^2)	Viscosity (cps)
1.5	5.75	0.30	0.070	1.217
3.0	11.50	0.70	0.163	1.417
6.0	23.00	1.40	0.326	1.417
12.0	46.00	2.75	0.640	1.391
30.0	115.00	6.70	1.560	1.355
60.0	230.00	13.30	3.095	1.346

TABLE B-53

VISCOMETRIC DATA

0.10 Percent Polyethylene Oxide WSR-205 in 0.2 Percent NaCl Solution

Run Number	53
Solution Temperature	76°F
Solution Density	0.990 gm/cm^3
Cannon-Fenske Viscosity	1.321 cps
Power Law Exponent, n	0.9759
Power Law Coefficient, k	0.0173

Viscometer Speed (rpm)	Shear Rate (sec^{-1})	Percent Full Scale Torque	Shear Stress ($dynes/cm^2$)	Viscosity (cps)
0.6	2.30	0.16	0.038	1.652
1.5	5.75	0.40	0.094	1.635
3.0	11.50	0.85	0.198	1.722
6.0	23.00	1.50	0.349	1.517
12.0	46.00	3.05	0.710	1.543
30.0	115.00	7.30	1.700	1.477
60.0	230.00	14.75	3.432	1.493

TABLE B-54

VISCOMETRIC DATA

0.25 Percent Polyethylene Oxide WSR-205 in 0.2 Percent NaCl Solution

Run Number	54
Solution Temperature	76°F
Solution Density	0.990 gm/cm^3
Cannon-Fenske Viscosity	2.100 cps
Power Law Exponent, n	0.9457
Power Law Coefficient, k	0.0335

Viscometer Speed (rpm)	Shear Rate (sec^{-1})	Percent Full Scale Torque	Shear Stress ($dynes/cm^2$)	Viscosity (cps)
0.3	1.15	0.15	0.035	3.043
0.6	2.30	0.30	0.698	2.933
1.5	5.75	0.75	0.174	3.037
3.0	11.50	1.50	0.349	3.034
6.0	23.00	3.05	0.710	3.087
12.0	46.00	5.70	1.326	2.883
30.0	115.00	13.25	3.083	2.679
60.0	230.00	23.35	5.433	2.363

TABLE B-55

VISCOMETRIC DATA

0.35 Percent Polyethylene Oxide WSR-205 in 0.2 Percent NaCl Solution

Run Number	55
Solution Temperature	76°F
Solution Density	0.990 gm/cm^3
Cannon-Fenske Viscosity	2.820 cps
Power Law Exponent, n	0.9691
Power Law Coefficient, k	0.0355

Viscometer Speed (rpm)	Shear Rate (sec^{-1})	Percent Full Scale Torque	Shear Stress ($dynes/cm^2$)	Viscosity (cps)
0.6	2.30	0.35	0.081	3.522
1.5	5.75	0.85	0.198	3.440
3.0	11.50	1.50	0.349	3.034
6.0	23.00	3.15	0.733	3.187
12.0	46.00	6.60	1.536	3.340
30.0	115.00	15.80	3.676	3.194
60.0	230.00	30.95	7.202	3.133

TABLE B-56

VISCOMETRIC DATA

0.50 Percent Polyethylene Oxide WSR-205 in 0.2 Percent NaCl Solution

Run Number	56
Solution Temperature	76°F
Solution Density	0.998 gm/cm^3
Cannon-Fenske Viscosity	4.079 cps
Power Law Exponent, n	0.8541
Power Law Coefficient, k	0.0880

Viscometer Speed (rpm)	Shear Rate (sec^{-1})	Percent Full Scale Torque	Shear Stress ($dynes/cm^2$)	Viscosity (cps)
0.3	1.15	0.45	0.105	9.130
0.6	2.30	0.85	0.198	8.609
1.5	5.75	1.50	0.349	6.069
3.0	11.50	3.00	0.698	6.069
6.0	23.00	5.50	1.278	5.557
12.0	46.00	8.60	2.001	4.350
30.0	115.00	22.40	5.212	4.529
60.0	230.00	41.15	9.575	4.165

TABLE B-57

VISCOMETRIC DATA

0.75 Percent Polyethylene Oxide WSR-205 in 0.2 Percent NaCl Solution

Run Number	57
Solution Temperature	76°F
Solution Density	0.998 gm/cm^3
Cannon-Fenske Viscosity	6.718 cps
Power Law Exponent, n	0.9424
Power Law Coefficient, k	0.0960

Viscometer Speed (rpm)	Shear Rate (sec^{-1})	Percent Full Scale Torque	Shear Stress ($dynes/cm^2$)	Viscosity (cps)
0.3	1.15	0.50	0.116	10.087
0.6	2.30	0.95	0.221	9.609
1.5	5.75	1.95	0.454	7.895
3.0	11.50	4.15	0.966	8.399
6.0	23.00	8.10	1.885	8.196
12.0	46.00	14.80	3.444	7.487
30.0	115.00	37.50	8.726	7.583
60.0	230.00	71.15	16.556	7.202

TABLE B-58

VISCOMETRIC DATA

1.00 Percent Polyethylene Oxide WSR-205 in 0.2 Percent NaCl Solution

Run Number	58
Solution Temperature	76°F
Solution Density	0.997 gm/cm^3
Cannon-Fenske Viscosity	11.182 cps
Power Law Exponent, n	0.9228
Power Law Coefficient, k	0.1940

Viscometer Speed (rpm)	Shear Rate (sec^{-1})	Percent Full Scale Torque	Shear Stress ($dynes/cm^2$)	Viscosity (cps)
0.3	1.15	1.00	0.233	20.261
0.6	2.30	1.85	0.430	18.695
1.5	5.75	4.30	1.000	17.391
3.0	11.50	7.90	1.838	15.981
6.0	23.00	15.40	3.583	15.579
12.0	46.00	29.00	6.748	14.670
30.0	115.00	68.95	16.044	13.942

TABLE B-59

VISCOMETRIC DATA

0.025 Percent Polyethylene Oxide WSR-301 in 0.2 Percent NaCl Solution

Run Number	59
Solution Temperature	76°F
Solution Density	0.996 gm/cm^3
Cannon-Fenske Viscosity	1.329 cps
Power Law Exponent, n	0.9827
Power Law Coefficient, k	0.0200

Viscometer Speed (rpm)	Shear Rate (sec^{-1})	Percent Full Scale Torque	Shear Stress (dynes/cm^2)	Viscosity (cps)
0.3	1.15	0.10	0.023	2.000
0.6	2.30	0.20	0.047	2.043
1.5	5.75	0.45	0.105	1.826
3.0	11.50	0.95	0.209	1.817
6.0	23.00	1.75	0.407	1.770
12.0	46.00	3.30	0.768	1.670
30.0	115.00	8.30	1.931	1.679
60.0	230.00	19.65	4.572	1.988

TABLE B-60

VISCOMETRIC DATA

0.05 Percent Polyethylene Oxide WSR-301 in 0.2 Percent NaCl Solution

Run Number	60
Solution Temperature	76°F
Solution Density	0.996 gm/cm^3
Cannon-Fenske Viscosity	1.923 cps
Power Law Exponent, n	0.9759
Power Law Coefficient, k	0.0310

Viscometer Speed (rpm)	Shear Rate (sec^{-1})	Percent Full Scale Torque	Shear Stress ($dynes/cm^2$)	Viscosity (cps)
0.3	1.15	0.15	0.035	3.043
0.6	2.30	0.30	0.069	3.000
1.5	5.75	0.80	0.186	3.235
3.0	11.50	1.50	0.349	3.035
6.0	23.00	3.05	0.710	3.087
12.0	46.00	5.95	1.385	3.011
30.0	115.00	14.15	3.293	2.863
60.0	230.00	27.25	6.341	2.757

TABLE B-61

VISCOMETRIC DATA

0.075 Percent Polyethylene Oxide WSR-301 in 0.2 Percent NaCl Solution

Run Number	61
Solution Temperature	76°F
Solution Density	0.996 gm/cm^3
Cannon-Fenske Viscosity	2.449 cps
Power Law Exponent, n	0.9099
Power Law Coefficient, k	0.0500

Viscometer Speed (rpm)	Shear Rate (sec^{-1})	Percent Full Scale Torque	Shear Stress ($dynes/cm^2$)	Viscosity (cps)
0.3	1.15	0.25	0.058	5.043
0.6	2.30	0.45	0.105	4.565
1.5	5.75	1.00	0.233	4.052
3.0	11.50	2.05	0.477	4.148
6.0	23.00	4.05	0.942	4.096
12.0	46.00	7.15	1.664	3.617
30.0	115.00	16.60	3.863	3.359
60.0	230.00	31.15	7.248	3.151

TABLE B-62

VISCOMETRIC DATA

0.1 Percent Polyethylene Oxide WSR-301 in 0.2 Percent NaCl Solution

Run Number	62
Solution Temperature	76°F
Solution Density	0.996 gm/cm^3
Cannon-Fenske Viscosity	3.064 cps
Power Law Exponent, n	0.9163
Power Law Coefficient, k	0.0555

Viscometer Speed (rpm)	Shear Rate (sec^{-1})	Percent Full Scale Torque	Shear Stress ($dynes/cm^2$)	Viscosity (cps)
0.3	1.15	0.25	0.058	5.043
0.6	2.30	0.50	0.116	5.043
1.5	5.75	1.40	0.326	5.669
3.0	11.50	2.65	0.617	5.365
6.0	23.00	4.70	1.094	4.756
12.0	46.00	8.85	2.059	4.476
30.0	115.00	19.40	4.514	3.925
60.0	230.00	35.75	8.319	3.617

TABLE B-63

VISCOMETRIC DATA

0.25 Percent Polyethylene Oxide WSR-301 in 0.2 Percent NaCl Solution

Run Number	63
Solution Temperature	76°F
Solution Density	0.996 gm/cm^3
Cannon-Fenske Viscosity	8.052 cps
Power Law Exponent, n	0.7673
Power Law Coefficient, k	0.2950

Viscometer Speed (rpm)	Shear Rate (sec^{-1})	Percent Full Scale Torque	Shear Stress ($dynes/cm^2$)	Viscosity (cps)
0.30	1.15	1.35	0.314	27.040
0.60	2.30	2.55	0.593	25.782
1.50	5.75	5.15	1.198	20.834
3.00	11.50	9.15	2.129	18.513
6.00	23.00	14.85	3.455	15.022
12.00	46.00	25.85	6.015	13.076
30.00	115.00	52.85	12.298	10.694
60.00	230.00	83.15	19.348	8.412

TABLE B-64

VISCOMETRIC DATA

0.35 Percent Polyethylene Oxide WSR-301 in 0.2 Percent NaCl Solution

Run Number	64
Solution Temperature	76°F
Solution Density	0.996 gm/cm^3
Cannon-Fenske Viscosity	13.014 cps
Power Law Exponent, n	0.7898
Power Law Coefficient, k	0.5190

Viscometer Speed (rpm)	Shear Rate (sec^{-1})	Percent Full Scale Torque	Shear Stress ($dynes/cm^2$)	Viscosity (cps)
0.3	1.15	2.40	0.558	48.521
0.6	2.30	4.55	1.059	46.043
1.5	5.75	9.45	2.199	38.243
3.0	11.50	16.40	3.816	33.182
6.0	23.00	27.90	6.492	28.226
12.0	46.00	46.40	10.797	23.472
30.0	115.00	90.75	21.117	18.362

TABLE B-65

VISCOMETRIC DATA

0.50 Percent Polyethylene Oxide WSR-301 in 0.2 Percent NaCl Solution

Run Number	65
Solution Temperature	76°F
Solution Density	0.996 gm/cm^3
Cannon-Fenske Viscosity	31.896 cps
Power Law Exponent, n	0.6619
Power Law Coefficient, k	1.544

Viscometer Speed (rpm)	Shear Rate (sec^{-1})	Percent Full Scale Torque	Shear Stress ($dynes/cm^2$)	Viscosity (cps)
0.3	1.15	6.70	1.559	135.564
0.6	2.30	11.60	2.699	117.347
1.5	5.75	22.30	5.422	94.294
3.0	11.50	35.35	8.226	71.530
6.0	23.00	55.20	12.844	55.843
12.0	46.00	85.00	19.779	23.269

TABLE B-66

VISCOMETRIC DATA

0.75 Percent Polyethylene Oxide WSR-301 in 0.2 Percent NaCl Solution

Run Number	66
Solution Temperature	76°F
Solution Density	0.996 gm/cm^3
Power Law Exponent, n	0.6224
Power Law Coefficient, k	3.9150

Viscometer Speed (rpm)	Shear Rate (sec^{-1})	Percent Full Scale Torque	Shear Stress ($dynes/cm^2$)	Viscosity (cps)
0.3	1.15	17.50	4.072	354.085
0.6	2.30	29.15	6.783	294.911
1.5	5.75	51.40	11.960	207.996
3.0	11.50	77.15	17.952	156.103

TABLE B-67

VISCOMETRIC DATA

0.025 Percent Polyacrylamide RC-300 in 0.2 Percent NaCl Solution

Run Number	67
Solution Temperature	76°F
Solution Density	0.994 gm/cm^3
Cannon-Fenske Viscosity	1.260 cps
Power Law Exponent, n	0.9545
Power Law Coefficient, k	0.9998
Standard Error of Estimation	0.0094

Viscometer Speed (rpm)	Shear Rate (sec^{-1})	Percent Full Scale Torque	Shear Stress (dynes/cm^2)	Viscosity (cps)
1.5	5.75	0.38	0.088	1.537
3.0	11.50	0.75	0.174	1.517
6.0	23.00	1.50	0.349	1.517
12.0	46.00	2.75	0.640	1.391
30.0	115.00	6.75	1.571	1.366
60.0	230.00	13.00	3.025	1.315

TABLE B-68

VISCOMETRIC DATA

0.04 Percent Polyacrylamide RC-300 in 0.2 Percent NaCl Solution

Run Number	68
Solution Temperature	76°F
Solution Density	0.993 gm/cm^3
Cannon-Fenske Viscosity	1.360 cps
Power Law Exponent, n	0.9951
Power Law Coefficient, k	0.0170
Standard Error of Estimation	0.0188

Viscometer Speed (rpm)	Shear Rate (sec^{-1})	Percent Full Scale Torque	Shear Stress ($dynes/cm^2$)	Viscosity (cps)
0.6	2.30	0.15	0.035	1.517
1.5	5.75	0.40	0.093	1.619
3.0	11.50	0.75	0.174	1.517
6.0	23.00	1.60	0.372	1.619
12.0	46.00	3.25	0.756	1.644
30.0	115.00	7.50	1.745	1.517
60.0	230.00	14.50	3.432	1.492

TABLE B-69

VISCOMETRIC DATA

0.071 Percent Polyacrylamide RC-300 in 0.2 Percent NaCl Solution

Run Number	69
Solution Temperature	76°F
Solution Density	0.991 gm/cm^3
Cannon-Fenske Viscosity	1.680 cps
Power Law Exponent, n	0.9449
Power Law Coefficient, k	0.0250
Standard Error of Estimation	0.0405

Viscometer Speed (rpm)	Shear Rate (sec^{-1})	Percent Full Scale Torque	Shear Stress ($dynes/cm^2$)	Viscosity (cps)
0.6	2.30	0.25	0.058	2.529
1.5	5.75	0.60	0.140	2.428
3.0	11.50	0.90	0.209	1.821
6.0	23.00	2.05	0.477	2.074
12.0	46.00	4.15	0.965	2.099
30.0	115.00	9.75	2.269	1.973
60.0	230.00	18.60	4.328	1.882

TABLE B-70

VISCOMETRIC DATA

0.10 Percent Polyacrylamide RC-300 in 0.2 Percent NaCl Solution

Run Number	70
Solution Temperature	76°F
Solution Density	0.993 gm/cm^3
Cannon-Fenske Viscosity	1.910 cps
Power Law Exponent, n	0.9248
Power Law Coefficient, k	0.0315
Standard Error of Estimation	0.0318

Viscometer Speed (rpm)	Shear Rate (sec^{-1})	Percent Full Scale Torque	Shear Stress ($dynes/cm^2$)	Viscosity (cps)
0.6	2.30	0.30	0.070	3.035
1.5	5.75	0.75	0.174	3.035
3.0	11.50	1.18	0.274	2.387
6.0	23.00	2.30	0.535	2.327
12.0	46.00	4.60	1.070	2.327
30.0	115.00	10.85	2.525	2.195
60.0	230.00	22.00	5.119	2.226

TABLE B-71

VISCOMETRIC DATA

0.25 Percent Polyacrylamide RC-300 in 0.2 Percent NaCl Solution

Run Number	71
Solution Temperature	76°F
Solution Density	0.996 gm/cm^3
Cannon-Fenske Viscosity	3.635 cps
Power Law Exponent, n	0.8593
Power Law Coefficient, k	0.0984
Standard Error of Estimation	0.0178

Viscometer Speed (rpm)	Shear Rate (sec^{-1})	Percent Full Scale Torque	Shear Stress ($dynes/cm^2$)	Viscosity (cps)
0.3	1.15	0.50	0.116	10.110
0.6	2.30	0.87	0.202	8.800
1.5	5.75	1.75	0.407	7.080
3.0	11.50	3.50	0.814	7.080
6.0	23.00	6.25	1.454	6.323
12.0	46.00	11.20	2.606	5.660
30.0	115.00	25.00	5.817	5.050
60.0	230.00	46.40	10.796	4.690

TABLE B-72

VISCOMETRIC DATA

0.40 Percent Polyacrylamide RC-300 in 0.2 Percent NaCl Solution

Run Number	72
Solution Temperature	76°F
Solution Density	0.996 gm/cm^3
Cannon-Fenske Viscosity	9.855 cps
Power Law Exponent, n	0.8783
Power Law Coefficient, k	0.1890
Standard Error of Estimation	0.0158

Viscometer Speed (rpm)	Shear Rate (sec^{-1})	Percent Full Scale Torque	Shear Stress ($dynes/cm^2$)	Viscosity (cps)
0.3	1.15	0.85	0.198	17.20
0.6	2.30	1.55	0.361	15.68
1.5	5.75	3.60	0.838	14.57
3.0	11.50	6.85	1.594	13.86
6.0	23.00	12.60	2.933	12.75
12.0	46.00	22.85	5.317	11.56
30.0	115.00	49.10	11.402	9.91
60.0	230.00	87.35	20.325	8.84

TABLE B-73

VISCOMETRIC DATA

0.71 Percent Polyacrylamide RC-300 in 0.2 Percent NaCl Solution

Run Number	73
Solution Temperature	76°F
Solution Density	0.996 gm/cm^3
Power Law Exponent, n	0.8565
Power Law Coefficient, k	0.4120
Standard Error of Estimation	0.0397

Viscometer Speed (rpm)	Shear Rate (sec^{-1})	Percent Full Scale Torque	Shear Stress ($dynes/cm^2$)	Viscosity (cps)
0.3	1.15	1.75	0.407	35.410
0.6	2.30	3.70	0.861	37.430
1.5	5.75	8.65	2.013	35.000
3.0	11.50	15.50	3.607	31.360
6.0	23.00	27.00	6.283	27.310
12.0	46.00	46.40	10.797	23.470
30.0	115.00	94.00	21.873	19.020

TABLE B-74

VISCOMETRIC DATA

1.00 Percent Polyacrylamide RC-300 in 0.2 Percent NaCl Solution

Run Number	74
Solution Temperature	76°F
Solution Density	0.996 gm/cm^3
Power Law Exponent, n	0.8443
Power Law Coefficient, k	0.5610
Standard Error of Estimation	0.0264

Viscometer Speed (rpm)	Shear Rate (sec^{-1})	Percent Full Scale Torque	Shear Stress ($dynes/cm^2$)	Viscosity (cps)
0.3	1.15	2.50	0.582	50.580
0.6	2.30	5.20	1.210	52.600
1.5	5.75	11.00	2.560	44.510
3.0	11.50	19.25	4.479	38.950
6.0	23.00	34.25	7.970	34.650
12.0	46.00	58.50	13.612	29.590

TABLE B-75

VISCOMETRIC DATA

0.025 Percent Polyacrylamide RC-301 in 0.2 Percent NaCl Solution

Run Number	75
Solution Temperature	76°F
Solution Density	0.991 gm/cm^3
Cannon-Fenske Viscosity	1.253 cps
Power Law Exponent, n	1.0985
Power Law Coefficient, k	0.0082
Standard Error of Estimation	0.0389

Viscometer Speed (rpm)	Shear Rate (sec^{-1})	Percent Full Scale Torque	Shear Stress ($dynes/cm^2$)	Viscosity (cps)
1.5	5.75	0.25	0.058	1.012
3.0	11.50	0.45	0.105	0.910
6.0	23.00	1.15	0.268	1.163
12.0	46.00	2.55	0.593	1.290
30.0	115.00	6.65	1.547	1.345
60.0	230.00	13.00	3.025	1.315

TABLE B-76

VISCOMETRIC DATA

0.04 Percent Polyacrylamide RC-301 in 0.2 Percent NaCl Solution

Run Number	76
Solution Temperature	76°F
Solution Density	0.994 gm/cm^3
Cannon-Fenske Viscosity	1.302 cps
Power Law Exponent, n	1.0909
Power Law Coefficient, k	0.0095
Standard Error of Estimation	0.0577

Viscometer Speed (rpm)	Shear Rate (sec^{-1})	Percent Full Scale Torque	Shear Stress ($dynes/cm^2$)	Viscosity (cps)
1.5	5.75	0.25	0.058	1.012
2.3	11.50	0.55	0.128	1.113
6.0	23.00	1.50	0.349	1.517
12.0	46.00	3.00	0.698	1.517
30.0	115.00	7.10	1.652	1.437
60.0	230.00	14.00	3.258	1.416

TABLE B-77

VISCOMETRIC DATA

0.071 Percent Polyacrylamide RC-301 in 0.2 Percent NaCl Solution

Run Number	77
Solution Temperature	76°F
Solution Density	0.994 gm/cm^3
Cannon-Fenske Viscosity	1.499 cps
Power Law Exponent, n	1.0306
Power Law Coefficient, k	0.0161
Standard Error of Estimation	0.0479

Viscometer Speed (rpm)	Shear Rate (sec^{-1})	Percent Full Scale Torque	Shear Stress ($dynes/cm^2$)	Viscosity (cps)
0.6	2.30	0.15	0.035	1.517
1.5	5.75	0.50	0.116	2.023
3.0	11.50	0.75	0.174	1.517
6.0	23.00	1.87	0.435	1.892
12.0	46.00	3.65	0.849	1.846
30.0	115.00	9.00	2.094	1.821
60.0	230.00	18.60	4.328	1.882

TABLE B-78

VISCOMETRIC DATA

0.10 Percent Polyacrylamide RC-301 in 0.2 Percent NaCl Solution

Run Number	78
Solution Temperature	76°F
Solution Density	0.993 gm/cm^3
Cannon-Fenske Viscosity	1.962 cps
Power Law Exponent, n	1.0413
Power Law Coefficient, k	0.0200
Standard Error of Estimation	0.0529

Viscometer Speed (rpm)	Shear Rate (sec^{-1})	Percent Full Scale Torque	Shear Stress (dynes/cm^2)	Viscosity (cps)
0.6	2.30	0.20	0.046	1.977
1.5	5.75	0.45	0.105	1.821
3.0	11.50	1.30	0.302	2.630
6.0	23.00	2.45	0.570	2.478
12.0	46.00	4.75	1.105	2.402
30.0	115.00	11.00	2.560	2.226
60.0	230.00	24.35	5.666	2.463

TABLE B-79

VISCOMETRIC DATA

0.25 Percent Polyacrylamide RC-301 in 0.2 Percent NaCl Solution

Run Number	79
Solution Temperature	76°F
Solution Density	0.99 gm/cm^3
Cannon-Fenske Viscosity	3.708 cps
Power Law Exponent, n	0.8226
Power Law Coefficient, k	0.0650
Standard Error of Estimation	0.0529

Viscometer Speed (rpm)	Shear Rate (sec^{-1})	Percent Full Scale Torque	Shear Stress ($dynes/cm^2$)	Viscosity (cps)
0.3	1.15	0.30	0.071	6.174
0.6	2.30	0.60	0.140	6.087
1.5	5.75	1.25	0.291	5.058
3.0	11.50	2.75	0.640	5.564
6.0	23.00	5.25	1.222	5.311
12.0	46.00	10.30	2.397	5.210
30.0	115.00	23.60	5.491	4.775
60.0	230.00	43.70	10.168	4.421

TABLE B-80

VISCOMETRIC DATA

0.40 Percent Polyacrylamide RC-301 in 0.2 Percent NaCl Solution

Run Number	80
Solution Temperature	76°F
Solution Density	0.991 gm/cm^3
Cannon-Fenske Viscosity	6.613 cps
Power Law Exponent, n	0.9407
Power Law Coefficient, k	0.0984
Standard Error of Estimation	0.0351

Viscometer Speed (rpm)	Shear Rate (sec^{-1})	Percent Full Scale Torque	Shear Stress ($dynes/cm^2$)	Viscosity (cps)
0.3	1.15	0.50	0.116	10.116
0.6	2.30	0.80	0.186	8.093
1.5	5.75	2.25	0.523	9.105
3.0	11.50	4.47	1.040	9.044
6.0	23.00	8.50	1.978	8.599
12.0	46.00	16.40	3.816	8.296
30.0	115.00	36.60	8.516	7.405
60.0	230.00	65.00	15.125	6.576

TABLE B-81

VISCOMETRIC DATA

0.71 Percent Polyacrylamide RC-301 in 0.2 Percent NaCl Solution

Run Number	81
Solution Temperature	76°F
Solution Density	0.994 gm/cm^3
Cannon-Fenske Viscosity	20.831 cps
Power Law Exponent, n	0.8479
Power Law Coefficient, k	0.4910
Standard Error of Estimation	0.0230

Viscometer Speed (rpm)	Shear Rate (sec^{-1})	Percent Full Scale Torque	Shear Stress ($dynes/cm^2$)	Viscosity (cps)
0.3	1.15	2.25	0.593	51.596
0.6	2.30	4.00	0.931	40.467
1.5	5.75	9.00	2.094	36.420
3.0	11.50	16.65	3.874	33.689
6.0	23.00	30.85	7.178	31.211
12.0	46.00	54.85	12.763	27.746

TABLE B-82

VISCOMETRIC DATA

1.00 Percent Polyacrylamide RC-301 in 0.2 Percent NaCl Solution

Run Number	82
Solution Temperature	76°F
Solution Density	0.994 gm/cm^3
Cannon-Fenske Viscosity	56.609 cps
Power Law Exponent, n	0.8183
Power Law Coefficient, k	1.4000
Standard Error of Estimation	0.0212

Viscometer Speed (rpm)	Shear Rate (sec^{-1})	Percent Full Scale Torque	Shear Stress (dynes/cm^2)	Viscosity (cps)
0.3	1.15	6.50	1.512	131.519
0.6	2.30	12.00	2.792	121.403
1.5	5.75	26.50	6.166	107.238
3.0	11.50	45.50	10.587	92.064
6.0	23.00	74.50	17.335	75.371

TABLE B-83

VISCOMETRIC DATA

0.025 Percent Polyacrylamide RC-322 in 0.2 Percent NaCl Solution

Run Number	83
Solution Temperature	76°F
Solution Density	0.993 gm/cm^3
Cannon-Fenske Viscosity	1.332 cps
Power Law Exponent, n	0.9924
Power Law Coefficient, k	0.0146
Standard Error of Estimation	0.0060

Viscometer Speed (rpm)	Shear Rate (sec^{-1})	Percent Full Scale Torque	Shear Stress ($dynes/cm^2$)	Viscosity (cps)
0.6	2.30	0.15	0.034	1.478
1.5	5.75	0.35	0.081	1.409
3.0	11.50	0.70	0.163	1.417
6.0	23.00	1.40	0.326	1.417
12.0	46.00	2.80	0.651	1.415
30.0	115.00	6.95	1.617	1.493
60.0	230.00	13.90	3.234	1.406

TABLE B-84

VISCOMETRIC DATA

0.05 Percent Polyacrylamide RC-322 in 0.2 Percent NaCl Solution

Run Number	84
Solution Temperature	76°F
Solution Density	0.993 gm/cm^3
Cannon-Fenske Viscosity	1.549 cps
Power Law Exponent, n	0.7627
Power Law Coefficient, k	0.0670
Standard Error of Estimation	0.0456

Viscometer Speed (rpm)	Shear Rate (sec^{-1})	Percent Full Scale Torque	Shear Stress ($dynes/cm^2$)	Viscosity (cps)
0.3	1.15	0.35	0.081	7.043
0.6	2.30	0.60	0.140	6.087
1.5	5.75	1.00	0.232	4.035
3.0	11.50	1.65	0.384	3.339
6.0	23.00	3.00	0.698	3.035
12.0	46.00	5.00	1.163	2.528
30.0	115.00	10.70	2.490	2.165
60.0	230.00	21.00	4.886	2.124

TABLE B-85

VISCOMETRIC DATA

0.075 Percent Polyacrylamide RC-322 in 0.2 Percent NaCl Solution

Run Number	85
Solution Temperature	76°F
Solution Density	0.990 gm/cm^3
Cannon-Fenske Viscosity	1.867 cps
Power Law Exponent, n	0.7954
Power Law Coefficient, k	0.0740
Standard Error of Estimation	0.0644

Viscometer Speed (rpm)	Shear Rate (sec^{-1})	Percent Full Scale Torque	Shear Stress ($dynes/cm^2$)	Viscosity (cps)
0.3	1.15	0.35	0.081	7.043
0.6	2.30	0.60	0.140	6.087
1.5	5.75	1.30	0.302	5.252
3.0	11.50	2.20	0.512	4.452
6.0	23.00	3.90	0.907	3.943
12.0	46.00	6.45	1.500	3.261
30.0	115.00	14.25	3.316	2.882
60.0	230.00	27.05	6.295	2.738

TABLE B-86

VISCOMETRIC DATA

0.10 Percent Polyacrylamide RC-322 in 0.2 Percent NaCl Solution

Run Number	86
Solution Temperature	76°F
Solution Density	0.986 gm/cm^3
Cannon-Fenske Viscosity	2.123 cps
Power Law Exponent, n	0.8116
Power Law Coefficient, k	0.0697
Standard Error of Estimation	0.0553

Viscometer Speed (rpm)	Shear Rate (sec^{-1})	Percent Full Scale Torque	Shear Stress ($dynes/cm^2$)	Viscosity (cps)
0.3	1.15	0.40	0.093	8.090
0.6	2.30	0.60	0.140	6.070
1.5	5.75	1.15	0.268	4.650
3.0	11.50	1.80	0.419	3.640
6.0	23.00	3.45	0.803	3.490
12.0	46.00	6.70	1.560	3.390
30.0	115.00	15.00	3.490	3.030
60.0	230.00	27.40	6.376	2.770

TABLE B-87

VISCOMETRIC DATA

0.25 Percent Polyacrylamide RC-322 in 0.2 Percent NaCl Solution

Run Number	87
Solution Temperature	76°F
Solution Density	0.993 gm/cm^3
Cannon-Fenske Viscosity	8.675 cps
Power Law Exponent, n	0.8224
Power Law Coefficient, k	0.3130
Standard Error of Estimation	0.0205

Viscometer Speed (rpm)	Shear Rate (sec^{-1})	Percent Full Scale Torque	Shear Stress (dynes/cm^2)	Viscosity (cps)
0.3	1.15	1.50	0.349	30.347
0.6	2.30	2.50	0.582	25.291
1.5	5.75	6.00	1.396	24.279
3.0	11.50	10.50	2.443	21.245
6.0	23.00	18.00	4.188	18.210
12.0	46.00	31.15	7.248	15.757
30.0	115.00	64.30	14.962	13.010

TABLE B-88

VISCOMETRIC DATA

0.75 Percent Polyacrylamide RC-322 in 0.2 Percent NaCl Solution

Run Number	88
Solution Temperature	76°F
Power Law Exponent, n	0.7319
Power Law Coefficient, k	1.0000

Viscometer Speed (rpm)	Shear Rate (sec^{-1})	Percent Full Scale Torque	Shear Stress ($dynes/cm^2$)	Viscosity (cps)
0.3	1.15	4.75	1.105	96.086
0.6	2.30	7.95	1.850	80.434
1.5	5.75	15.25	3.548	61.703
3.0	11.50	24.65	5.736	49.870
6.0	23.00	40.85	9.505	41.330
12.0	46.00	71.40	16.614	36.120

TABLE B-89

SODIUM CHLORIDE CONCENTRATION TEST DATA

0.05 Percent Polyacrylamide Pusher 700 in 0.00 Percent NaCl Solution

Run Number	89
Solution Temperature	76°F
Solution Density	0.990 gm/cm^3
Cannon-Fenske Viscosity	8.759 cps
Power Law Exponent, n	0.5228
Power Law Coefficient, k	1.2350

Viscometer Speed (rpm)	Shear Rate (sec^{-1})	Percent Full Scale Torque	Shear Stress (dynes/cm^2)	Viscosity (cps)
0.3	1.15	5.50	1.280	111.304
0.6	2.30	8.60	2.001	86.999
1.5	5.75	13.35	3.106	54.016
3.0	11.50	18.50	4.305	37.432
6.0	23.00	26.85	6.248	27.166
12.0	46.00	38.25	8.900	19.349
30.0	115.00	61.85	14.392	12.507
60.0	230.00	90.65	21.093	9.175

TABLE B-90

SODIUM CHLORIDE CONCENTRATION TEST DATA

0.05 Percent Polyacrylamide Pusher 700 in 0.5 Percent NaCl Solution

Run Number	90
Solution Temperature	76°F
Solution Density	0.996 gm/cm^3
Cannon-Ferske Viscosity	2.428 cps
Power Law Exponent, n	0.8391
Power Law Coefficient, k	0.0820

Viscometer Speed (rpm)	Shear Rate (sec^{-1})	Percent Full Scale Torque	Shear Stress (dynes/cm^2)	Viscosity (cps)
0.3	1.15	0.40	0.093	8.096
0.6	2.30	0.75	0.174	7.565
1.5	5.75	1.75	0.400	6.956
3.0	11.50	2.65	0.616	5.356
6.0	23.00	4.70	1.093	4.752
12.0	46.00	8.60	2.001	4.350
30.0	115.00	18.90	4.398	3.822
60.0	230.00	35.60	8.284	3.603

TABLE B-91

SODIUM CHLORIDE CONCENTRATION TEST DATA

0.05 Percent Polyacrylamide Pusher 700 in 1.0 Percent NaCl Solution

Run Number	91
Solution Temperature	76°F
Solution Density	1.000 gm/cm^3
Cannon-Fenske Viscosity	2.092 cps
Power Law Exponent, n	0.8785
Power Law Coefficient, k	0.0515

Viscometer Speed (rpm)	Shear Rate (sec^{-1})	Percent Full Scale Torque	Shear Stress (dynes/cm^2)	Viscosity (cps)
0.3	1.15	0.25	0.058	5.043
0.6	2.30	0.50	0.116	5.043
1.5	5.75	1.00	0.233	4.052
3.0	11.50	1.65	0.384	3.339
6.0	23.00	3.40	0.791	3.439
12.0	46.00	6.45	1.500	3.261
30.0	115.00	15.00	3.490	3.033
60.0	230.00	34.20	7.958	3.462

TABLE B-92

SODIUM CHLORIDE CONCENTRATION TEST DATA

0.05 Percent Polyacrylamide Pusher 700 in 2.0 Percent NaCl Solution

Run Number	92
Solution Temperature	76°F
Solution Density	1.007 gm/cm^3
Cannon-Fenske Viscosity	1.849 cps
Power Law Exponent, n	0.9163
Power Law Coefficient, k	0.0305

Viscometer Speed (rpm)	Shear Rate (sec^{-1})	Percent Full Scale Torque	Shear Stress (dynes/cm^2)	Viscosity (cps)
0.6	2.30	0.30	0.070	3.043
1.5	5.75	0.60	0.140	2.433
3.0	11.50	1.15	0.266	2.313
6.0	23.00	2.15	0.500	2.174
12.0	46.00	4.15	0.965	2.098
30.0	115.00	9.75	2.269	1.972
60.0	230.00	19.35	4.502	1.958

TABLE B-93

SODIUM CHLORIDE CONCENTRATION TEST DATA

0.05 Percent Polyacrylamide Pusher 700 in 4.0 Percent NaCl Solution

Run Number	93
Solution Temperature	76°F
Solution Density	1.022 gm/cm^3
Cannon-Fenske Viscosity	1.692 cps
Power Law Exponent, n	1.0212
Power Law Coefficient, k	0.0132

Viscometer Speed (rpm)	Shear Rate (sec^{-1})	Percent Full Scale Torque	Shear Stress ($dynes/cm^2$)	Viscosity (cps)
1.5	5.75	0.35	0.810	1.409
3.0	11.50	0.60	0.140	1.217
6.0	23.00	1.35	0.314	1.365
12.0	46.00	3.15	0.733	1.593
30.0	115.00	7.60	1.768	1.536
60.0	230.00	14.60	3.398	1.478

TABLE B-94

SODIUM CHLORIDE CONCENTRATION TEST DATA

0.05 Percent Polyacrylamide Pusher 700 in 7.0 Percent NaCl Soltuion

Run Number	94
Solution Temperature	76°F
Power Law Exponent, n	1.0538
Power Law Coefficient, k	0.0145

Viscometer Speed (rpm)	Shear Rate (sec^{-1})	Percent Full Scale Torque	Shear Stress ($dynes/cm^2$)	Viscosity (cps)
1.5	5.75	0.40	0.093	1.617
3.0	11.50	0.80	0.186	1.617
6.0	23.00	1.65	0.384	1.670
12.0	46.00	3.95	0.919	1.998
30.0	115.00	9.85	2.292	1.992
60.0	230.00	19.50	4.537	1.973

TABLE B-95

SODIUM CHLORIDE CONCENTRATION TEST DATA

0.05 Percent Polyacrylamide Pusher 700 in 10.0 Percent NaCl Solution

Run Number	95
Solution Temperature	76°F
Power Law Exponent, n	1.0464
Power Law Coefficient, k	0.0170

Viscometer Speed (rpm)	Shear Rate (sec^{-1})	Percent Full Scale Torque	Shear Stress ($dynes/cm^2$)	Viscosity (cps)
1.5	5.75	0.45	0.105	1.826
3.0	11.50	0.95	0.221	1.922
6.0	23.00	2.00	0.465	2.022
12.0	46.00	4.15	0.965	2.098
30.0	115.00	10.60	2.466	2.143
60.0	230.00	21.70	5.049	2.196

TABLE B-96

SODIUM CHLORIDE CONCENTRATION TEST DATA

0.10 Percent Polyacrylamide "Reten" A-5 in 0.00 Percent NaCl Solution

Run Number	96
Solution Temperature	76°F
Solution Density	0.993 gm/cm^3
Power Law Exponent, n	0.6297
Power Law Coefficient, k	7.1500

Viscometer Speed (rpm)	Shear Rate (sec^{-1})	Percent Full Scale Torque)	Shear Stress ($dynes/cm^2$)	Viscosity (cps)
0.3	1.15	33.50	7.795	677.826
0.6	2.30	52.15	12.135	527.605
1.5	5.75	93.00	21.640	376.341

TABLE B-97

SODIUM CHLORIDE CONCENTRATION TEST DATA

0.10 Percent Polyacrylamide "Reten" A-5 in 0.50 Percent NaCl Solution

Run Number	97
Solution Temperature	76°F
Solution Density	0.996 gm/cm^3
Cannon-Fenske Viscosity	3.307 cps
Power Law Exponent, n	0.8754
Power Law Coefficient, k	0.1035

Viscometer Speed (rpm)	Shear Rate (sec^{-1})	Percent Full Scale Torque	Shear Stress ($dynes/cm^2$)	Viscosity (cps)
0.3	1.15	0.50	0.116	10.087
0.6	2.30	0.90	0.209	9.087
1.5	5.75	2.40	0.558	9.704
3.0	11.50	3.65	0.849	7.382
6.0	23.00	6.70	1.556	6.765
12.0	46.00	12.25	2.850	6.196
30.0	115.00	28.30	6.585	5.722
60.0	230.00	52.80	12.286	5.344

TABLE B-98

SODIUM CHLORIDE CONCENTRATION TEST DATA

0.1 Percent Polyacrylamide "Reten" A-5 in 1.0 Percent NaCl Solution

Run Number	98
Solution Temperature	76°F
Solution Density	1.000 gm/cm^3
Cannon-Fenske Viscosity	2.615 cps
Power Law Exponent, n	0.9759
Power Law Coefficient, k	0.0253

Viscometer Speed (rpm)	Shear Rate (sec^{-1})	Percent Full Scale Torque	Shear Stress ($dynes/cm^2$)	Viscosity (cps)
0.6	2.30	0.25	0.058	2.522
1.5	5.75	0.65	0.151	2.626
3.0	11.50	1.25	0.291	2.530
6.0	23.00	2.55	0.593	2.578
12.0	46.00	4.90	1.140	2.478
30.0	115.00	12.30	2.862	2.478
60.0	230.00	23.05	5.363	2.333

TABLE B-99

SODIUM CHLORIDE CONCENTRATION TEST DATA

0.1 Percent Polyacrylamide "Reten" A-5 in 2.0 Percent NaCl Solution

Run Number	99
Solution Temperature	76°F
Solution Density	1.007 gm/cm^3
Cannon-Fenske VIscosity	2.397 cps
Power Law Exponent, n	0.9827
Power Law Coefficient, k	0.0217

Viscometer Speed (rpm)	Shear Rate (sec^{-1})	Percent Full Scale Torque	Shear Stress (dynes/cm^2)	Viscosity (cps)
0.6	2.30	0.20	0.046	2.000
1.5	5.75	0.50	0.116	2.017
3.0	11.50	1.05	0.244	2.122
6.0	23.00	2.15	0.500	2.174
12.0	46.00	4.35	1.012	2.200
30.0	115.00	10.45	2.432	2.113
60.0	230.00	20.30	4.724	2.055

TABLE B-100

SODIUM CHLORIDE CONCENTRATION TEST DATA

0.1 Percent Polyacrylamide "Reten" A-5 in 4.0 Percent NaCl Solution

Run Number	100
Solution Temperature	76°F
Solution Density	1.018 gm/cm^3
Cannon-Fenske Viscosity	2.068 cps
Power Law Exponent, n	1.0176
Power Law Coefficient, k	0.0140

Viscometer Speed (rpm)	Shear Rate (sec^{-1})	Percent Full Scale Torque	Shear Stress (dynes/cm^2)	Viscosity (cps)
1.5	5.75	0.35	0.081	1.409
3.0	11.50	0.75	0.174	1.513
6.0	23.00	1.30	0.302	1.313
12.0	46.00	3.15	0.733	1.593
30.0	115.00	8.15	1.896	1.648
60.0	230.00	16.15	3.758	1.635

TABLE B-101

SODIUM CHLORIDE CONCENTRATION TEST DATA

0.1 Percent Polyacrylamide "Reten" A-5 in 7.0 Percent NaCl Solution

Run Number	101
Solution Temperature	76°F
Power Law Exponent, n	0.9004
Power Law Coefficient, k	0.0262

Viscometer Speed (rpm)	Shear Rate (sec^{-1})	Percent Full Scale Torque	Shear Stress ($dynes/cm^2$)	Viscosity (cps)
0.3	1.15	0.15	0.036	3.130
0.6	2.30	0.30	0.070	3.043
1.5	5.75	0.75	0.174	3.026
3.0	11.50	1.15	0.267	2.321
6.0	23.00	2.30	0.535	2.326
12.0	46.00	4.05	0.942	2.048
30.0	115.00	9.75	2.269	1.972
60.0	230.00	19.15	4.456	1.938

TABLE B-102

SODIUM CHLORIDE CONCENTRATION TEST DATA

0.1 Percent Polyacrylamide "Reten" A-5 in 10.0 Percent NaCl Solution

Run Number	102
Solution Temperature	76°F
Power Law Exponent, n	0.9004
Power Law Coefficient, k	0.0320

Viscometer Speed (rpm)	Shear Rate (sec^{-1})	Percent Full Scale Torque	Shear Stress ($dynes/cm^2$)	Viscosity (cps)
0.6	2.30	0.35	0.081	3.522
1.5	5.75	0.80	0.186	3.235
3.0	11.50	1.65	0.384	3.339
6.0	23.00	2.50	0.582	2.530
12.0	46.00	5.00	1.163	2.528
30.0	115.00	11.85	2.757	2.396
60.0	230.00	22.85	5.317	2.313

TABLE B-103

SODIUM CHLORIDE CONCENTRATION TEST DATA

0.075 Percent Polyacrylamide RC-319 in 0.00 Percent NaCl Solution

Run Number	103
Solution Temperature	76°F
Solution Density	0.991 gm/cm^3
Cannon-Fenske Viscosity	15.839 cps
Power Law Exponent, n	0.6032
Power Law Coefficient, k	1.0165

Viscometer Speed (rpm)	Shear Rate (sec^{-1})	Percent Full Scale Torque	Shear Stress (dynes/cm^2)	Viscosity (cps)
0.3	1.15	5.00	1.163	101.130
0.6	2.30	8.50	1.978	85.999
1.5	5.75	16.65	3.641	60.190
3.0	11.50	23.70	5.515	47.956
6.0	23.00	35.10	8.167	35.508
12.0	46.00	51.00	11.867	25.798
30.0	115.00	82.95	19.303	16.784

TABLE B-104

SODIUM CHLORIDE CONCENTRATION TEST DATA

0.075 Percent Polyacrylamide RC-319 in 0.5 Percent NaCl Solution

Run Number	104
Solution Temperature	76°F
Solution Density	0.996 gm/cm^3
Cannon-Fenske Viscosity	2.433 cps
Power Law Exponent, n	0.9457
Power Law Coefficient	0.0400

Viscometer Speed (rpm)	Shear Rate (sec^{-1})	Percent Full Scale Torque	Shear Stress (dynes/cm^2)	Viscosity (cps)
0.3	1.15	0.20	0.046	4.000
0.6	2.30	0.40	0.093	4.043
1.5	5.75	0.85	0.198	3.443
3.0	11.50	1.60	0.372	3.235
6.0	23.00	3.40	0.791	3.439
12.0	46.00	6.45	1.500	3.261
30.0	115.00	15.15	3.525	3.065
60.0	230.00	29.60	6.887	2.994

TABLE B-105

SODIUM CHLORIDE CONCENTRATION TEST DATA

0.075 Percent Polyacrylamide RC-319 in 0.1 Percent NaCl Solution

Run Number	105
Solution Temperature	76°F
Solution Density	1.000 gm/cm^3
Cannon-Fenske Viscosity	1.973 cps
Power Law Exponent, n	0.9556
Power Law Coefficient, k	0.0320

Viscometer Speed (rpm)	Shear Rate (sec^{-1})	Percent Full Scale Torque	Shear Stress ($dynes/cm^2$)	Viscosity (cps)
0.3	1.15	0.15	0.035	3.043
0.6	2.30	0.30	0.070	3.043
1.5	5.75	0.80	0.186	3.235
3.0	11.50	1.40	0.326	2.835
6.0	23.00	2.80	0.651	2.830
12.0	46.00	5.30	1.233	2.680
30.0	115.00	12.85	2.990	2.600
60.0	230.00	26.15	6.085	2.646

TABLE B-106

SODIUM CHLORIDE CONCENTRATION TEST DATA

0.075 Percent Polyacrylamide RC-319 in 2.0 Percent NaCl Solution

Run Number	106
Solution Temperature	76°F
Solution Density	1.003 gm/cm^3
Cannon-Fenske Viscosity	2.554 cps
Power Law Exponent, n	0.9793
Power Law Coefficient, k	0.0255

Viscometer Speed (rpm)	Shear Rate (sec^{-1})	Percent Full Scale Torque	Shear Stress (dynes/cm^2)	Viscosity (cps)
0.3	1.15	0.10	0.023	2.000
0.6	2.30	0.25	0.058	2.522
1.5	5.75	0.60	0.140	2.435
3.0	11.50	1.15	0.267	2.322
6.0	23.00	2.55	0.593	2.578
12.0	46.00	4.90	1.140	2.478
30.0	115.00	12.20	2.839	2.469
60.0	230.00	24.30	5.654	2.458

TABLE B-107

SODIUM CHLORIDE CONCENTRATION TEST DATA

0.075 Percent Polyacrylamide RC-319 in 4.0 Percent NaCl Solution

Run Number	107
Solution Temperature	76°F
Solution Density	1.016 gm/cm^3
Cannon-Fenske Viscosity	1.728 cps
Power Law Exponent, n	1.1343
Power Law Coefficient, k	0.0076

Viscometer Speed (rpm)	Shear Rate (sec^{-1})	Percent Full Scale Torque	Shear Stress ($dynes/cm^2$)	Viscosity (cps)
1.5	5.75	0.25	0.058	1.008
3.0	11.50	0.45	0.105	0.913
6.0	23.00	1.15	0.267	1.160
12.0	46.00	2.55	0.593	1.289
30.0	115.00	7.55	1.757	1.528
60.0	230.00	16.75	3.897	1.694

TABLE B-108

SODIUM CHLORIDE CONCENTRATION TEST DATA

0.075 Percent Polyacrylamide RC-319 in 7.0 Percent NaCl Solution

Run Number	108
Solution Temperature	76°F
Power Law Exponent, n	1.1106
Power Law Coefficient, k	0.0097

Viscometer Speed (rpm)	Shear Rate (sec^{-1})	Percent Full Scale Torque	Shear Stress ($dynes/cm^2$)	Viscosity (cps)
0.6	2.30	0.10	0.023	1.000
1.5	5.75	0.30	0.070	1.217
3.0	11.50	0.65	0.151	1.313
6.0	23.00	1.40	0.326	1.417
12.0	46.00	3.05	0.710	1.543
30.0	115.00	8.60	2.001	1.740
60.0	230.00	18.50	4.305	1.872

TABLE B-109

SODIUM CHLORIDE CONCENTRATION TEST DATA

0.075 Percent Polyacrylamide RC-319 in 10.0 Percent NaCl Solution

Run Number	109
Solution Temperature	76°F
Power Law Exponent, n	1.0799
Power Law Coefficient, k	0.0130

Viscometer Speed (rpm)	Shear Rate (sec^{-1})	Percent Full Scale Torque	Shear Stress ($dynes/cm^2$)	Viscosity (cps)
0.6	2.30	0.15	0.035	1.522
1.5	5.75	0.35	0.081	1.408
3.0	11.50	0.75	0.174	1.513
6.0	23.00	1.60	0.372	1.617
12.0	46.00	3.55	0.826	1.796
30.0	115.00	9.60	2.234	1.942
60.0	230.00	20.30	4.724	2.054

TABLE B-110

ELEVATED TEMPERATURE RUN DATA

0.075 Percent Polyacrylamide "Separan" NP-10 Solution

Run Number	110
Solution Temperature	87.8°F
Power Law Exponent, n	0.9974
Power Law Coefficient, k	0.0132
Standard Error of Estimation	0.0690

Viscometer Speed (rpm)	Shear Rate (sec^{-1})	Percent Full Scale Torque	Shear Stress ($dynes/cm^2$)	Viscosity (cps)
0.6	2.30	0.15	0.035	1.522
1.5	5.75	0.40	0.093	1.617
3.0	11.50	1.00	0.233	2.026
6.0	23.00	2.05	0.477	2.074
12.0	46.00	4.05	0.942	2.048
30.0	115.00	9.90	2.304	2.002
60.0	230.00	19.15	4.456	1.938

TABLE B-111

ELEVATED TEMPERATURE RUN DATA

0.075 Percent Polyacrylamide "Separan" NP-10 Solution

Run Number	111
Solution Temperature	104°F
Power Law Exponent, n	1.1694
Power Law Coefficient, k	0.0077
Standard Error of Estimation	0.1436

Viscometer Speed (rpm)	Shear Rate (sec^{-1})	Percent Full Scale Torque	Shear Stress ($dynes/cm^2$)	Viscosity (cps)
1.5	5.75	0.35	0.081	1.409
3.0	11.50	0.75	0.175	1.522
6.0	23.00	1.55	0.361	1.569
12.0	46.00	3.15	0.733	1.594
30.0	115.00	7.85	1.827	1.588
60.0	230.00	15.15	3.525	1.533

TABLE B-112

ELEVATED TEMPERATURE RUN DATA

0.075 Percent Polyacrylamide "Separan" NP-10 Solution

Run Number	112
Solution Temperature	131°F
Power Law Exponent, n	1.0370
Power Law Coefficient, k	0.0096
Standard Error of Estimation	0.0020

Viscometer Speed (rpm)	Shear Rate (sec^{-1})	Percent Full Scale Torque	Shear Stress ($dynes/cm^2$)	Viscosity (cps)
1.5	5.75	0.25	0.058	1.009
3.0	11.50	0.50	0.116	1.009
6.0	23.00	1.15	0.268	1.165
12.0	46.00	2.20	0.512	1.113
30.0	115.00	5.65	1.315	1.143
60.0	230.00	11.35	2.641	1.149

TABLE B-113

ELEVATED TEMPERATURE RUN DATA

0.075 Percent Polyacrylamide "Separan" NP-10 Solution

Run Number	113
Solution Temperature	167°F
Power Law Exponent, n	1.1307
Power Law Coefficient, k	0.0038
Standard Error of Estimation	0.0538

Viscometer Speed (rpm)	Shear Rate (sec^{-1})	Percent Full Scale Torque	Shear Stress ($dynes/cm^2$)	Viscosity (cps)
3.0	11.50	0.30	0.069	0.599
6.0	23.00	0.60	0.140	0.608
12.0	46.00	1.30	0.302	0.656
30.0	115.00	3.30	0.768	0.667
60.0	230.00	7.30	1.699	0.739

TABLE B-114

ELEVATED TEMPERATURE RUN DATA

0.075 Percent Polyacrylamide "Separan" NP-10 Solution

Run Number	114
Solution Temperature	185°F
Power Law Exponent, n	1.0115
Power Law Coefficient, k	0.0057
Standard Error of Estimation	0.0750

Viscometer Speed (rum)	Shear Rate (sec^{-1})	Percent Full Scale Torque	Shear Stress ($dynes/cm^2$)	Viscosity (cps)
3.0	11.50	0.25	0.058	0.504
6.0	23.00	0.50	0.116	0.504
12.0	46.00	1.00	0.233	0.507
30.0	115.00	2.70	0.628	0.646
60.0	230.00	6.00	1.396	0.607

TABLE B-115

ELEVATED TEMPERATURE RUN DATA

0.10 Percent Polyacrylamide "Reten" A-1 Solution

Run Number	115
Solution Temperature	86.9°F
Power Law Exponent, n	0.8941
Power Law Coefficient, k	0.0750

Viscometer Speed (rpm)	Shear Rate (sec^{-1})	Percent Full Scale Torque	Shear Stress ($dynes/cm^2$)	Viscosity (cps)
0.3	1.15	0.35	0.081	7.043
0.6	2.30	0.65	0.151	6.565
1.5	5.75	1.50	0.349	6.070
3.0	11.50	2.45	0.570	4.956
6.0	23.00	5.40	1.257	5.465
12.0	46.00	10.00	2.327	5.059
30.0	115.00	22.35	5.201	4.520
60.0	230.00	40.40	9.401	4.089

TABLE B-116

ELEVATED TEMPERATURE RUN DATA

0.10 Percent Polyacrylamide "Reten" A-1 Solution

Run Number	116
Solution Temperature	104°F
Power Law Exponent, n	0.9163
Power Law Coefficient, k	0.0435

Viscometer Speed (rpm)	Shear Rate (sec^{-1})	Percent Full Scale Torque	Shear Stress ($dynes/cm^2$)	Viscosity (cps)
0.6	2.30	0.40	0.093	4.043
1.5	5.75	0.95	0.221	3.843
3.0	11.50	1.75	0.407	3.539
6.0	23.00	3.30	0.768	3.339
12.0	46.00	6.70	1.559	3.389
30.0	115.00	15.30	3.560	3.094
60.0	230.00	28.85	6.713	2.920

TABLE B-117

ELEVATED TEMPERATURE RUN DATA

0.10 Percent Polyacrylamide "Reten" A-1 Solution

Run Number	117
Solution Temperature	131°F
Power Law Exponent, n	0.8693
Power Law Coefficient, k	0.0386

Viscometer Speed (rpm)	Shear Rate (sec^{-1})	Percent Full Scale Torque	Shear Stress ($dynes/cm^2$)	Viscosity (cps)
0.6	2.30	0.35	0.081	3.522
1.5	5.75	0.75	0.175	3.042
3.0	11.50	1.30	0.302	2.626
6.0	23.00	2.40	0.558	2.426
12.0	46.00	4.65	1.082	2.352
30.0	115.00	10.45	2.432	2.113
60.0	230.00	19.05	4.433	1.928

TABLE B-118

ELEVATED TEMPERATURE RUN DATA

0.10 Percent Polyacrylamide "Reten" A-1 Solution

Run Number	118
Solution Temperature	158.9°F
Power Law Exponent, n	0.9523
Power Law Coefficient, k	0.0145

Viscometer Speed (rpm)	Shear Rate (sec^{-1})	Percent Full Scale Torque	Shear Stress ($dynes/cm^2$)	Viscosity (cps)
1.5	5.75	0.35	0.081	1.409
3.0	11.50	0.60	0.140	1.217
6.0	23.00	1.20	0.279	1.213
12.0	46.00	2.20	0.512	1.113
30.0	115.00	5.30	1.233	1.071
60.0	230.00	11.25	2.618	1.139

TABLE B-119

ELEVATED TEMPERATURE RUN DATA

0.10 Percent Polyacrylamide "Reten" A-1 Solution

Run Number	119
Solution Temperature	185.9°F
Power Law Exponent, n	0.9523
Power Law Coefficient, k	0.0096

Viscometer Speed (rpm)	Shear Rate (sec^{-1})	Percent Full Scale Torque	Shear Stress ($dynes/cm^2$)	Viscosity (cps)
0.3	1.15	0.05	0.012	1.043
0.6	2.30	0.10	0.023	1.000
1.5	5.75	0.25	0.058	1.009
3.0	11.50	0.45	0.105	0.913
6.0	23.00	0.85	0.198	0.861
12.0	46.00	1.70	0.396	0.861
30.0	115.00	3.70	0.861	0.748
60.0	230.00	8.25	1.200	0.835

TABLE B-120

ELEVATED TEMPERATURE RUN DATA

0.071 Percent Polyacrylamide RC-301 Solution

RUN NUMBER	120
Solution Temperature	95.9°F
Power Law Exponent, n	0.9163
Power Law Coefficient, k	0.0214
Standard Error of Estimation	0.0562

Viscometer Speed (rpm)	Shear Rate (sec^{-1})	Percent Full Scale Torque	Shear Stress ($dynes/cm^2$)	Viscosity (cps)
1.5	5.75	0.47	0.109	1.902
3.0	11.50	0.70	0.163	1.416
6.0	23.00	1.50	0.349	1.517
12.0	46.00	3.00	0.698	1.517
30.0	115.00	7.50	1.745	1.517
60.0	230.00	14.50	3.374	1.467

TABLE B-121

ELEVATED TEMPERATURE RUN DATA

0.071 Percent Polyacrylamide RC-301 Solution

Run Number	121
Solution Temperature	113°F
Power Law Exponent, n	1.0760
Power Law Coefficient, k	0.0091
Standard Error of Estimation	0.0238

Viscometer Speed (rpm)	Shear Rate (sec^{-1})	Percent Full Scale Torque	Shear Stress ($dynes/cm^2$)	Viscosity (cps)
0.6	2.30	0.10	0.023	1.012
1.5	5.75	0.25	0.058	1.012
3.0	11.50	0.50	0.116	1.012
6.0	23.00	1.20	0.279	1.214
12.0	46.00	2.55	0.593	1.290
30.0	115.00	6.50	1.512	1.325
60.0	230.00	13.33	3.101	1.348

TABLE B-122

ELEVATED TEMPERATURE RUN DATA

0.071 Percent Polyacrylamide RC-301 Solution

Run Number	122
Solution Temperature	140°F
Power Law Exponent, n	1.0200
Power Law Coefficient, k	0.0099
Standard Error of Estimation	0.0142

Viscometer Speed (rpm)	Shear Rate (sec^{-1})	Percent Full Scale Torque	Shear Stress ($dynes/cm^2$)	Viscosity (cps)
0.6	2.30	0.10	0.023	1.012
1.5	5.75	0.25	0.058	1.012
3.0	11.50	0.50	0.116	1.012
6.0	23.00	1.10	0.256	1.113
12.0	46.00	2.15	0.500	1.087
30.0	115.00	5.20	1.210	1.052
60.0	230.00	11.00	2.560	1.113

TABLE B-123

ELEVATED TEMPERATURE RUN DATA

0.071 Percent Polyacrylamide RC-30 Solution

Run Number	123
Solution Temperature	176°F
Power Law Exponent, n	0.9581
Power Law Coefficient, k	0.0080
Standard Error of Estimation	0.0781

Viscometer Speed (rpm)	Shear Rate (sec^{-1})	Percent Full Scale Torque	Shear Stress ($dynes/cm^2$)	Viscosity (cps)
0.6	2.30	0.10	0.023	1.012
1.5	5.75	0.15	0.035	0.607
3.0	11.50	0.35	0.081	0.708
6.0	23.00	0.60	0.140	0.607
12.0	46.00	1.25	0.291	0.632
30.0	115.00	3.35	0.779	0.678
60.0	230.00	7.25	1.687	0.733

TABLE B-124

ELEVATED TEMPERATURE RUN DATA

0.25 Percent Polyethylene Oxide "Polyox" WSR-301 Solution

Run Number	124
Solution Temperature	88.7°F
Power Law Exponent, n	0.8724
Power Law Coefficient, k	0.1600

Viscometer Speed (rpm)	Shear Rate (sec^{-1})	Percent Full Scale Torque	Shear Stress ($dynes/cm^2$)	Viscosity (cps)
0.3	1.15	0.65	0.151	13.130
0.6	2.30	1.40	0.326	14.174
1.5	5.75	3.55	0.826	14.365
3.0	11.50	6.70	1.559	13.556
6.0	23.00	12.05	2.804	12.191
12.0	46.00	21.80	5.073	11.028
30.0	115.00	47.75	10.646	9.257
60.0	230.00	79.00	18.383	7.993

TABLE B-125

ELEVATED TEMPERATURE RUN DATA

0.25 Percent Polyethylene "Polyox" WSR-301 Solution

Run Number	125
Solution Temperature	104°F
Power Law Exponent, n	0.8878
Power Law Coefficient, k	0.1070

Viscometer Speed (rpm)	Shear Rate (sec^{-1})	Percent Full Scale Torque	Shear Stress ($dynes/cm^2$)	Viscosity (cps)
0.3	1.15	0.50	0.116	10.087
0.6	2.30	1.05	0.244	10.609
1.5	5.75	2.05	0.477	8.296
3.0	11.50	4.15	0.966	8.400
6.0	23.00	7.95	1.850	8.043
12.0	46.00	14.75	3.432	7.461
30.0	115.00	32.60	7.586	6.596
60.0	230.00	57.95	13.484	5.863

TABLE B-126

ELEVATED TEMPERATURE RUN DATA

0.25 Percent Polyethylene "Polyox" WSR-301 Solution

Run Number	126
Solution Temperature	131°F
Power Law Exponent, n	0.9827
Power Law Coefficient, k	0.0325

Viscometer Speed (rpm)	Shear Rate (sec^{-1})	Percent Full Scale Torque	Shear Stress ($dynes/cm^2$)	Viscosity (cps)
0.3	1.15	0.15	0.035	3.043
0.6	2.30	0.35	0.081	3.522
1.5	5.75	0.85	0.198	3.443
3.0	11.50	1.50	0.349	3.035
6.0	23.00	3.15	0.733	3.187
12.0	46.00	6.40	1.489	3.237
30.0	115.00	16.15	3.458	3.007
60.0	230.00	30.80	7.167	3.116

TABLE B-127

ELEVATED TEMPERATURE RUN DATA

0.25 Percent Polyethylene Oxide "Polyox" WSR-301 Solution

Run Number	127
Solution Temperature	158.9°F
Power Law Exponent, n	0.9163
Power Law Coefficient, k	0.0212

Viscometer Speed (rpm)	Shear Rate (sec^{-1})	Percent Full Scale Torque	Shear Stress ($dynes/cm^2$)	Viscosity (cps)
0.3	1.15	0.10	0.023	2.000
0.6	2.30	0.20	0.046	2.000
1.5	5.75	0.50	0.116	2.017
3.0	11.50	0.85	0.196	1.704
6.0	23.00	1.50	0.349	1.517
12.0	46.00	2.75	0.628	1.365
30.0	115.00	6.60	1.536	1.336
60.0	230.00	13.80	3.211	1.396

TABLE B-128

ELEVATED TEMPERATURE RUN DATA

0.25 Percent Polyethylene Oxide "Polyox" WSR-301 Solution

Run Number	128
Solution Temperature	196.7°F
Power Law Exponent, n	0.8481
Power Law Coefficient, k	0.0186

Viscometer Speed (rpm)	Shear Rate (sec^{-1})	Percent Full Scale Torque	Shear Stress ($dynes/cm^2$)	Viscosity (cps)
3.0	11.50	0.75	0.175	1.522
6.0	23.00	1.25	0.291	1.265
12.0	46.00	2.15	0.500	1.087
30.0	115.00	4.05	0.942	1.819
60.0	230.00	8.80	2.048	0.890

TABLE B-129

ELEVATED TEMPERATURE RUN DATA

0.05 Percent Polysaccharide "Kelzan" M Solution

Run Number	129
Solution Temperature	104°F
Power Law Exponent, n	0.7785
Power Law Coefficient, k	0.0960

Viscometer Speed (rpm)	Shear Rate (sec^{-1})	Percent Full Scale Torque	Shear Stress ($dynes/cm^2$)	Viscosity (cps)
0.3	1.15	0.45	0.105	9.130
0.6	2.30	0.75	0.174	7.565
1.5	5.75	1.50	0.349	6.069
3.0	11.50	2.75	0.640	5.565
6.0	23.00	4.90	1.140	4.957
12.0	46.00	8.35	1.943	4.224
30.0	115.00	16.25	3.781	3.286
60.0	230.00	27.25	6.341	2.758

TABLE B-130

ELEVATED TEMPERATURE RUN DATA

0.05 Percent Polysaccharide "Kelzan" M Solution

Run Number	130
Solution Temperature	122°F
Power Law Exponent, n	0.7481
Power Law Coefficient, k	0.0830

Viscometer Speed (rpm)	Shear Rate (sec^{-1})	Percent Full Scale Torque	Shear Stress ($dynes/cm^2$)	Viscosity (cps)
0.3	1.15	0.40	0.093	8.087
0.6	2.30	0.65	0.151	6.565
1.5	5.75	1.40	0.326	5.669
3.0	11.50	2.35	0.547	4.756
6.0	23.00	3.80	0.884	3.844
12.0	46.00	6.45	1.501	3.263
30.0	115.00	12.75	2.967	2.578
60.0	230.00	21.45	4.991	2.171

TABLE B-131

ELEVATED TEMPERATURE RUN DATA

0.05 Percent Polysaccharide "Kelzan" M Solution

Run Number	131
Solution Temperature	158°F
Power Law Exponent, n	0.8012
Power Law Coefficient, k	0.0547

Viscometer Speed (rpm)	Shear Rate (sec^{-1})	Percent Full Scale Torque	Shear Stress ($dynes/cm^2$)	Viscosity (cps)
0.3	1.15	0.25	0.058	5.043
0.6	2.30	0.50	0.116	5.043
1.5	5.75	1.00	0.233	4.052
3.0	11.50	1.75	0.407	3.539
6.0	23.00	3.05	0.709	3.083
12.0	46.00	5.30	1.233	2.680
30.0	115.00	10.80	2.513	2.184
60.0	230.00	18.40	4.281	1.862

TABLE B-132

ELEVATED TEMPERATURE RUN DATA

0.05 Percent Polysaccharide "Kelzan" M Solution

Run Number	132
Solution Temperature	195.8°F
Power Law Exponent, n	0.7983
Power Law Coefficient, k	0.0407

Viscometer Speed (rpm)	Shear Rate (sec^{-1})	Percent Full Scale Torque	Shear Stress ($dynes/cm^2$)	Viscosity (cps)
1.5	5.75	0.75	0.174	3.026
3.0	11.50	1 '5	0.291	2.530
6.0	23.00	1.90	0.442	1.922
12.0	46.00	3.65	0.849	1.846
30.0	115.00	7.05	1.640	1.425
60.0	230.00	14.40	3.351	1.458

APPENDIX C

POLYMER SOLUTION DISPLACEMENT DATA

TABLE C-1

RESISTANCE FACTOR DATA AND CALCULATIONS

0.075 Percent RC-322 in 2 Percent NaCl Solution

Run No. 1 — Water Viscosity 1.012 cps
Core No. 15 — Polymer Viscosity 1.377 cps

Pressure Drop ΔP (atm)	Flow Rate $Qx10^2$ (cm^3/sec)	Polymer Mobility $\lambda_p = \frac{QL}{\Delta PA}$	Linear Pore Velocity V (ft/day)	$R = \frac{\lambda_w}{\lambda_p}$
23.816	116.70	0.038	1570.40	10.82
20.924	91.70	0.034	1235.90	12.10
17.488	66.70	0.030	898.60	13.70
14.290	46.90	0.026	632.10	15.81
11.840	33.70	0.022	453.50	18.68
7.485	19.50	0.020	263.60	20.55
3.470	8.80	0.020	119.10	20.55
2.722	6.70	0.019	90.70	21.63
2.041	4.70	0.018	62.40	22.83
1.361	3.10	0.018	42.50	22.83
0.680	1.30	0.015	17.00	27.40
0.340	0.90	0.021	11.30	19.57

TABLE C-2

RESISTANCE FACTOR DATA AND CALCULATIONS

0.075 Percent RC-322 in 2 Percent NaCl Solution

Run No. 2 — Water Viscosity 1.012 cps
Core No. 18 — Polymer Viscosity 1.377 cps

Pressure Drop ΔP (atm)	Flow Rate $Qx10^2$ (cm^3/sec)	Polymer Mobility $\lambda_p = \frac{QL}{\Delta PA}$	Linear Pore Velocity V (ft/day)	$R = \frac{\lambda_w}{\lambda_p}$
34.022	248.00	0.057	3120.89	8.95
27.490	179.00	0.051	2253.51	10.00
21.978	120.00	0.043	1510.84	11.86
18.848	90.00	0.037	1133.84	13.78
15.378	62.00	0.031	779.51	16.45
11.568	38.00	0.026	479.05	19.61
7.689	21.00	0.022	263.62	23.18
2.722	6.00	0.017	76.53	30.00
2.041	4.00	0.015	51.02	34.00
1.360	2.00	0.012	25.51	42.50
0.680	1.00	0.012	11.34	42.50

TABLE C-3

RESISTANCE FACTOR DATA AND CALCULATIONS

0.075 Percent RC-322 in 2 Percent NaCl Solution

Run No. 1 — Water Viscosity 1.012 cps
Core No. 15 — Polymer Viscosity 1.377 cps

Pressure Drop ΔP (atm)	Flow Rate $Qx10^3$ (cm^3/sec)	Polymer Mobility $\lambda_p = \left(\frac{QL}{\Delta PA}\right) x10^3$	Linear Pore Velocity V (ft/day)	$R = \frac{\lambda_w}{\lambda_p}$
26.946	1250.00	37.00	1641.20	17.11
21.026	750.00	28.00	943.60	22.61
15.651	456.00	23.00	598.10	27.52
10.513	258.00	20.00	337.30	31.65
6.805	154.00	18.00	201.30	35.17
3.402	70.00	16.00	90.70	39.56
2.722	51.00	15.00	68.00	42.20
2.041	31.00	12.00	39.70	52.75
0.680	10.00	12.00	14.20	52.75
0.340	5.00	12.00	5.70	52.75

TABLE C-4

RESISTANCE FACTOR DATA AND CALCULATIONS

0.075 Percent RC-322 in 2 Percent NaCl Solution

Run No. 4 — Water Viscosity 1.012 cps
Core No. 21 — Polymer Viscosity 1.377 cps

Pressure Drop ΔP (atm)	Flow Rate $Qx10^2$ (cm^3/sec)	Polymer Mobility $\lambda_p = \frac{QL}{\Delta PA}$	Linear Pore Velocity V (ft/day)	$R = \frac{\lambda_w}{\lambda_p}$
21.162	203.00	0.046	4654.40	5.30
18.032	161.00	0.043	3690.60	5.67
14.630	110.00	0.036	2522.80	6.78
10.819	67.00	0.025	1536.40	9.76
7.145	33.00	0.022	748.30	11.09
5.171	20.00	0.019	459.20	12.84
3.674	13.00	0.017	297.60	14.35
2.858	10.00	0.017	229.60	14.35
2.246	7.00	0.016	161.60	15.25
1.429	4.00	0.013	90.70	18.77
0.680	2.00	0.014	45.40	17.43

TABLE C-5

RESISTANCE FACTOR DATA AND CALCULATIONS

0.074 Percent RC-322 in 2 Percent NaCl Solution

Run No. 5 — Water Viscosity 1.012 cps
Core No. 22 — Polymer Viscosity 1.377 cps

Pressure Drop ΔP (atm)	Flow Rate $Qx10^3$ (cm^3/sec)	Polymer Mobility $\lambda_p = \left(\frac{QL}{\Delta PA}\right) x10^3$	Linear Pore Velocity V (ft/day)	$R = \frac{\lambda_w}{\lambda_p}$
7.281	265.00	17.318	495.84	17.61
4.083	161.10	18.769	295.15	16.25
3.402	138.30	19.348	252.40	15.76
2.722	116.70	20.416	212.99	14.94
2.041	96.70	22.528	176.48	13.54
1.361	70.00	24.458	127.76	12.47
0.953	58.30	29.107	106.38	10.48
0.680	37.50	26.272	68.54	11.61
0.544	28.30	24.719	51.65	12.34
0.408	20.80	24.199	37.67	12.60
0.272	11.70	20.394	21.34	14.96
0.136	5.20	17.981	9.52	16.96

TABLE C-6

RESISTANCE FACTOR DATA AND CALCULATIONS

0.05 Percent RC-302 in 2 Percent NaCl Solution

Run No. 6 — Water Viscosity 1.012 cps
Core No. 7 — Polymer Viscosity 1.148 cps

Pressure Drop ΔP (atm)	Flow Rate $Qx10^3$ (cm^3/sec)	Polymer Mobility $\lambda_p = \left(\frac{QL}{\Delta PA}\right) x 10^3$	Linear Pore Velocity V (ft/day)	$R = \frac{\lambda_w}{\lambda_p}$
7.077	800.00	92.318	936.57	6.323
5.784	594.00	84.478	695.37	6.960
4.219	400.00	77.992	468.23	7.539
3.266	275.00	69.282	321.93	8.487
2.722	203.00	61.342	237.66	9.586
2.041	133.00	53.619	155.65	10.966
1.361	71.10	42.958	83.282	13.688
1.021	42.60	34.339	49.851	17.123
0.817	16.70	16.870	19.50	34.855
0.680	11.70	14.148	13.66	41.561
0.544	5.00	7.482	5.81	78.589
0.408	2.00	4.082	2.41	144.047
0.204	0.80	3.175	0.88	185.197

TABLE C-7

RESISTANCE FACTOR DATA AND CALCULATIONS

0.05 Percent RC-302 in 2 Percent NaCl Solution

Run No. 7 — Water Viscosity 1.012 cps
Core No. 9 — Polymer Viscosity 1.148 cps

Pressure Drop ΔP (atm)	Flow Rate $Qx10^3$ (cm^3/sec)	Polymer Mobility $\lambda_p = \left(\frac{QL}{\Delta PA}\right) \times 10^3$	Linear Pore Velocity V (ft/day)	$R = \frac{\lambda_w}{\lambda_p}$
3.538	1000.00	207.074	1515.80	4.250
2.654	700.00	193.232	1060.95	4.554
2.041	516.70	185.483	783.21	4.744
1.361	328.30	176.733	497.62	4.979
0.749	169.00	165.293	256.17	5.324
0.544	110.00	148.166	166.79	5.939
0.408	76.70	137.689	116.33	6.391
0.272	49.20	132.522	74.58	6.640
0.136	23.70	127.632	35.89	6.895

TABLE C-8

RESISTANCE FACTOR DATA AND CALCULATIONS

0.075 Percent NP-10 in 2 Percent NaCl Solution

Run No. 8 — Water Viscosity 1.012 cps
Core No. 8 — Polymer Viscosity 1.224 cps

Pressure Drop ΔP (atm)	Flow Rate $Qx10^3$ (cm^3/sec)	Polymer Mobility $\lambda_p = \left(\frac{QL}{\Delta PA}\right) x10^3$	Linear Pore Velocity V (ft/day)	$R = \frac{\lambda_w}{\lambda_p}$
10.547	813.00	58.00	861.72	9.55
8.437	589.00	52.00	620.78	10.65
6.804	455.00	50.00	479.05	11.08
6.192	400.00	48.00	422.35	11.54
5.444	333.00	45.00	351.49	12.31
4.763	248.00	39.00	261.63	14.20
4.083	211.00	38.00	222.80	14.58
3.402	166.00	36.00	175.18	15.39
2.722	127.00	34.70	134.08	15.96
2.041	96.00	35.00	101.19	15.83
1.361	62.00	33.90	65.48	16.34
0.861	36.00	32.80	37.98	16.89

TABLE C-9

RESISTANCE FACTOR DATA AND CALCULATIONS

0.075 Percent NP-10 in 2 Percent NaCl Solution

Run No. 9
Core No. 17

Water Viscosity 1.012 cps
Polymer Viscosity 1.224 cps

Pressure Drop ΔP (atm)	Flow Rate $Q \times 10^3$ (cm^3/sec)	Polymer Mobility $\lambda_p = \left(\frac{QL}{\Delta PA}\right) \times 10^3$	Linear Pore Velocity V (ft/day)	$R = \frac{\lambda_w}{\lambda_p}$
15.718	1216.00	59.90	1411.63	8.80
12.248	868.00	54.90	1006.28	10.35
10.071	667.00	51.30	773.84	10.27
8.165	500.00	47.40	581.09	11.12
6.804	400.00	45.60	464.87	11.56
6.124	330.00	41.80	382.67	12.61
5.444	278.00	39.60	323.14	13.31
4.763	241.00	39.20	279.77	13.44
4.083	193.00	36.60	223.93	14.40
3.402	157.00	35.70	182.26	14.76
3.062	130.00	32.90	150.80	16.02
2.722	117.00	33.30	135.77	15.83
2.041	83.00	31.50	96.35	16.73
1.361	53.00	30.10	61.51	17.50
0.680	28.00	31.90	32.51	16.52

TABLE C-10

RESISTANCE FACTOR DATA AND CALCULATIONS

0.199 Percent Polyox WSR-301 Solution

Run No. 10 — Water Viscosity 1.012 cps
Core No. 3 — Polymer Viscosity 4.062 cps

Pressure Drop ΔP (atm)	Flow Rate $Qx10^3$ (cm^3/sec)	Polymer Mobility $\lambda_p = \left(\frac{QL}{\Delta PA}\right) x10^3$	Linear Pore Velocity V (ft/day)	$R = \frac{\lambda_w}{\lambda_p}$
38.990	76.67	1.548	86.85	525.80
33.683	56.67	1.324	64.19	614.80
29.600	47.22	1.256	53.49	648.10
26.538	42.22	1.252	47.83	650.20
23.204	36.94	1.253	41.85	649.60
18.100	30.06	1.307	33.99	622.80
13.133	23.06	1.382	26.12	589.00
9.731	17.50	1.416	19.83	574.90
7.485	15.00	1.577	16.99	516.20
4.151	9.72	1.844	11.01	441.40
2.858	6.11	1.683	6.92	483.70
1.361	3.33	1.928	3.47	422.20
0.680	1.83	2.123	2.07	383.40

TABLE C-11

RESISTANCE FACTOR DATA AND CALCULATIONS

0.199 Percent Polyox WSR-301 Solution

Run No. 11 — Water Viscosity 1.012 cps
Core No. 5 — Polymer Viscosity 4.062 cps

Pressure Drop ΔP (atm)	Flow Rate $Qx10^3$ (cm^3/sec)	Polymer Mobility $\lambda_p = \left(\frac{QL}{\Delta PA}\right) x10^3$	Linear Pore Velocity V (ft/day)	$R = \frac{\lambda_w}{\lambda_p}$
40.001	47.17	0.964	49.29	672.20
35.724	33.61	0.769	35.124	842.70
30.621	26.67	0.712	27.87	910.10
25.177	21.39	0.695	22.35	932.40
20.754	17.50	0.690	18.29	939.10
18.100	15.83	0.715	16.54	906.30
13.541	11.94	0.721	12.48	898.80
10.547	9.03	0.700	9.30	925.70
7.213	5.98	0.677	6.24	957.20
3.402	2.78	0.668	2.903	970.10
2.041	1.46	0.584	1.52	1109.60

TABLE C-12

RESISTANCE FACTOR DATA AND CALCULATIONS

0.199 Percent Polyox WSR-301 Solution

Run No. 12 — Water Viscosity 1.012 cps
Core No. 6 — Polymer Viscosity 4.062 cps

Pressure Drop ΔP (atm)	Flow Rate $Qx10^3$ (cm^3/sec)	Polymer Mobility $\lambda_p = \left(\frac{QL}{\Delta PA}\right)x10^3$	Linear Pore Velocity V (ft/day)	$R = \frac{\lambda_w}{\lambda_p}$
39.603	19.44	0.399	19.61	278.20
36.745	13.61	0.301	13.73	368.80
33.955	11.67	0.279	11.77	397.80
31.301	8.33	0.217	8.40	511.50
27.899	6.67	0.194	6.72	572.20
23.952	5.00	0.170	5.04	652.90
20.550	3.96	0.157	3.99	707.00
16.467	2.50	0.123	2.52	902.4
13.745	2.08	0.123	2.10	902.4
10.479	1.46	0.113	1.47	982.30

TABLE C-13

RESISTANCE FACTOR DATA AND CALCULATIONS

0.199 Percent Polyox WSR-301 Solution

Run No. 13 — Water Viscosity 1.012 cps
Core No. 10 — Polymer Viscosity 4.062 cps

Pressure Drop ΔP (atm)	Flow Rate $Qx10^3$ (cm^3/sec)	Polymer Mobility $\lambda_p = \left(\frac{QL}{\Delta PA}\right) x10^3$	Linear Pore Velocity V (ft/day)	$R = \frac{\lambda_w}{\lambda_p}$
40.691	40.00	0.822	39.29	419.70
35.248	26.67	0.632	26.19	545.00
30.621	21.94	0.599	21.55	576.00
26.130	17.78	0.569	17.46	606.30
21.094	15.00	0.594	14.73	580.80
17.079	12.50	0.612	12.28	563.70
13.609	9.44	0.580	9.27	594.80
10.207	6.25	0.512	6.14	673.80
6.805	4.167	0.512	4.09	673.80
3.811	2.22	0.487	2.18	708.40

TABLE C-14

RESISTANCE FACTOR DATA AND CALCULATIONS

0.199 Percent Polyox WSR-301 Solution

Run No. 14 — Water Viscosity 1.012 cps
Core No. 16 — Polymer Viscosity 4.062 cps

Pressure Drop ΔP (atm)	Flow Rate $Qx10^3$ (cm^3/sec)	Polymer Mobility $\lambda_p = \left(\frac{QL}{\Delta PA}\right) x10^3$	Linear Pore Velocity V (ft/day)	$R = \frac{\lambda_w}{\lambda_p}$
39.398	76.67	1.645	85.47	321.00
33.206	49.44	1.258	55.12	419.70
26.538	28.89	0.920	32.21	573.90
21.979	20.00	0.769	22.30	686.60
17.352	15.56	0.758	17.34	696.60
13.065	10.28	0.665	12.14	794.00
10.683	8.33	0.659	9.29	801.20
6.805	4.44	0.552	4.95	956.50
4.899	3.19	0.551	3.56	958.3
3.062	1.94	0.536	2.17	985.10
1.497	0.83	0.470	0.93	1123.40

TABLE C-15

RESISTANCE FACTOR DATA AND CALCULATIONS

0.05 Percent Pusher 700 in 2 Percent NaCl Solution

Run No. 15 — Water Viscosity 1.012 cps
Core No. 14 — Polymer Viscosity 1.437 cps

Pressure Drop ΔP (atm)	Flow Rate $Qx10^3$ (cm^3/sec)	Polymer Mobility $\lambda_p = \left(\frac{QL}{\Delta PA}\right) x10^3$	Linear Pore Velocity V (ft/day)	$R = \frac{\lambda_w}{\lambda_p}$
8.778	268.00	24.986	356.910	26.01
7.349	252.00	28.073	335.56	23.15
6.260	223.00	29.153	296.93	22.30
4.967	197.00	32.472	262.29	20.02
3.743	170.00	37.176	226.35	17.48
2.314	127.00	44.939	169.09	14.46
1.429	89.20	51.097	118.83	12.72
0.680	55.80	67.159	74.30	9.68
0.544	45.00	67.704	59.98	9.60
0.408	26.70	53.580	35.52	12.13
0.272	15.40	46.512	20.97	13.97
0.136	7.30	30.096	9.72	21.60

TABLE C-16

RESISTANCE FACTOR DATA AND CALCULATIONS

0.05 Percent Pusher 700 in 2 Percent NaCl Solution

Run No. 16 — Water Viscosity 1.012 cps
Core No. 19 — Polymer Viscosity 1.437 cps

Pressure Drop ΔP (atm)	Flow Rate $Qx10^3$ (cm^3/sec)	Polymer Mobility $\lambda_p = \left(\frac{QL}{\Delta PA}\right) x10^3$	Linear Pore Velocity V (ft/day)	$R = \frac{\lambda_w}{\lambda_p}$
12.861	326.00	19.808	432.14	21.91
10.547	288.00	21.261	380.41	20.41
7.893	229.00	22.675	303.51	19.14
5.240	193.00	28.787	255.88	15.08
3.879	152.00	30.615	210.43	14.18
2.722	127.00	36.396	168.265	11.92
1.701	93.30	42.736	123.647	10.15
1.021	61.70	47.266	81.723	9.18
0.680	46.70	53.645	61.965	8.09
0.544	34.20	49.119	45.383	8.84
0.408	21.30	40.724	28.205	10.66
0.272	13.80	39.754	18.255	10.92
0.136	4.70	27.149	6.180	15.98

TABLE C-17

CORRECTION DATA AND CALCULATIONS

2.0 Percent NaCl Solution

Run No. 17
Core No. 1

Water Viscosity 0.977 cps
Water Density 0.994 gm/cm^3

Pressure Drop $\Delta P \times 10^{-5}$ (dynes/cm^2)	Flow Rate Q (cm^3/sec)	Velocity $V_o = \frac{q}{A}$ (cm/sec)	$f_r = \left(\frac{\Delta P}{2L\rho V_o^2}\right) \times 10^{-6}$	$R_r = \frac{V_o \rho}{\mu}$
62.052	2.483	0.230	6.801	0.234
43.437	1.561	0.144	12.143	0.146
24.131	0.783	0.072	27.010	0.073
7.584	0.217	0.020	109.913	0.020

TABLE C-18

CORRECTION DATA AND CALCULATIONS

2.0 Percent NaCl Solution

Run No. 18
Core No. 3

Water Viscosity 0.977 cps
Water Density 0.994 gm/cm^3

Pressure Drop $\Delta P \times 10^5$ (dynes/cm^2)	Flow Rate Q (cm^3/sec)	Velocity $V_o = \frac{q}{A}$ (cm/sec)	$f_r = \left(\frac{\Delta P}{2L\rho V_o^2}\right) \times 10^{-6}$	$R_r = \frac{V_o}{\mu}$
68.947	3.444	0.319	4.014	0.324
45.505	2.156	0.200	6.740	0.203
20.684	0.941	0.087	16.188	0.088
8.963	0.358	0.033	48.712	0.034

TABLE C-19

CORRECTION DATA AND CALCULATIONS

2.0 Percent NaCl Solution

Run No. 19
Core No. 5

Water Viscosity 0.977 cps
Water Density 0.994 gm/cm^3

Pressure Drop $\Delta P \times 10^{-5}$ (dynes/cm^2)	Flow Rate Q (cm^3/sec)	Velocity $V_o = \frac{q}{A}$ (cm/sec)	$f_r = \left(\frac{\Delta P}{2L\rho V_o^2}\right) \times 10^{-6}$	$R_r = \frac{V_o \rho}{\mu}$
73.084	3.542	0.326	4.005	0.332
46.194	2.078	0.192	7.104	0.195
22.063	0.833	0.077	21.091	0.078
6.895	0.225	0.021	88.853	0.021

TABLE C-20

CORRECTION DATA AND CALCULATIONS

2.0 Percent NaCl Solution

Run No. 20
Core No. 6

Water Viscosity 0.977 cps
Water Density 0.994 gm/cm^3

Pressure Drop $\Delta P \times 10^{-5}$ (dynes/cm^2)	Flow Rate Q (cm^3/sec)	Velocity $V_o = \frac{q}{A}$ (cm/sec)	$f_r = \left(\frac{\Delta P}{2L\rho V_o^2}\right) \times 10^{-6}$	$R_r = \frac{V_o}{\mu}$
208.909	0.489	0.045	588.974	0.0458
144.789	0.283	0.026	1218.763	0.0264
95.836	0.250	0.023	1034.946	0.0234
53.089	0.083	0.008	5056.095	0.0081

TABLE C-21

CORRECTION DATA AND CALCULATIONS

2.0 Percent NaCl Solution

Run No. 21
Core No. 7

Water Viscosity 0.977 cps
Water Density 0.994 gm/cm^3

Pressure Drop $\Delta P \times 10^{-5}$ (dynes/cm^2)	Flow Rate Q (cm^3/sec)	Velocity $V_o = \frac{q}{A}$ (cm/sec)	$f_r = \left(\frac{\Delta P}{2L\rho V_o^2}\right) \times 10^{-6}$	$R_r = \frac{V_o \rho}{\mu}$
61.363	2.583	0.239	6.077	0.243
42.747	1.650	0.153	10.329	0.156
28.238	1.033	0.096	17.342	0.098
10.342	0.350	0.032	57.360	0.033

TABLE C-22

CORRECTION DATA AND CALCULATIONS

2.0 Percent NaCl Solution

Run No. 22
Core No. 9

Water Viscosity 0.977 cps
Water Density 9.994 gm/cm^3

Pressure Drop $\Delta P \times 10^{-5}$ ($dynes/cm^2$)	Flow Rate Q (cm^3/sec)	Velocity $V_o = \frac{q}{A}$ (cm/sec)	$f_r = \left(\frac{\Delta P}{2L\rho V_o^2}\right) \times 10^{-6}$	$R_r = \frac{V_o \rho}{\mu}$
54.468	2.817	0.252	5.275	0.256
37.921	1.900	0.170	8.069	0.173
13.789	0.650	0.058	25.236	0.059
6.895	0.317	0.028	53.376	0.028

TABLE C-23

CORRECTION DATA AND CALCULATIONS

2.0 Percent NaCl Solution

Run No. 23
Core No. 10

Water Viscosity 0.977 cps
Water Density 0.994 gm/cm^3

Pressure Drop $\Delta P \times 10^{-5}$ (dynes/cm^2)	Flow Rate Q (cm^3/sec)	Velocity $V_o = \frac{q}{A}$ (cm/sec)	$f_r = \left(\frac{\Delta P}{2L\rho V_o^2}\right) \times 10^{-6}$	$R_r = \frac{V_o \rho}{\mu}$
62.052	1.067	0.099	35.398	0.101
43.092	0.625	0.058	71.677	0.059
24.131	0.281	0.026	198.283	0.026
6.205	0.067	0.006	861.806	0.006

TABLE C-24

CORRECTION DATA AND CALCULATIONS

2.0 Percent NaCl Solution

Run No. 24
Core No. 14

Water Viscosity 0.977 cps
Water Density 0.994 gm/cm^3

Pressure Drop $\Delta P \times 10^{-5}$ (dynes/cm^2)	Flow Rate Q (cm^3/sec)	Velocity $V_o = \frac{q}{A}$ (cm/sec)	$f_r = \left(\frac{\Delta P}{2L\rho V_o^2}\right) \times 10^{-6}$	$R_r = \frac{V_o \rho}{\mu}$
70.326	2.067	0.192	10.906	0.195
44.816	1.167	0.109	21.564	0.111
20.684	0.483	0.045	58.246	0.046
7.584	0.183	0.017	149.586	0.017

TABLE C-25

CORRECTION DATA AND CALCULATIONS

2.0 Percent NaCl Solution

Run No. 25
Core No. 16

Water Viscosity 0.977 cps
Water Density 0.994 gm/cm

Pressure Drop $\Delta P \times 10^{-5}$ (dynes/cm^2)	Flow Rate Q (cm^3/sec)	Velocity $V_o = \frac{q}{A}$ (cm/sec)	$f_r = \left(\frac{\Delta P}{2L\rho V_o^2}\right) \times 10^{-6}$	$R_r = \frac{V_o \rho}{\mu}$
78.600	3.067	0.290	5.251	0.295
49.642	1.739	0.164	10.368	0.167
20.684	0.656	0.062	30.262	0.063
8.274	0.192	0.018	145.158	0.018

TABLE C-26

CORRECTION DATA AND CALCULATIONS

2.0 Percent NaCl Solution

Run No. 26
Core No. 19

Water Viscosity 0.977 cps
Water Density 0.994 gm/cm^3

Pressure Drop $\Delta P \times 10^{-5}$ (dynes/cm^2)	Flow Rate Q (cm^3/sec)	Velocity $V_o = \frac{q}{A}$ (cm/sec)	$f_r = \left(\frac{\Delta P}{2L_c V_o^2}\right) \times 10^{-6}$	$R_r = \frac{V_o c}{\mu}$
70.326	2.967	0.261	5.842	0.265
48.263	1.800	0.158	10.941	0.161
20.684	0.733	0.064	28.545	0.065
7.584	0.250	0.022	89.434	0.022

TABLE C-27

CORRELATION DATA AND CALCULATIONS

0.05 Percent RC-302 in 2 Percent NaCl Solution

Run No. 27
Core No. 7

Polymer Viscosity 1.148 cps
Polymer Density 1.008 gm/cm^3

Pressure Drop $\Delta P \times 10^{-6}$ (dynes/cm^2)	Flow Rate $Q \times 10^3$ (cm^3/sec)	Velocity $V_o = \left(\frac{q}{A}\right) \times 10^2$ (cm/sec)	$f_r = \left(\frac{\Delta P}{2L\rho V_o^2}\right) \times 10^{-8}$	$R_r = \left(\frac{V_o \rho}{\mu}\right) \times 10^2$
7.17	800.00	7.401	0.730	6.498
5.86	594.00	5.495	1.083	4.825
4.27	400.00	3.700	1.740	3.249
3.31	275.00	2.544	2.853	2.234
2.76	203.00	1.878	4.365	1.649
2.07	133.00	1.230	7.631	1.080
1.38	71.10	0.658	17.777	0.578
1.03	42.60	0.394	37.064	0.346
0.83	16.70	0.154	193.023	0.135
0.69	11.70	0.108	320.930	0.095
0.55	5.00	0.046	1527.778	0.040
0.41	2.00	0.019	6833.333	0.017
0.21	0.80	0.007	21000.000	0.006

TABLE C-28

CORRELATION DATA AND CALCULATIONS

0.05 Percent RC-302 in 2 Percent NaCl Solution

Run No. 28
Core No. 9

Polymer Viscosity 1.148 cps
Polymer Density 1.008 gm/cm^3

Pressure Drop $\Delta P \times 10^{-6}$ (dynes/cm^2)	Flow Rate $Q \times 10^3$ (cm^3/sec)	Velocity $V_o = \left(\frac{q}{A}\right) \times 10^2$ (cm/sec)	$f_r = \left(\frac{\Delta P}{2L\rho V_o^2}\right) \times 10^{-8}$	$R_r = \left(\frac{V_o \rho}{\mu}\right) \times 10^2$
3.59	100.00	9.251	0.241	8.122
2.69	70.00	6.475	0.369	5.685
2.07	51.67	4.780	0.521	4.197
1.38	32.83	3.037	0.861	2.666
0.76	16.90	1.563	1.789	1.372
0.55	11.00	1.018	2.706	0.894
0.41	7.67	0.710	4.678	0.623
0.28	4.92	0.455	7.780	0.399
0.14	2.37	0.219	16.766	0.192

TABLE C-29

CORRELATION DATA AND CALCULATIONS

0.075 Percent RC-322 in 2 Percent NaCl Solution

Run No. 29
Core No. 1

Polymer Viscosity 1.377 cps
Polymer Density 1.009 gm/cm^3

Pressure Drop $\Delta P \times 10^{-5}$ (dynes/cm^2)	Flow Rate $Q \times 10^3$ (cm^3/sec)	Velocity $V_o = \left(\frac{q}{A}\right) \times 10^2$ (cm/sec)	$f_r = \left(\frac{\Delta P}{2L\rho V_o^2}\right) \times 10^{-8}$	$R_r = \left(\frac{V_o \rho}{\mu}\right) \times 10^3$
159.30	519.00	4.801	3.947	35.190
68.90	214.00	1.980	10.034	14.510
55.20	172.00	1.591	12.457	11.660
40.00	132.00	1.221	15.323	8.950
27.60	96.70	0.895	19.681	6.560
20.70	74.20	0.686	25.103	5.030
15.20	53.20	0.493	35.731	3.610
11.70	41.70	0.386	44.845	2.830
9.70	28.90	0.267	78.037	1.960
8.30	22.20	0.205	112.925	1.500
6.20	15.80	0.146	168.478	1.070
4.80	10.80	0.100	227.457	.730
3.80	5.00	0.046	1085.714	.340
1.70	1.50	0.014	4250.000	.100

TABLE C-30

CORRELATION DATA AND CALCULATIONS

0.199 Percent Polyox WSR-301 Solution

Run No. 30
Core No. 3

Polymer Viscosity 4.062 cps
Polymer Density 0.993 gm/cm^3

Pressure Drop $\Delta P \times 10^{-6}$ (dynes/cm^2)	Flow Rate $Q \times 10^3$ (cm^3/sec)	Velocity $V_o = \left(\frac{q}{A}\right) \times 10^4$ (cm/sec)	$f_r = \left(\frac{\Delta P}{2L\rho V_o^2}\right) \times 10^{-10}$	$R_r = \left(\frac{V_o \rho}{\mu}\right) \times 10^4$
39.51	76.67	71.080	4.638	17.344
34.13	56.67	52.538	7.333	12.819
29.99	47.22	43.781	9.279	10.683
26.89	42.22	39.145	10.408	9.551
23.51	36.94	34.252	11.885	8.357
18.34	30.06	27.819	13.956	6.788
13.31	23.06	21.376	17.277	5.216
9.86	17.50	16.225	22.207	3.959
7.58	15.00	13.907	23.244	3.393
4.21	9.72	9.014	30.708	2.199
2.90	6.11	5.666	53.604	1.383
1.38	3.33	3.090	86.250	0.754
0.69	1.83	1.699	140.816	0.415

TABLE C-31

CORRELATION DATA AND CALCULATIONS

0.199 Percent Polyox WSR-301 Solution

Run No. 31
Core No. 5

Polymer Viscosity 4.062 cps
Polymer Density 0.993 gm/cm^3

Pressure Drop $\Delta P \times 10^{-6}$ (dynes/cm^2)	Flow Rate $Q \times 10^3$ (cm^3/sec)	Velocity $V_o = \left(\frac{q}{A}\right) \times 10^4$ (cm/sec)	$f_r = \left(\frac{\Delta P}{2L\rho V_o^2}\right) \times 10^{-10}$	$R_r = \left(\frac{V_o \rho}{\mu}\right) \times 10^4$
40.54	47.17	43.472	12.173	10.607
36.20	33.61	30.978	21.407	7.559
31.03	26.67	24.578	29.150	5.997
25.51	21.39	19.713	39.367	4.810
21.03	17.50	16.129	45.883	3.935
18.34	15.83	14.593	48.868	3.561
13.72	11.94	11.008	76.648	2.686
10.69	9.03	8.321	87.695	2.030
7.31	5.97	5.504	136.891	1.343
3.45	2.78	2.560	297.414	0.625
2.07	1.46	1.344	646.875	0.328

TABLE C-32

CORRELATION DATA AND CALCULATIONS

0.199 Percent Polyox WSR-301 Solution

Run No. 32
Core No. 6

Polymer Viscosity 4.062 cps
Polymer Density 0.993 gm/cm^3

Pressure Drop $\Delta P \times 10^{-6}$ (dynes/cm^2)	Flow Rate $Q \times 10^3$ (cm^3/sec)	Velocity $V_o = \left(\frac{q}{A}\right) \times 10^4$ (cm/sec)	$f_r = \frac{\Delta P}{2L\rho V_o^2} \times 10^{-10}$	$R_r = \left(\frac{V_o \rho}{\mu}\right) \times 10^4$
40.13	19.44	17.987	70.564	4.389
37.23	13.61	12.591	133.632	3.072
34.40	11.67	10.793	167.969	2.633
31.72	8.33	7.709	303.831	1.881
28.27	6.67	6.167	423.204	1.505
24.27	5.00	4.625	645.479	1.129
20.82	3.96	3.661	882.203	0.893
16.69	2.50	2.313	1794.624	0.564
13.93	2.08	1.927	2143.077	0.470
10.62	1.46	1.349	3318.750	0.329

TABLE C-33

CORRELATION DATA AND CALCULATIONS

0.199 Percent Polyox WSR-301 Solution

Run No. 33
Core No. 10

Polymer Viscosity 4.062 cps
Polymer Density 0.993 gm/cm^3

Pressure Drop $\Delta P \times 10^{-6}$ (dynes/cm^2)	Flow Rate $Q \times 10^3$ (cm^3/sec)	Velocity $V_o = \left(\frac{q}{A}\right) \times 10^4$ (cm/sec)	$f_r = \left(\frac{\Delta P}{2L\rho V_o^2}\right) \times 10^{-10}$	$R_r = \left(\frac{V_o \rho}{\mu}\right) \times 10^4$
42.39	40.00	37.144	17.153	9.063
35.71	26.67	24.763	32.582	6.042
31.03	21.94	20.377	41.819	4.972
26.48	17.78	16.508	54.363	4.028
21.37	15.00	13.929	61.621	3.399
17.31	12.50	11.607	71.885	2.832
13.79	9.44	8.770	100.291	2.140
10.34	6.25	5.804	171.761	1.416
6.89	4.17	3.869	257.090	0.944
3.86	2.22	2.063	501.299	0.503

TABLE C-34

CORRELATION DATA AND CALCULATIONS

0.199 Percent Polyox WSR-301 Solution

Run No. 34
Core No. 16

Polymer Viscosity 4.062 Cps
Polymer Density 0.993 gm/cm^3

Pressure Drop $\Delta P \times 10^{-6}$ (dynes/cm^2)	Flow Rate $Q \times 10^3$ (cm^3/sec)	Velocity $V_o = \left(\frac{q}{A}\right) \times 10^4$ (cm/sec)	$f_r = \frac{\Delta P}{2LV_o^2} \times 10^{-10}$	$R_r = \left(\frac{V_o \rho}{\mu}\right) \times 10^4$
39.92	76.67	72.368	4.287	17.368
33.65	49.44	46.672	8.688	11.388
26.89	28.89	27.269	20.337	6.654
22.27	20.00	18.879	34.143	4.606
17.58	15.56	14.684	45.883	3.583
13.24	10.28	10.278	70.501	2.508
10.82	8.33	7.866	98.274	1.919
6.89	4.44	4.195	220.128	1.024
4.96	3.19	3.015	307.407	0.736
3.10	1.94	1.835	508.197	0.448
1.52	0.83	0.786	1381.818	0.192

TABLE C-35

CORRELATION DATA AND CALCULATIONS

0.05 Percent Pusher 700 in 2 Percent NaCl Solution

Run No. 35
Core No. 14

Polymer Viscosity 1.437 cps
Polymer Density 1.009 gm/cm^3

Pressure Drop $\Delta P \times 10^{-6}$ (dynes/cm^2)	Flow Rate $Q \times 10^3$ (cm^3/sec)	Velocity $V_o = \left(\frac{q}{A}\right) \times 10^2$ (cm/sec)	$f_r = \left(\frac{\Delta P}{2L\rho V_o^2}\right) \times 10^{-8}$	$R_r = \left(\frac{V_o \rho}{\mu}\right) \times 10^2$
8.89	268.00	2.493	8.055	1.750
7.45	252.00	2.344	7.636	1.646
6.34	223.00	2.074	8.301	1.456
5.03	197.00	1.832	8.440	1.286
3.79	170.00	1.581	8.537	1.110
2.34	127.00	1.181	9.446	0.829
1.45	89.20	0.830	11.851	0.583
0.69	55.80	0.519	14.444	0.364
0.55	45.00	0.419	17.600	0.294
0.41	26.70	0.248	37.239	0.174
0.28	15.40	0.143	78.873	0.100
0.18	7.30	0.068	262.240	0.048

TABLE C-36

CORRELATION DATA AND CALCULATIONS

0.05 Percent Pusher 700 in 2 Percent NaCl Solution

Run No. 36
Core No. 19

Polymer Viscosity 1.437 cps
Polymer Density 1.009 gm/cm^3

Pressure Drop $\Delta P \times 10^{-6}$ (dynes/cm^2)	Flow Rate $Q \times 10^3$ (cm^3/sec)	Velocity $V_o = \left(\frac{q}{A}\right) \times 10^2$ (cm/sec)	$f_r = \left(\frac{\Delta P}{2L_o V_o^2}\right) \times 10^{-8}$	$R_r = \left(\frac{V_o \rho}{\mu}\right) \times 10^2$
13.03	326.00	2.866	8.842	2.012
10.69	287.00	2.523	9.360	1.771
8.00	229.00	2.013	11.005	1.413
5.31	193.00	1.697	10.277	1.191
3.93	152.00	1.336	12.272	0.938
2.76	127.00	1.116	12.357	0.783
1.72	93.30	0.820	14.267	0.576
1.03	61.70	0.542	19.529	0.380
0.69	46.70	0.411	22.757	0.288
0.55	34.20	0.301	33.701	0.211
0.41	21.30	0.187	65.286	0.131
0.28	13.80	0.121	104.089	0.085
0.14	4.70	0.041	388.880	0.029

TABLE C-37

OIL DISPLACEMENT DATA AND CALCULATIONS

2.0 Percent NaCl Solution

Run No. 37
Core No. 13
Oil Viscosity 1.512 cps
Water Viscosity 1.012 cps

Core Pore Volume 19.383cc
Initial Oil in PLace (I.O.I.P.) 12.60 cc
Ultimate Oil Recovered 4.79 cc

Water Injected (cc)	Cumulative Water Injected (cc)	Cumulative Water Injected (pore volume)	Oil Produced (cc)	Cumulative Oil Produced (cc)	Cumulative Oil Produced %(I.O.I.P.)	Cumulative Water Produced (cc)	Water Oil Ratio
0.97	0.97	0.050	0.97	0.97	7.71	0.00	0.000
0.48	1.45	0.075	0.48	1.45	11.51	0.00	0.000
0.51	1.96	0.100	0.51	1.96	15.55	0.00	0.000
0.56	2.52	0.130	0.56	2.52	20.00	0.00	0.000
0.58	3.10	0.160	0.58	3.10	24.60	0.00	0.000
0.39	3.49	0.180	0.39	3.49	27.70	0.00	0.000
0.58	4.07	0.210	0.58	4.07	32.30	0.00	0.000
0.29	4.36	0.225	0.29	4.36	34.60	0.00	0.000
0.48	4.84	0.250	0.23	4.59	36.50	0.25	0.054
0.97	5.81	0.300	0.02	4.61	36.62	1.20	0.260
1.46	7.27	0.375	0.01	4.62	36.65	2.65	0.574
3.87	11.14	0.575	0.00	4.62	36.70	6.52	1.411
1.46	12.60	0.650	0.01	4.63	36.75	7.97	1.721

TABLE C-37 (Continued)

Water Injected (cc)	Cumulative Water Injected (cc)	Cumulative Water Injected (pore volume)	Oil Produced (cc)	Cumulative Oil Produced (cc)	Cumulative Oil Produced %(I.O.I.P.)	Cumulative Water Produced (cc)	Water Oil Ratio
4.84	17.44	0.900	0.02	4.65	36.90	12.79	2.751
4.36	21.80	1.125	0.01	4.66	37.00	17.14	3.678
6.30	28.10	1.450	0.03	4.69	37.25	23.41	4.991
4.36	32.46	1.675	0.03	4.72	37.50	27.74	5.877
5.33	37.79	1.950	0.02	4.74	37.60	33.05	6.973
2.91	40.70	2.100	0.00	4.74	37.65	35.96	7.586
2.90	43.60	2.250	0.02	4.76	37.75	38.84	8.160
2.33	45.93	2.370	0.01	4.77	37.90	41.16	8.629
4.46	50.39	2.600	0.02	4.79	38.06	45.60	9.520
3.87	54.26	2.800	0.00	4.79	38.06	49.47	10.328
3.88	58.14	3.000	0.00	4.79	38.06	53.35	11.138
11.63	69.77	3.600	0.00	4.79	38.06	64.98	13.566
17.44	87.21	4.500	0.00	4.79	38.06	82.42	17.207
9.69	96.90	5.000	0.00	4.79	38.06	92.11	19.230

TABLE C-37 (Continued)

OIL DISPLACEMENT DATA AND CALCULATIONS

0.05 Percent Polyox WSR-301 in 2 Percent NaCl Solution

Run No. 38
Core No. 13
Oil Viscosity 1.512 cps
Polymer Viscosity 1.843 cps

Core Pore Volume 19.383 cc
Initial Oil in PLace (I.O.I.P.) 12.98 cc
Ultimate Oil Recovered 5.54 cc

Polymer Injected (cc)	Cumulative Polymer Injected (cc)	Cumulative Polymer Injected (pore volume)	Oil Produced (cc)	Cumulative Oil Produced (cc)	Cumulative Oil Produced %(I.O.I.P.)	Cumulative Polymer Produced (cc)	Polymer Oil Ratio
0.97	0.97	0.050	0.97	0.97	7.47	0.00	0.000
0.58	1.55	0.080	0.58	1.55	11.94	0.00	0.000
0.58	2.13	0.110	0.58	2.13	16.41	0.00	0.000
1.16	3.29	0.170	1.16	3.29	25.35	0.00	0.000
0.29	3.58	0.185	0.29	3.58	27.58	0.00	0.000
0.24	3.82	0.197	0.24	3.82	29.43	0.00	0.000
0.15	3.97	0.205	0.15	3.97	30.58	0.00	0.000
0.14	4.11	0.212	0.14	4.11	31.66	0.00	0.000
0.15	4.26	0.220	0.15	4.26	32.82	0.00	0.000
0.10	4.36	0.225	0.10	4.36	33.59	0.00	0.000
0.23	4.59	0.235	0.54	4.90	37.75	0.00	0.000
0.25	4.84	0.250	0.06	4.96	38.25	0.00	0.000
0.97	5.81	0.300	0.10	5.06	39.00	0.75	0.148

TABLE C-37 (Continued)

Polymer Injected (cc)	Cumulative Polymer Injected (cc)	Cumulative Polymer Injected (pore volume)	Oil Produced (cc)	Cumulative Oil Produced (cc)	Cumulative Oil Produced %(I.O.I.P.)	Cumulative Polymer Produced (cc)	Polymer Oil Ratio
1.46	7.27	0.375	0.02	5.08	39.12	2.19	0.431
1.45	8.72	0.450	0.01	5.09	39.25	3.63	0.713
6.30	15.02	0.775	0.04	5.13	39.50	9.89	1.928
2.42	17.44	0.900	0.10	5.23	40.30	12.21	2.335
5.81	23.25	1.200	0.09	5.32	41.00	17.93	3.370
3.30	26.55	1.370	0.03	5.35	41.25	21.20	3.963
3.97	30.52	1.575	0.04	5.39	41.50	25.19	4.673
5.82	36.34	1.875	0.06	5.45	42.00	30.89	5.668
4.36	40.70	2.100	0.03	5.48	42.25	35.22	6.427
5.81	46.51	2.400	0.03	5.51	42.50	41.00	7.441
2.91	49.42	2.550	0.03	5.54	42.70	43.88	7.921
6.78	56.20	2.900	0.00	5.54	42.70	50.66	9.144
15.50	71.70	3.700	0.00	5.54	42.70	65.16	11.762
16.02	87.72	4.500	0.00	5.54	42.70	81.18	14.653
7.24	94.96	4.900	0.00	5.54	42.70	89.42	17.765

TABLE C-38

OIL DISPLACEMENT DATA AND CALCULATIONS

2.0 Percent NaCl Solution

Run No. 39
Core No. 11
Oil Viscosity 2.723 cps
Water Viscosity 1.012 cps

Core Pore Volume 18.588 cc
Initial Oil in Place (I.O.I.P.) 11.75 cc
Ultimate Oil Recovered 5.41 cc

Water Injected (cc)	Cumulative Water Injected (cc)	Cumulative Water Injected (pore volume)	Oil Produced (cc)	Cumulative Oil Produced (cc)	Cumulative Oil Produced %(I.O.I.P.)	Cumulative Water Produced (cc)	Water Oil Ratio
0.93	0.93	0.050	0.93	0.93	7.91	0.00	0.000
0.46	1.39	0.075	0.46	1.39	11.83	0.00	0.000
0.84	2.23	0.120	0.94	2.23	19.83	0.00	0.000
0.37	2.60	0.140	0.37	2.60	22.13	0.00	0.000
0.65	3.25	0.175	0.65	3.25	27.66	0.00	0.000
0.65	3.90	0.210	0.65	3.90	33.19	0.00	0.000
0.56	4.46	0.240	0.56	4.46	37.96	0.00	0.000
0.30	4.76	0.255	0.30	4.76	40.51	0.00	0.000
0.17	4.93	0.265	0.17	4.93	41.96	0.00	0.000
0.46	5.39	0.290	0.28	5.21	44.38	0.18	0.035
0.43	5.82	0.313	0.08	5.29	45.00	0.53	0.100
0.69	6.51	0.350	0.05	5.35	45.50	1.16	0.217
0.93	7.44	0.400	0.00	5.40	45.92	2.04	0.378

TABLE C-38 (Continued)

Water Injected (cc)	Cumulative Water Injected (cc)	Cumulative Water Injected (pore volume)	Oil Produced (cc)	Cumulative Oil Produced (cc)	Cumulative Oil Produced %(I.O.I.P.)	Cumulative Water Produced (cc)	Water Oil Ratio
4.72	12.16	0.654	0.00	5.40	45.92	6.76	1.252
4.57	16.73	0.900	0.00	5.40	45.95	11.33	2.098
12.21	28.94	1.557	0.00	5.40	45.95	23.54	4.359
6.85	35.79	1.925	0.00	5.40	45.95	30.39	5.628
8.83	44.62	2.400	0.01	5.41	46.00	39.21	7.248
14.87	59.49	3.200	0.00	5.41	46.00	54.08	9.996
11.15	70.64	3.800	0.00	5.41	46.00	65.23	12.057
10.23	80.87	4.350	0.00	5.41	46.00	75.46	13.948
11.15	92.02	4.950	0.00	5.41	46.00	86.61	16.009
5.95	97.97	5.270	0.00	5.41	46.00	92.56	17.109

TABLE C-38 (Continued)

OIL DISPLACEMENT DATA AND CALCULATIONS

0.05 Percent Polyox WSR-301 in 2 Percent NaCl Solution

Run No. 40
Core No. 11
Oil Viscosity 2.723 cps
Polymer Viscosity 1.843 cps

Core Pore Volume 18.588 cc
Initial Oil in Place (I.O.I.P.) 11.80 cc
Ultimate Oil Recovered 6.03 cc

Polymer Injected (cc)	Cumulative Polymer Injected (cc)	Cumulative Polymer Injected (pore volume)	Oil Produced (cc)	Cumulative Oil Produced (cc)	Cumulative Oil Produced %(i.O.I.P.)	Cumulative Polymer Produced (cc)	Polymer Oil Ratio
0.93	0.93	0.050	0.93	0.93	0.00	0.00	0.000
0.65	1.58	0.085	0.65	1.58	7.88	0.00	0.000
0.74	2.32	0.125	0.74	2.32	13.39	0.00	0.000
0.47	2.79	0.150	0.47	2.79	19.66	0.00	0.000
0.28	3.07	0.165	0.28	3.07	23.64	0.00	0.000
0.65	3.72	0.200	0.65	3.72	26.02	0.00	0.000
0.93	4.65	0.250	0.93	4.65	31.53	0.00	0.000
0.74	5.39	0.290	0.74	5.39	39.41	0.00	0.000
0.47	5.86	0.325	0.40	5.79	45.68	0.07	0.012
0.39	6.25	0.337	0.06	5.85	49.06	0.40	0.068
0.72	6.97	0.375	0.05	5.90	49.56	1.07	0.181
0.93	7.90	0.425	0.04	5.94	50.02	1.96	0.330
1.95	9.85	0.530	0.02	5.96	50.34	3.89	0.653

TABLE C-38 (Continued)

Polymer Injected (cc)	Cumulative Polymer Injected (cc)	Cumulative Polymer Injected (pore volume)	Oil Produced (cc)	Cumulative Oil Produced (cc)	Cumulative Oil Produced %(I.O.I.P.)	Cumulative Polymer Produced (cc)	Polymer Oil Ratio
3.53	13.38	0.720	0.00	5.96	50.54	7.49	1.245
3.72	17.10	0.920	0.02	5.98	50.54	11.12	1.860
5.21	23.31	1.200	0.01	5.99	50.70	16.32	2.725
8.36	30.67	1.650	0.04	6.03	50.80	24.64	4.086
10.23	40.90	2.200	0.00	6.03	51.10	34.87	5.783
19.52	60.42	3.250	0.00	6.03	51.10	54.39	9.020
13.94	74.36	4.000	0.00	6.03	51.10	68.33	11.332
20.45	94.81	5.100	0.00	6.03	51.10	88.78	14.723
13.01	107.82	5.800	0.00	6.03	51.10	100.79	16.715

TABLE C-39

OIL DISPLACEMENT DATA AND CALCULATIONS

2.0 Percent NaCl Solutions

Run No. 41
Core No. 4
Oil Viscosity 26.392 cps
Water Viscosity 1.012 cps

Core Pore Volume 21.272 cc
Initial Oil in Place (I.O.I.P.) 14.78 cc
Ultimate Oil Recovered 5.91 cc

Water Injected (cc)	Cumulative Water Injected (cc)	Cumulative Water Injected (pore volume)	Oil Produced (cc)	Cumulative Oil Produced (cc)	Cumulative Oil Produced %(I.O.I.P.)	Cumulative Water Produced (cc)	Water Oil Ratio
0.94	0.94	0.044	0.94	0.94	6.35	0.00	0.000
0.57	1.51	0.071	0.57	1.51	10.20	0.00	0.000
1.44	2.95	0.141	1.44	2.95	20.00	0.00	0.000
0.74	3.69	0.171	0.74	3.69	25.00	0.00	0.000
1.11	4.80	0.232	1.11	4.80	32.50	0.00	0.000
0.74	5.54	0.245	0.74	5.54	37.50	0.00	0.000
0.53	6.38	0.300	0.14	5.68	38.44	0.70	0.123
1.06	7.44	0.350	0.05	5.73	38.74	1.71	0.298
1.06	8.50	0.400	0.04	5.77	39.04	2.73	0.473
2.13	10.63	0.500	0.00	5.77	39.05	4.86	0.842
7.45	18.08	0.850	0.00	5.77	39.07	12.31	2.133
3.19	21.27	1.000	0.01	5.78	39.09	15.49	2.680
4.25	25.52	1.200	0.00	5.78	39.12	19.74	3.415

TABLE C-39 (Continued)

Water Injected (cc)	Cumulative Water Injected (cc)	Cumulative Water Injected (pore volume)	Oil Produced (cc)	Cumulative Oil Produced (cc)	Cumulative Oil Produced %(I.O.I.P.)	Cummulative Water Produced (cc)	Water Oil Ratio
4.26	29.78	1.400	0.05	5.83	39.47	23.95	4.108
8.50	38.28	1.800	0.04	5.87	39.69	32.41	5.521
4.26	42.54	2.000	0.02	5.89	39.89	36.65	6.222
8.50	51.04	2.400	0.00	5.89	39.89	45.15	7.666
4.26	55.30	2.600	0.02	5.91	40.00	49.39	8.357
2.12	57.42	2.700	0.00	5.91	40.00	51.51	8.716
6.38	63.80	3.000	0.00	5.91	40.00	57.89	9.795
31.91	95.71	4.500	0.00	5.91	40.00	89.80	15.195
10.64	106.35	5.000	0.00	5.91	40.00	100.44	16.995
21.27	127.62	6.000	0.00	5.91	40.00	121.71	20.594

TABLE C-39 (Continued)

OIL DISPLACEMENT DATA AND CALCULATION

0.05 Percent Polyox WSR-301 in 2 Percent NaCl Solution

Run No. 42
Core No. 4
Oil Viscosity 26.392 cps
Polymer Viscosity 1.843 cps

Core Pore Volume 21.272 cc
Initial Oil in Place (I.O.I.P.) 14.61 cc
Ultimate Oil Recovered 6.53 cc

Polymer Injected (cc)	Cumulative Polymer Injected (cc)	Cumulative Polymer Injected (pore volume)	Oil Produced (cc)	Cumulative Oil Produced (cc)	Cumulative Oil Produced %(I.O.I.P.)	Cumulative Polymer Produced (cc)	Polymer Oil Ratio
0.93	0.93	0.04	0.93	0.93	6.40	0.00	0.000
0.52	1.45	0.07	0.52	1.45	9.90	0.00	0.000
0.38	1.83	0.09	0.38	1.83	12.50	0.00	0.000
0.36	2.19	0.10	0.36	2.19	15.00	0.00	0.000
0.73	2.92	0.14	0.73	2.92	20.00	0.00	0.000
0.46	3.38	0.16	0.46	3.38	23.12	0.00	0.000
1.00	4.38	0.21	1.00	4.38	30.00	0.00	0.000
0.64	5.02	0.24	0.64	5.02	34.37	0.00	0.000
0.46	5.48	0.26	0.46	5.48	37.50	0.00	0.000
0.18	6.38	0.30	0.18	5.66	38.75	0.72	0.127
1.06	7.44	0.35	0.36	6.02	41.25	1.42	0.236
2.13	9.57	0.45	0.01	6.03	41.31	3.54	0.587
2.12	11.69	0.55	0.17	6.20	42.50	5.49	0.885

TABLE C-39 (Continued)

Polymer Injected (cc)	Cumulative Polymer Injected (cc)	Cumulative Polymer Injected (pore volume)	Oil Produced (cc)	Cumulative Oil Produced (cc)	Cumulative Oil Produced %(I.O.I.P.)	Cumulative Polymer Produced (cc)	Polymer Oil Ratio
3.20	14.89	0.70	0.03	6.23	42.90	8.66	1.390
2.11	17.00	0.80	0.04	6.27	43.00	10.73	1.711
4.27	21.27	1.00	0.02	6.28	43.75	14.99	2.387
6.91	28.18	1.32	0.11	6.39	44.50	21.79	3.410
3.72	31.90	1.50	0.11	6.50	44.50	25.40	3.908
6.39	38.29	1.80	0.00	6.50	44.50	31.79	4.891
4.25	42.54	2.00	0.00	6.50	44.50	36.04	5.545
10.63	53.17	2.50	0.00	6.50	44.50	46.67	7.183
9.64	63.81	3.00	0.00	6.50	44.50	57.31	8.817
21.27	85.08	4.00	0.00	6.50	44.50	78.58	12.089
31.90	116.98	5.50	0.00	6.50	44.50	110.43	16.989
21.27	138.25	6.50	0.00	6.50	44.50	131.75	20.269

TABLE C-40

OIL DISPLACEMENT DATA AND CALCULATIONS

2.0 Percent NaCl Solution

Run No. 43
Core No. 2
Oil Viscosity 44.156 cps
Water Viscosity 1.012 cps

Core Pore Volume 23.160 cc
Initial Oil in Place (I.O.I.P.) 17.11 cc
Ultimate Oil Recovered 8.24 cc

Water Injected (cc)	Cumulative Water Injected (cc)	Cumulative Water Injected (pore volume)	Oil Produced (cc)	Cumulative Oil Produced (cc)	Cumulative Oil Produced %(I.O.I.P.)	Cumulative Water Produced (cc)	Water Oil Ratio
0.93	0.93	0.040	0.93	0.93	5.44	0.00	0.000
1.39	2.32	0.100	1.39	2.32	13.56	0.00	0.000
1.15	3.47	0.150	1.15	3.47	20.28	0.00	0.000
0.81	4.28	0.185	0.81	4.28	25.01	0.00	0.000
0.35	4.63	0.200	0.35	4.63	27.06	0.00	0.000
0.93	5.56	0.240	0.93	5.56	32.50	0.00	0.000
0.92	6.48	0.280	0.92	6.48	37.87	0.00	0.000
0.70	7.25	0.310	0.77	7.25	42.37	0.00	0.000
0.35	7.53	0.325	0.02	7.27	42.50	0.26	0.036
0.57	8.10	0.350	0.21	7.48	43.75	0.62	0.083
1.16	9.26	0.400	0.18	7.66	44.75	1.60	0.209
1.74	11.00	0.475	0.09	7.75	45.31	3.25	0.419
0.58	11.58	0.500	0.06	7.81	45.62	3.77	0.485

TABLE C-40 (Continued)

Water Injected (cc)	Cumulative Water Injected (cc)	Cumulative Water Injected (pore volume)	Oil Produced (cc)	Cumulative Oil Produced (cc)	Cumulative Oil Produced %(I.O.I.P.)	Cumulative Water Produced (cc)	Water Oil Ratio
1.16	12.74	0.550	0.05	7.86	45.94	4.88	0.621
1.73	14.47	0.625	0.12	7.98	46.65	6.49	0.813
1.74	16.21	0.700	0.05	8.03	46.95	8.18	1.019
4.63	20.84	0.900	0.04	8.07	47.15	12.77	1.582
3.48	24.32	1.050	0.01	8.08	47.25	16.24	2.010
8.68	33.00	1.425	0.07	8.15	47.62	24.85	3.049
6.95	39.95	1.725	0.01	8.15	47.65	31.80	3.902
4.63	44.58	1.925	0.02	8.17	47.75	36.41	4.457
8.69	53.27	2.300	0.02	8.19	47.87	45.08	5.504
11.58	64.85	2.800	0.05	8.24	48.15	56.61	6.870
12.73	77.58	3.350	0.00	8.24	48.15	69.34	8.415
26.64	104.22	4.500	0.00	8.24	48.15	95.98	11.637
22.00	126.22	5.450	0.00	8.24	48.15	117.98	14.318
24.32	150.54	6.500	0.00	8.24	48.15	142.30	17.269

TABLE C-40 (Continued)

OIL DISPLACEMENT DATA AND CALCULATIONS

0.05 Percent Polyox WSR-301 in 2 Percent NaCl Solution

Run No. 44
Core No. 2
Oil Viscosity 44.156 cps
Polymer Viscosity 1.843 cps

Core Pore Volume 23.160 cc
Initial Oil in Place (I.O.I.P.) 17.13 cc
Ultimate Oil Recovered 9.07 cc

Polymer Injected (cc)	Cumulative Polymer Injected (cc)	Cumulative Polymer Injected (pore volume)	Oil Produced (cc)	Cumulative Oil Produced (cc)	Cumulative Oil Produced %(I.O.I.P.)	Cumulative Polymer Produced (cc)	Polymer Oil Ratio
0.58	0.58	0.025	0.58	0.58	3.39	0.00	0.000
0.58	1.16	0.050	0.58	1.16	6.77	0.00	0.000
0.58	1.74	0.075	0.58	1.74	10.16	0.00	0.000
0.81	2.55	0.110	0.81	2.55	14.89	0.00	0.000
0.78	3.33	0.144	0.78	3.33	19.44	0.00	0.000
1.07	4.40	0.190	1.07	4.40	25.69	0.00	0.000
0.46	4.86	0.210	0.46	4.86	28.37	0.00	0.000
0.94	5.80	0.250	0.94	5.80	33.86	0.00	0.000
0.54	6.34	0.274	0.54	6.34	37.01	0.00	0.000
0.95	7.29	0.315	0.97	7.29	42.65	0.00	0.000
0.28	7.57	0.327	0.08	7.39	43.12	0.18	0.024
0.53	8.10	0.350	0.01	7.40	43.18	0.70	0.095
0.58	8.68	0.375	0.20	7.60	44.37	1.08	0.142

TABLE C-40 (Continued)

Polymer Injected (cc)	Cumulative Polymer Injected (cc)	Cumulative Polymer Injected (pore volume)	Oil Produced (cc)	Cumulative Oil Produced (cc)	Cumulative Oil Produced %(I.O.I.P.)	Cumulative Polymer Produced (cc)	Polymer Oil Ratio
0.86	9.54	0.412	0.11	7.71	45.00	1.83	0.237
0.60	10.14	0.438	0.05	7.76	45.31	2.38	0.307
0.67	10.81	0.467	0.05	7.81	45.62	3.00	0.384
1.07	11.88	0.513	0.11	7.92	46.25	3.96	0.500
0.56	12.44	0.537	0.06	7.98	46.56	4.46	0.559
2.03	14.47	0.625	0.17	8.15	47.60	6.32	0.775
1.16	15.63	0.675	0.07	8.22	48.00	7.41	0.901
1.74	17.37	0.750	0.12	8.34	48.67	9.03	1.083
2.32	19.69	0.850	0.04	8.38	48.92	11.31	1.350
2.89	22.58	0.975	0.07	8.45	49.32	14.13	1.672
2.59	25.17	1.087	0.06	8.51	49.65	16.66	1.958
2.63	27.80	1.200	0.04	8.56	49.95	19.24	2.248
2.31	30.11	1.300	0.05	8.61	50.27	21.50	2.497
5.21	35.32	1.525	0.11	8.72	50.90	26.60	3.050
4.91	40.32	1.737	0.11	8.83	51.52	31.40	3.556
7.25	47.48	2.050	0.10	8.93	52.15	38.55	4.317
4.05	51.53	2.225	0.06	8.99	52.46	42.54	4.732

TABLE C-40 (Continued)

Polymer Injected (cc)	Cumulative Polymer Injected (cc)	Cumulative Polymer Injected (pore volume)	Oil Produced (cc)	Cumulative Oil Produced (cc)	Cumulative Oil Produced %(I.O.I.P.)	Cumulative Polymer Produced (cc)	Polymer Oil Ratio
5.21	56.74	2.450	0.04	9.03	52.71	47.71	5.283
3.48	60.22	2.600	0.04	9.07	52.95	51.15	5.639
11.58	71.88	3.100	0.00	9.07	52.95	62.73	6.916
20.84	92.64	4.000	0.00	9.07	52.95	82.57	9.104
11.58	104.22	4.500	0.00	9.07	52.95	95.15	10.491
30.11	134.33	4.800	0.00	9.07	52.95	125.26	13.810

TABLE C-41

OIL DISPLACEMENT DATA AND CALCULATIONS

2.0 Percent NaCl Solution

Run No. 45
Core No. 12
Oil Viscosity 2.723 cps
Water Viscosity 1.012 cps

Core Pore Volume 15.320 cc
Initial Oil in Place (I.O.I.P.) 8.78 cc
Ultimate Oil Recovered 3.71 cc

Water Injected (cc)	Cumulative Water Injected (cc)	Cumulative Water Injected (pore volume)	Oil Produced (cc)	Cumulative Oil Produced (cc)	Cumulative Oil Produced %(I.O.I.P.)	Cumulative Water Produced (cc)	Water Oil Ratio
0.92	0.92	0.060	0.92	0.92	10.48	0.00	0.000
0.23	1.15	0.075	0.23	1.15	13.10	0.00	0.000
0.54	1.69	0.110	0.54	1.69	19.25	0.00	0.000
0.61	2.30	0.150	0.61	2.30	26.20	0.00	0.000
0.23	2.53	0.165	0.23	2.53	28.82	0.00	0.000
0.30	2.83	0.185	0.30	2.83	32.23	0.00	0.000
0.39	3.22	0.210	0.39	3.22	36.67	0.00	0.000
0.23	3.45	0.225	0.23	3.45	39.29	0.00	0.000
0.15	3.60	0.235	0.13	3.58	40.80	0.02	0.006
0.23	3.83	0.250	0.03	3.61	41.10	0.22	0.061
1.61	5.44	0.355	0.05	3.66	41.70	1.78	0.486
2.22	7.66	0.500	0.04	3.69	42.00	3.97	1.027
3.83	11.49	0.750	0.00	3.69	42.20	7.80	2.114

TABLE C-41 (Continued)

Water Injected (cc)	Cumulative Water Injected (cc)	Cumulative Water Injected (pore volume)	Oil Produced (cc)	Cumulative Oil Produced (cc)	Cumulative Oil Produced %(I.O.I.P.)	Cumulative Water Produced (cc)	Water Oil Ratio
3.06	14.55	0.950	0.01	3.70	42.25	10.85	2.932
3.83	18.38	1.200	0.00	3.70	42.25	14.68	3.968
3.07	21.45	1.400	0.01	3.71	42.30	17.74	4.782
6.13	27.58	1.800	0.00	3.71	42.30	23.87	6.434
12.25	39.83	2.600	0.00	3.71	42.30	36.12	9.736
12.23	52.06	3.400	0.00	3.71	42.30	43.35	13.032
10.75	62.81	4.100	0.00	3.71	42.30	59.10	15.930
16.85	79.66	5.200	0.00	3.71	42.30	75.95	20.472
15.79	95.75	6.250	0.00	3.71	42.30	92.04	24.906

TABLE C-41 (Continued)

OIL DISPLACEMENT DATA AND CALCULATIONS

0.04 Percent Polyox WSR-301 in 2 Percent NaCl Solution

Run No. 46
Core No. 12
Oil Viscosity 2.723 cps
Polymer Viscosity 1.493 cps

Core Pore Volume 15.320 cc
Initial Oil in Place (I.O.I.P.) 8.85 cc
Ultimate Oil Recovered 4.13 cc

Polymer Injected (cc)	Cumulative Polymer Injected (cc)	Cumulative Polymer Injected (pore volume)	Oil Produced (cc)	Cumulative Oil Produced (cc)	Cumulative Oil Produced %(I.O.I.P.)	Cumulative Polymer Produced (cc)	Polymer Oil Ratio
0.61	0.61	0.040	0.61	0.61	6.89	0.00	0.000
0.81	1.41	0.092	0.80	1.41	15.93	0.00	0.000
0.44	1.85	0.121	0.44	1.85	20.90	0.00	0.000
0.40	2.25	0.147	0.40	2.25	25.42	0.00	0.000
0.39	2.64	0.172	0.39	2.64	29.83	0.00	0.000
0.35	2.99	0.195	0.35	2.99	33.79	0.00	0.000
0.30	3.29	0.215	0.30	3.29	37.18	0.00	0.000
0.16	3.45	0.225	0.30	3.45	38.98	0.00	0.000
0.12	3.57	0.233	0.16	3.65	41.25	0.00	0.000
0.14	3.71	0.242	0.20	3.68	41.56	0.03	0.008
0.14	3.85	0.251	0.03	3.71	41.87	0.14	0.038
1.86	5.71	0.373	0.07	3.78	42.70	1.93	0.511
1.95	7.66	0.500	0.06	3.84	43.34	3.82	0.995

TABLE C-41 (Continued)

Polymer Injected (cc)	Cumulative Polymer Injected (cc)	Cumulative Polymer Injected (pore volume)	Oil Produced (cc)	Cumulative Oil Produced (cc)	Cumulative Oil Produced %(I.O.I.P.)	Cumulative Polymer Produced (cc)	Polymer Oil Ratio
2.60	10.26	0.670	0.06	3.90	44.04	6.36	1.631
1.25	11.51	0.751	0.04	3.94	44.55	7.57	1.921
2.62	14.13	0.922	0.11	4.05	45.75	10.08	2.489
3.11	17.24	1.125	0.01	4.06	45.90	12.18	3.000
1.91	19.15	1.250	0.03	4.09	46.20	15.04	3.677
3.83	22.98	1.500	0.04	4.13	46.70	18.85	4.564
6.13	29.11	1.900	0.00	4.13	46.70	24.98	6.048
9.19	38.30	2.500	0.00	4.13	46.70	33.17	8.031
18.38	56.68	3.700	0.00	4.13	46.70	52.55	12.724
7.66	64.34	4.200	0.00	4.13	46.70	60.21	14.579
21.45	85.79	5.600	0.00	4.13	46.70	81.66	19.772
16.85	102.64	6.700	0.00	4.13	46.70	98.51	23.852